CYCLIC DISTILLATION FOR ENERGY CONSERVATION IN SPIRIT PRODUCTION

By

Nicole Elizabeth Shriner

A DISSERTATION

Submitted to
Michigan State University
in partial fulfillment of the requirements
for the degree of

Chemical Engineering – Doctor of Philosophy

2018

ABSTRACT

CYCLIC DISTILLATION FOR ENERGY CONSERVATION IN SPIRIT PRODUCTION

By

Nicole Elizabeth Shriner

Distillation technology has been used worldwide throughout the chemical industry for many years, originally being invented in China around 800 BC. There are currently over 40,000 columns in operation worldwide [29]. Although there are many variations in column types, sizes, tray configurations, etc., the underlying principle is the same. Distillation is the physical process of heating a liquid mixture to separate components based the relative volatilities of each component. Distilleries consume about 40% of the total energy used to operate plants in the chemical industry, and over 95% of that energy is used in separation processes [31]. Therefore, improving distillation technology is one area that chemical engineers are working to transform into a more efficient process by use of process intensification. The purpose of this research was to investigate the possible economic and energy impacts of a form of process intensification called ‘cyclic distillation’ as well as its application to the distilled spirits industry.

Cyclic distillation is an alternate mode of operation first proposed and studied by Cannon and McWhirter in the 1960’s. The ‘cycle’ consists of alternating between two periods, vapor flow and liquid flow. During the vapor flow period heat is supplied to the column, vapor flow upwards and distillate is collected as in normal operation. During the liquid flow period, the heat source is ceased and the liquid on each tray is transferred to the tray below. The cycle of alternating between the two periods is continued for the entire distillation. Cyclic distillation has been applied to many different systems and configurations and has been demonstrated experimentally and theoretically to increase column throughput, lower energy requirements and achieve higher separation performance.

In this study, a 150 L Carl © still was used to distill fermented apple cider and apple brandy low wines. Cyclic distillation and conventional operation were compared using the same system. Distillation samples were collected and analyzed using a gas chromatograph. The system was also simulated using MATLAB.

In summary, cyclic distillation on the batch column used was able to show a decrease in energy (steam) requirements for finishing runs but not in stripping runs. Cyclic distillation trends included ethanol concentration decreased at a slower rate compared to conventional operation and as a result temperature profiles mimicked this phenomenon. It was shown that the volume of hearts (product) was increased and volume of tails and heads (unwanted by-products) was decreased. This research has shown that the application of cyclic distillation on spirit production is a viable option for distilleries large and small. In extension of this work, it is suggested that cyclic distillation is applied to other types of spirits and to columns with a larger number of trays, and to trays with true plug flow capability.

This dissertation is dedicated to my mom, Dr. Tamara Shriner. Thank you for pushing me to achieve my highest potential even when I was slightly opposed to continue my academic path. Thank you for instilling in me that I can do anything I set my mind to. Thank you for showing me how a hardworking and independent woman carries herself. I am forever indebted and grateful to you.

I love you.

ACKNOWLEDGEMENTS

I would like to acknowledge and thank my advisor, Dr. Kris Berglund. Without him I would not have found my passion in the fermented beverage industry or have the connections and opportunities that I have and will continue to receive. His confidence in me since undergrad has helped to instill confidence in myself and in my work. I would also like to thank my colleagues Jacob Rochte, Yasheen Jadidi, and John Szfranski. Without their help I would likely still be googling how to fix things in the lab, getting a lot less hours of sleep, and still working on errors in my mat lab code. THANK YOU!

TABLE OF CONTENTS

LIST OF TABLES

LIST OF FIGURES

KEY TO SYMBOLS

Nomenclature

x − *liquid mole fraction*

y − *vapor mole fraction*

k *or* K − *equilbrium constant*

F − *feed*

W − *hold up (liquid)*

U − *hold up (vapor)*

D − *distillate*

B − *bottoms*

M − *holdup*

V − *vapor flow rate*

L − *liquid flow rate*

R − *reflux*

Q − *heat duty*

H *or* h − *enthalpy/specific enthalpy*

γ − *activity coefficient*

t − *time*

P − *pressure*

T − *temperature*

NT − *total number of stages*

O_L − *quantity of liquid that flows from stage to stage during the liquid flow period*

Super Scripts

$(V) - end\ of\ vapor\ flow\ period$

$(L) - end\ of\ liquid\ flow\ period$

$c - cycle\ number$

Subscripts

$i, j, k - stage\ number$

$F - feed$

$D - distillate$

$B - reboiler\ or\ bottoms$

$sat - saturation$

$vap - vapor\ flow$

CHAPTER 1: Introduction

1.1 Distillation Theory and Background

Distillation technology has been used worldwide throughout the chemical industry for many years, originally being invented in China around 800 BC. There are currently over 40,000 columns in operation worldwide [29]. Although there are many variations in column types, sizes, tray configurations, etc., the main principle is the same. Distillation is the physical process of heating a liquid mixture to separate components based on the relative volatilities of each component.

There are primarily two main types of distillation, continuous distillation and batch distillation. Continuous distillation requires a continuous feed into the column at an optimal tray, bottoms product and distillate product are continuously collected. This process can theoretically continue forever at steady state if there is feed to the column. Multiple feeds can be fed at different locations as well as multiple product distillates may be taken off at different stages in the column. In batch distillation a still pot is used to hold a certain initial volume of liquid to be separated, known as the feed. The mixture is heated, and distillate is collected until processing of the feed is completed. The distillate may be collected all together or ‘cuts’ maybe be taken as concentrations in the distillate change over time. In both types of distillation, heat is supplied by direct fire, steam, or electric heating. As the mixture is heated, the most volatile component, the one with the lowest boiling point, will vaporize first and travel upward through the column. The column can have any number of trays ranging from 3 up to 40 or more depending on the size of production and products being made. Trays allow for rectification of the feed throughout the column. There are many different tray types, but each serve the purpose of allowing some of the vapor to condense to liquid on the tray and some of the vapor to continue up the column. Each additional tray increases rectification and causes the vapor at the top of the column to have the highest concentration of the most volatile component at any time during the distillation. Finally, the vapor may travel through either a partial or total condenser. Partial condensers partially condense the vapor sending some liquid back into the column, known as reflux. Total condensers totally condense the vapor into liquid and the product exits the system, known as the distillate. In batch distillation there are two operation modes that are commonly discussed in academia, constant reflux or constant distillate composition. When the reflux is held constant the distillate will initially start with a high concentration of the most volatile component in the system and gradually decrease over time. If a constant distillate composition is desired, then the reflux ratio can be adjusted throughout the distillation. In general, increasing the reflux increases rectification, so as the distillate composition begins to decrease, the reflux will be increased to keep the distillate at a constant composition.

1.2 Distillation Improvement and Cyclic Distillation

Distillation is the most widely used separation method. Consequently, distilleries consume about 40% of the total energy used to operate plants in the chemical industry, and over 95% of the energy used in separation processes [31]. Therefore, improving distillation technology is one area that chemical engineers are working to transform into a more efficient process by use of process intensification. Process intensification (PI) is a design philosophy that aims to improve the efficiency of an already existing machine or process. In general, it can be a change in equipment or a change in a method to increase efficiency. In distillation, PI aims to improve product quality, lower energy requirements, increase capacity, reduce time from raw material to market and increase safety by design. Overall, PI aims to safely increase the speed and quality of production while decreasing capital and operating costs. The four domains that PI should make use of include: spatial (structure), thermodynamic (energy), functional (synergy), and temporal (time) [30]. There are many PI distillation technologies that have been suggested including heat pump assisted distillation, membrane distillation with its various designs, HiGee technology, cyclic distillation, dividing wall column, and reactive distillation [29].

The purpose of this research was to investigate the possible economic and energy impacts of cyclic distillation as well as its application to the distilled spirits industry. Cyclic distillation is an alternate mode of operation first proposed and studied by Cannon and McWhirter in the 1960's. The 'cycle' consists of alternating between two periods, vapor flow and liquid flow. During the vapor flow period heat is supplied to the column, vapor flow upwards and distillate is collected as in normal operation. During the liquid flow period, the heat source is ceased and the liquid on each tray is transferred to the tray below. The cycle of alternating between the two periods is continued for the entire distillation. Cyclic distillation has been applied to many different systems and configurations and has been demonstrated experimentally and theoretically to increase column throughput, lower energy requirements and achieve higher separation performance. Previous studies on cyclic distillation and current usage will be discussed in the proceeding chapter.

1.3 Cyclic Distillation Application to Spirits Industry

The distilled spirits industry is a rapidly growing industry. The US Distilled Spirits Council reported an 8th consecutive year of market share gains in 2017, "supplied sales were up 4 percent, rising $1 billion to a total of $26.2 billion, while volumes rose 2.6 percent to 226 million cases, up 5.8 million cases from the prior year. These results reflect adult consumers' ongoing taste for higher-end distilled products across most categories [40].” Increasing demand for higher-end products causes manufactures to look for technologies that can increase efficiency of their process and profit for their company. Cyclic distillation can help meet and exceed these higher demands.

Distilled spirits are different from other distilled products in that they are eventually going to be consumed as a beverage by the consumer. In many processes the end goal is to concentrate one or more products with as high purity as possible, in distilled spirits this is not necessarily the case. To make a distilled spirit product, first the grain is milled into a flour like constituency. The grain is then mixed with water to form a slurry, known as the mash, in a large vat called a mashtun. During the mashing process, the mash is heated, and alpha and beta amylase enzymes are added at the appropriate time, temperature and pH to enable the breakdown of starch into simple sugars, like glucose, that yeast can consume. The mash is then cooled and transferred to a fermenter to ferment for 1-2 weeks. During fermentation of the mash, yeast produce mainly ethanol and carbon dioxide but also by products including other alcohols as well as esters, aldehydes, and ketones. The distilling industry refers to the other compounds as congeners. The concentration of the fermentation at the end is roughly 8-12% alcohol by volume. The next step in the process is stripping the mash into low wines. The fermented mash is pumped into a designated stripping still which may or may not have trays. The purpose of stripping is to separate and concentrate the volatile components formed during fermentation from the solid and non-volatile components. The distillate called low wines is collected entirely and is usually 25-40% alcohol by volume. The next step is the finishing run in another distillation column. In large operations, this is done on a continuous column and the product is pulled off the column at the appropriate ethanol concentration for the product being made.

Batch distillation for both the stripping and finishing run is used widely throughout the craft spirits industry. Many craft distilleries pride themselves on their beautiful copper stills that look like pieces of art in their distilleries. In batch finishing, a certain volume of low wines is added to the still and distillate is collected. During batch distillation of spirits, fractions of the distillate are separated into different volumes known as cuts. The first distillate product is known as the heads cut, which is heavily concentrated with ethanol as well as the most volatile components mainly acetone, acetaldehyde, methanol and ethyl acetate. Once those compounds are out of the system, detected by the distiller by the flavor and aroma of the distillate, the actual product is collected and known as hearts. The hearts cut has primarily ethanol, but other compounds also come through in low concentrations such as methanol, isoamyl alcohol and other higher alcohols. Towards the end of the distillation the higher alcohols start to increase in concentration in the distillate and the flavor and aroma of the distillate become undesirable; this is when the tails cut is made. The tails cut still contains a high amount of ethanol, so it is oftentimes re-distilled to collect as much hearts as possible. Since the ethanol concentration is high and has other hazardous compounds, it cannot go down the drain and must be disposed of properly. Tails storage and disposal is a big problem from smaller distilleries with small facilities while trying to balance the energy requirement of re-distillation with the actual profit it lends. While ethanol is the primary contributor to the average spirit flavor and aroma profile, concentrations near the ppm level of the other compounds mentioned are found and desired to make a balanced and flavorful product. Therefore, it is important to investigate the trends of the congeners during cyclic distillation. Thus far cyclic distillation has not been applied to distilling spirits. The next few chapters intend to investigate a thorough literature review of cyclic distillation, to model the proposed batch cyclic distillation method, as well as to present the experimental methods and data collected while cyclically distilling apple brandy on an industry sized batch column still.

CHAPTER 2: Literature Review

Cyclic distillation was first proposed by Cannon in 1961. The ‘cycle’ he proposed consisted of two periods, a vapor flow period, and a liquid flow period. Cannon used a cycle timer with an automated valve to allow the periods to be specifically timed. While the valve was open, the vapor flowed through the column, and did not allow liquid to travel down through the trays. When the valve was closed, the lack of vapor thrust allowed the liquid to fall to the preceding tray. This removed the need for downcomers on plates because the liquid and vapor flowed through the same area at different times. Cannon concluded the advantages of controlled cycling in distillation were higher capacity, simpler and cheaper plate design, and high flexibility due to a choice of operating conditions dependent on cycle times [1].

Cannon and others applied controlled cycling to sieve and screen plate towers as well as packed-plate columns [2,3]. Gaska and Cannon reported experimental data on a distillation of a mixture of benzene and toluene using two test towers, one with 9 plates spaced 18 ½ inches apart, and the other with 17 plates spaced 9 ½ inches apart. The data showed a 48% increase in total vapor load at a fixed column pressure drop. They reported a significant increase in column capacity based on the average vapor velocity achieved which is shown graphically below.

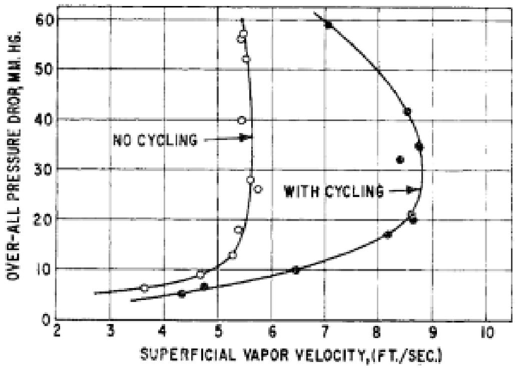

Figure 2.1 Cycling Increases Column Capacity for Type-Two Plates [2]

Gaska and Cannon concluded that the maximum rate of phase flow was not dictated by solely the equipment size and properties of the system, but was also dependent on the mode of operation of the column [2]. McWhirter and Cannon also found that it was possible to produce maximum tower efficiency, maximum tower capacity or anywhere in between these via controlled cycling of a packed plate tower [3]. McWhirter later demonstrated in his Ph.D. thesis that it was possible to double the stage efficiency and triple the throughput of a column simultaneously through theoretical and experimental investigations. McWhirter also demonstrated that while over multiple cycles the column appeared to be in steady-state operation, during a single cycle it was in unsteady-state. At any instance during the vapor flow period, the composition of the liquid on a tray varied with time, and thus the composition of the vapor leaving the stage also varied with time. He also showed that the average driving forces for mass transfer in a cyclic column were considerably greater than those in a conventional column. McWhirter believed that the high stage efficiencies of a cyclic column were difficult, if not impossible, to rationalize in terms of conventional operation. Lastly, McWhirter used these ideas to develop computer simulations of cycled columns by solving the unsteady-state material balance equations describing compositions as a function of time by using the finite-difference method [3]. Schrodt was the next to study controlled cyclic distillation and implement this operation mode on a plant-scale [4,5,6,7]. First Schrodt and others re-introduced a simple model to describe the controlled cycle column [6]. They constructed figures relating vapor compositions xiV as a function of the fraction of plate holdup dropped (ϕ).

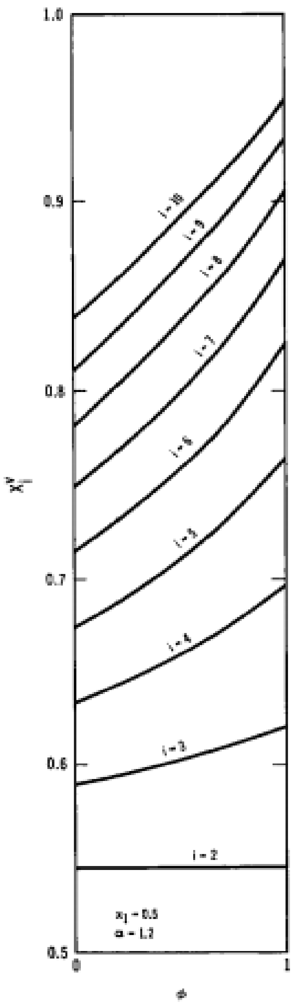

Figure 2.2 Compositions $\boldsymbol{xi\ V}$ as a Function of Fraction of Plate Holdup Dropped ($\boldsymbol{\phi}$) [6]

Figure 2.2 illustrates the concept that with the closer to true plug flow and more cycles, the purer the resulting vapor composition, which is not dependent on the number of plates. Schrodt defined the effective plate efficiency as:

$$E_{0,i} = \frac{x_{i+1}^V - x_i^V}{k_i x_i^V - x_i^V} \tag{2.1}$$

Where, ki, is a term used to calculate the equilibrium relationship. In addition, Figure 2.3 was generated which illustrated the effective plate efficiency as a function of plate number.

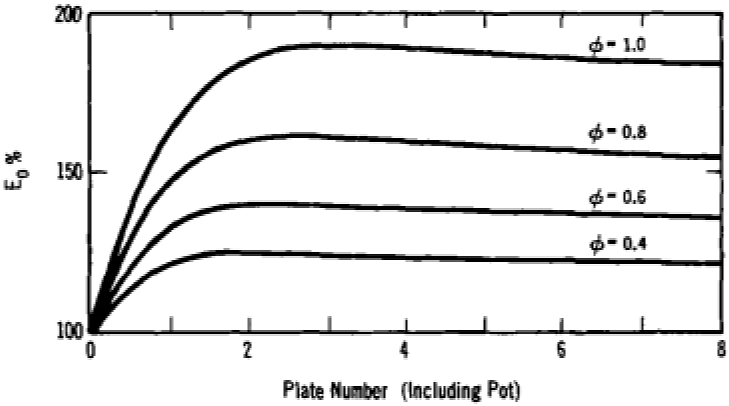

Figure 2.3 Effective Plate Efficiency $E0$ as a Function of Plate Number [6]

Next, Schrodt and others developed a computational method for obtaining the theoretical number of stages similar to the McCabe-Thiele. The current method will be presented later in this paper. The next paper published by Schrodt and others reported the results of computer simulations of controlled cyclic distillation to investigate the theoretical effects of various parameters on the separating ability of controlled cycling [5]. At this point is important to remind the reader of the definition of various efficiencies below in Table 2.1.

Table 2.1 Definition of Various Efficiencies [5]

Efficiency	Symbol	Definition
Murphree (vapor) point efficiency	E	Local vapor efficiency at a point in time and space
Instantaneous plate efficiency	-	Over-all vapor efficiency of a plate at a point in time
Effective plate efficiency	E_0	Over-all efficiency of a plate computed on the basis of liquid-phase plate compositions
Over-all column efficiency	E^0	Number of theoretical stages ($E_0 = 100\%$) corresponding to a given separation divided by the number of actual plates in the column

The Murphree point efficiency is assumed to be the same and equal for all plates and is defined as:

$$E = \frac{y_n - y_{n-1}}{y_n^* - y_{n-1}} \tag{2.2}$$

Where $yn *$ is the composition of the vapor that would be in equilibrium with the liquid on the nth stage and is given by the vapor-liquid equilibrium relationship assumed.

For computer simulations, Schrodt used the previously developed equations to see how the plate compositions varied with time as well as how the column approached its pseudo-steady-state conditions [5]. The pseudo steady state was defined as the composition profile remaining constant at the end of successive cycles. For the simulation, a binary system with a constant volatility of 1.2 was assumed. It ran in total reflux and assumed a boil-up rate and liquid hold up of 0.1 g mole/sec and 0.2 g mole, respectively. In addition, the initial pot was charged with 10 g moles, the Murphree efficiency was assumed to be 1, the fraction of plate holdup dumped to the plate below was assumed to be 1, and N was assumed to be 5. Lastly, the initial composition of the still pot was 0.5.

The results from the computer simulation gave graphical insight to how a controlled cycled column operates. It was found that the pseudo steady state condition was achieved after roughly 150 cycles.

The effect of fraction of plate holdup dropped was studied for values of ϕ ranging from 0 to 3.0. The effective numbers of theoretical plates in the column ($Neff$) was calculated from the values of the still-pot and condenser compositions at the end of the vapor flow period once the pseudo-steady-state condition was achieved, using the Fenske equation below:

$$N_{eff} = \left(\frac{\log\left[\frac{x_c}{1-x_c}\,\frac{1-x_1}{x_1}\right]}{\log\alpha} \right) - 1 \tag{2.3}$$

The overall column efficiency ($E0$) was then determined by dividing $Neff$ by the number of actual plates. The resulting data can be seen below in Figure 2.4.

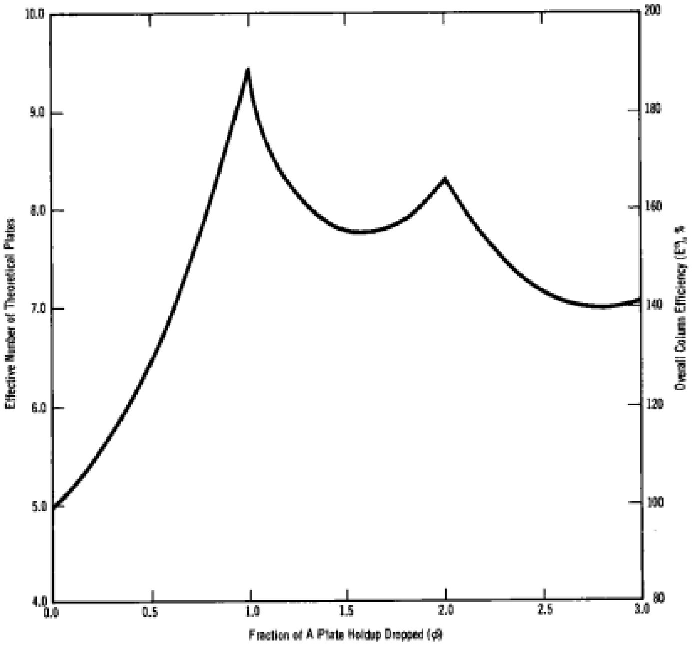

Figure 2.4 Effect of Fraction of Plate Holdup Dropped During the Liquid Flow Period on the Over-all Efficiency of a Controlled Cycling Rectification Still at Total Reflux [5]

The results from Schrodt's computer simulations agreed with McWhirter's theoretical studies that maxima occur at integral values of ϕ, with the maximum of these occurring at ϕ = 1. It is important to note that ϕ = 0 corresponds to conventional column operation.

The next parameter studied was the effect of mixing during the liquid flow period. Values of τ equal to 0.5, 1.0 and 2.0 seconds were investigated which correspond to ϕ = 0.25, 0.5 and 1.0, respectively. Results of these simulations can be seen in Table 1.2 below.

Table 2.2 Effects of Mixing During the Liquid Flow Period on the Separating Ability of a Controlled Cycle Rectification Still at Total Reflux [5]

Duration of the vapor-flow period $\tau(=\tau_L), sec$	Effective number of theoretical plates, N_{eff}	Over-all column efficiency, $E^0, \%$
0.5	4.96	99.1
1.0	4.93	98.7
2.0	4.83	96.6

The data presented in Table 2.2 illustrates that complete mixing during the liquid flow period decreased the separation advantages that were gained in cyclic operation.

The next effect studied was the effect of relative volatility. The results are shown below in Table 2.3.

Table 2.3 Effect of Relative Volatility on the Overall Column Efficiency of a Controlled Cycling Rectification Still at Total Reflux [5]

Relative volatility, α	Effective number of theoretical plates, N_{eff}	Over-all column efficiency, $E^0, \%$
1.05	9.56	191.1
1.10	9.54	190.8
1.20	9.46	189.2
1.30	9.35	187.0
1.40	9.23	184.6
1.50	9.12	182.4
1.50[a]	9.26	185.3

[a] $x_1^0 = 0.3$

The results in Table 2.3 show that the overall column efficiency decreased with an increase in the relative volatility of the distilled mixture.

Next, the effect of Murphree plate efficiency was studied and it was concluded that the over-all column efficiency of a controlled cyclic distillation column increased rapidly as the individual plate efficiencies were increased. This conclusion was also in agreement with McWhirter's earlier findings. Lastly, the effect of the number of plates, N, was studied via computer simulations. In this case, a straight-line equilibrium relationship was assumed. From these simulations, it was found that the over-all column efficiency of a controlled cycling column increased to an asymptotic value as the number of actual plates in the still increased. These findings are illustrated in Figure 2.5 below.

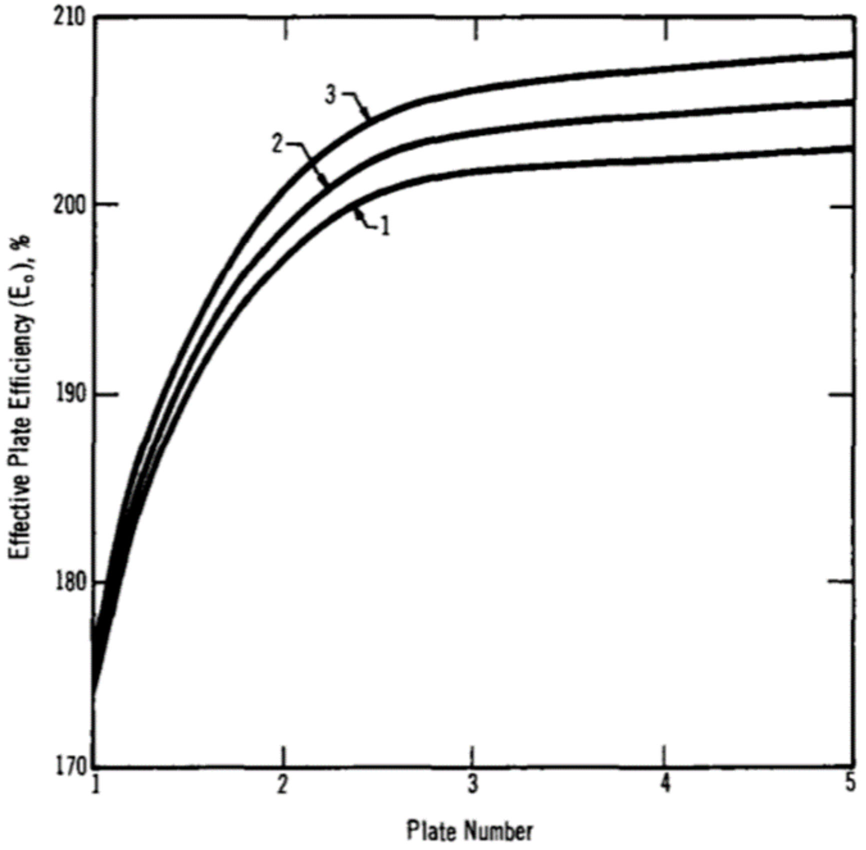

Figure 2.5 Effective Plate Efficiencies (E_0) in a Controlled Cycling Rectification Column Still at Total Reflux [5]

To study plant-scale operation, a 20-plate column was designed to separate a mixture of acetone and water [7]. Schrodt and others found that the use of a conventional column in a cyclic operational mode resulted in substantial capacity improvements, if the number of trays was less than 12. This was assumed to be due to pressure drops throughout the column which caused trays to mix with each other during the liquid flow period. They suggested that an 100% efficiency increase, and 2 to 3 times capacity increases were still possible if true plug flow was observed.

True plug flow would be achieved if the volume from tray 4 only dropped to tray 3, and none of the liquid from tray 5 would mix with the liquid of tray 3 [7].

In 1967, Robinson and Engel presented a theoretical analysis that demonstrated the advantages of cycled mass transfer operations [9]. Considering a classic paper by Lewis on the effect of liquid phase composition profiles applicable to cyclic operation, Robinson and Engel developed time-axis concentration gradients on each stage, analogous to those developed for conventional columns with lateral concentration gradients to predict column performance. Lewis' paper considering three cases. Case 1, vapor flowing to the tray, liquid flows at uniform composition at all points. Case 2, vapor laterally unmixed flowing between stages, liquid flows in same lateral direction on all stages. Case 3, vapor laterally unmixed flowing between stages, liquid flows in opposite directions on alternate stages. Robinson and Engel decided that the plate directly above the reboiler was analogous to a Lewis Case 1 with constant composition vapor flowing to it over short times of one cycle. The rest of the plates corresponded to Lewis Case 2 plates. Robinson and Engel then used the mathematical analyses developed by Lewis to derive a vapor flow period material balance and solutions to case 1 and case 2. The plate efficiency was found to be dependent on the fraction of liquid on the plate that drained to the plate below during cycling. The results of this analysis were like the results of McWhirter and Schrodt, therefore the equations and figures have not been presented [9].

In 1967, Horn published a paper on periodic countercurrent processes. The report discussed how the overall stage efficiency of a periodically operated distillation column is complicated and depends on the number of stages as well as the equilibrium and transport parameters. Horn developed accurate asymptotic formulas for the stage efficiency that proved the idea that the performance of a distillation column can be drastically improved by periodic operation [8].

In 1968, Horn and May developed a simple asymptotic relation which described the stage efficiency of a periodically operated distillation column. The relation developed used parameters which are a function of Murphree efficiency, transport number, and separation factor. Horn and May defined an important number, the transport number as the ratio of the quantity of liquid transported per cycle to the liquid hold up of a stage. They also investigated the effect of mixing on stage efficiency of a periodically operated countercurrent process for the case of difficult separations. They did so by modeling each stage, during the time of liquid transport, by a series of well stirred tanks [10,11].

Gel'perin, Polotskii, and Potapov experimented with a bubble-cap fractionating column in a cyclic regime [13]. The column contained six sections having an internal diameter of 80 mm and a height of 250 mm, each with five single cap plates in between the sections. The experiment allowed for varying total cycle time from 5 to 60 seconds, operated at total reflux and atmospheric pressure. To incorporate the cyclic regime, electromagnetic solenoid valves were used in the vapor feed and reflux lines and controlled by two-time relays through the rectifier. From the resulting data, they determined an optimum total cycle time and ratio of vapor to liquid feed periods. The experiments confirmed the presence of a beneficial effect from the use of the cycle regime with bubble-cap plates as seen in Figure 1.5 below.

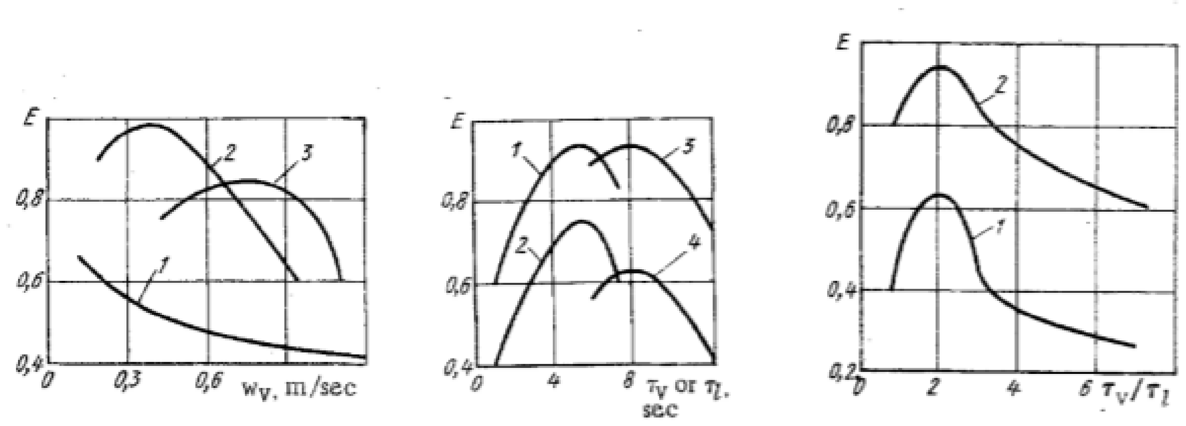

(a) **(b)** **(c)**

Figure 2.6 (a) Dependence of Column Separation Efficiency E on Mean Vapor Velocity W_v (b) Dependence of Column Separation Efficiency E on Vapor Feed Time τ_v and on Liquid-feed Time τ_l (c) Dependence of Column Separation Efficiency E on the Ratio of Feed Periods of Phases τ_v/τ_l for Various Velocities [13]

In the Figure 1.6(a) line 1 is the stationary regime, line 2 is cyclic regime with $\tau_v = 8\ sec$ and $\tau_l = 5\ sec$, and line 3 is cyclic regime with $\tau_v = 12\ sec$ and $\tau_l = 3\ sec$. The cyclic regime was clearly more efficient than the stationary mode of operation. The maxima in the cyclic regime lines indicates a maximum vapor flow rate corresponding to a maximum efficiency. In Figure 1.6(b) line 1 is for $\tau_v = 8\ sec$, line 2 is for $\tau_v = 12\ sec$, line 3 if for $\tau_l = 5\ sec$ and line 4 is for $\tau_l = 1\ sec$. This figure allowed for the assumption of the optimal vapor feed time of 8 seconds and the optimal liquid feed time to be 5 seconds. It is important to note that the optimal duration of liquid feed to the column was determined by the time to replace the liquid on each plate and was a function of plate construction and properties of the liquid. In Figure 1.6(c) line 1 corresponds to a mean vapor velocity $W_v = 1.0\ m/sec$ and line 2 corresponds to $W_v = 0.8\ m/sec$. From the data it is evident that for this column, the optimum total cycle time is about 13 sec, and the ratio of the feed periods for vapor and liquid is in the range from 1 to 3 [13].

Up to this point, most of the research done was comparing cyclic columns to conventional operation. In 1977, Rivas developed a short cut method for preliminary design of ideal cyclic distillation columns. Material balance differential equations on each plate of a cyclic distillation column were used to develop analytical equations to calculate the ideal number of trays for cyclic countercurrent processes like distillation, absorption, and stripping [14].

One year later, Furzer studied fluid flow in a distillation column by taking measurements of the discrete residence time distribution [16]. The column had five sieve plates spaced 635 mm apart. A microprocessor was used to obtain periodic control. The data yielded the parameters in the (2S) model which described the fluid flow. Furzer concluded that in order to achieve maximum separation, modifications to the column internals were required. A few years later in 1980, Furzer and Goss studied fluid mixing and mass transfer separations of mixtures of methylcyclohexane and n-heptane under periodically cycled conditions [17]. The theoretical improvements of 200% reported by McWhirter and Lloyd could not be reproduced. Goss and Furzer concluded that liquid bypassing the plates caused the reduction to 107-126% improvement. However, the (2S) model was successful in modeling both the fluid mixing and the mass transfer separations in the periodically cycled column.

Baron, Wajc and Lavie developed a theory of stepwise periodic distillation [18,19]. The major difference in stepwise periodic versus controlled cycling is in stepwise the liquid flow is controlled directly instead of through pulsations of the vapor flow rate. The researchers developed this based on the idea that preventing axial mixing could improve the separation. Their research goal was to compare the two operating models for total reflux and for continuous distillation, as well as construct a lab-scale stepwise periodic column for data collection. The column analyzed consisted of a boiler, a total condenser, N trays numbered starting at the bottom and N reservoirs specific to each tray. The schematic can be seen below in Figure 2.7.

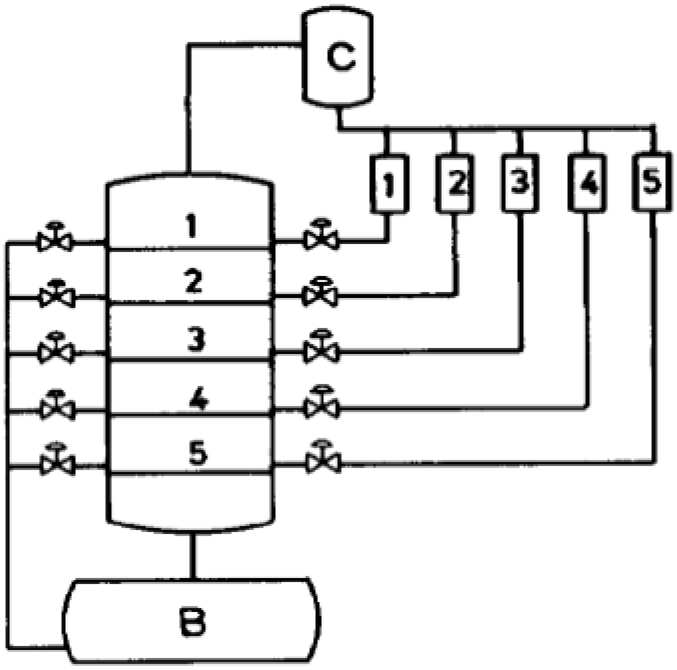

Figure 2.7 Schematic of Column Used for Stepwise Period Distillation [18]

Each tray is fitted with an inlet and an outlet with on-off valves. The trays had no downcomers but could be completely emptied via the outlet to the reboiler. The reservoirs collected the condensate from each tray via the inlet. One periodic cycle started with vapor alone flowing through the column exchanging mass with the stationary liquid on each tray. The condensate was then collected in the reservoirs corresponding to each tray. When the bottom tray (tray N) was full, all outlet valves were opened to empty all plates into the boiler. Next, the outlet values were closed, and inlet valves were opened to all the reservoirs to empty to their corresponding plates. Lastly, all valves were closed again, and the cycle starts again. Baron and others compared controlled cycling and stepwise periodic distillation. They showed that the two processes have the same asymptotic efficiencies for large values of N while periodic distillation is

10 to 30% more efficient for a finite number of trays [18]. In a follow-up study, they described separating a binary mixture using stepwise periodic operation mode. They proposed a model and simulation algorithm for both controlled and periodic cycling. Through an extensive parametric study, it was concluded again that stepwise periodic operation was superior to ideal controlled cycling [19].

In 1984, Matsubara, Watanbe, and Kurimoto analyzed the work of Cannon and Baron-Wajc in hopes to combine the advantages of both schemes [20]. They successfully developed a composite scheme which could vary from the ideal cannon scheme to the Baron-Wajc scheme by changing various parameters. In a second paper published in 1985, a laboratory-scale periodic distillation column using the idealized Cannon scheme was constructed and experimented with to view energy conservation performance [21]. They used a five-stage column to separate water and methanol. The experimental results showed an 84.6% increase in energy efficiency due to an average vapor flow rate roughly 50-20% lower than in conventional continuous column operation and achieving the same separation.

Around the same time, Thompson and Furzer developed hydrodynamic modeling for liquid holdup in periodically cycled plate columns [22]. Their objective was to predict the holdup distribution in a periodically-cycled column, for a specific set of design and operating conditions. They confirmed their models were satisfactory by experimenting with a 600 mm diameter Perspex column containing four sieve plates. The column was fitted with Time Delay Plates to improve plug flow pressure equalization at the start of the liquid flow period [22]. Szonyi and Furzer then developed a new tray design to increase column performance using a periodic cycle operating method [23]. They ran computer simulations which predicted 200% greater column performance for systems with nonlinear equilibrium curves. They also conducted experiments distilling methanol-water mixtures to verify the computer predictions. Using a single-plate the simulations expectations were confirmed. A new tray design was then implemented in a five-plate insulated mild steel column of 610mm I.D. The new trays consisted of a sieve tray plus inclined surfaces and a vessel in between each sieve tray. The new tray design can be seen in Figure 2.8 below.

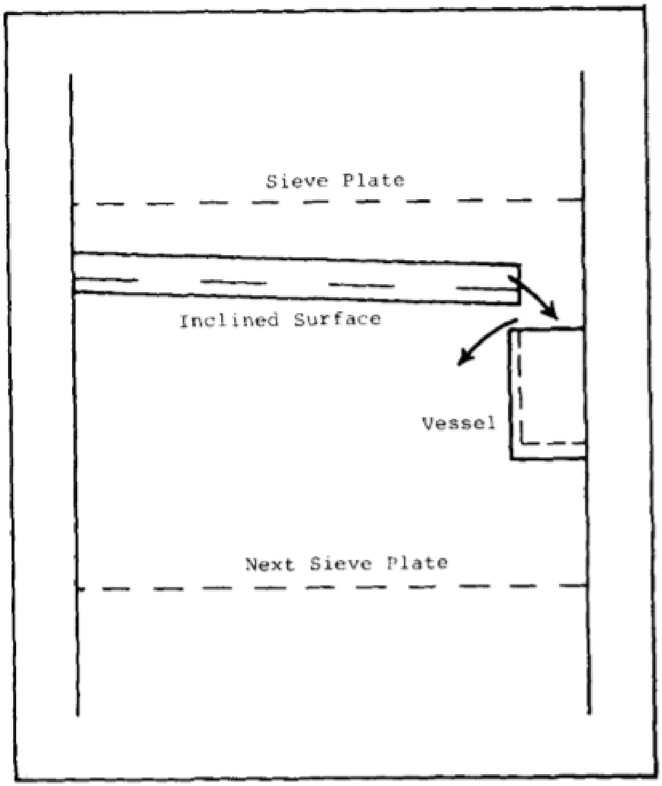

Figure 2.8 New Tray Design for Period Cycling Distillation [23]

The trays collected liquid from the sieve plate above and directed it via the inclined surface to the vessel. In doing so, the liquid in the vessel experienced a time delay before flowing to the sieve plate below. The trays were experimentally effective at obtaining true plug flow but were limited by lack of ventilation and consequently were only able to achieve 140% greater column efficiencies compared to conventional distillation. Szonyi and Furzer recommend further improvements be made by hardware modification [23].

In 1989, Toftegard and Jorgensen developed an integration method for the dynamic simulation of cycled processes. Application of the method was demonstrated on a simulation of controlled cycling distillation. The time to compute the transient was reduced by 90% compared to using a conventional integration method [37].

Finally, in 1997 Sorensen and Prenzler applied cyclic distillation theory to batch distillation [38]. The cycle applied to a batch column was a repeated filling and dumping of the reflux drum. In the beginning of the cycle the reflux drum was filled. Then the column ran under total reflux, and the maximum attainable separation in the column was achieved. During total reflux the light component accumulated in the reflux drum until the column reached equilibrium or steady state. At the end of the cycle, the drum was dumped, and the product was withdrawn. An illustration of each period can be seen below in Figure 2.9.

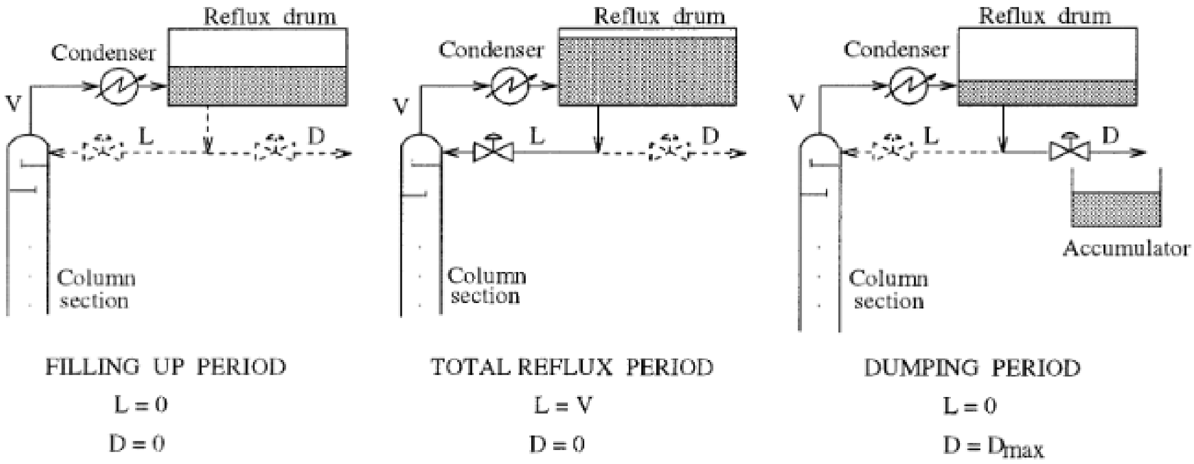

Figure 2.9 The Three Characteristic Periods in the Cyclic Operation of a Regular Batch Distillation Column [39]

Sorensen concluded that the best operating procedure was to adjust the reflux drum holdup online based on measurements of distillate composition as a function of time. If the purity is too low the drum holdup could be reduced and vice versa. A laboratory batch column with 8 sieve trays was used to implement this method [39]. A schematic of the column can be seen below in Figure 2.10.

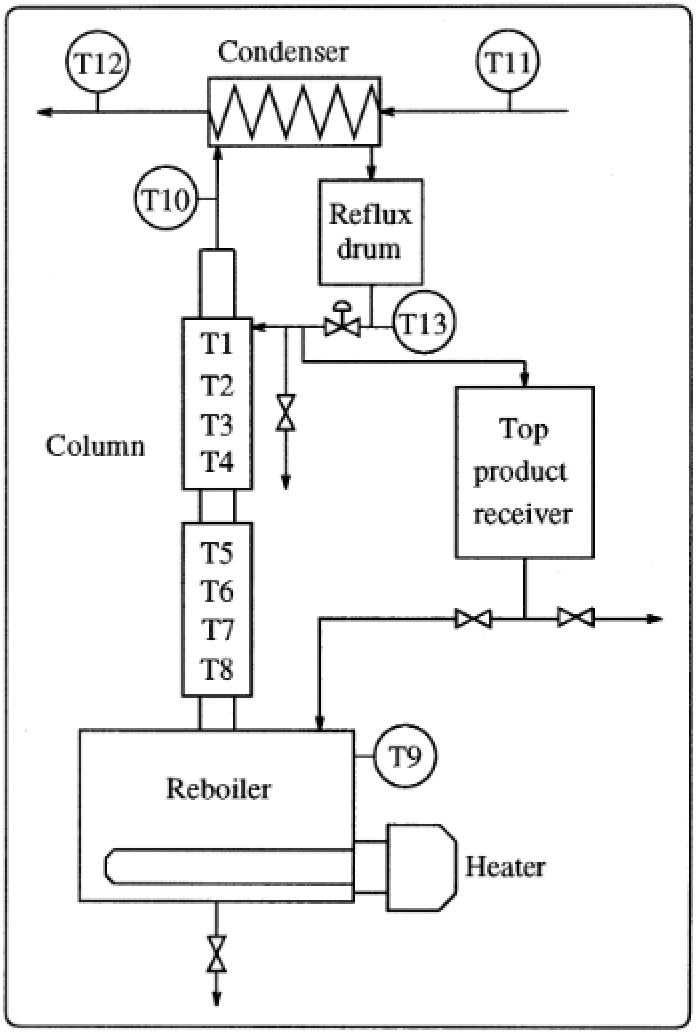

Figure 2.10 Lab Batch Column Used to Apply a Batch Cyclic Operating Theory [39]

The still consisted of a 12 L reboiler, a column with 8 sieve trays, inner diameter of 50 mm, a condenser, a reflux drum with a maximum holdup of 4 L, a reflux valve, and a top product receiver. The reflux valve was a three-way solenoid valve. Samples could be taken through a manual valve as the condensate was returned through the column. In addition, samples of the reboiler and top product were taken. The feed consisted of 10 L of a 25 mol% methanol and 75 mol% water. The required amount of product was 4 L with recovery of methanol at least 75 vol%, which corresponded to 65 mol%. The column started with a cold feed which was heated to the boiling point at roughly 78 ºC. The first cycle started when the mixture began to boil, the reflux drum began to fill, and temperatures in the column increased. Once the drum was filled to a desired level, reflux back to the column started, and the temperatures in the column started to decrease. This was the beginning of the second total reflux period. Once the temperatures in the column stabilized, steady state was achieved which happened after about 95 minutes of operation. The reflux drum was then dumped to the product receiver for a duration of 1 min. A new cycle was then started, and the previous procedure was repeated for another two cycles. At the end of 305 minutes of operation, 68mol% methanol was achieved in the final product which was within the specifications. The policy was found to be easy to implement with the only interaction being the dumping of the reflux drum. The main difficulty was determining the end of the total reflux period which was chosen to be when the temperatures in the column did not change more than 0.1 ºC within in a 5 min period [39].

In 2000, Bausa and Tsatsaronis studied the optimal profiles for all important control variables in continuous cyclic distillation systems [24]. These variables included the flow rates of feed, products, reflux and vapor. They studied two examples. In the first, an ideal ternary mixture was separated into two fractions. In the second, the same mixture was separated into three fractions using a column with a side stream. The optimal control problem was formulated and solved using the software Optimal Control Code Generator for Maple (OCOMA). In the first example, the energy demand of a column with 16 trays for separating a three-component mixture operating at 22.7% higher than minimum energy demand, was reduced by 4.2%. The study showed that the possible energy savings were higher for columns operating at considerable higher energy demands.

The second example was the first study on a column with a side stream. The study showed that the potential energy-savings can be reduced by approximately 48%. Lastly, the authors concluded that the inclusion of oscillations in the optimal control profiles can be extended for the batch distillation and could lead to large energy savings [24].

In 2012, Flodman and Timm studied batch distillation employing cyclic rectification and stripping operations. The authors experimented with three modes of operation: (1) a conventional batch still with a fractionation column configured for rectification, (2) an inverted batch still with the column configured for stripping and (3) an operating policy where the column is sequentially used for batch rectification and stripping. The aim for the third mode was to demonstrate a mode that potentially could reduce operating costs by maintaining high product rates with fluids having modest differences in volatilities. The policy was implemented on an educational batch rectifying/stripping still equipped with a total condenser, partial reboiler, and six, 3-inch diameter sieve trays. The control diagram for batch rectification is illustrated below in Figure 2.11.

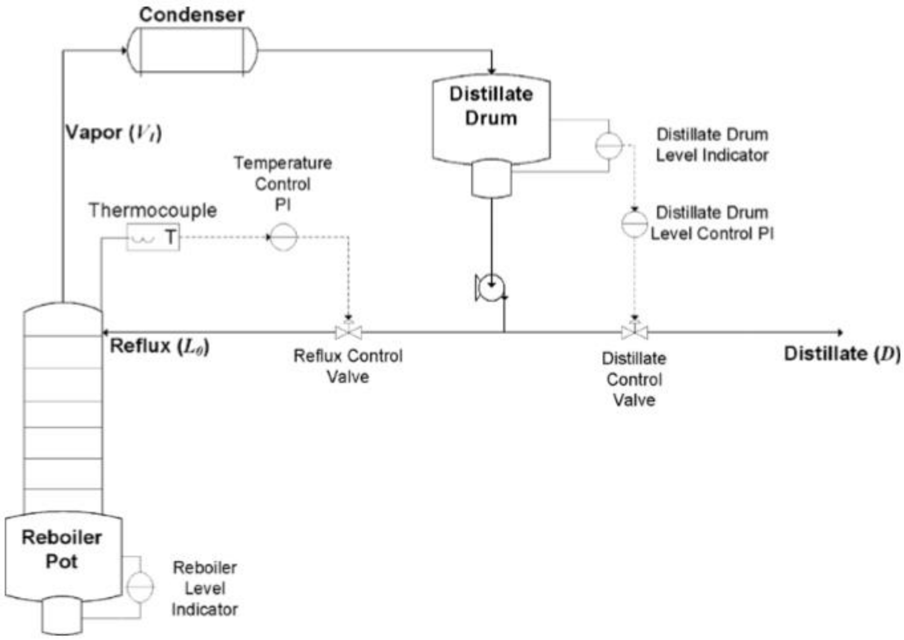

Figure 2.11 Batch Rectification Control Diagram [25]

The control diagram for batch stripping is illustrated below in Figure 1.12.

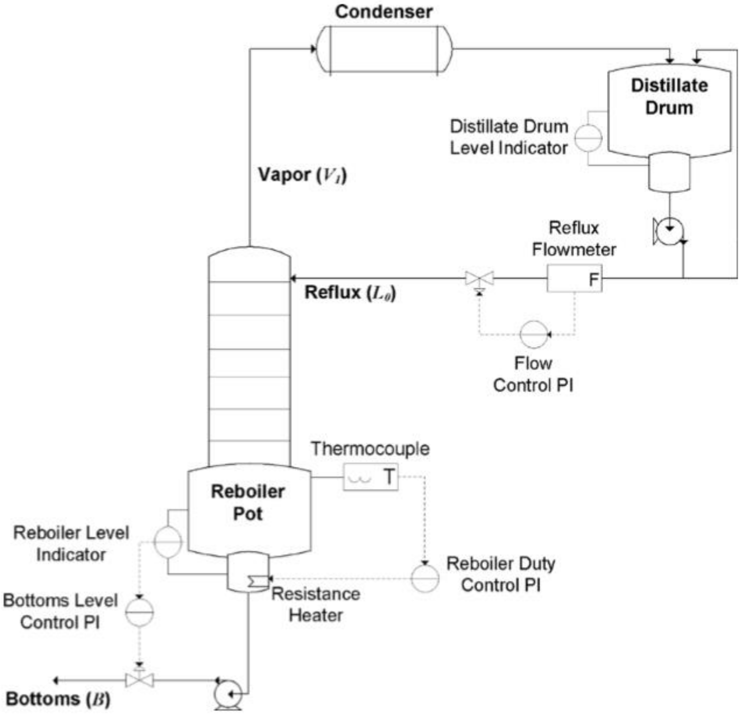

Figure 2.12 Batch Stripping Control Diagram [25]

Conventional batch rectification and inverted batch stripping was used to promote high product flow rates for a binary fractionation. While rectifying, the light component was removed as distillate, concentrating the heavy component in the reboiler. As the distillate decreased with time, the still was then switched to stripping mode. The heavy component was removed as bottoms product, concentrating the light component in the distillate drum. For startup and for liquid transfer, tubing allowed the bottoms to be pumped to the distillate drum, or the distillate to be transferred to the reboiler. The mode was not optimized; however, they demonstrated energy and time savings compared to conventional batch or inverted batch distillation alone. The advantages of this cyclic batch operation were the simultaneous concentration for both the light and heavy components, as well as the capability of fractionating nearly the entire contents of the initial charge. Lastly, the authors suggested that a minimal capital investment would be required to convert a conventional batch still to be capable of this type of cyclic operation [25].

Up to this point, most of the modeling done for cyclic distillation involved an assumption of a linear equilibrium relationship. Lita, Bilde, and Kiss filled this gap in 2012 by modeling the design and control of cyclic distillation systems for the general case of nonlinear equilibrium [26]. The authors developed a complete model and an innovative graphical method similar to the McCabe-Thiele diagram, as well as demonstrated the controllability of cyclic distillation columns. Through their study, they concluded that the energy requirements for cyclic distillation are greatly reduced especially for high purity products. Moreover, the number of trays required is reduced by nearly 50% when the same purity is obtained with the same vapor flow rate. The authors also discovered that a minimum vapor-flow rate exists corresponding to an infinite number of trays, as well as the opposite. A minimum number of trays exists with a corresponding infinite vapor flow rate. Lastly, the authors suggested that columns could be easily controlled by adjusting the reflux and the vapor flow rate to sustain required product purities [26].

Finally, in 2012 Maleta and Maleta patented the first official tray to be used for cyclic distillation [27]. They called it a “mass exchange contact device.” The patented tray or contact device works as follows. During the vapor period, the gas phase lifts a movable valve in such a way that the upper plate closes the bottom, opening of the above tray. The vapor getting under the upper plate is allowed through small orifices and enters a barbotage unit while passing through the liquid layer therein. At the end of the vapor period, the valve moves down due to the weight of the liquid on the above tray. The liquid from the barbotage zone on tray 1 passes through the windows and into the liquid (which is limited by a casing) on the lower tray. The overall design of the trays is a combination of bubble trays and sluice chambers under each tray. The liquid can move from one tray to another without mixing of liquids from adjacent trays. A figure of the trays and a complete column set up can be viewed below in Figure 2.13.

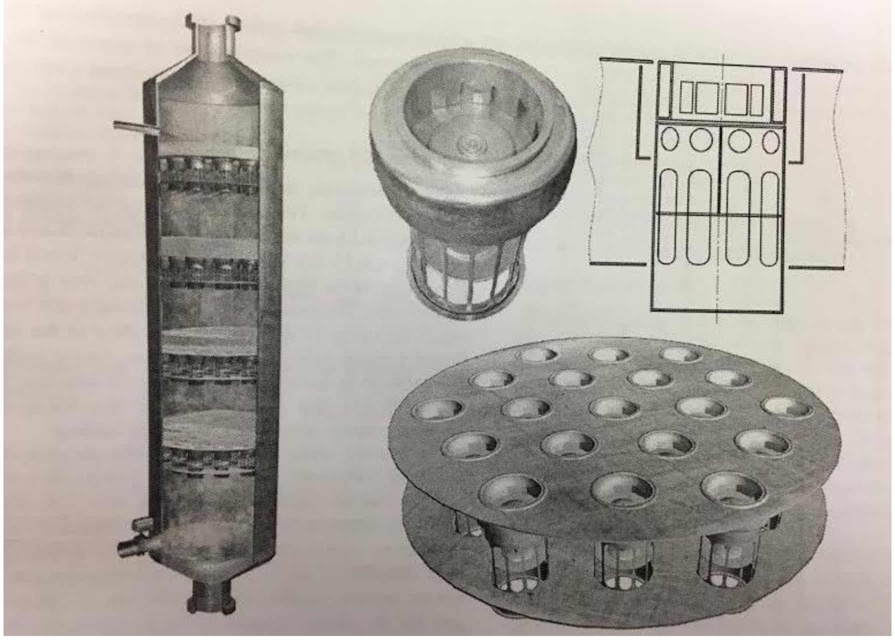

Figure 2.13 Mass Exchange Contact Device and Column [28]

The most recent study on cyclic distillation was published in 2015 [28]. Maleta, Shevchenko, Bedryk, and Kiss reported on the performance of a pilot-scale distillation column for ethanol-water separation operated in cyclic mode. The column had a diameter of 310 mm, height 5500 mm, and had 10 Maleta trays spaced 500 mm apart. The study was set up to feed two separate columns at the same time using a splitter to allow for optimal performance comparison of both operation modes. The study resulted in higher throughput and equipment productivity in the cyclic operated column. With a beer mash feed of 4-12% ethanol, cyclic distillation had a steam usage of 1.4 times less while using 2.6 times fewer trays as compared with classical distillation. The maximum efficiency of the process corresponded to the minimum steam consumption due to a finite number of trays within a given column. The pilot scale distillation column was 100-160% per the perfect mixing theoretical stage model (classis distillation), or 40-90% per the perfect displacement model. The authors concluded that potential applications include biofuel production, organic synthesis, specialty chemicals, gas processing, petrochemicals, and pharmaceuticals.

CHAPTER 3: Modeling Overview

3.1 Batch Distillation

3.1.1 Alembic Distillation – The Rayleigh Equation

The simplest type of distillation is binary distillation using no trays and consequently no rectification, also known as Rayleigh distillation. In the spirits industry, Rayleigh distillation is also known as alembic distillation. The pot is charged with an initial feed which is connected directly to a condenser. As the feed is boiled, the resulting initial vapor will be rich in the most volatile component. As the distillation continues, the concentration of the most volatile component will decrease in the pot. Figure 3.1 is a schematic of simple batch distillation or Rayleigh distillation.

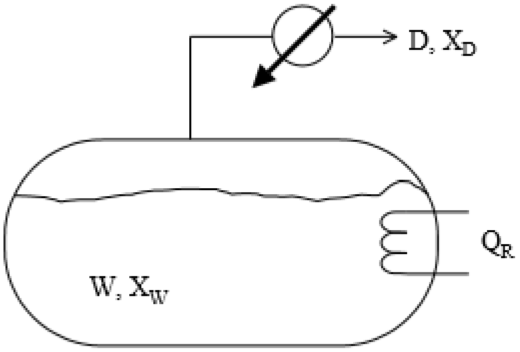

Figure 3.1 Simple Batch Distillation Schematic

Mass balances can be written around the entire system:

$$F = W_{final} + D_{total} \tag{3.1}$$

$$Fx_F = x_{W,final}W_{final} + D_{total}x_{D,avg} \tag{3.2}$$

The feed variables F , x_F are known, as well as the desired final distillate or pot concentration either $x_{W,final}$ or $x_{D,avg}$. Given there are 3 unknowns and 2 equations, a third equation was derived known as the Rayleigh equation. An assumption is applied that the holdup in the accumulator and column are negligible. Using this assumption, a differential mass balance can be applied to the system. The differential amount of a component -dW with concentration xD is removed from the system, resulting in the following differential mass balance:

$$-x_d dW = -d(Wx_W) = -WdX_w - x_W dW \tag{3.3}$$

Rearranging and integration gives:

$$ln\left[\frac{W_{final}}{F}\right] = -\int_{x_{W,final}}^{xF} \frac{dx_W}{x_D - x_W} \tag{3.4}$$

In simple batch distillations, the vapor and liquid are in equilibrium. When a total condenser is used the substitution of $y = x_D$ is used, resulting in:

$$ln\left[\frac{W_{final}}{F}\right] = -\int_{x_{W,final}}^{xF} \frac{dx}{y-x} = \int_{x_{W,final}}^{xF} \frac{dx}{f(x)-x} \tag{3.5}$$

Here x and y are in equilibrium which can be expressed as $y = f(x,p)$. This is the common form of the Rayleigh equation which shows the relationship between total moles remaining in the still and the mole fraction of the more volatile component in the still at any given time.

3.1.2 Multistage Batch Distillation

Multistage distillation refers to distillation involving one or more trays. Within these systems the mole fraction in the distillate, x_D and the mole fraction in the pot, x_W are no longer in equilibrium. Therefore, a relationship between x_D and x_W must be found using stage by stage calculations. Below is a schematic of multistage distillation.

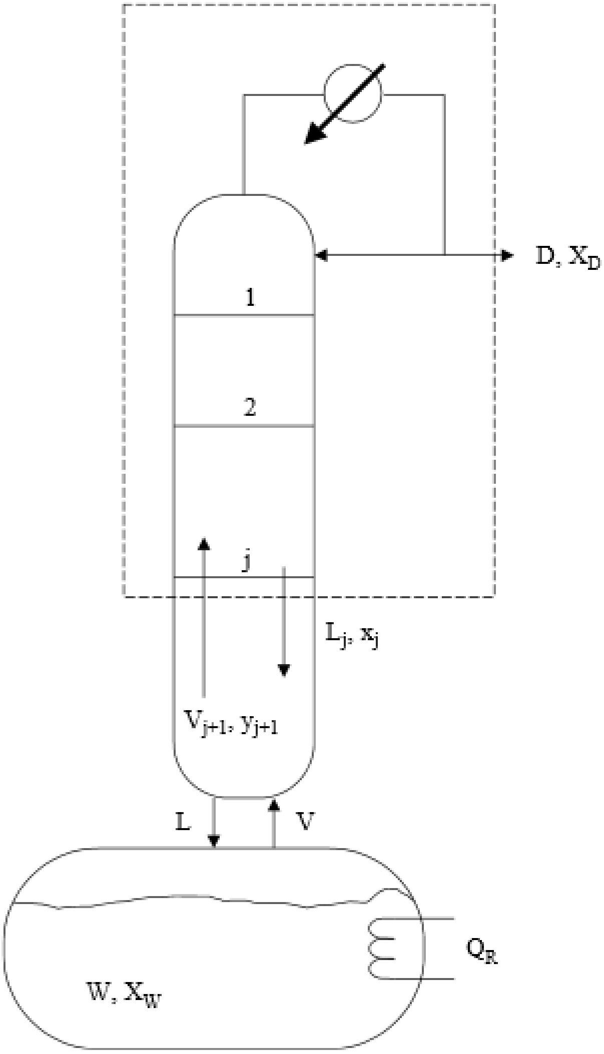

Figure 3.2 Multistage Batch Distillation

An assumption is made that the liquid hold up on each tray, condenser and pot is negligible. Therefore, mass, material and energy balances can be written around stage j and at the top of the column at any time t as follows:

$$V_{j+1} = L_{j+1} + D \tag{3.6}$$

$$V_{j+1}y_{j+1} = L_j x_j + Dx_D \tag{3.7}$$

$$Q_C + V_{j+1}H_{j+1} = L_j h_j + Dh_D \tag{3.8}$$

When constant molal overflow for vapor, liquid and distillate is assumed, the energy balance is no longer needed, and the component balance also known as the operating line becomes:

$$y_{j+1} = \frac{L}{V} x_j + \left(1 - \frac{L}{V}\right) x_D \tag{3.9}$$

The previous equation is a straight line on an equilibrium x-y diagram, with the slope L/V and the intercept with the y=x line at x_D. During batch distillation, either x_D or L/V will need to vary to satisfy the equation, and therefore the operating line. The McCabe-Thiele method for multistage distillation with variable reflux can be seen in Figure 3.3 below.

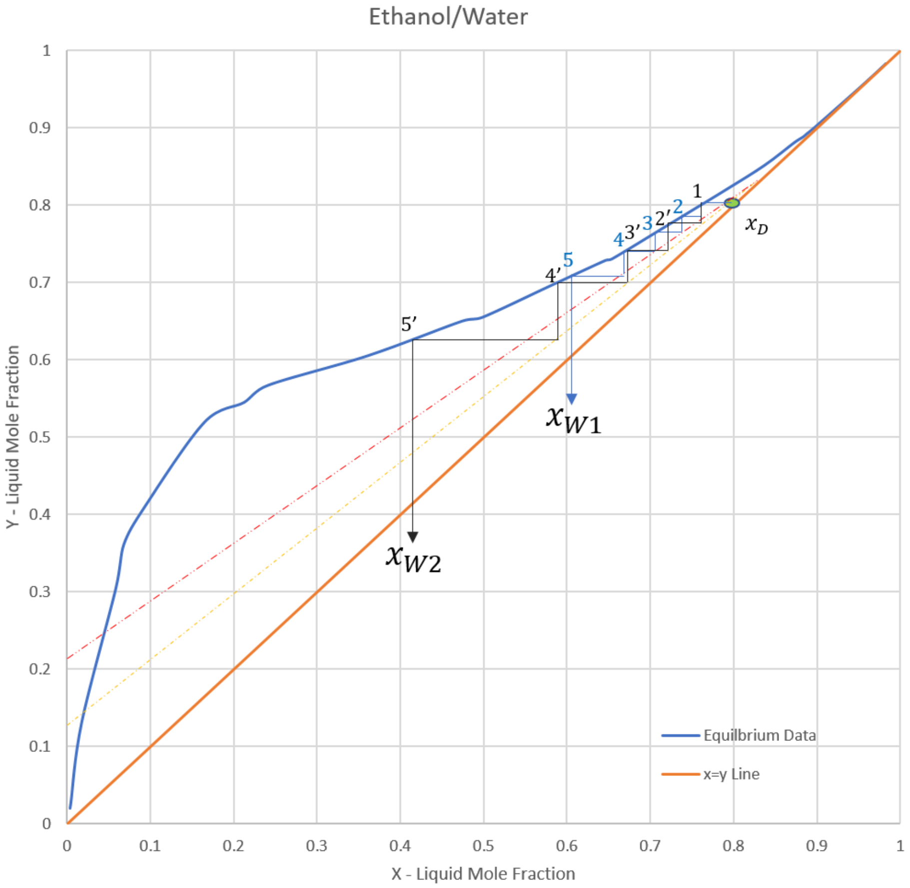

Figure 3.3 McCabe-Thiele Diagram for Multistage Batch Distillation of Ethanol/Water with Varibale Reflux

3.1.3 Stage-By-Stage Methods for Batch Rectification

To design or simulate a multicomponent batch distillation system, stage by stage temperature, flow rates and composition profiles as a function of time are required. The calculations are in depth but can be solved with either of two types of computer-based methods using differential-algebraic equations which can be solved in two ways. The model presented by Boston, is based on the multicomponent batch-rectification operation [42]. The system consists of a partial reboiler (still-pot), a column with N equilibrium stages and a total condenser with a reflux drum. To start the distillation, the feed is charged to the pot and heat is supplied. As the mixture in the pot beings to vaporize it travels upwards through the column. When the vapor leaves stage 1 at the top of the column it is condensed and passes to the reflux drum. At first, a total-reflux condition is established for a steady-state, fixed-overhead vapor flow rate. Starting at t=0, distillate is removed from the reflux drum and accumulated in the receiving tank at a constant molar flow rate, and a reflux ratio is established. The heat-transfer rate to the reboiler is adjusted to maintain the overhead-vapor molar flow rate. The model is broken down into three separate sections and model equations are derived for component material balances, a total material balance and an energy balance. These can be seen respectively below.

For section 1:

$$\frac{d\left(M_0 x_{i,0}\right)}{dt} = V_1 y_{i,1} - L_0 x_{i,0} - D_{x_i 0} \tag{3.10}$$

$$\frac{dM_0}{dt} = V_1 - L_0 - D \tag{3.11}$$

$$Q_0 + \frac{d\left(M_0 h_{L_0}\right)}{dt} = V_1 h_{V1} - (L_0 + D) h_{L_0} \tag{3.12}$$

The derivative terms are accumulations due to holdup, which is assumed to be perfectly mixed. To relate the vapor and liquid mole fractions at Stage 1, we have the phase equilibrium equation:

$$y_{i,1} = K_{i,1} x_{i,1} \tag{3.13}$$

By combining the component material balance with the previous equation, a revised component material balance is derived in terms of liquid-phase compositions. By combining the total material and energy balances, a revised energy balance equation is derived that does not include dM_0/dt. Equations for sections II and III are derived similarly. Below is the resulting model for $t = 0^+$, where i refers to the component, j refers to the stage, and M is the molar liquid holdup.

1. Component mole balances for the overhead-condensing system, column stages, and reboiler, respectively:

$$\frac{dx_{i,0}}{dt} = -\left[\frac{L_0 + D + \frac{dM_0}{dt}}{M_0}\right] x_{i,0} + \left[\frac{V_1 K_{i,1}}{M_0}\right] x_{i,1} \tag{3.14}$$

$$i = 1 \; to \; C$$

$$\frac{dx_{i,j}}{dt} = \left[\frac{L_{j-1}}{M_j}\right] x_{i,j-1} - \left[\frac{L_j + K_{i,j} V_j + \frac{dM_j}{dt}}{M_j}\right] x_{i,j} + \left[\frac{K_{i,j+1} V_{j+1}}{M_j}\right] x_{i,j+1} \tag{3.15}$$

$$i = 1 \; to \; C, j = 1 \; to \; N$$

$$\frac{dx_{i,N+1}}{dt} = \left(\frac{L_N}{M_{N+1}}\right) x_{i,N} - \left[\frac{V_{N+1} K_{i,N+1} + \frac{dM_{N+1}}{dt}}{M_{N+1}}\right] x_{i,N+1} \tag{3.16}$$

$$i = 1 \; to \; C$$

   Where $L_0 = RD$.

2. Total mole balances for overhead-condensing system and column stages, respectively:

$$V_1 = D(R+1) + \frac{dM_0}{dt} \tag{3.17}$$

$$L_j = V_{j+1} + L_{j-1} - V_j - \frac{dM_j}{dt} \tag{3.18}$$

$$j = 1 \; to \; N$$

3. Enthalpy balances around overhead-condensing system, adiabatic column stages, and reboiler, respectively:

$$Q_0 = V_1\left(h_{V_1} - h_{L_0}\right) - M_0 \frac{dh_{L_0}}{dt} \tag{3.19}$$

$$V_{j+1} = \frac{1}{\left(h_{V_{j+1}} - h_{L_j}\right)} \times \left[V_j\left(h_{V_j} - h_{L_j}\right) - L_{j-1}\left(h_{L_{j-1}} - h_{L_j}\right) + M_j \frac{dh_{L_j}}{dt}\right] \tag{3.20}$$

$$j = 1 \; to \; N$$

$$Q_{N+1} = V_{N+1}\left(h_{V_{N+1}} - h_{L_{N+1}}\right) - L_N\left(h_{L_N} - h_{L_{N+1}}\right) + M_{N+1}\left(\frac{dh_{V_{N+1}}}{dt}\right) \tag{3.21}$$

4. Phase equilibrium on the stages and in the reboiler:

$$y_{i,j} = K_{i,j} x_{i,j} \tag{3.22}$$

$$i = 1 \; to \; C, j = 1 \; to \; N+1$$

5. Mole-fractions sums at column stages and in the reboiler:

$$\sum_{i=1}^{C} y_{i,j} = \sum_{i=1}^{C} K_{i,j} x_{i,j} = 1.0 \tag{3.23}$$

$$j = 0 \; to \; N+1$$

6. Molar holdups in the condenser system and on the column stages, based on constant-volume holdups, G_j.

$$M_0 = G_0 \rho_0 \tag{3.24}$$

$$M_j = G_j \rho_j, \quad j = 1 \; to \; N \tag{3.25}$$

Where ρ is liquid molar density.

7. Variation of molar holdup in the reboiler, where M_{N+1}^0 is the initial charge to the reboiler.

$$M_{N+1} = M_{N+1}^0 - \sum_{j=0}^{N} M_j - \int_0^t D \, dt \tag{3.26}$$

The previous described equations make up an initial-value problem for a system of ordinary differential and algebraic equations. The total number of equations is $(2CN + 3C + 4N + 7)$. If variables $N, D, R = \frac{L_0}{D}, M_{N+1}^0$, and all G_j are specified, and if correlations are available for computing liquid densities, vapor and liquid enthalpies, and K-values, the number of unknown variables, distributed as follows, is equal to the number of equations.

Table 3.1 Variables and Total Number of Equations for Multicomponent Batch Distillation

$x_{i,j}$	$CN + 2C$
$y_{i,j}$	$CN + C$
L_j	N
V_j	$N + 1$
T_j	$N + 2$
M_j	$N + 2$
Q_0	1
Q_{N+1}	1
	$2CN + 3C + 4N + 7$

Initial values at $t = 0$ for all the above variables are obtained from steady-state, total reflux calculations which depend on the values of $N, M_{N+1}^0, x_{N+1}^0, G_j$, and V_1. The previous equations in section 1, 2 and 3 include first derivatives of $x_{i,j}, M_j$, and h_{Lj}. With the exception of M_{N+1}, derivatives of the other two variables can be approximated by incremental changes over the previous time step. If the reflux ratio is high, M_{N+1} may also be approximated. This reduces the ODE's to only $C(N+2)$ equations for the component material balances to be integrated in terms of the $x_{i,j}$ dependent variables.

3.1.4 Governing Equations and Thermodynamic Model for System in Study

Applying the previous modeling method provides differential and algebraic equations which will be used to model the system in study. Below is schematic of the column and flows in study.

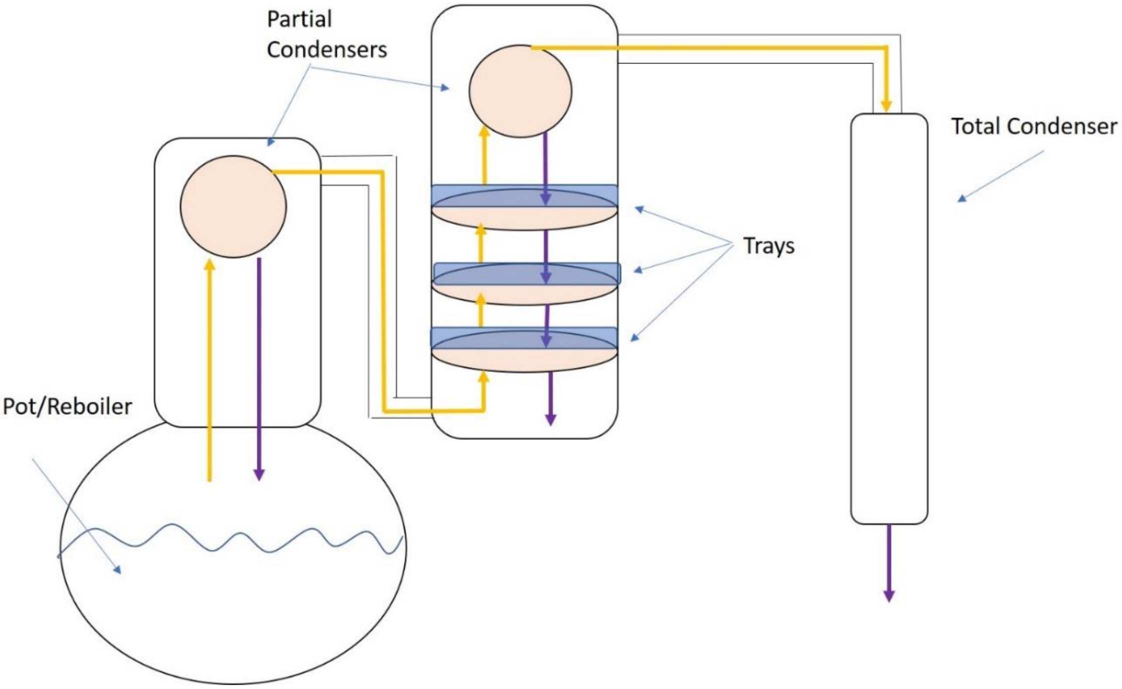

Figure 3.4 Schematic of Cyclic Distillation on Carl Still

The partial condensers are assumed to act like stages and will be modeled as such. The material balance equations for the stages (N=1-5) in the column is:

$$\frac{dx_N}{dt} = \frac{L(x_{N-1} - x_N) + V(y_{N+1} - y_N)}{M_H} \tag{3.27}$$

The material balance for the condenser is:

$$\frac{dx_0}{dt} = \frac{Vy_1}{M_{H0}} - \frac{(L+D)x_0}{M_{H0}} \tag{3.28}$$

The material balance for the reboiler is:

$$\frac{dx_B}{dt} = L(x_5 - x_B) - V(y_B - x_B) \tag{3.29}$$

A solution of water and ethanol is considered as a non-ideal mixture because it presents an azeotrope at 89% mole fraction of ethanol. Therefore, modified Raoult's law was used to determine the vapor mole fraction given a temperature and liquid mole fraction.

$$y_i P = x_i \gamma P_i^{sat} \tag{3.30}$$

Where γ is an activity coefficient that can be calculated by using a specific thermodynamic model. In this study, the NRTL method was the thermodynamic model chosen based on a study which reported that the NRTL method fit experimental data accurately to an RMS value of 0.403% [41]. It was important to pick a model that accurately modeled the azeotrope between water and ethanol. The NRTL activity model is calculated using parameters G_{ij} and τ_{ij}:

$$ln(\Upsilon_1) = x_2^2 * \left(\tau_{21} * \left(\frac{G_{21}}{x_1 + x_2 * G_{21}}\right)^2 + \tau_{12} * \frac{G_{12}}{(x_2 + x_1 * G_{12})^2}\right) \tag{3.31}$$

$$ln(\Upsilon_1) = x_1^2 * \left(\tau_{12} * \left(\frac{G_{12}}{x_2 + x_1 * G_{12}}\right)^2 + \tau_{21} * \frac{G_{21}}{(x_1 + x_2 * G_{21})^2}\right) \tag{3.32}$$

Where $G_{ij} = \exp(-0.3 * \tau_{ij}), \tau_{ij} = \frac{A_{ij}}{RT}$

The parameters A_{12} and A_{21} were found within literature to be -633 and 5823.1, respectively [41]. To determine the vapor pressure the Antoine equation was used:

$$log_{10} P_{sat} = A - \frac{B}{T+C} \tag{3.33}$$

Where pressure is in mmHg and temperature is in is in °C. Finally, the total pressure was calculated as the sum of the partial pressures using the follow equation:

$$P = x_1 \Upsilon_1 P_1^{sat} + x_2 \Upsilon_2 P_2^{sat} \tag{3.34}$$

3.2 Cyclic Continuous Distillation Modeling Approach

As previously stated, cyclic column operation consists of two parts, a vapor flow period, and a liquid flow period. Since the operation is two separate parts, the mathematical analysis must be done in two parts as well. Sections 3.2.1 – 3.2.5 describe the method first published by Lita, Bilde and Kiss for the modeling of continuous cyclic distillation systems and comparison against conventional distillation.

3.2.1 Assumptions

The current accepted modeling approach is derived using the following assumptions:

- Binary (mixture) distillation
- Ideal stages (vapor-liquid equilibrium is reached)
- Equal heat of vaporization (constant molar holdup and vapor flow rate)
- Perfect mixing on each stage
- Negligible vapor holdup
- Saturated liquid feed

3.2.2 Operational Constraints

From the condenser and reboiler mass balance, for one operating cycle:

$$V *\ t_{vap} = D + L \tag{3.35}$$

$$L + F = V *\ t_{vap} + B \tag{3.36}$$

the condition follows that:

$$L < V * t_{vap} < L + F \tag{3.37}$$

3.2.3 Model of Vapor Flow Period

The model for the vapor flow period involves using equations to describe the evolution in time of stage holdup and composition.

$$Condenser\text{:}\ \ \frac{dM_{1\,V*t_{vap}=D+L}}{dt} = V;\ M_1\frac{dx_1}{dt} = V(y_2 - x_1) \tag{3.38}$$

$$Trays\text{:}\ \ \frac{dM_k}{dt} = 0;\ M_k\frac{dx_k}{dt} = V(y_{k+1} - y_k) \tag{3.39}$$

$$Reboiler\text{:}\ \ \frac{dM_{NT}}{dt} = -V; M_{NT}\frac{dx_{NT}}{dt} = V(x_{NT} - y_{NT}) \tag{3.40}$$

$$Initial\ conditions\text{:}\ at\ t = 0, (M, x) = \left(M^{(L)}, x^{(L)}\right) \tag{3.41}$$

Integration of these equations from $t = 0$ to $t = t_{vap}$ gives the state of the system at the end of the vapor flow period, $\left(M^{(V)}, x^{(V)}\right)$ [26].

3.2.4 Model of Liquid Flow Period

The model for the liquid flow period uses the following equations:

$$Condenser\text{:}\ \ M_1^{(L)} = M_1^{(V)} - D - L;\ x_1^{(L)} = x_1^{(V)} \tag{3.42}$$

$$Trays, rectifying\ section\text{:}\ \ M_k^{(L)} = L;\ x_k^{(L)} = x_{k-1}^{(V)} \tag{3.43}$$

$$Feed\ tray\colon M_{NF+1}^{(L)} = L + F;\ x_{NF+1}^{(L)} = \frac{Lx_{NF}^{(V)} + Fx_F}{(L+F)} \tag{3.44}$$

$$Reboiler\colon\ M_{NT}^{(L)} = M_{NT}^{(V)} - B + M_{NT-1}^{(V)};\ x_{NT}^{(L)} = \frac{\left(M_{NT}^{(V)} - B\right)x_{NT}^{(V)} + M_{NT-1}^{(V)}x_{NT-1}^{(V)}}{M_{NT}^{(L)}} \tag{3.45}$$

3.2.5 Solution Method

For the solution, the previous equations are written in condensed form, where $\Phi^{(V)}$ and $\Phi^{(L)}$ are mappings which relate the state at the beginning and at the end of the liquid and vapor flow periods, respectively:

$$\left(M^{(V)}, x^{(V)}\right) = \Phi^{(V)}(M, x) \tag{3.46}$$

$$\left(M^{(L)}, x^{(L)}\right) = \Phi^{(L)}(M, x) \tag{3.47}$$

Which implies the following condition:

$$\left(M^{(L)}, x^{(L)}\right) = \Phi^{(L)} \circ \Phi^{(V)}\left(M^{(L)}, x^{(L)}\right) \tag{3.48}$$

A solution to the above equation can be found by considering an initial state and applying relationships for $\left(M^{(V)}, x^{(V)}\right)$ and $\left(M^{(L)}, x^{(L)}\right)$ until the difference between two iterations becomes small. Alternatively, the convergence of the iterations can also be done by applying numerical methods and can be solved in MATLAB © [26]. Below is a graphically representation of the energy requirements in cyclic distillation compared to classic distillation.

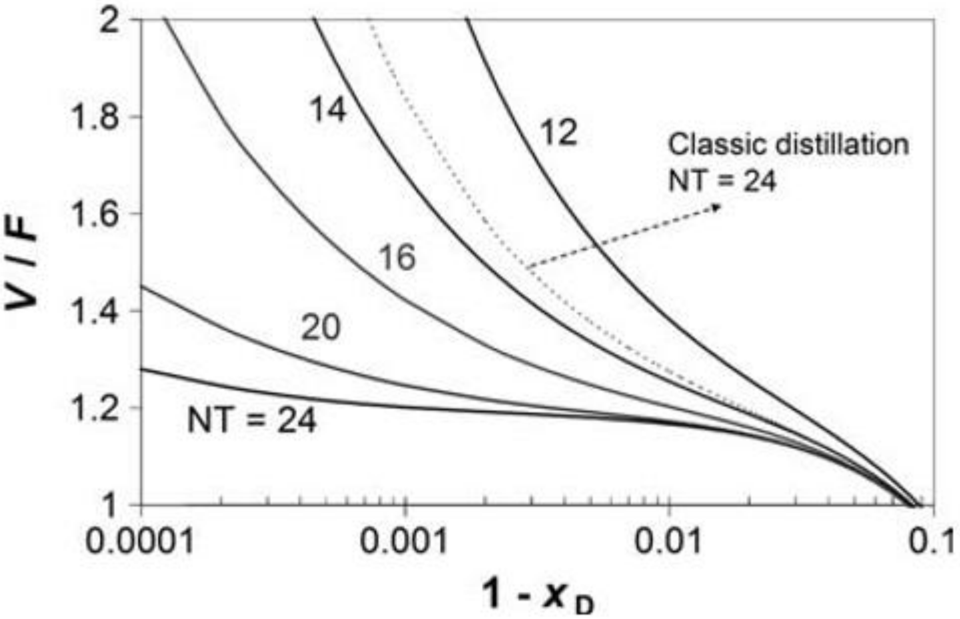

Figure 3.5 Comparison of Energy Requirements in Cyclic Distillation versus Conventional Distillation [26]

The vapor/feed ratio is comparable to the energy requirements of a distillation column. The higher the ratio, the more energy required. $1 - x_D$ represents the product purity. The energy requirements are greatly reduced and is reduced even greater when the product purity is higher.

3.3 Design of Cyclic Distillation

3.3.1 Design Methodology

First given the feed (F, x_F) and the required performance (x_D, x_B) the mass balance over one operating cycle is used to find the product flow rates (D, B).

$$F = D + B \tag{3.49}$$

$$F * x_F = D * x_D + B * x_B \tag{3.50}$$

Next the vapor flow rate $V$and the duration of the vapor-flow period, t_{vap}, are specified. The liquid transferred from the condenser to the top tray can be calculated.

$$L = V * t_{vap} - D \tag{3.51}$$

For tray holdups in rectifying section $M_k = L$ and for the stripping section we have $M_k = L + F$.

It is important to check hydrodynamics of the column including, column diameter, vapor velocity and pressure drop.

To determine the state of the reboiler at the end of the vapor-flow period the following needs to be specified:

- Holdup, $M_{NT}(t_{vap})$. Although the results of this design procedure are independent of this value it is still necessary to specify.
- Composition, $x_{NT}(t_{vap}) = x_B$. At the end of the vapor-flow period, the reboiler is richer in the heavy component and therefore is the time to remove the bottom product if possible.

To find the holdup and reboiler composition at the beginning of the vapor-flow period, $M_{NT}(0), x_{NT}(0)$, equations (3.32) are integrated from $t = t_{vap}$ to $t = 0$. Next determine the state of the last tray (stage NT-1) at the end of the vapor flow period, using the mass balance for the liquid flow period:

$$M_{NT-1}(t_{vap}) = L + F \tag{3.52}$$

$$x_{NT-1}(t_{vap}) = \frac{M_{NT}(0) * x_{NT}(0) - \left(M_{NT}(t_{vap}) - B\right) * x_{NT}(t_{vap})}{L + F} \tag{3.53}$$

Next find the state of the reboiler and last tray at the beginning of the vapor flow period by integrating equations 3.30 and 3.31 from $t = t_{vap}\ to\ t = 0$. Next add one more tray, whose state at the end of the vapor-flow period is

$$M_{NT-2}(t_{vap}) = L + F \tag{3.54}$$

$$x_{NT-2}(t_{vap}) = x_{NT-1}(0) \tag{3.55}$$

And integrate the resulting set of equations from $t = t_{vap}\ to\ t = 0$. Repeat until the feed composition is reached for the tray NF+1. Then find the state of the feed tray at the end of the vapor flow period.

$$M_{NF}(t_{vap}) = L \tag{3.56}$$

$$x_{NF}(t_{vap}) = \frac{M_{NF+1} * x_{NF+1}(0) - F * x_F}{M_{NF}} \tag{3.57}$$

And integrate from $t = t_{vap}\ to\ t = 0$. Similarly, repeat addition of one tray, finding its state at the end of the vapor-flow period and integration of the resulting equations until the distillate composition is reached. The previously discussed process is illustrated in Figure 3.5 below.

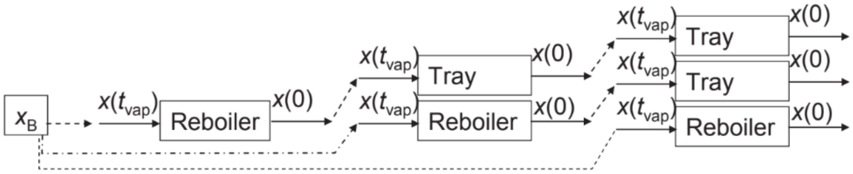

Figure 3.6 Cyclic Distillation Design Approach

3.4 Batch Cyclic Distillation Dynamic Analysis

The basis of the dynamic analysis of batch cyclic distillation comes from McWhirter's dissertation from the 1960's. The equations developed were written for a continuously fed batch system. Here the equations are re-written to apply to batch distillation where necessary. Below is a schematic of the distillation column used for cyclic operation in the lab. As seen in Figure 3.6 below, in terms of dynamic modeling partial condensers act similarly to stages therefore the partial condensers are modeled as such. The following sections will provide the equations written to model the system in study.

3.4.2 Vapor Flow Period

During the vapor flow period, only vapor flows up through the partial condensers and the column and ideally no liquid flows down the column. The column liquid hold up is trapped and held on the stages in the column during this vapor flow period. A detailed analysis will be made for stage N. The material balance for the most volatile component on stage N is written as:

$$\frac{d(U_N Y_N)}{dt} + \frac{d(W_N X_N)}{dt} = V_{N+1} Y_{N+1} - V_N Y_N \qquad (3.58)$$

Where,

$U_N = vapor\ hold\ up\ on\ stage\ N, moles$

$W_N = liquid\ holdup\ on\ stage\ N, moles$

$Y_N = average\ vapor\ mole\ fraction\ of\ more\ volatile\ component\ leaving\ stage\ N$

$X_N = average\ liquid\ mole\ fraction\ of\ more\ volatile\ component\ on\ stage\ N$

$V_N = vapor\ flow\ rate\ from\ stage\ N, moles/min$

$t = time\ in\ mins$

The energy balance relationship is then:

$$\frac{d(U_N H_N)}{dt} + \frac{d(W_N h_N)}{dt} = V_{N+1} H_{N+1} - V_N H_N - Q_N \qquad (3.59)$$

Where,

$H_N = average\ enthalpy\ of\ vapor\ leaving\ stage\ N, kJ\ \ per\ mole$

$h_N = average\ enthalpy\ of\ liquid\ on\ stage\ N, kJ\ per\ mole$

$Q_N = heat\ loss\ from\ stage\ N, kJ\ per\ hour$

The average enthalpies are a function of the liquid mole fraction and temperature on stage N. For simplicity, the difference between enthalpies $(H_{N+1} - h_N)$ is assumed independent of composition. This allows for the assumption of constant value of h_N on each stage. Also, the vapor hold up is assumed negligible in comparison to liquid hold up. With these assumptions the energy balance becomes:

$$\frac{dW_N}{dt} = 0 \tag{3.60}$$

The liquid holdup per stage during the vapor flow period is constant and equal for all stages. Using this and the previous assumptions, the material balance becomes:

$$\frac{dX_N}{dt} = \frac{V(Y_{N+1} - Y_N)}{W} \tag{3.61}$$

The previous equation completely describes the material balance and must be written for each stage in the column of study and all must be satisfied.

The reflux to the column is assumed to be cycled in phase with the liquid flow period. Also, the condenser is assumed to have a holdup equal to the amount of vapor introduced into it during the vapor flow period. Consequently, the entire contents of the condenser will be returned as reflux or withdrawn as distillate product during each cycle.

The overall material balance expression for the reboiler is:

$$\frac{dW_B}{dt} + \frac{dU_B}{dt} = -V \tag{3.62}$$

Where,

$W_B = reboiler\ liquid\ holdup, pound\ moles$

$U_B = reboiler\ vapor\ holdup, pound\ moles$

$V = constant\ molar\ vapor\ rate, pound\ moles\ per\ hour$

The contents of the reboiler is assumed to be perfectly mixed. The material balance on the most volatile component is:

$$\frac{d(W_B x_B)}{dt} + \frac{d(U_B Y_B)}{dt} = -VY_B \tag{3.63}$$

Similarly, the vapor hold up is considered negligible in comparison to the liquid hold up. Using this assumption and substituting the material balance becomes:

$$\frac{dx_B}{dt} = \frac{-V}{w_B}(Y_B - x_B) \tag{3.64}$$

Adding equations for the reboiler to the previous stage equations completely models the vapor flow period for the system in study.

3.4.3 Liquid Flow Period

During the liquid flow period ideally only liquid flows down the column to the preceding tray and there is no vapor traveling up the column. Since the relative velocity between the phases will be almost zero and the vapor hold up is essentially negligible, no mass transfer will be assumed to take place during the liquid flow period. Consequently, time is not a factor in any calculations for the liquid flow period. Plug flow of the liquid from stage to stage down the column is assumed.

The volume of liquid that flows from stage to stage is assumed equal for all stages and constant for all liquid flow periods. The following equation gives a material balance for stage N:

$$x_N^{C+1} = \frac{O_L x_{N-1}^C}{W} + \frac{(W - O_L)}{W} x_N^C \tag{3.65}$$

Where,

O_L

$= quantity\ of\ liquid\ which\ flows\ from\ stage\ to\ stage\ during\ the\ liquid\ flow\ period, lb\ moles$

$$c = cycle\ number$$

The material balance calculates the value of the concentration of the liquid on stage N at the start of a new vapor flow period from the values at the end of the preceding vapor flow period. To simplify Equation 3.60, a new quantity is introduced, $\emptyset$, which is the ratio of the quantity of liquid which flows during the liquid flow period to the liquid holdup per stage. Using this variable, Equation 3.60 becomes:

$$x_N^{C+1} = \emptyset x_{N-1}^C + (1 - \emptyset) x_N^C \tag{3.66}$$

The previous equation is valid for values of $\emptyset$ from zero to one, but when values are larger than one the following will apply:

For $1.0 \leq \emptyset \leq 2.0$

$$x_N^{C+1} = (\emptyset - 1.0) x_{N-2}^C + (2.0 - \emptyset) x_{N-1}^C \tag{3.67}$$

For $2.0 \leq \emptyset \leq 3.0$

$$x_N^{C+1} = (\emptyset - 2.0) x_{N-3}^C + (3.0 - \emptyset) x_{N-2}^C \tag{3.68}$$

During the liquid flow period, no vapor leaves the reboiler, but reflux from the partial condenser is re-introduced back into the reboiler. The average composition of the reflux from the partial condenser depends on the value of $\emptyset$.

For $0.0 \leq \emptyset \leq 1.0$

$$x_L = x_{NOS} \tag{3.69}$$

Where $x_L = average\ composition\ of\ reflux\ from\ bottom\ of\ column$

$x_{NOS} = average\ composition\ of\ liquid\ on\ bottom\ stage\ at\ end\ of\ vapor\ flow\ period$

For $1.0 \leq \emptyset \leq 2.0$

$$x_L = \frac{(\emptyset - 1.0)x_{NOS-1}}{\emptyset} + \frac{x_{NOS}}{\emptyset} \tag{3.70}$$

For $2.0 \leq \emptyset \leq 3.0$

$$x_L = \frac{(\emptyset - 2.0)x_{NOS-2}}{\emptyset} + \frac{x_{NOS-1} + x_{NOS}}{\emptyset} \tag{3.71}$$

The material balance for the most volatile component for the reboiler during the liquid flow period is given below:

$$x_B^{C+1} = \frac{W_B x_B^C}{W_{BI}} + \frac{\emptyset(W)(x_L)}{W_{BI}} \tag{3.72}$$

Where $W_{BI} = initial\ reboiler\ holdup\ at\ start\ of\ vapor\ flow\ period, pound\ moles$

$x_B^{C+1} = reboiler\ composition\ at\ start\ of\ next\ vapor\ flow\ period$

Equations 3.53 through 3.65 describe the operation of the column throughout one entire cycle. The equations with correct subscripts can be found Appendix B.

3.4.4 Solution Method

Like how the continuous equations are solved, each cycle requires the end point of the previous cycle. Therefore, to start the vapor flow period equations are used to solve with initial conditions for the state of the system at the end of vapor flow period 1. Those values are then used to solve for the state of the system at the end of liquid flow period 1. Those numbers are then used to solve for the state of the system at the end of vapor flow period 2. This process continues until the final condenser ABV drops below 10%. The MATLAB script written for the solution and modeling of cyclic batch distillation can be found in Appendix B. The results can be found in Appendix B and Chapter 5, Results.

CHAPTER 4: Methods

4.1 Materials and Equipment

Raw materials used for this research included: fermented apple cider, previously distilled apple brandy, standard solutions, and cleaning agents. Equipment used for this research included: 165 L Carl batch still, leur lock syringes, copper tubing, centrifugal pump, GC-2010 gas chromatograph, plastic GC vials, storage tanks, hydrometer, and miscellaneous glassware.

4.1.1 Manufacturing Equipment

To monitor the tray composition during distillation, four site glasses on the distillation column where replaced with a new piece of glass made of borosilicate, which had a precut hole to allow for a sampling apparatus to be installed. Borosilicate was chosen due to its high melting point and non-reactivity with the compounds being distilled. The sampling apparatus consisted of a luer-lock system with copper tubing going to the column and resting on the tray. Outside of the column a syringe allowed a 1 mL sample to be extracted from the tray. A schematic of the self-manufactured sampling equipment can be seen below.

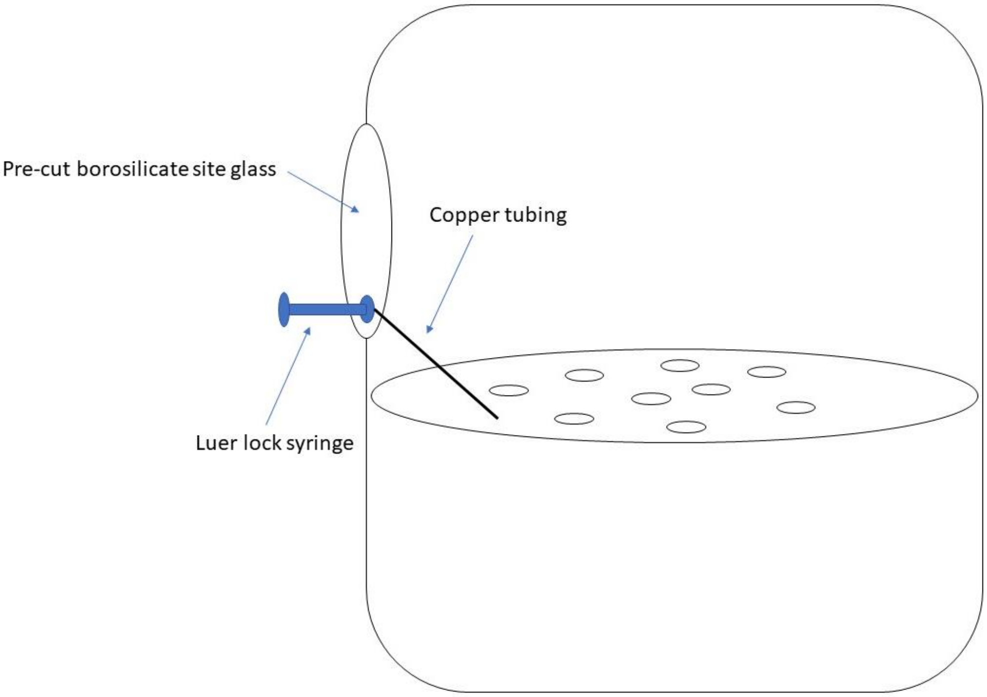

Figure 4.1 Manufactured Sampling Apparatus

In addition to the fabrication of sample ports, an extra valve between the steam condensate outlet to the drain was installed to allow for the collection of the condensate. This allowed for the condensate to be collected into buckets, transported to a larger container and measured. The volume was then converted to pounds of steam and reported as pounds of steam in the data.

4.2 Measurement Methods

4.2.1 GC Method

A gas chromatograph was used to analyze the samples withdrawn from the still. Below is a list of compounds that were of importance and their respective boiling points.

Table 4.1 Detected Compounds [44]

Compound	Boiling Point (°C)	Retention TIME (MIN)
Acetaldehyde	20.8	1.532
Acetone	56.2	2.194
Ethyl Acetate	77.0	2.913
Methanol	64.7	3.091
Isopropanol	82.6	3.509
Ethanol	78.0	3.615
Propanol	97.0	5.184
Isobutanol	108	6.132
Butanol	117.7	6.944
Isoamyl Alcohol	132.0	7.887

The above compounds were selected based on previous knowledge of the compounds metabolized by common yeast strains used in fermented beverage production and are volatile enough to come through to the final product in distilled alcoholic beverages. Although there are many other compounds that yeast produce including aldehydes, ketones, and esters, the compounds chosen to have the most impact on the flavor and aroma profile of sprits. Sample chromatograph results can be seen in Figure C.1 in Appendix C.

Standards with four different levels of concentrations ranging from 0.1 – 10 g/L were made to form a method for the GC-2010 gas chromatograph. The column used was a 30 m Stabliwax column with 0.32 mm ID and film thickness of 0.50 um. The oven temperature started at 35 °C and ramping up to 100 °C over a period of 8.5 minutes. The carrier gas used was helium with a linear velocity of 45 cm/sec and a split ratio of 50. The auto injector AOC-20i was paired with the GC to analyze 12 samples in one batch.

4.3 Research Design

Multiple distillations were carried out to understand how cyclic distillation compares to conventional distillation in the 165 L batch still. Table 4.2 shows all distillations performed and the operating conditions associated with each distillation including: the duration of the liquid and vapor flow periods during cyclic operation, the initial volume and ABV, and whether reflux to the partial condensers was being utilized or not.

Table 4.2 Distillation Conditions

Distillation #	Operation Type (Vapor, Liquid)	Initial Volume (gals)	Initial ABV	Reflux to Partial Condensers
1	Conventional	47	35%	Off
2	Conventional	48	25%	Off
3	Conventional	49	40%	Off
4	Cyclic (9 min, 3 min)	47	36%	Off
5	Cyclic (6 min, 3 min)	45	38%	Off
6	Cyclic (3 min, 3 min)	39	36%	Off
7	Conventional	25	8%	Off
8	Cyclic (9 min, 3 min)	25	8%	Off
9	Cyclic (6 min, 3 min)	25	7.4%	Off
10	Cyclic (4 min, 3 min)	25	6.3%	Off
11	Conventional	36	19%	On
12	Conventional	36	27%	Off
13	Cyclic (6 min, 3 min) Tray by Tray	36	28%	On
14	Cyclic (6 min, 3min) Tray by Tray	33	27%	On
15	Cyclic (6 min, 3min) Tray by Tray	33	30%	On

4.4 Procedures

To begin a distillation, the pot was filled with the intended initial volume. The door was then shut tightly, and steam valves opened. The condensate valve to the steam jacket was then opened to release any water remaining in the jacket from the previous distillation and then closed. In the beginning of every distillation, steam was supplied to the steam jacket until the first volume of distillate was collected. The distillate flowrate and pressure reading were monitored throughout the distillation throughout each distillation. If the flowrate dropped below average levels, the steam was increased using the gate valve to keep a relatively constant distillate flowrate. During conventional operation, steam was supplied to the column for the entire duration of the distillation, until the hydrometer read below 10% ABV.

During cyclic distillation, the first vapor flow period started when the first distillate was collected. After the appropriate vapor flow time, the main steam valve was closed. This started the liquid flow period. During the liquid flow period, the tray valves were opened to allow the liquid to flow to the tray below. The bottom tray was first opened for around 10-15 seconds, until the stream coming down from the tray nearly stopped. Next, the valve was closed, and the middle tray was opened. Lastly, the top tray valve was opened to allow the contents to fall to the middle tray and then closed again. The distillation continued until the hydrometer read under 10% ABV at the beginning of a vapor flow period.

4.5 Data Collection and Analysis

Throughout each distillation temperature, pressure, distillate flow rate, and total volume collected were taken at time increments roughly 10 minutes apart. Samples from each tray, the bottom of the column, and of the distillate were taken roughly 10 minutes apart and taken during each vapor period for cyclic operation. The samples were placed directly into GC vials and labeled. Steam condensate was collected into buckets and stored in a large storage tank to record overall volume after the distillation was complete. The distillate flow rate was measured using a stopwatch and graduated cylinder, collected distillate over a 10 second period and recorded as mL/s. The distillate was collected into volume incremented containers. After every distillation was complete samples were taken of the final contents of the pot and of the overall distillate, as well as of cuts if they were taken.

After the distillation was complete, each sample was run through the GC-2010 gas chromatograph to analyze the concentration of each component in each sample. The results can be seen in Chapter 5.

CHAPTER 5: Results

5.1 Results

A complete set of graphical results for every distillation and every compound studied can be found in Appendix A. Within this section are key results which will be discussed and referred to in the discussion section

5.1.1 All Distillation Results

Table 5.1 is a summary table of all the distillations, included in it is the initial parameters, % recovered, and steam and time efficiencies.

Table 5.1 Distillation Efficiency Results

Distillation #	Type (V,L)	Reflux	Initial	Distilled	Recovered	Final Pot	Steam Used	Efficiency	Time	Time Eff.
			PG	PG	%	ABV %	lbs	lbs steam/ PG	hours	PG/hr
3	Normal Operation	Off	39	34	0.87	1.2%	284	8.4	4.1	8.3
4	Cyclic (9 min, 3 min)	Off	34	32	0.95	0.6%	266	8.3	4.5	7.1
5	Cyclic(6 min, 3 min)	Off	34	31	0.90	1.3%	242	7.9	5.9	5.2
6	Cyclic(4 min, 3 min)	Off	28	27	0.96	2.0%	223	8.3	6.0	4.5
7	Normal Operation - Low Wines	Off	4	4	0.90	0.50%	114	31.7	1.3	2.8
8	Cyclic -Low Wines (9min, 3 min)	Off	4	4	0.88	0.70%	116	33.1	2.2	1.6
9	Cyclic - Low Wines (6min, 3min)	Off	4	4	0.99	0.40%	126	34.3	3.3	1.1
10	Cyclic - Low Wines (4min, 3min)	Off	3	3	0.96	0.40%	134	44.2	3.2	0.9
11	Normal Operation (Brandy)	On	14	13	0.92	0.20%	183	14.2	2.2	6.0
12	Normal Operation (Brandy)	Off	20	18	0.92	0.80%	175	9.7	2.6	6.9
13	Cyclic (6min, 3min) - Tray by Tray	On	20	19	0.92	0.20%	246	13.1	3.6	5.2
14	Cyclic (6min, 3min) - Tray by Tray	On	18	17	0.93	0.20%	225	13.5	2.7	6.1
15	Cyclic (6min, 3min) - Tray by Tray	On	20	18	0.92	0.20%	224	12.3	2.8	6.5

Figure 5.1 shows the hydrometer reading versus time throughout every distillation. D1 is not shown because not enough data was collected.

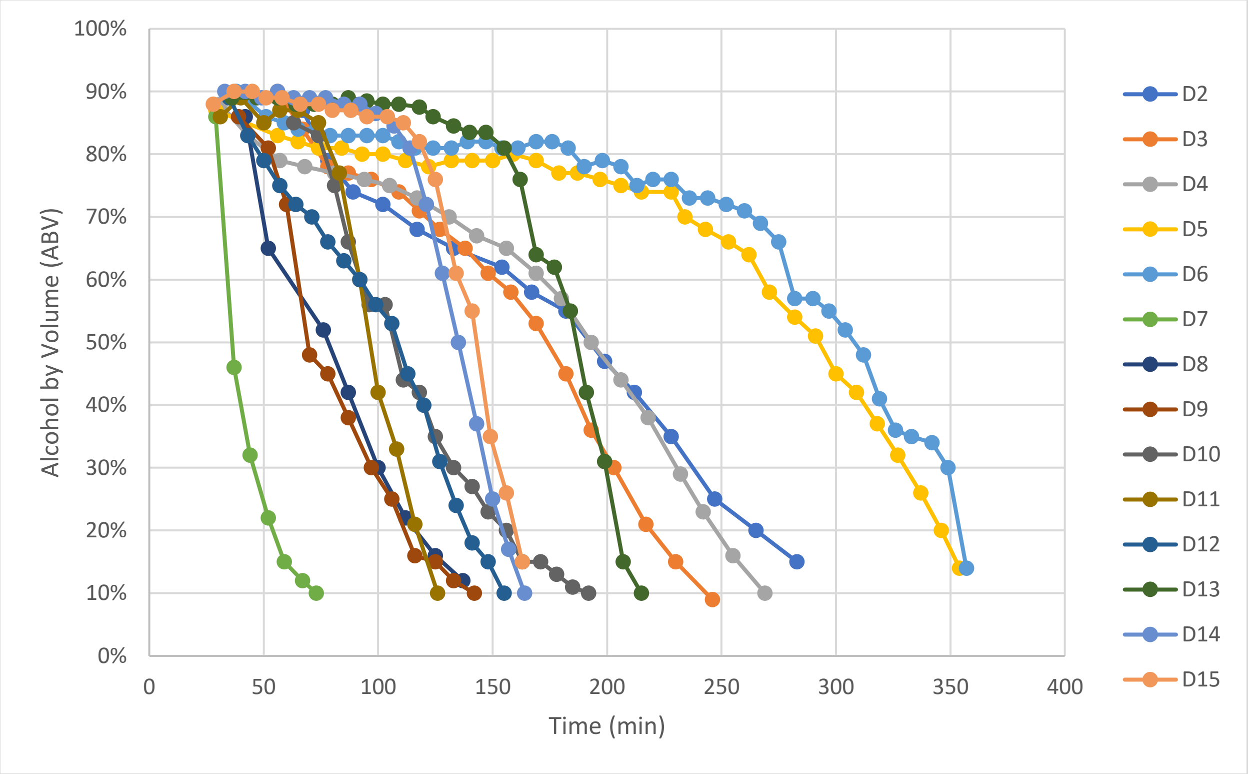

Figure 5.1 Ethanol Concentration in Distillate vs Time for All Distillations

Figure 5.2 shows the hydrometer reading vs volume for distillations D7 through D15. These distillations are the only distillations in which volume distilled data was collected, so they were selected for comparison.

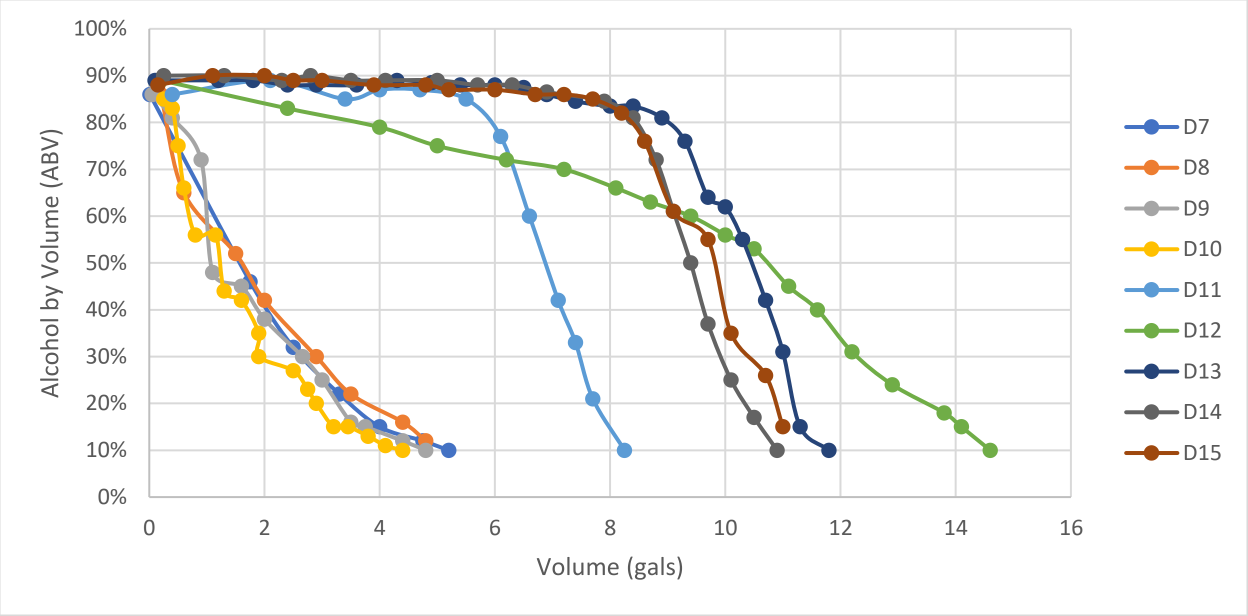

Figure 5.2 Ethanol Concentration vs Volume for Distillations D7 – D15

As you can see in Figure 5.2, not all distillations collected the same volume of distillate, therefore to compare the data, the x-axis was normalized by dividing the volume at a given point by the overall volume collected. This can be seen graphically in Figure 5.3 below.

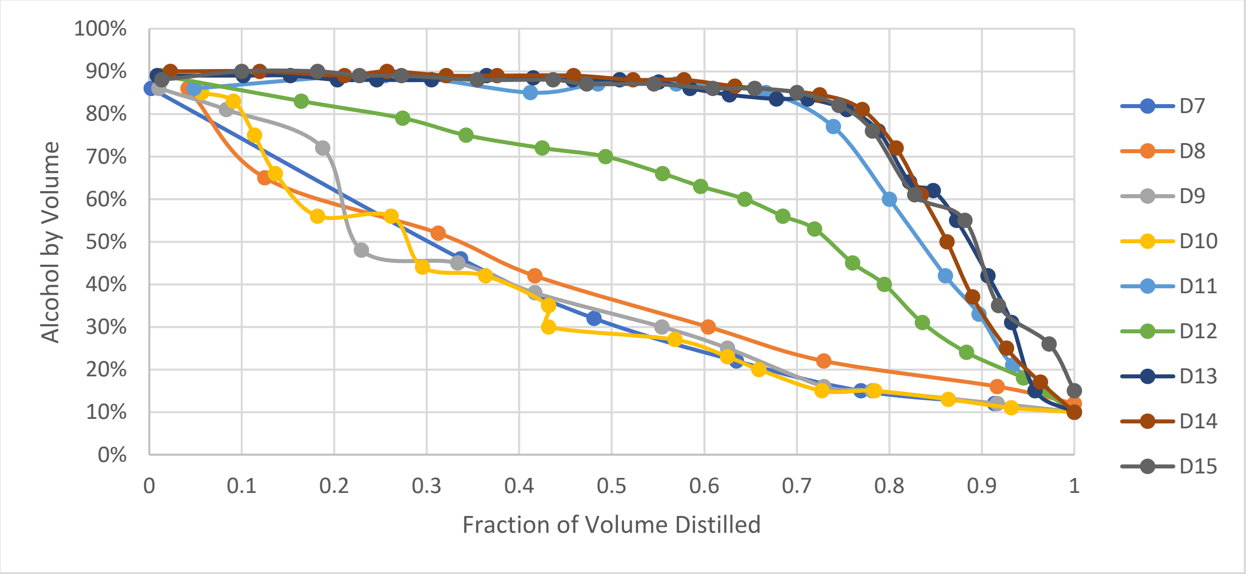

Figure 5.3 Normalized Ethanol Concentration vs Volume for Distillations D7-D15

5.1.2 Component Concentration Results

Figures 5.4 – 5.11 show the trend in compound concentration versus fraction of volume distilled for distillation D7 – D15.

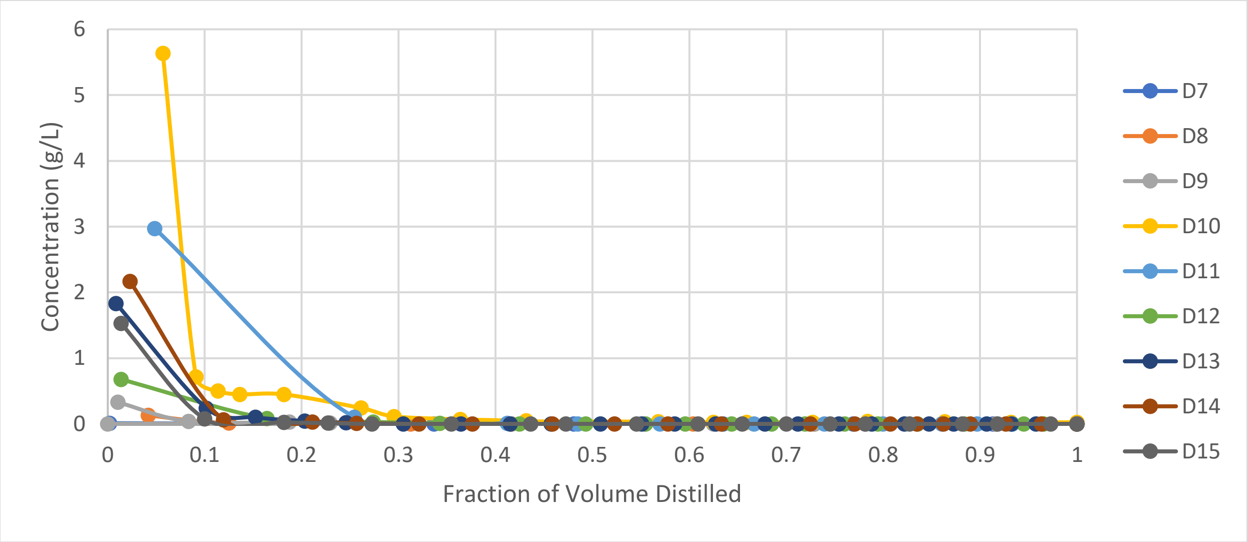

Figure 5.4 Normalized Acetaldehyde Concentration vs Volume for Distillations D7-D15

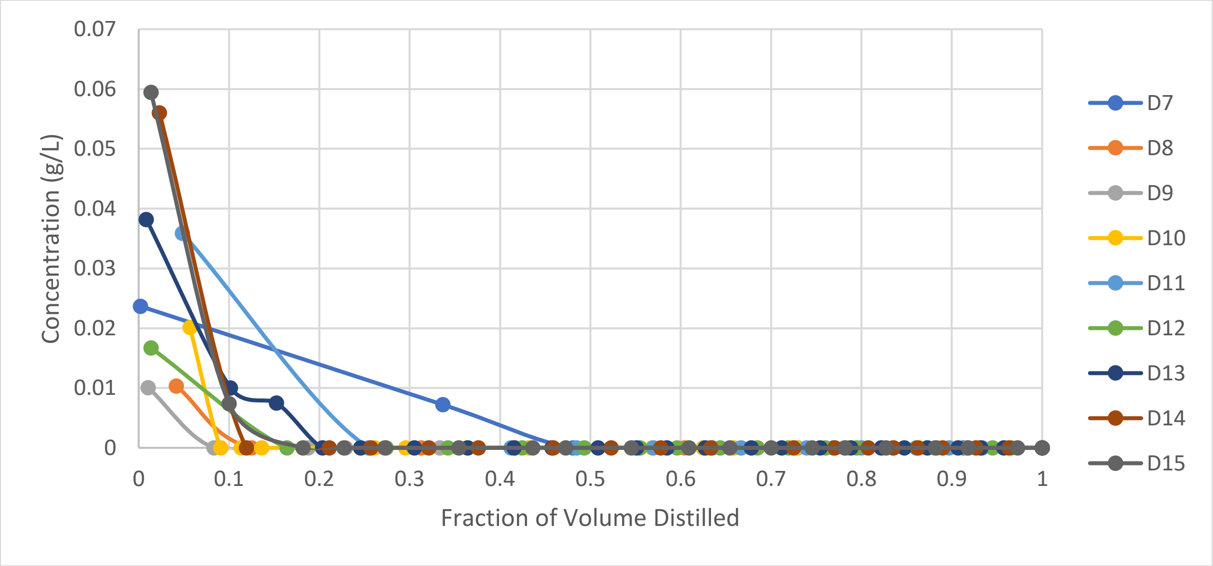

Figure 5.5 Normalized Acetone Concentration vs Volume for Distillations D7-D15

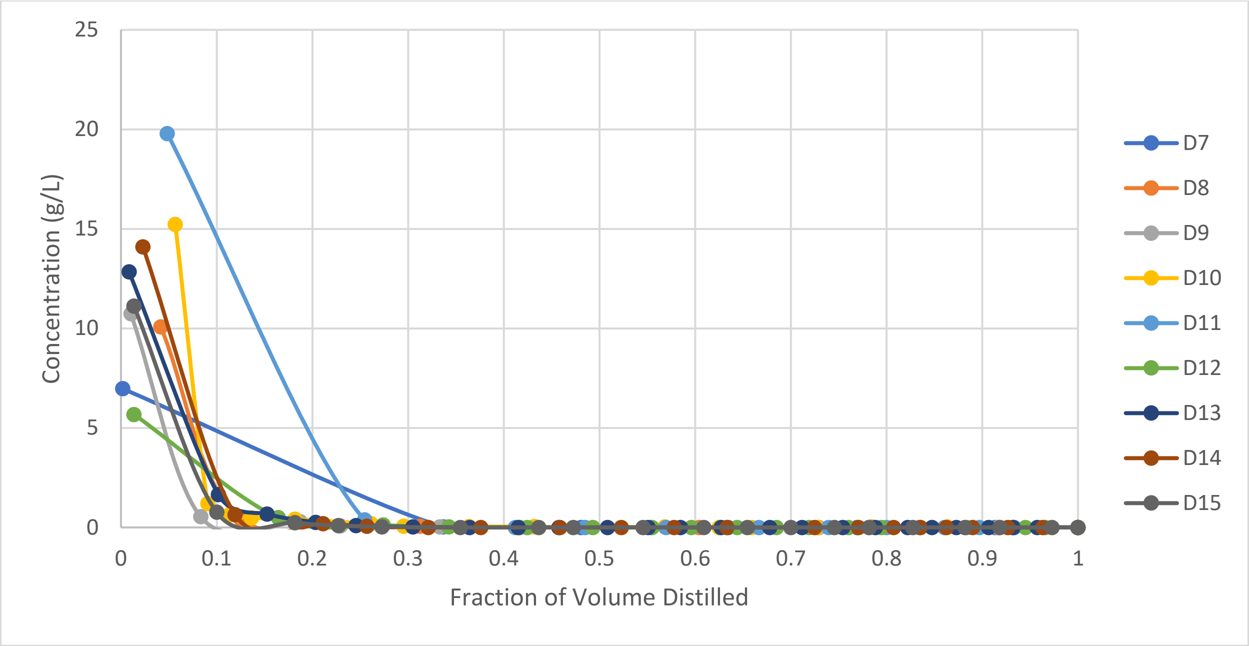

Figure 5.6 Normalized Ethyl Acetate Concentration vs Volume for Distillations D7-D15

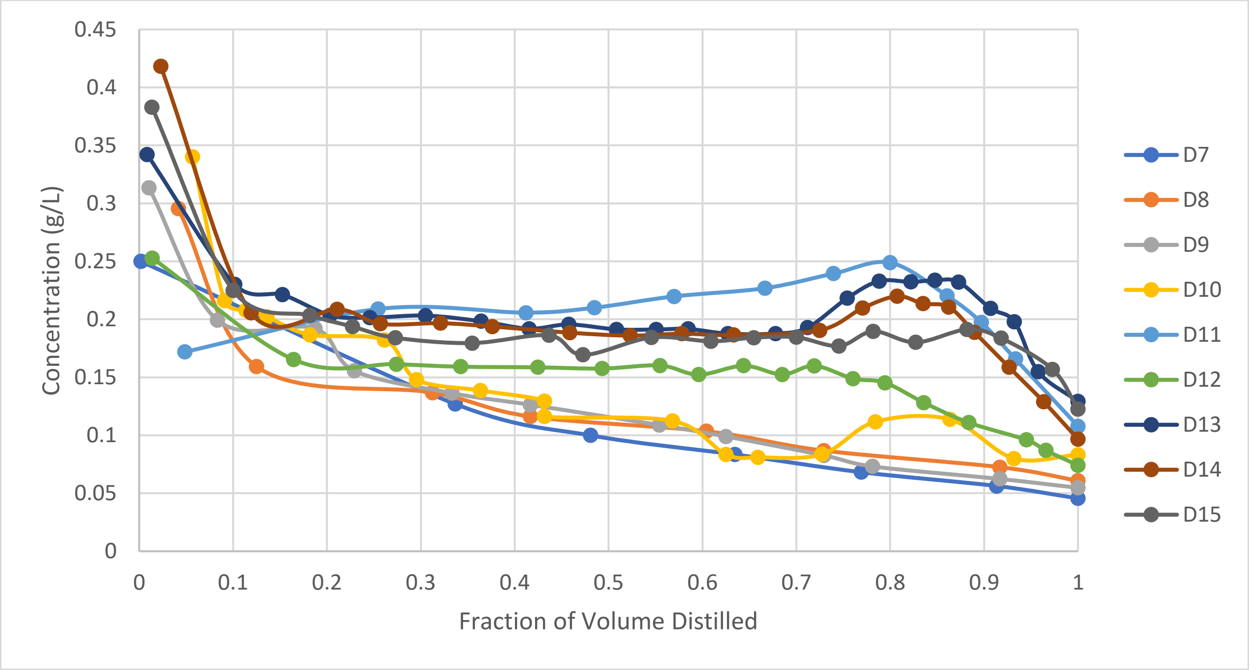

Figure 5.7 Normalized Methanol Concentration vs Volume for Distillations D7-D15

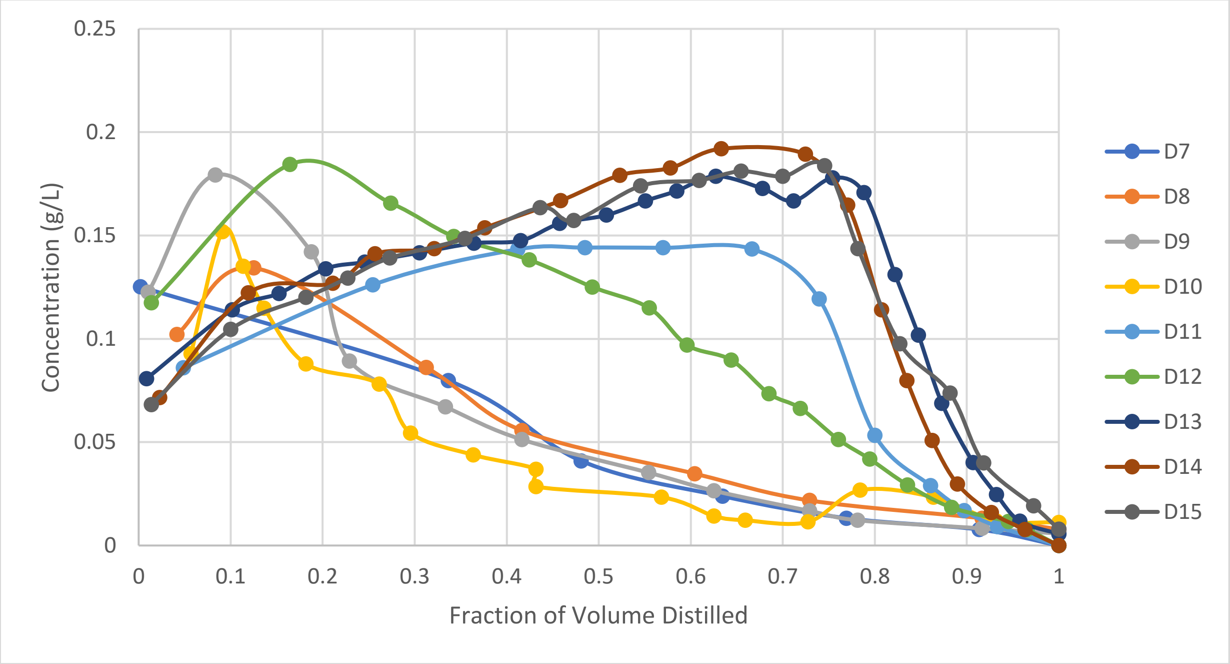

Figure 5.8 Normalized Propanol Concentration vs Volume for Distillations D7-D15

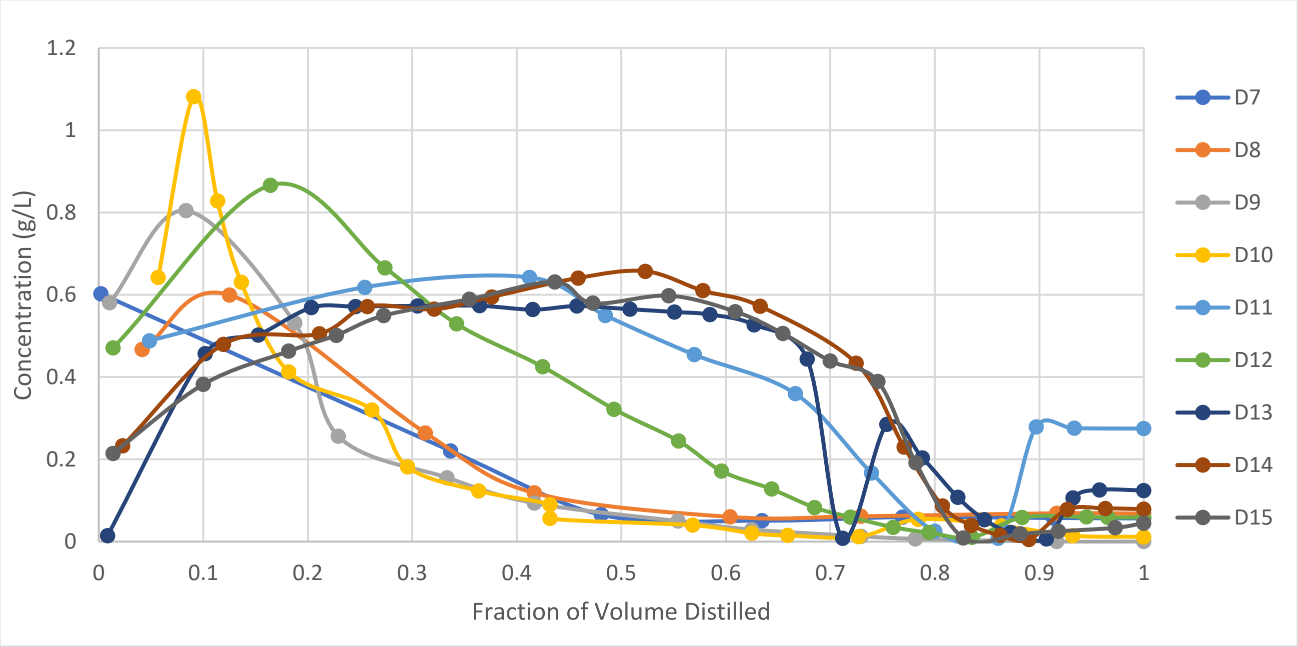

Figure 5.9 Normalized Isobutanol Concentration vs Volume for Distillations D7-D15

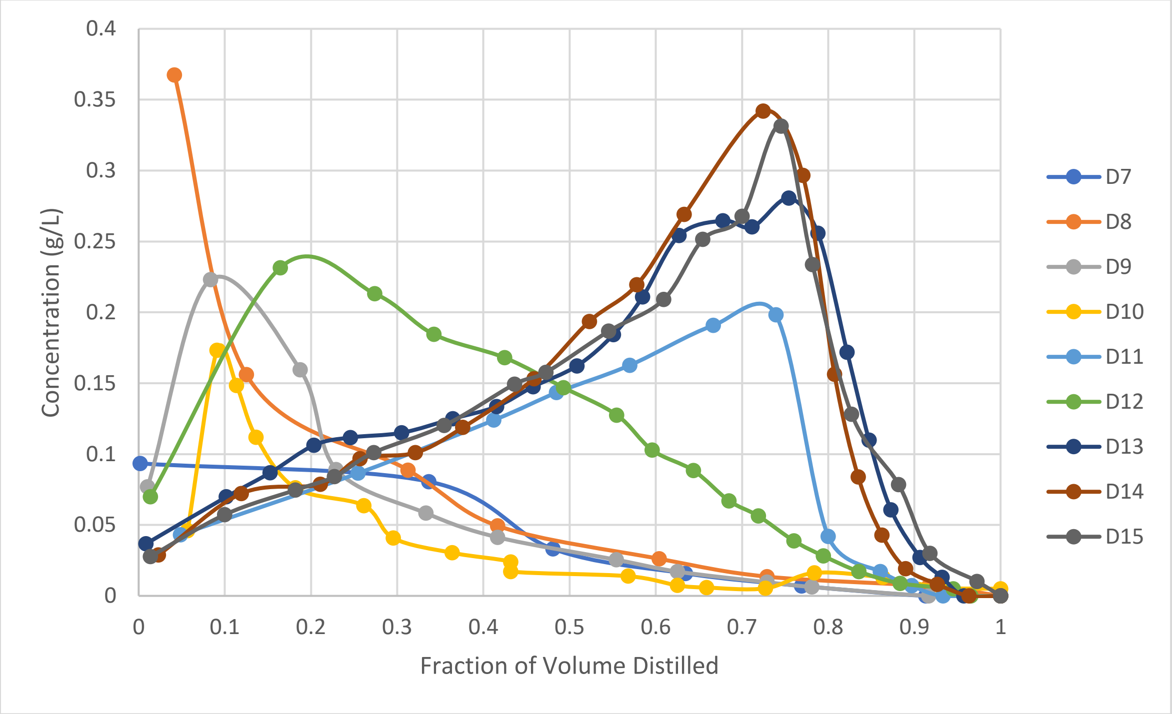

Figure 5.10 Normalized Butanol Concentration vs Volume for Distillations D7-D14

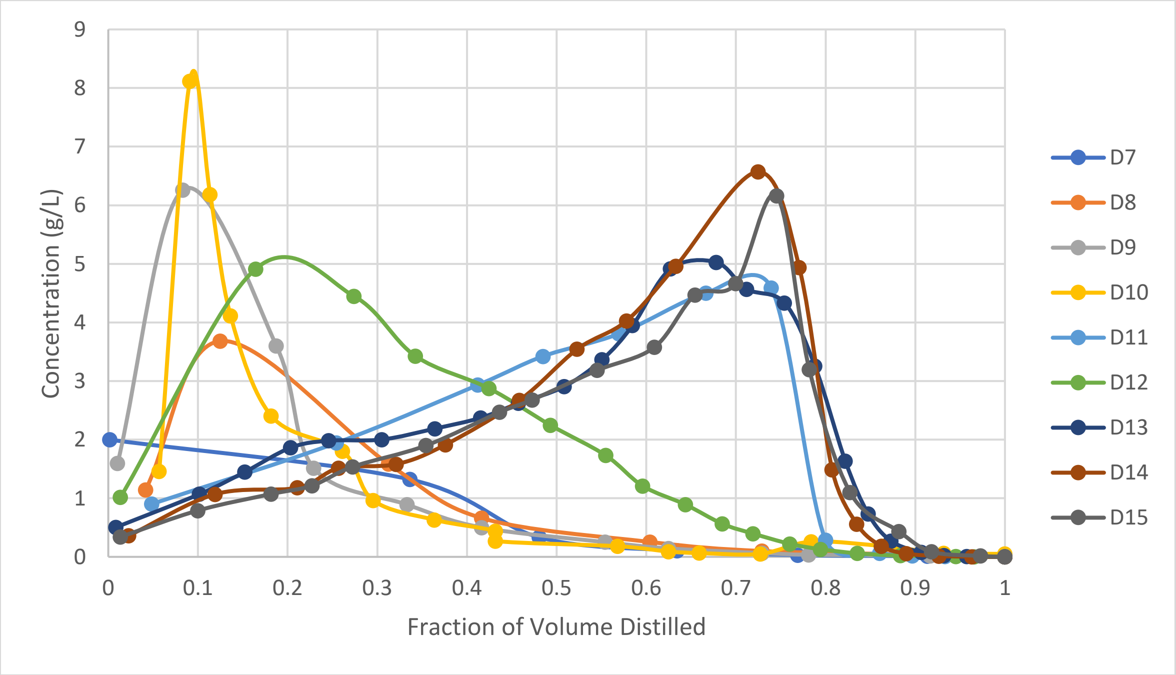

Figure 5.11 Normalized Isoamyl Alcohol Concentration vs Volume for Distillations D7-D15

5.1.3 Results by Type of Distillation

Overall, there were multiple types of distillations with and without reflux and with varying initial feed to the pot. Cyclic versus conventional operation, as well as, low wines distillation versus finishing run distillation. Below is a comparison table of operating parameters which led to the separation of the distillations graphically into four different categories.

Table 5.2 Distillations Separated by Type

Operation Type	Conventional Operation	Conventional Operation	Cyclic Operation	Cyclic Operation
Distillation Type	Low Wines	Finishing	Low Wines	Finishing
Distillation #	D7	D3,D11,D12	D8,D9,D10	D4,D5,D6,D13,D14,D15

Low Wines Distillation Results

Figure 5.12 below illustrates the low wines distillate results for cyclic versus conventional operation.

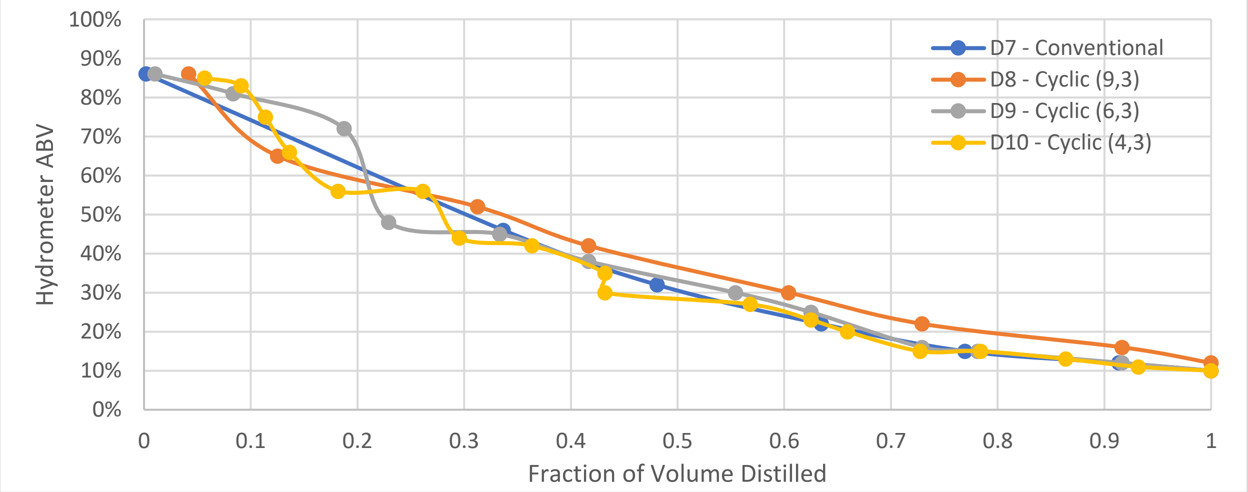

Figure 5.12 Hydrometer ABV Reading vs Fraction of Volume Distilled for Low Wine Distillations

Another important parameter to look at is the steam efficiency of each distillation. Steam efficiency was calculated as the lbs. of steam used per proof gallon distilled. For low wines, this can be seen in Figure 5.13 below.

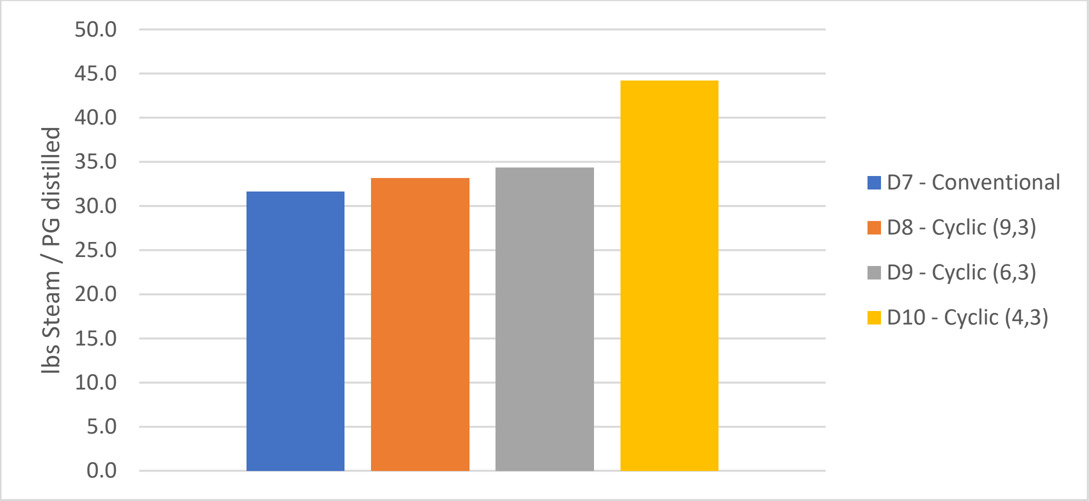

Figure 5.13 Steam Efficiency for All Low Wine Distillations

The last measure of efficiency was percent recovery which was calculated by dividing the total proof gallons distilled by the total initial proof gallons fed into the pot. For low wines this is illustrated in Figure 5.14 below.

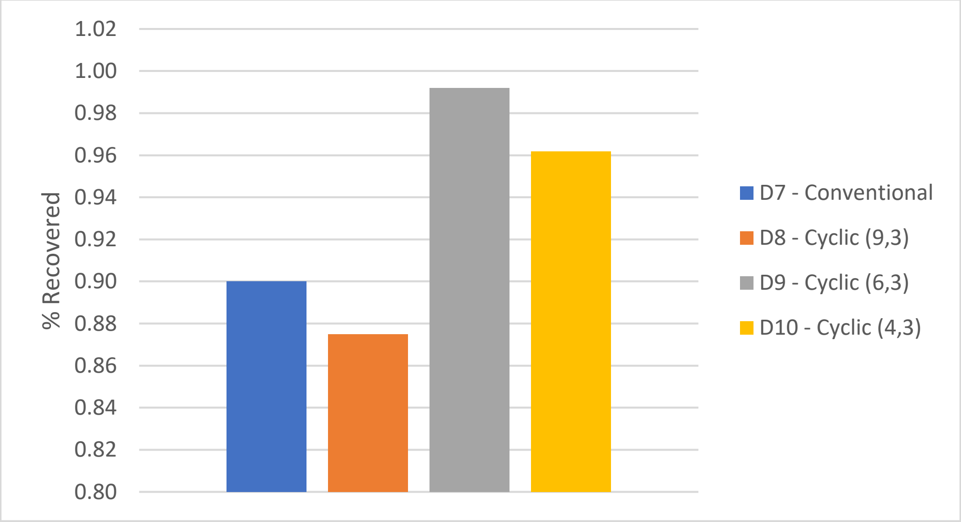

Figure 5.14 Percent Recovery for All Low Wine Distillations

Finishing Distillation Results

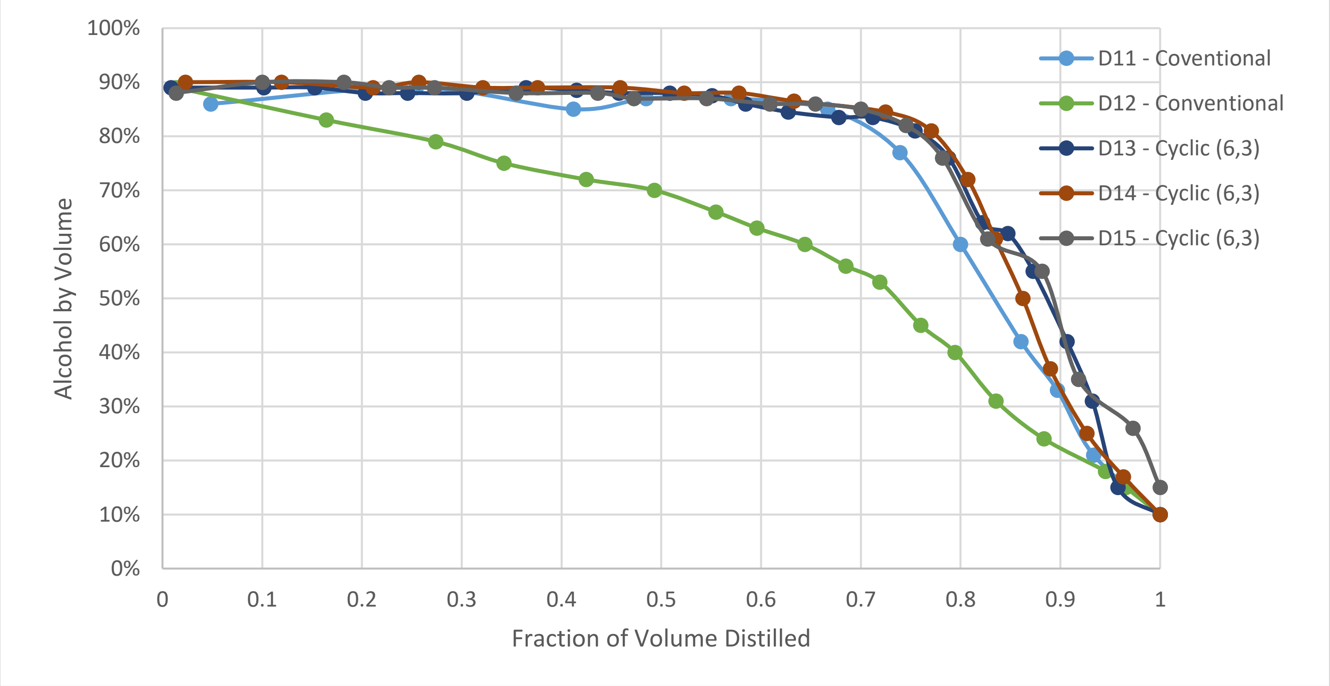

Figure 5.15 Hydrometer ABV Reading vs Fraction of Volume Distilled for Finishing Distillations

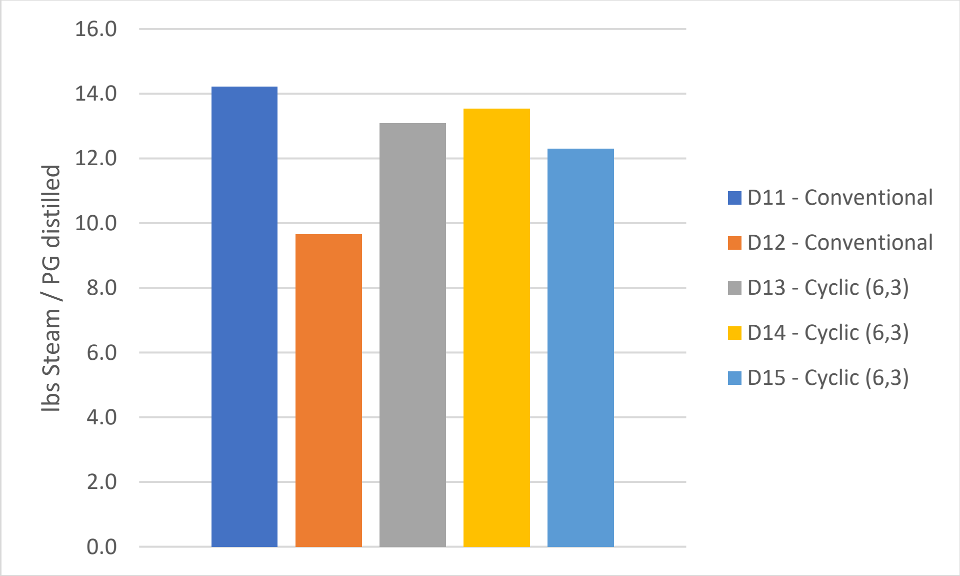

Figure 5.16 Steam Efficiency for All Finishing Distillations

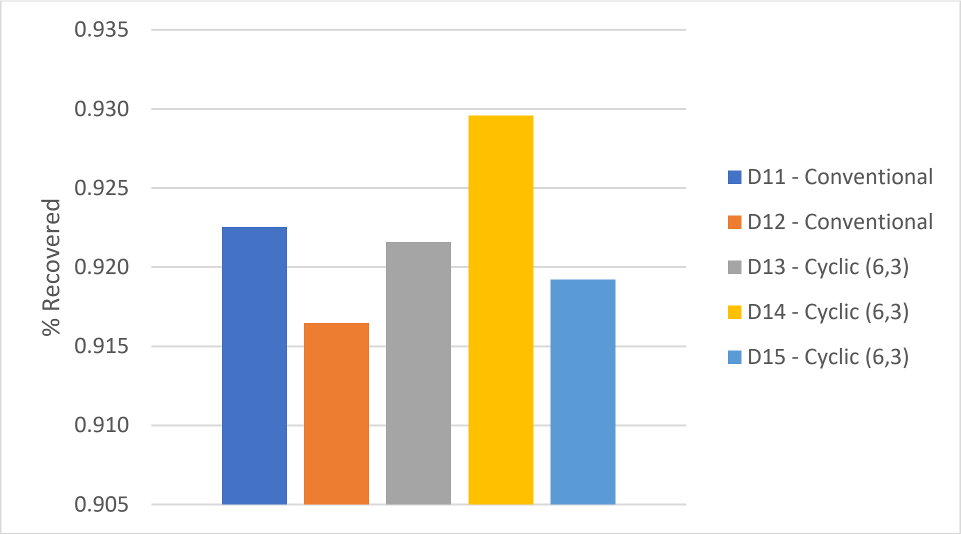

Figure 5.17 Percent Recovery for All Finishing Distillations

5.1.4 Results of Cuts Taken

Table 5.3 is a summary table of all the distillations in which cuts were taken. It shows the cuts by volume, and the concentrations of the key components initially and in each cut.

Table 5.3 Cut Results for Distillations 11, 12, 13, 14 & 15

		Volume	Acetaldehyde	Acetone	Methanol	Ethanol	Ethyl Acetate	Propanol	Isobutanol	Butanol	Isoamyl Alcohol	ABV
		gal	g/L	g/L	g/L	g/L	g/L	g/L	g/L	g/L	g/L	%
Initial Pot	D11	36	0.03	0.00	0.06	151	0.13	0.03	0.09	0.03	0.50	0.19
	D12	36	0.03	0.00	0.07	215	0.13	0.04	0.13	0.04	0.70	0.27
	D13	36	0.02	0.00	0.07	222	0.15	0.04	0.13	0.05	0.77	0.28
	D14	33	0.02	0.00	0.07	214	0.12	0.04	0.13	0.04	0.72	0.27
	D15	33	0.01	0.00	0.07	241	0.13	0.05	0.15	0.05	0.84	0.31
Heads	D11	1.0	0.76	0.01	0.26	708	6.47	0.12	0.63	0.08	1.89	0.90
	D12	1.4	0.41	0.01	0.21	713	3.23	0.14	0.64	0.11	2.00	0.90
	D13	0.9	0.49	0.02	0.25	724	4.62	0.12	0.47	0.07	1.10	0.92
	D14	1.1	0.31	0.02	0.25	710	3.43	0.09	0.01	0.05	0.67	0.90
	D15	1.0	0.29	0.02	0.28	764	3.60	0.09	0.01	0.05	0.61	0.92
Hearts	D11	5.3	0.03	0.00	0.22	709	0.10	0.14	0.52	0.14	3.35	0.90
	D12	7.7	0.02	0.00	0.16	599	0.11	0.14	0.49	0.17	3.12	0.76
	D13	9.1	0.02	0.00	0.19	694	0.12	0.15	0.49	0.17	3.02	0.88
	D14	8.2	0.00	0.00	0.18	663	0.04	0.15	0.48	0.17	2.91	0.84
	D15	8.0	0	0	0.19	714	0	0.17	0.54	0.19	3.20	0.91
Tails	D11	2.1	0.00	0.00	0.19	288	0.00	0.02	0.01	0.02	0.12	0.37
	D12	5.8	0.00	0.00	0.13	293	0.00	0.04	0.03	0.03	0.21	0.37
	D13	1.8	0.00	0.00	0.15	250	0.00	0.02	0.01	0.02	0.07	0.32
	D14	1.6	0.00	0.00	0.14	215	0.00	0.02	0.02	0.01	0.05	0.27
	D15	2.2	0	0	0.16	320	0.00	0.04	0.02	0.04	0.25	0.41

To best compare these values, the volumes were converted into proof gallons, which as a reminder is a gallon of alcohol at 50% alcohol by volume. The values were then normalized by dividing the proof gallons of a given cut by the overall proof gallons fed into the still. This shows are more direct comparisons of the amount of each cut produced as a percent of the initial volume. Figures 5.18 – 5.20 show quantitatively the normalized proof gallon of each cut in comparison by distillation.

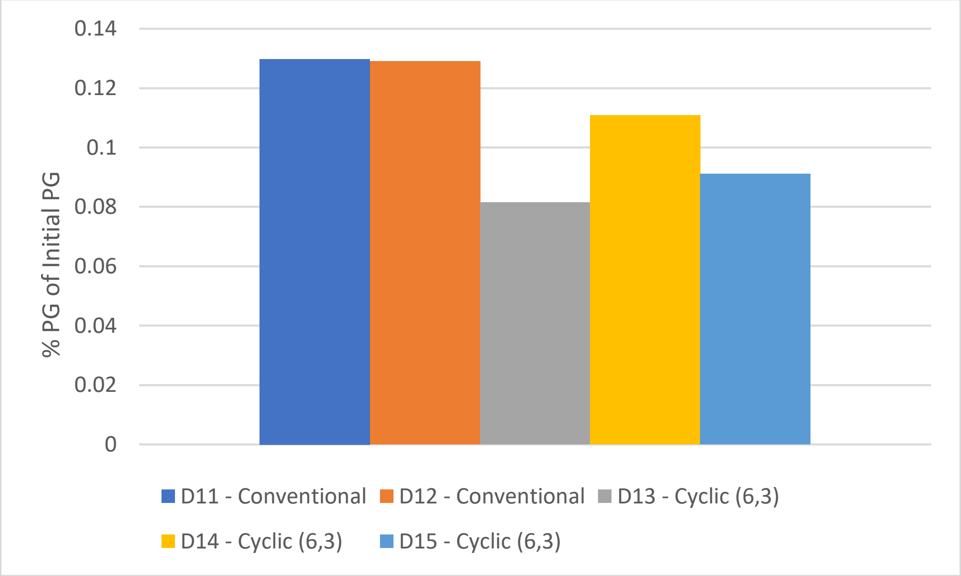

Figure 5.18 Normalized Proof Gallon of Heads Cut by Distillation

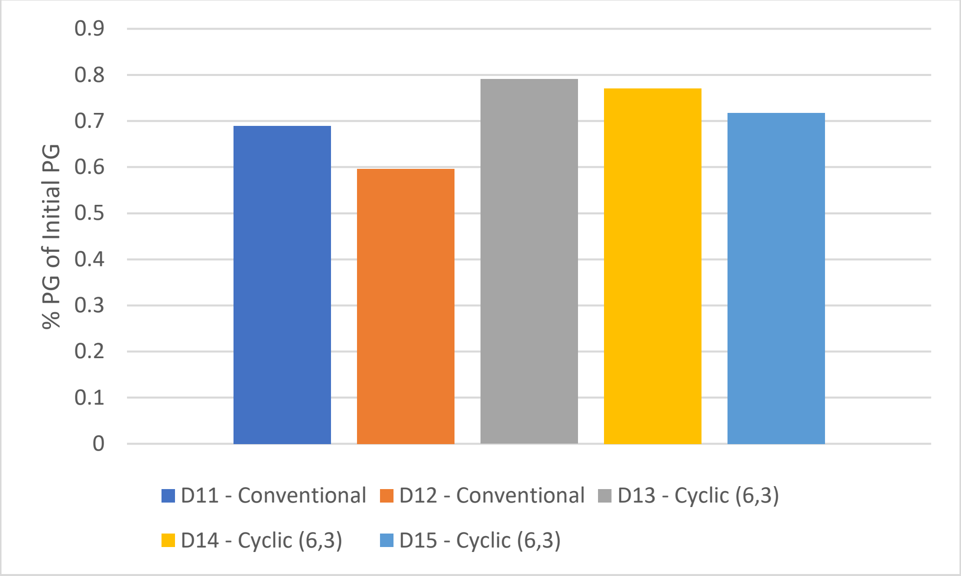

Figure 5.19 Normailized Proof Gallon of Hearts Cut by Distillation

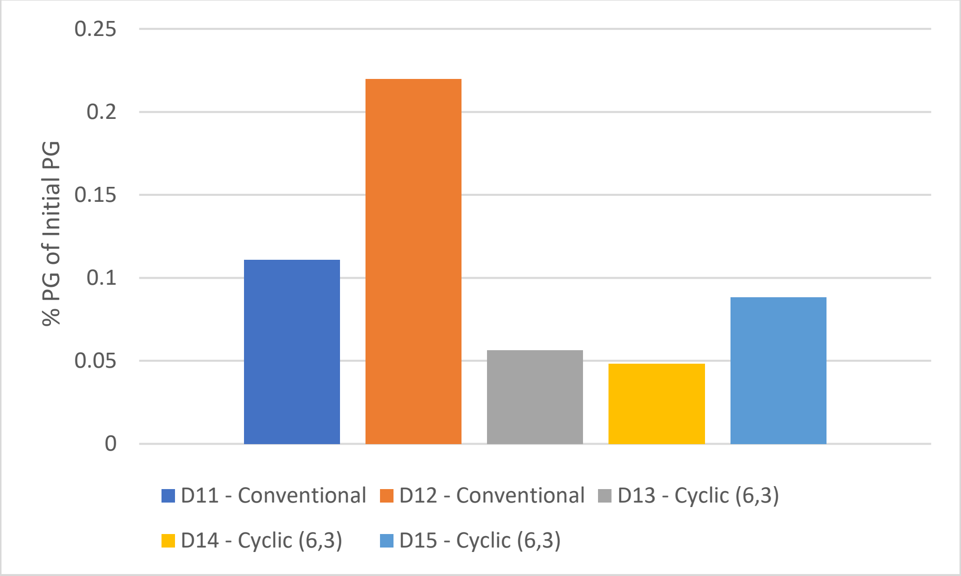

Figure 5.20 Normailized Proof Gallon of Tails Cut by Distillation

5.1.5 Temperature Profile Results

Temperatures throughout the still and column were recorded during each distillation. Figures 5.21-22 show conventional and cyclic temperature profiles for D11 and D 13.

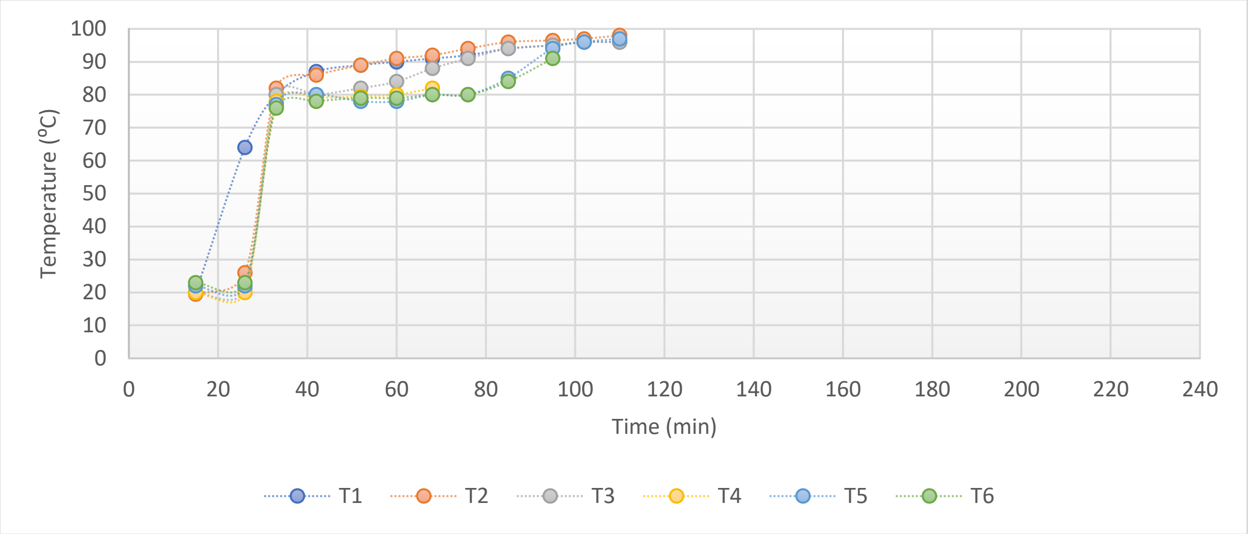

Figure 5.21 Temperature vs Time Profile for Conventional Operation (D11)

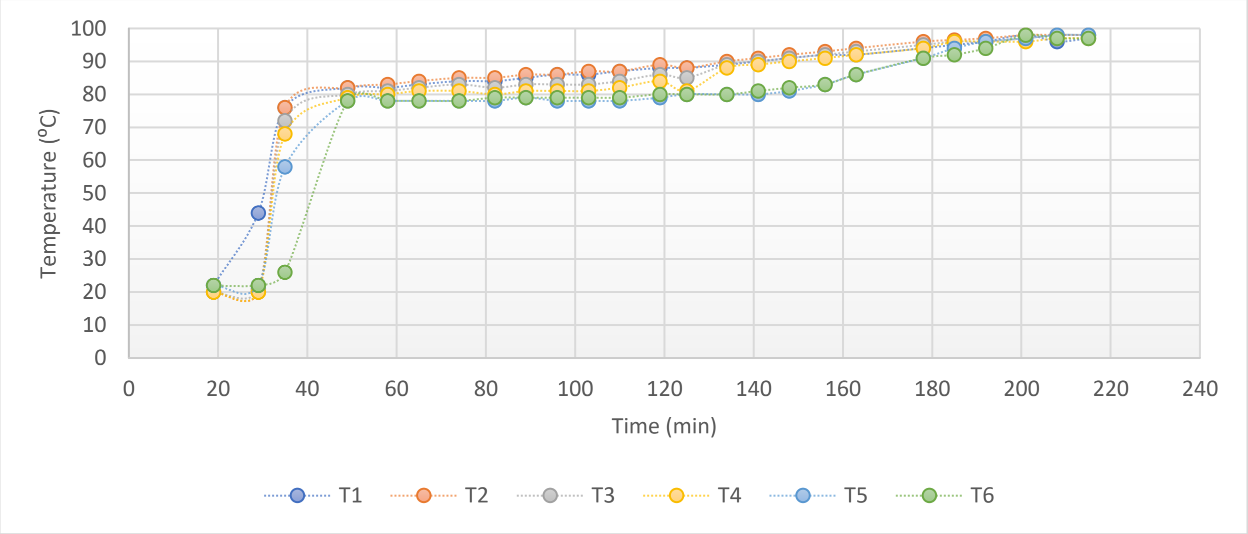

Figure 5.22 Temperature vs Time Profile for Cyclic Operation (D13)

5.2 Simulation Results

The previous modeling methods were applied to the system studied using MATLAB. The MATLAB codes can be viewed in Appendix B. The initial conditions and other known parameters used for the simulations can be seen below in Table 5.4.

Table 5.4 Parameters for Batch Distillation Simulation

Vapor Flow Rate (mole/min)	15
Reflux Ratio	1
Reboiler Hold Up (moles)	7000
Vapor Flow Period (min)	6
Total Operation Time (min)	185
Stage/Tray hold-up (moles)	56
Initial Condenser Mole fraction and Temperature (°C) (X1,T1)	0.73,55
Initial Reboiler mole fraction and Temperature (°C) (X2,T2)	0.64,55
Bottom tray mole fraction and Temperature (°C) (X3,T3)	0.61,55
Middle tray mole fraction and Temperature (°C) (X4,T4)	0.56,55
Top Tray mole fraction and Temperature (°C) (X5,T5)	0.49,55
Partial condenser 2 mole fraction and Temperature (°C) (X6,T6)	0.36,55
Initial Reboiler mole fraction and Temperature (°C) (X7,T7)	0.10,55

For conventional operation, the partial differential and algebraic equations were set up in the MATLAB function ‘Ethanol_Water_Conventional.’ initial values were entered into the global code ‘EthanolWater_main’ which uses ODE15s to solve and plot the tray and still composition and temperature over time. The resulting figures can be seen below in Figures 5.23 – 5.26.

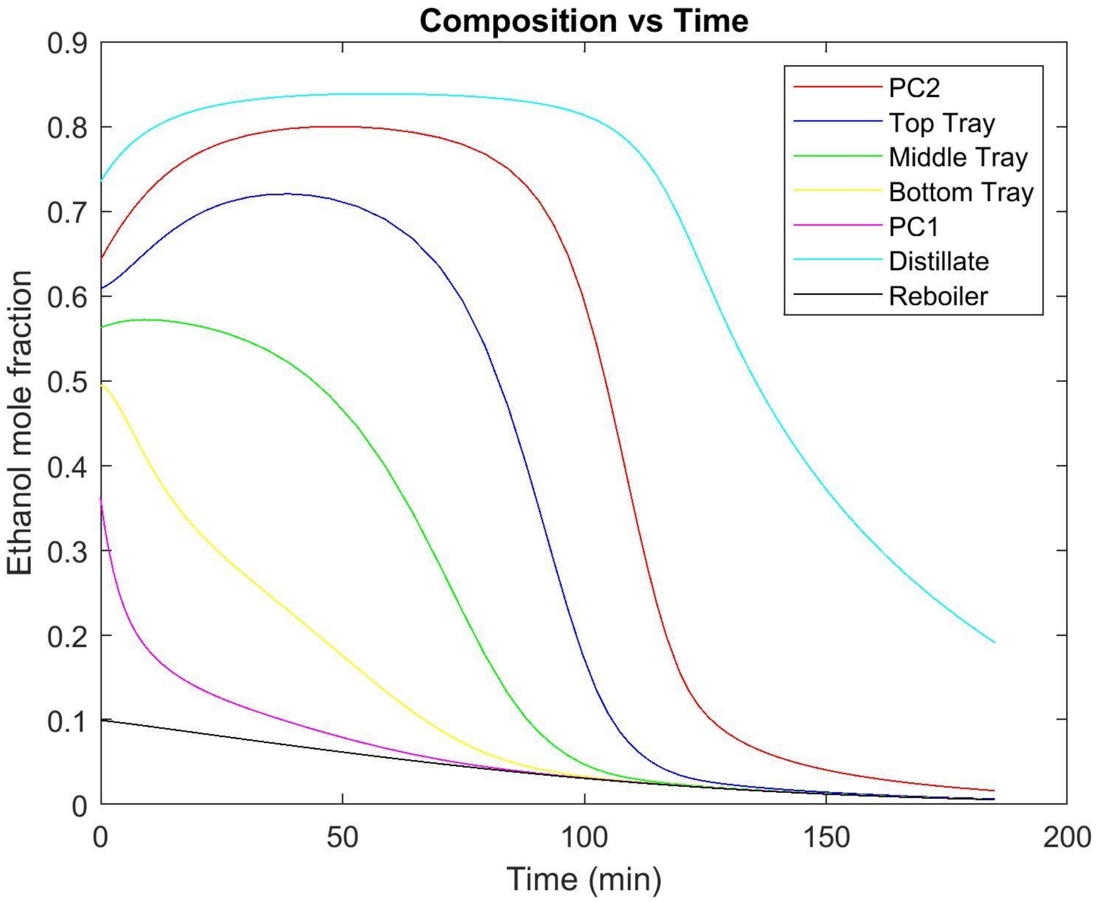

Figure 5.23 MATLAB Simulation of Conventional Distillation: Composition vs Time

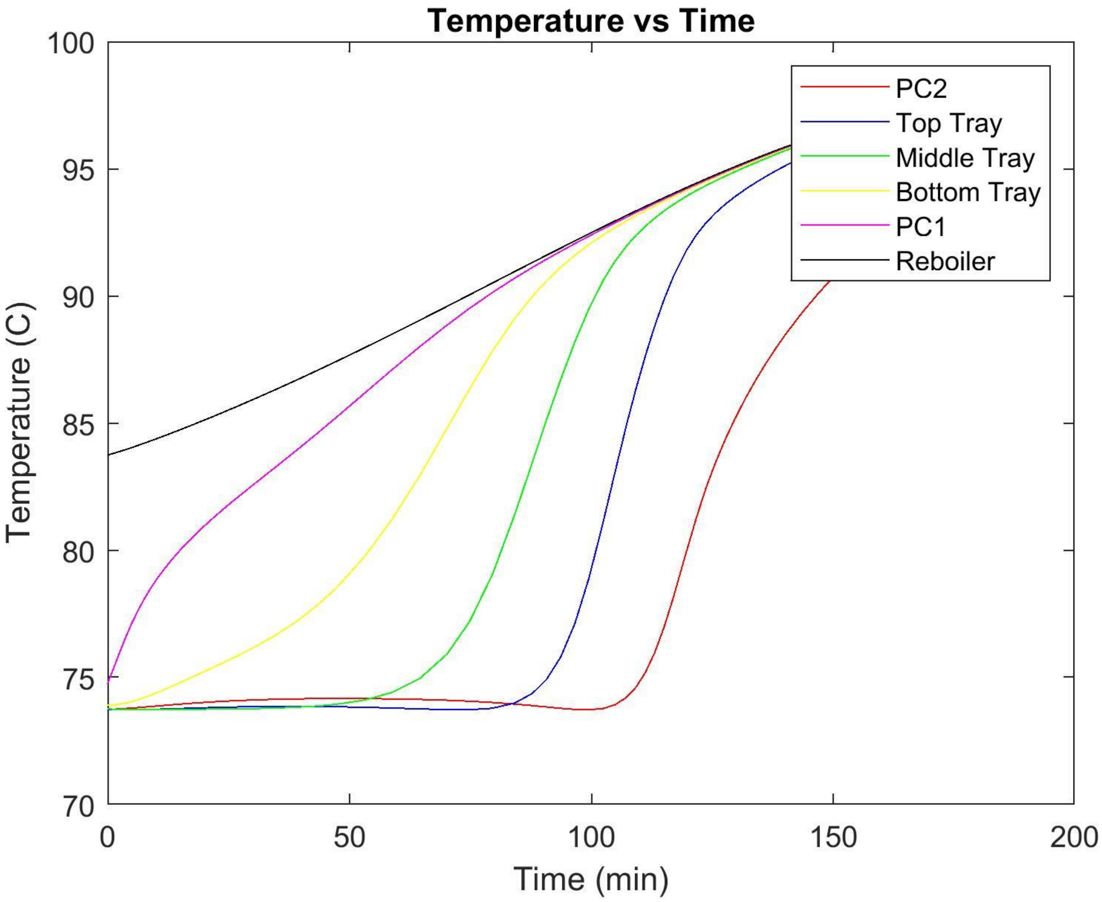

Figure 5.24 MATLAB Simulation of Conventional Distillation: Temperature vs Time

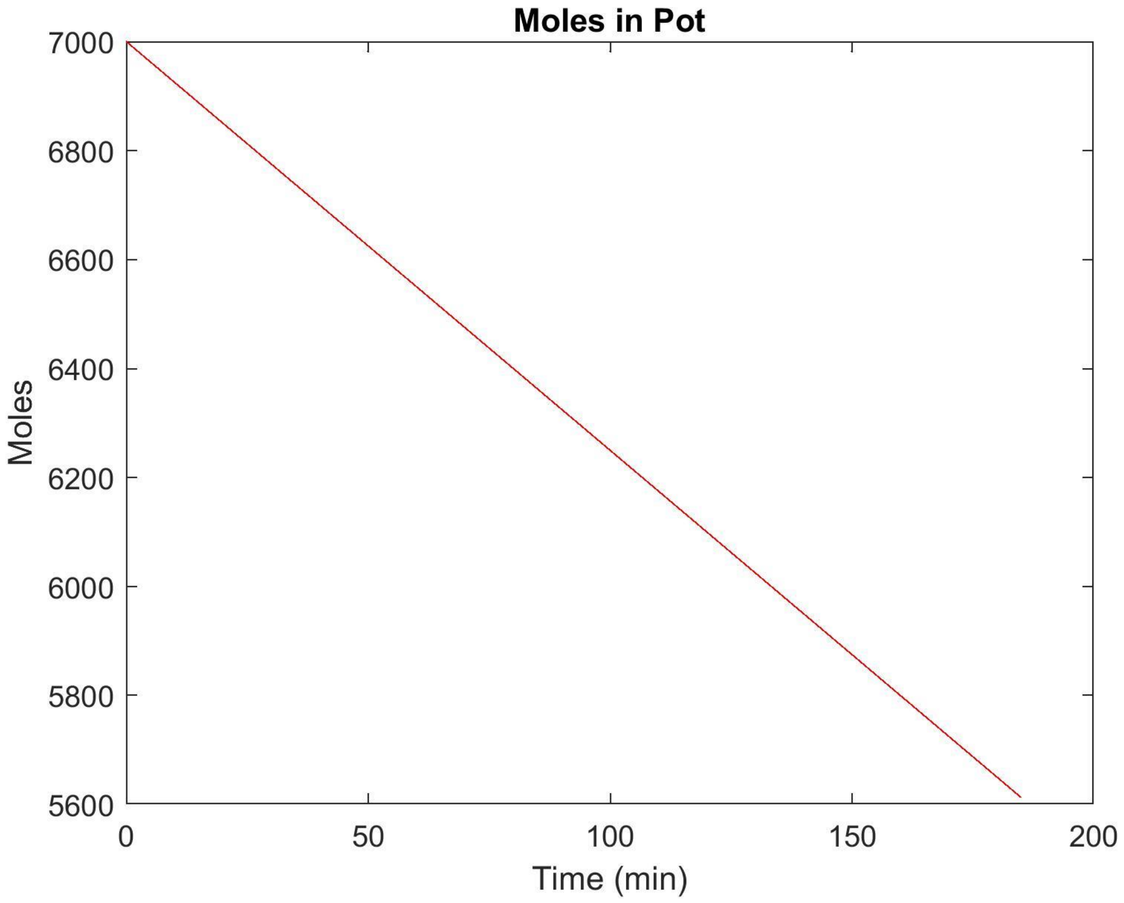

Figure 5.25 MATLAB Simulation of Conventional Distillation: Moles in Pot vs Time

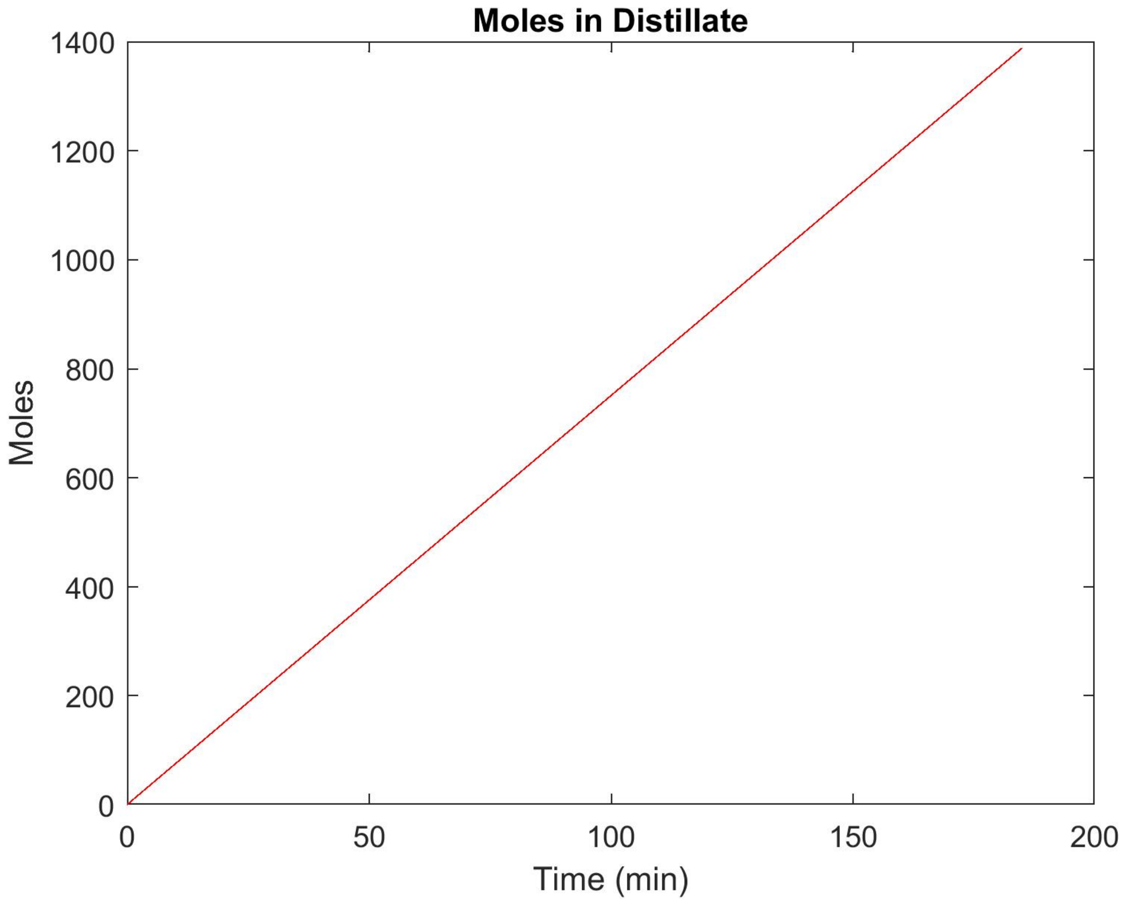

Figure 5.26 MATLAB Simulation of Conventional Distillation: Moles in Distillate vs Time

For cyclic distillation modeling, the script ‘cyclic global’ was first ran to determine the state of the system at the end of the vapor flow period. Plots of composition and temperature on the stages as a function of time were generated for each vapor flow period. The results of the first vapor flow period can be seen in Figures 5.27-28 below.

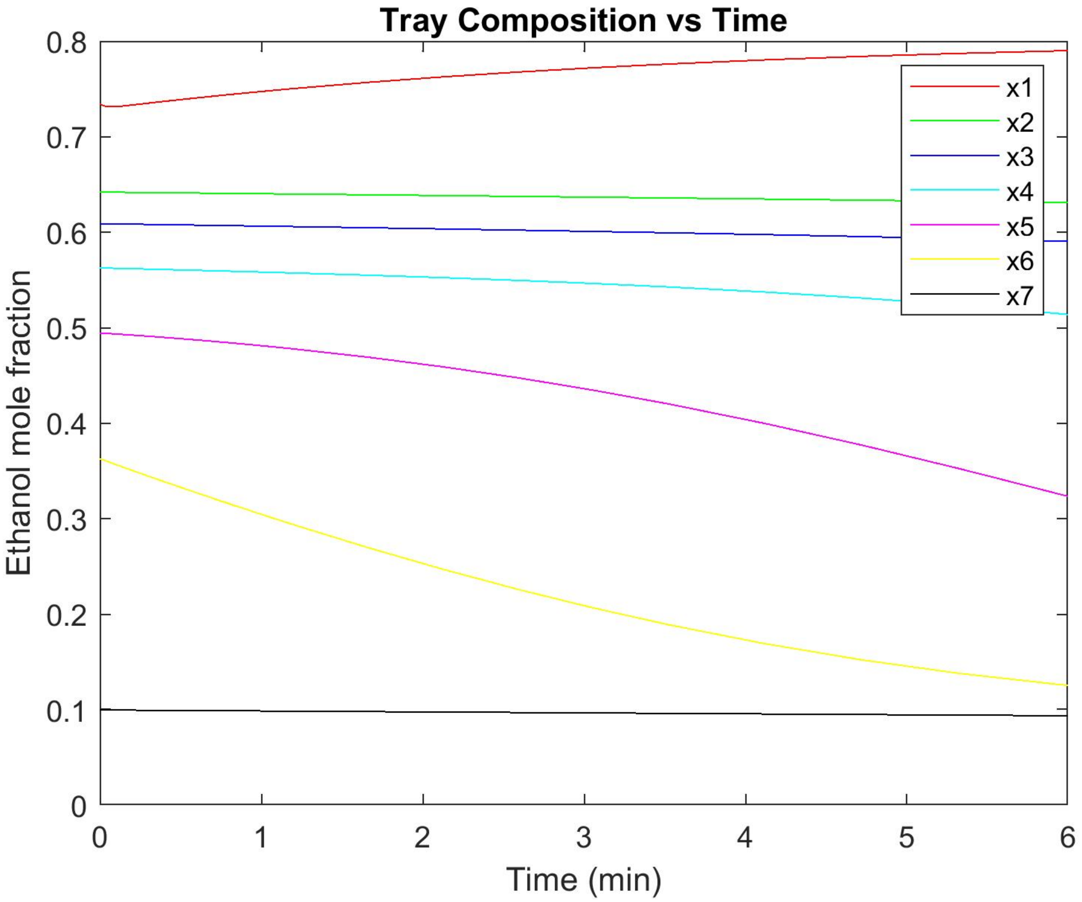

Figure 5.27 Stage and Reboiler Composition vs Time for First Vapor Flow Period

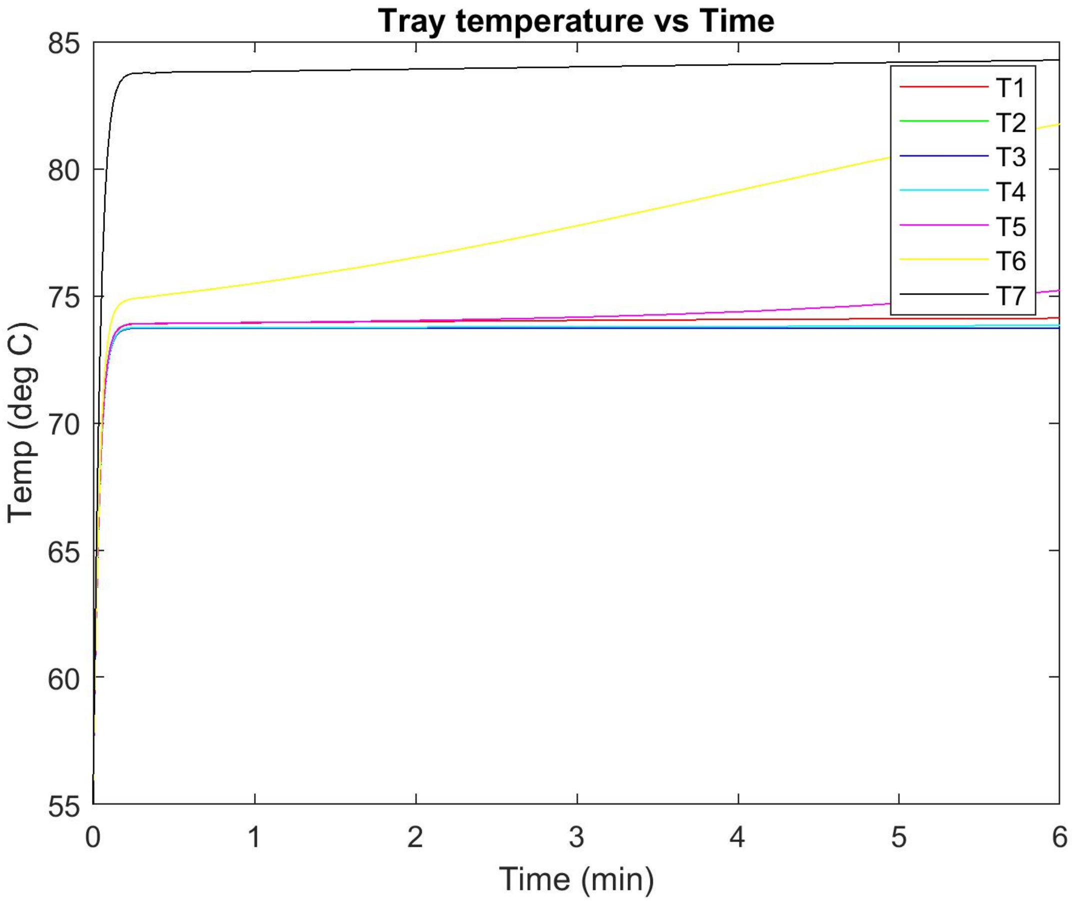

Figure 5.28 Stage and Reboiler Temperature vs Time for First Vapor Flow Period

The values obtained were then input into the script ‘liquid flow’ to determine the state of the system at the end of the liquid flow period. The values obtained were then entered back into the script ‘cyclic global’ to determine the state of the system at the end of second vapor flow period. This process continued for 25 cycles. The data was entered in an excel spreadsheet as it was collected. The tables can be found in Appendix B. The graphical representation of the results can be seen in Figures 5.29-30 below.

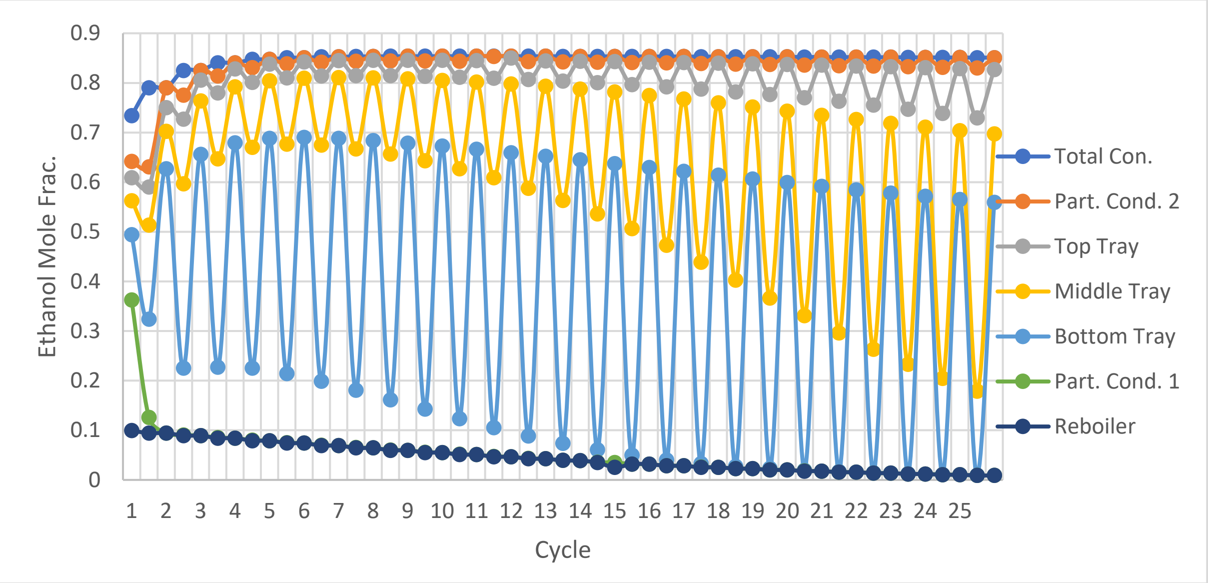

Figure 5.29 Cyclic Batch Distillation Tray and Still Composition vs Time for 25 Cycles

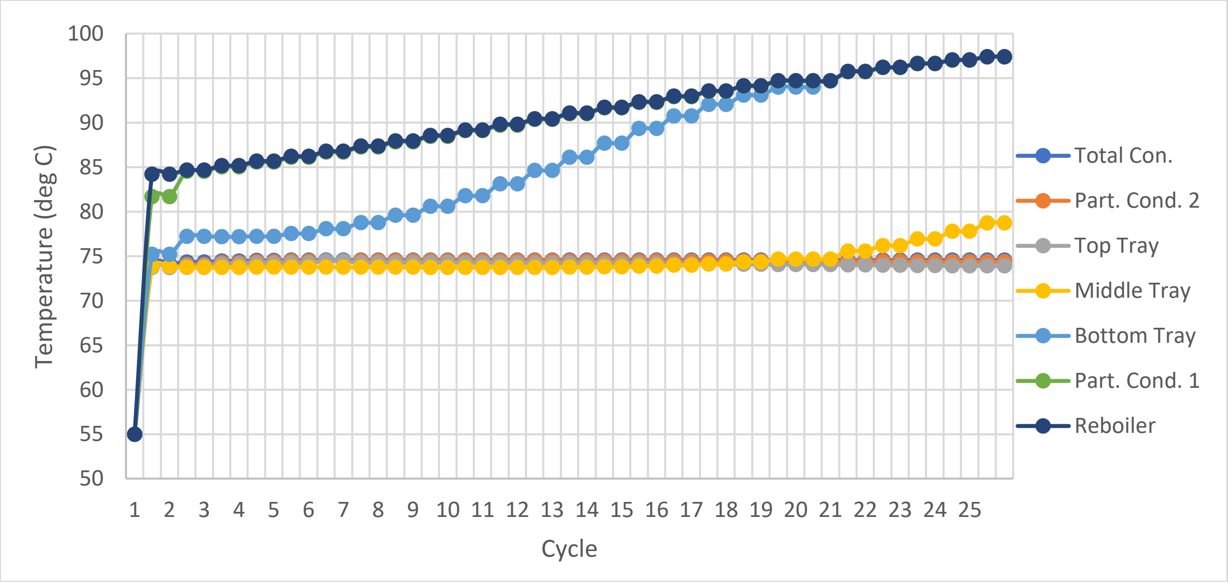

Figure 5.30 Cyclic Batch Distillation Tray and Still Temperature vs Time for 25 Cycles

5.3 Reproducibility

Due to the length of each distillation to run as well as to analyze the samples, one triplication experiment was run under the same conditions D13, D14 and D15 to prove reproducibility. The normalized heads, hearts, and tails cuts were used to compare to the normalized cuts taken in D11 and D12. First the heads, hearts and tails percentages were averaged. Next, the standard deviation was calculated and used to determine a range of values which would be accepted as within one standard deviation and therefore statistically the same. Then the values from D11 and D12 were determined to be within or outside the respected ranges. The values can be seen in Table 5.5 below.

Table 5.5 Statistical Analysis of Reproducibility

	D13	D14	D15	AVG	STD	Low End	High End	D11	D12
Heads	0.08	0.11	0.09	0.09	0.01	0.08	0.11	0.13	0.13
Hearts	0.79	0.77	0.72	0.76	0.03	0.73	0.79	0.69	0.60
Tails	0.06	0.05	0.09	0.06	0.01	0.05	0.08	0.11	0.22

As seen in Table 5.4, the standard deviation of the triplicate is very small averaging around 0.017, deeming the distillation results as the same and therefore reproducible. The distillation results of D11 and D12 were determined to be statistically different from D13, D14 and D15 because the values were all out of the range of 1 standard deviation.

CHAPTER 6: Discussion

6.1 Summary

In summary, cyclic distillation on the batch column used was able to show a decrease in energy (steam) requirements for finishing runs but not in stripping runs. Cyclic distillation trends included the following: ethanol concentration decreased at a slower rate compared to conventional operation and as a result temperature profiles mimicked this phenomenon. It was shown that the volume of hearts (product) was increased and volume of tails and heads (unwanted by-products) was decreased. This research has shown that the application of cyclic distillation on spirit production is a viable option for distilleries large and small. It is suggested that cyclic distillation is applied to other types of spirits, to columns with a larger number of trays, and to trays with true plug flow capability.

6.2 Conclusions

6.2.1 All Distillation Discussion

There are a few key differences when broadly comparing cyclic to conventional operation. First, it was observed that for nearly the same initial volume and ABV as feed into the still, cyclic operation took much longer to process than conventional operation. This trend makes sense because during conventional operation, distillate is always being collected. During cyclic operation distillate is only being collected during the vapor flow period, and during the beginning of the liquid flow period when the condenser is draining.

Secondly, it was noticed that over time and over volume collected the hydrometer reading stayed higher for longer. This is illustrated in Figure 5.3. Rather than start high and decrease gradually throughout the distillation like in conventional operation, during cyclic operation the distillate concentration stayed high and then dramatically decreased towards the end of the distillation. Additionally, it was observed during each distillation that during conventional operation the hydrometer reading started high, near 90% ABV, and then gradually decreased over time. However, during cyclic operation, the hydrometer started high, near 90% ABV and gradually decreased during the vapor flow period. However, it was also observed that in the beginning of a vapor flow period, the hydrometer reading would increase about 3-5% from what it was at the end of the liquid flow period. Both phenomena can be explained by the collected and essentially re-distillation of the column and piping vapor and liquid contents. Rather than allowing the feed to vaporize and condense and increasingly become less concentrated as the distillation continues, some of the ethanol and other alcohols return to the pot and column, therefore causing a disruption in this trend.

Lastly, Figures 5.21-22 display that the temperature in the column and top of the still helmet increase at a slower rate during cyclic distillation compared to during conventional operation. The temperature profiles were as expected because as the ethanol concentration decreases, the water concentration increases. Since water has a higher boiling point than ethanol, when there is a lower mole fraction of ethanol, the boiling point of the mixture is expected to increase. As the ethanol concertation decreases at a slower rate throughout the pot and column, the temperatures will increase at a slower rate as well.

6.2.2 Component Concentration Trends

Some compounds were not affected by cyclic operation including acetaldehyde, acetone, and ethyl aetate. The trends can be seen in Figures 5.4 -5.6. This makes sense because of the relative boiling points of these compounds compared to ethanol. The boiling point of these compounds are all lower than ethanol, therefore they are concentrated in the distillate in the beginning of the distillation and are not subject to cyclic operation.

Methanol also has a lower boiling point than ethanol (64.7°C) however it is well known in industry and literature to start at a high concentration in the heads, decrease throughout the hearts cut and then increase again in the tails cut. The trend observed in Figure 5.7 is like the trend Claus and Berglund found in distilling a cherry distillate [43].

Higher alcohols including propanol, isobutanol, butanol and isoamyl alcohol with higher boiling points than ethanol all exhibited similar trends and trend changes. A normal trend seen in the previous report is a gradual increase from the beginning to the end of the distillation and a big increase in the tails fraction [43]. This trend was inverted for the distillations when the reflux was not engaged to the partial condensers. When the partial condensers are active, the vapor the heavier and less volatile components of the vapor that travels through them are more likely to condense in turn holding them back from entering the final condenser and into the distillate.

6.2.3 Low Wines vs Finishing Tends

Cyclic distillation of low wines did not seem to have any noticeable changes when compared to conventional distillation of low wines. The efficiency measures compared in Figure 5.13 and 5.14 show conventional operation to be more efficient than cyclic operation. This is attributed to the fact that the initial ABV of the feed is very low, roughly 10% ABV and that there are only three trays which can allow cyclic distillation to occur. In distilled sprit products this is one of the most energy intensive operations, because it takes more energy to heat a mixture that is 90% water than a mixture that is 70-75% water, and thus would be an ideal application of the benefits of cyclic distillation. It is believed that with more trays and trays that allow true plug flow, the energy saving advantage of cyclic distillation would be observed.

Increases in efficiency measures were seen in the finishing runs observed in Figures 5.15-17. In cyclic distillations D13-D15 the ABV reading on the hydrometer remained higher for longer compared to the identical distillation D11 for the reasons already explained in the 'All Distillation Discussion.' Additionally, the steam usage per proof gallon distilled was the lower for D13-D15 compared to the identical conventional operation D11, proving an increasing in energy efficiency. Lastly, the percent recovery values were too spread out to be able to confirm the percent recovery was better in cyclic versus conventional operation.

6.2.4 Effects on Cuts

The last five distillations were used to identify what effect cyclic distillation had on the heads, hearts and tails cuts. The results can be referred to in Table 5.3 and Figures 5.18 -20. The heads cut was statistically smaller during cyclic operation than in conventional operation. The hearts cut was larger for cyclic operation than in conventional operation and lastly the tails cut was drastically smaller for cyclic operation than in conventional operation.

This is best explained by the earlier mentioned phenomenon that the ethanol concentration stays higher for longer throughout the distillation during cyclic operation. If the ethanol concentration remains high and the fusel oils/ congeners do not start coming through, the distillate remains clean and pleasant to the distiller and the hearts cut increases in proof gals. This consequence allows most of the ethanol to remain in the hearts cut. Since the proof gallons collected in the hearts cut increased, the proof gallons in the tails cut decreased.

Based on the previous observations it can be concluded that cyclic distillation causes an increase in proof gallon of hearts. This in turn increases the production efficiency and decreases energy requirement per proof gal of product. In addition, decreasing the volume of by products produced reduces the storage and processing requirements, decreasing cost per proof gal produced.

6.2.6 Reflux Observations and Discussion

It was observed that regardless of mode of operation, when reflux to the partial condenser was turned on a smaller volume of hearts was collected, however it was higher in alcohol by volume. This is because when the partial condensers are active, they act as an additional stage by sending some condensed vapor to the preceding tray or to the reboiler/pot, depending on the location of the partial condenser. When the partial condensers are not active, vapor travels past this ‘stage.’ Overall, not having the partial condensers active causes less rectification in the column therefore it is suitable to assume they will be used when making most types of spirits.

6.2.7 Simulation Discussion

Results from the simulation and modeling of conventional and cyclic operation can be seen in Figures 5.23 -5.26 and Figures 5.27-5.30, respectively. The trends seen in the data were also seen in the simulations. Temperatures in conventional operation increased at a faster rate than in cyclic operation. Distillate ethanol concentration decreased over time at a faster rate than in cyclic operation. During cyclic distillation modeling, some of the ethanol is transferred to the tray below, causing the ethanol to be held back in the column and thus the tray composition to increase and decrease slightly from cycle to cycle. This trend of cyclic tray composition is seen graphically in Figure 5.29. The model calculates the temperature based on the ethanol composition, therefore temperature and concentration are directly proportional and can be seen in Figure 5.30.

Lastly, given the same processing time cyclic operation was able to process less moles in the pot than in conventional operation. This was also seen in the data and can be explained on the basis that during the liquid flow period, no distillate is collected, leading to a longer distillation time.

6.3 Limitations and Sources of Error

One key limitation is the lack of separation between liquids drained from tray to tray. The trays in the Carl still have small holes that allow the liquid to fall to the previous tray regardless of whether it is during the vapor flow or the liquid flow period. Therefore, it was not possible to separate the liquid hold up traveling from tray to tray during each liquid flow period. Since the still used was not specifically designed for cyclic distillation, the still was not able to achieve the 200% efficiency increase predicted by theoretical models.

Is it important to note that cuts are taken by the distiller and are predominantly made by sensory analysis. In industry, it is common for distillers to go through specific sensory training to become more attune with the flavor and aroma of the compounds in the spirit. The distiller of this research has two-year part-time experience distilling which is more than the average researcher, but less than a full-time trained distiller. Many factors play a role in sensory analysis including what and what time the distiller has last ate or drank can affect the sensory perception, therefore cuts cannot be 100% consistent.

Another important note is the inconsistency of initial volume and proof gallons in the feed. When large volume and large equipment is used, it becomes increasingly hard to duplicate an exact volume and initial ABV due to the necessary pumping into the still, and losses associated with the hoses.

6.4 Recommendations for Future Research and Application

It is strongly suggested that cyclic distillation be applied to other types of spirits. This research was solely based on brandy made from fermented apple cider, both the stripping and the finishing runs. While the energy requirements are mostly likely the same, different spirits are fermented with different yeast strains and ultimately have very different components and concentrations of key flavor and aroma attributes. Rum, whiskey, gin and vodka production are all sprits that can be further investigated. Legally, vodka must be distilled to 95% alcohol by volume, so its production requires more trays than all other spirits. Therefore, the application of cyclic distillation for vodka production is a promising addition to this research for both energy conservation and efficiency purposes. In addition to other spirits, implementing the already designed Maleta© trays or a new tray design which maximizes true plug flow would increase the positive effects of cyclic distillation.

APPENDICES

APPENDIX A: Graphical Distillation Results

Tray by Tray Results:

Distillation

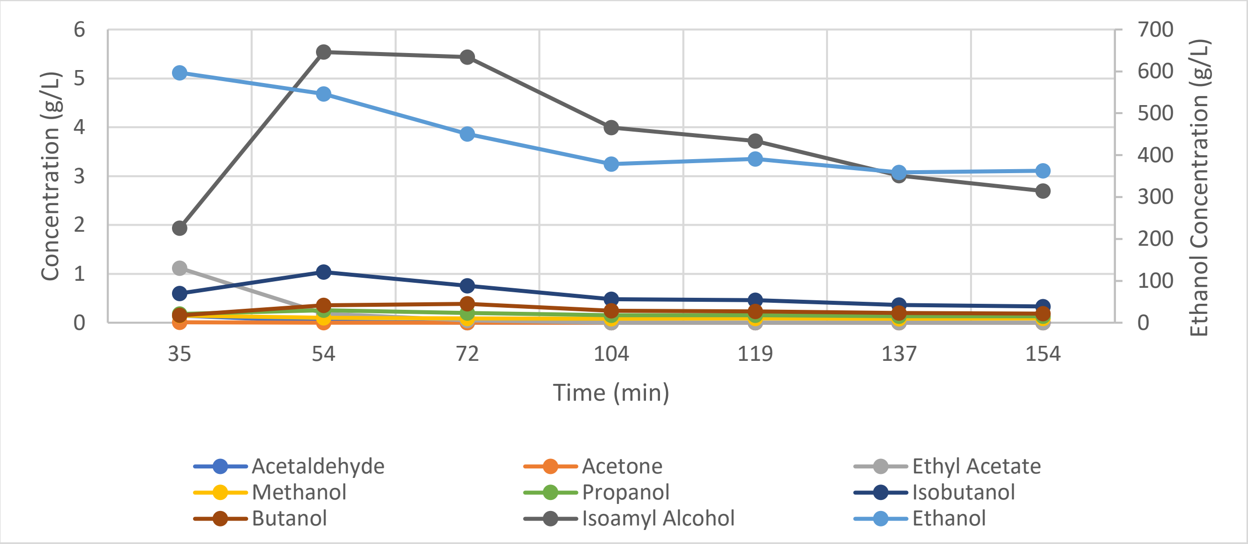

Figure A.1 Normal Operation 1, Tray 1 Graphical Results

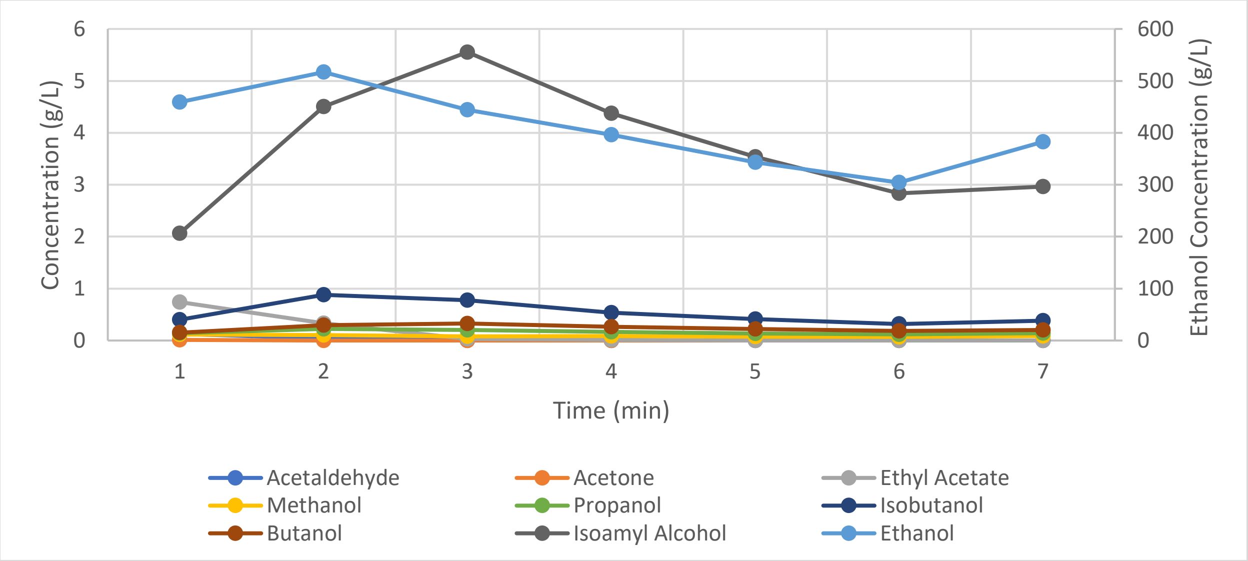

Figure A.2 Normal Operation 1, Tray 2 Graphical Results

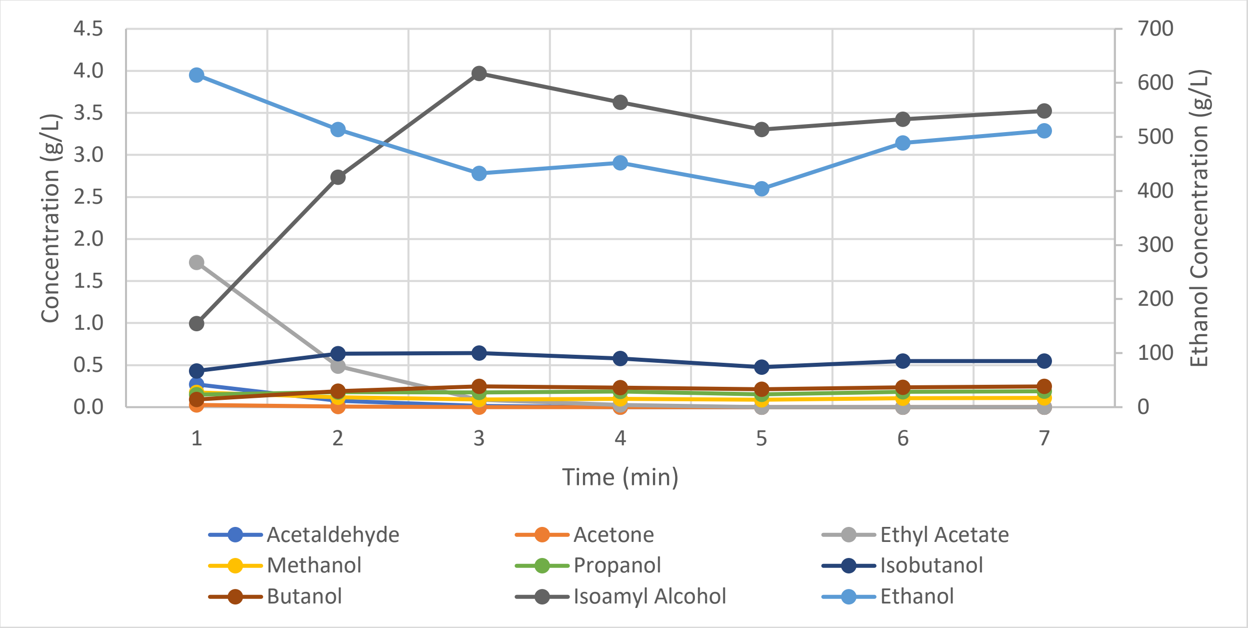

Figure A.3 Normal Operation 1, Tray 3 Graphical Results

Distillation 2

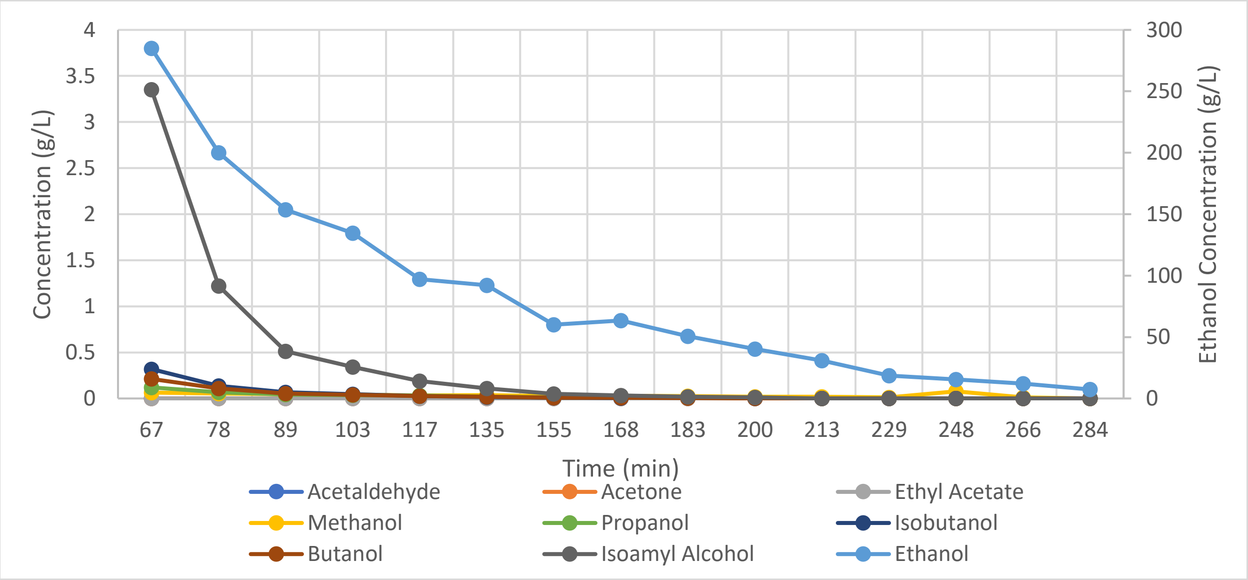

Figure A.4 Normal Operation 2 , Tray 1 Graphical Results

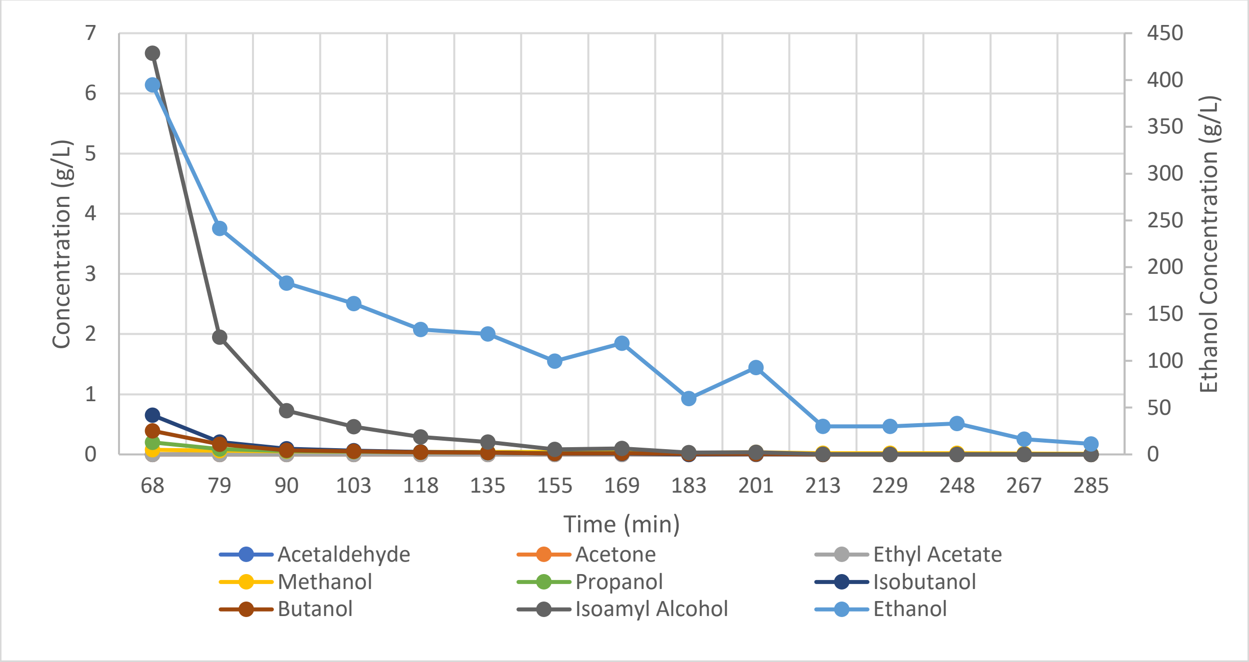

Figure A.5 Normal Operation 2 , Tray 2 Graphical Results

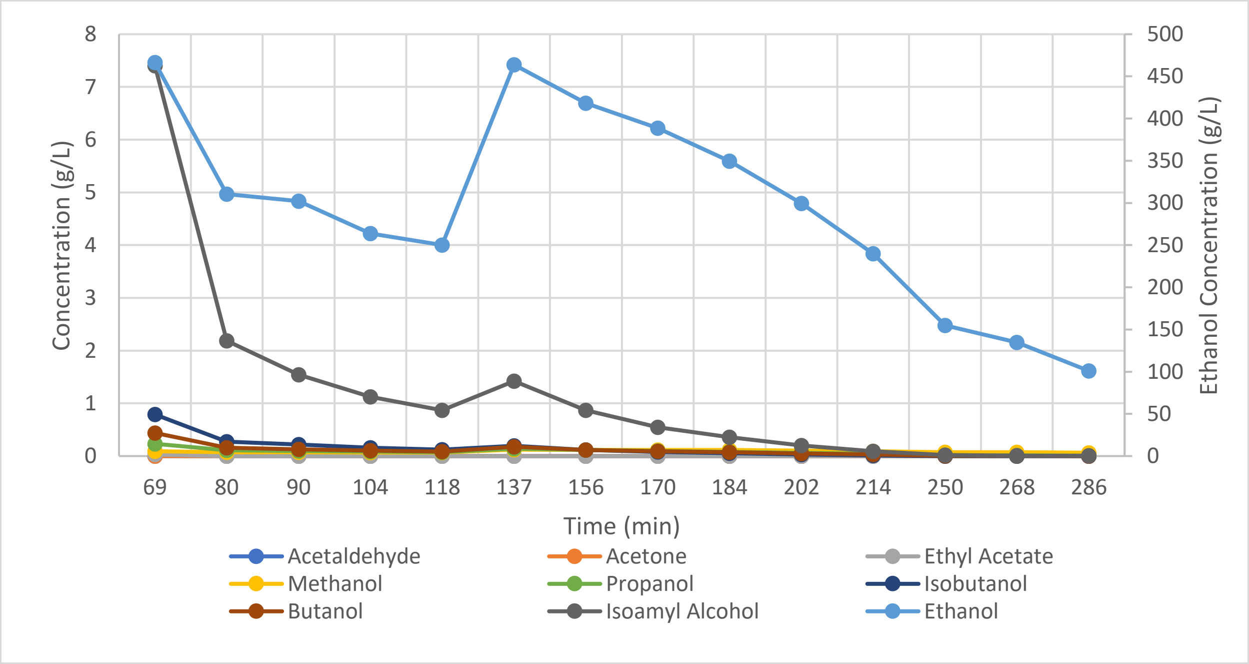

Figure A.6 Normal Operation 2 , Tray 3 Graphical Results

Distillation 3

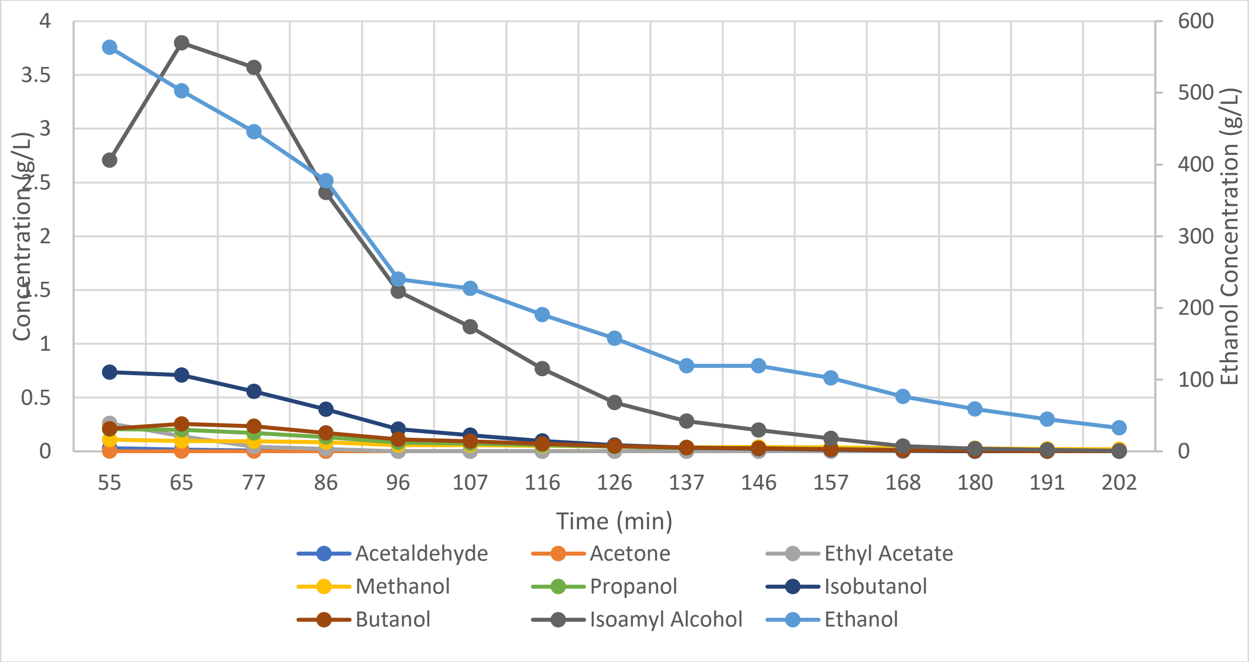

Figure A.7 Normal Operation 3 , Tray 1 Graphical Results

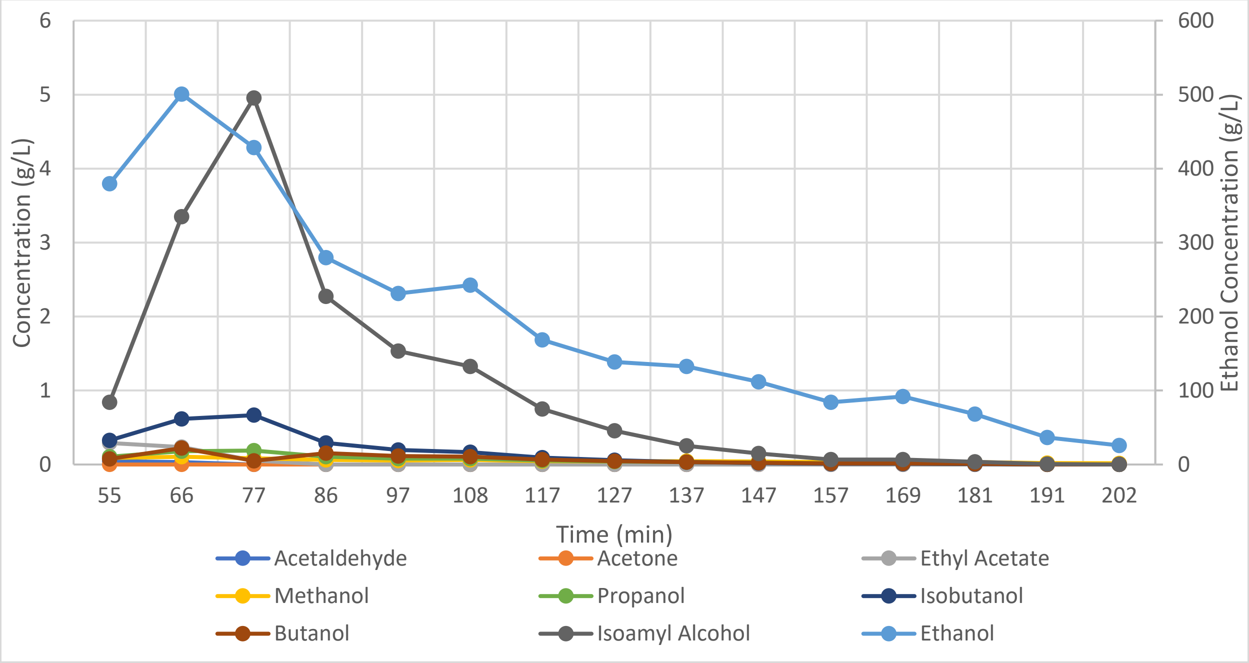

Figure A.8 Normal Operation 3 , Tray 2 Graphical Results

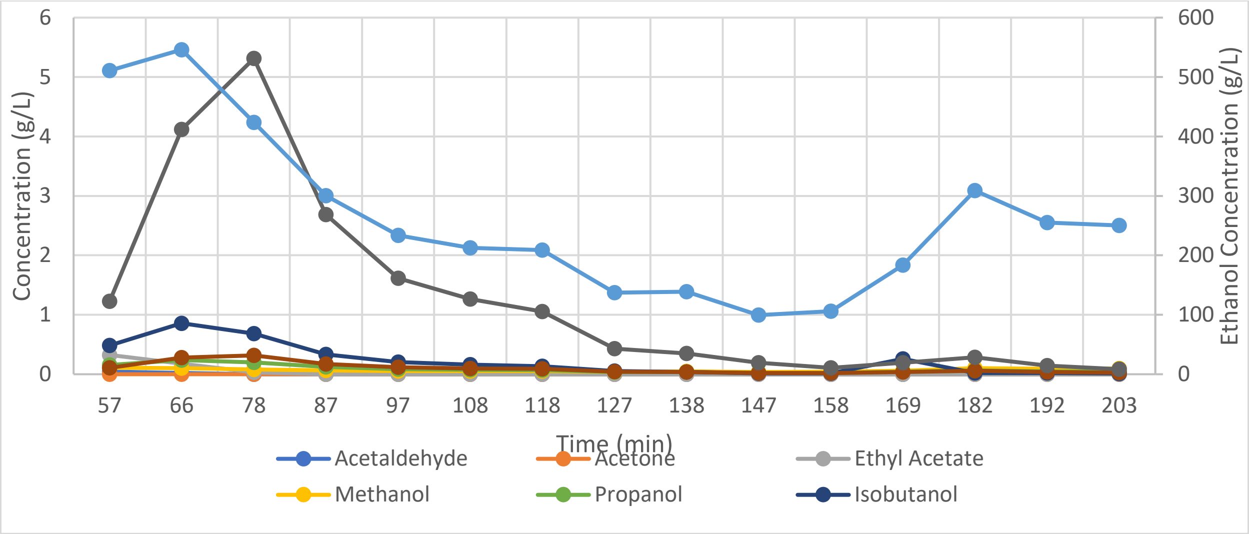

Figure A.9 Normal Operation 3 , Tray 3 Graphical Results

Distillation 4

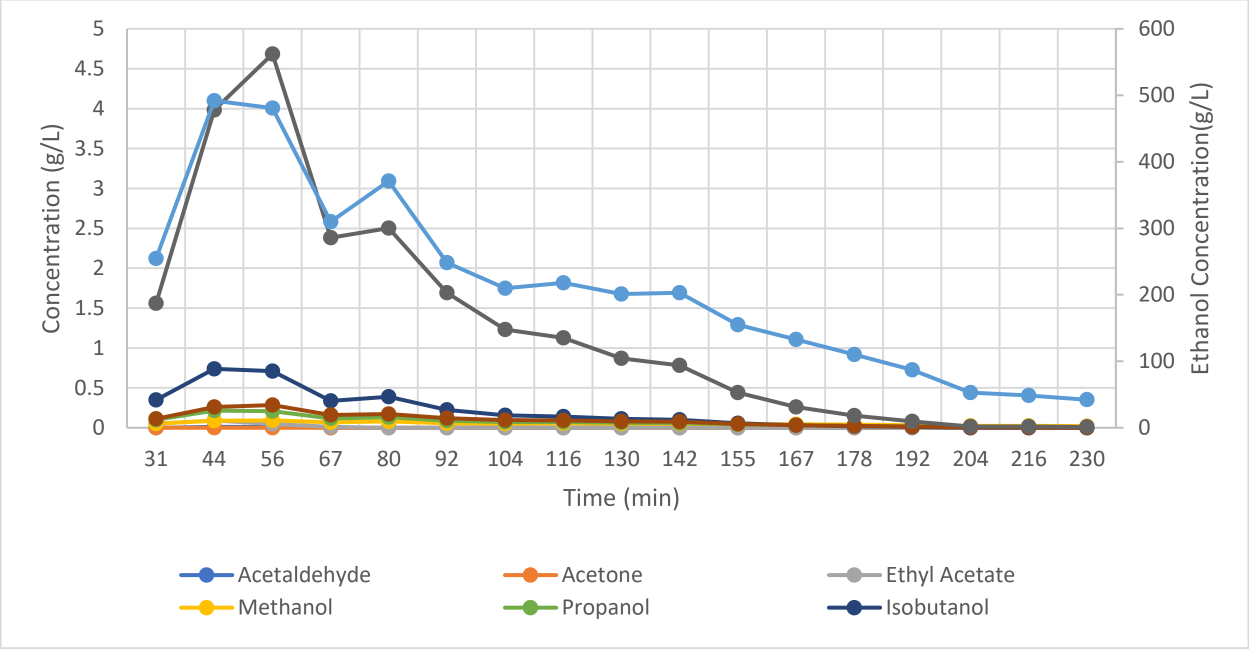

Figure A.10 Cyclic Distillation 1 (Vapor 9 min, Liquid 3 min) , Tray 1 Graphical Results

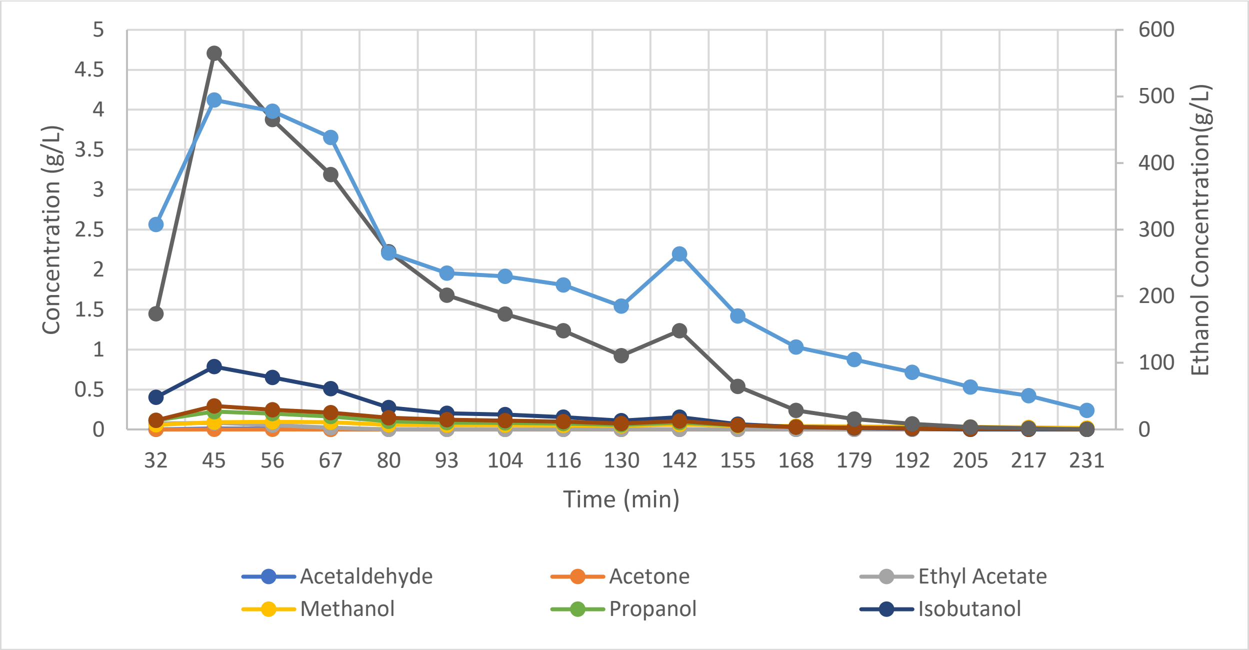

Figure A.11 Cyclic Distillation 1 (Vapor 9 min, Liquid 3 min) , Tray 2 Graphical Results

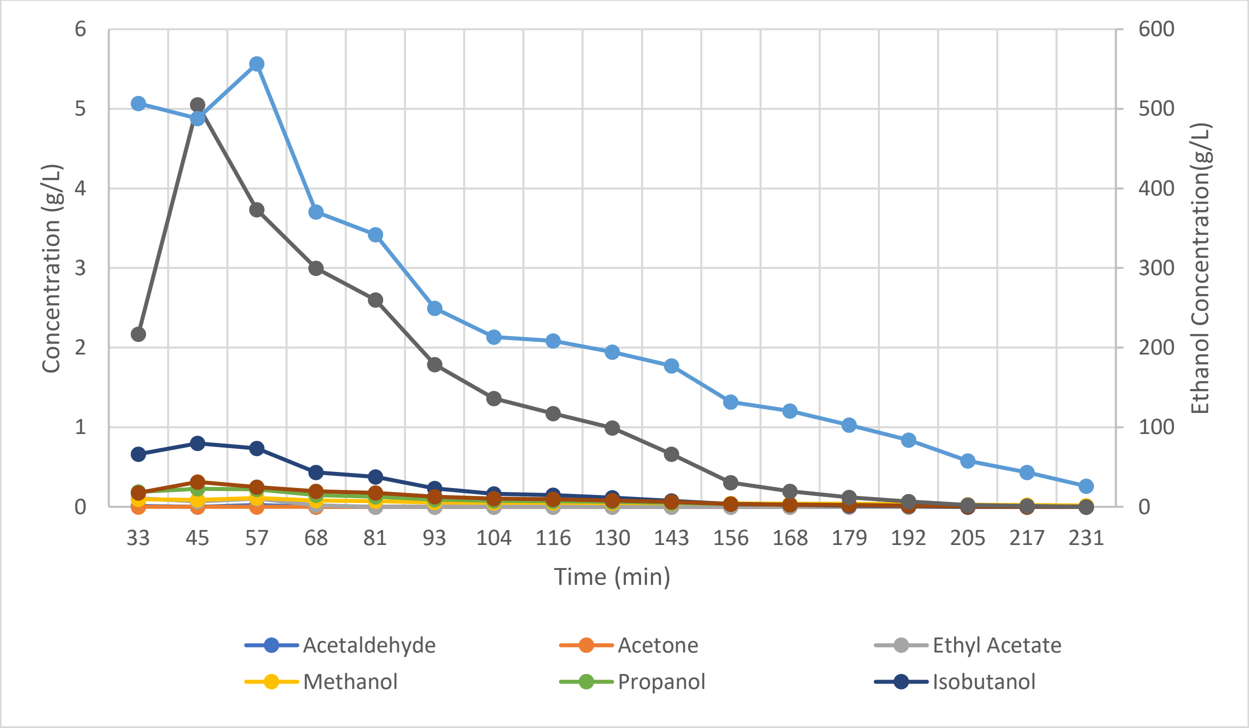

Figure A.12 Cyclic Distillation 1 (Vapor 9 min, Liquid 3 min) , Tray 3 Graphical Results

Distillation 5

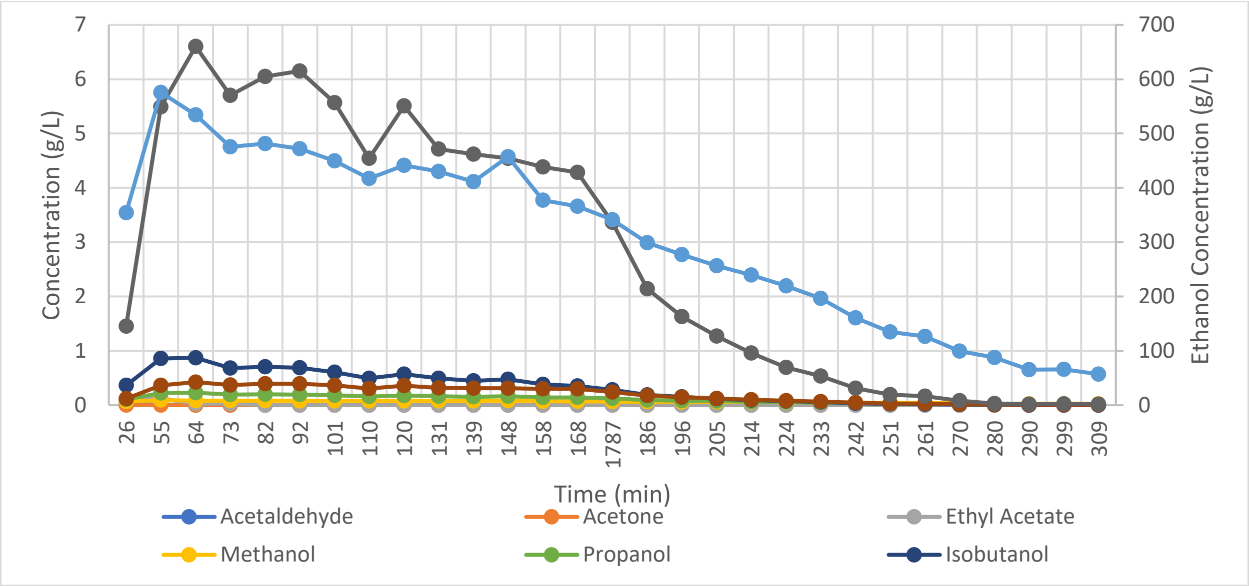

Figure A.13 Cyclic Distillation 2 (Vapor 6 min, Liquid 3 min) , Tray 1 Graphical Results

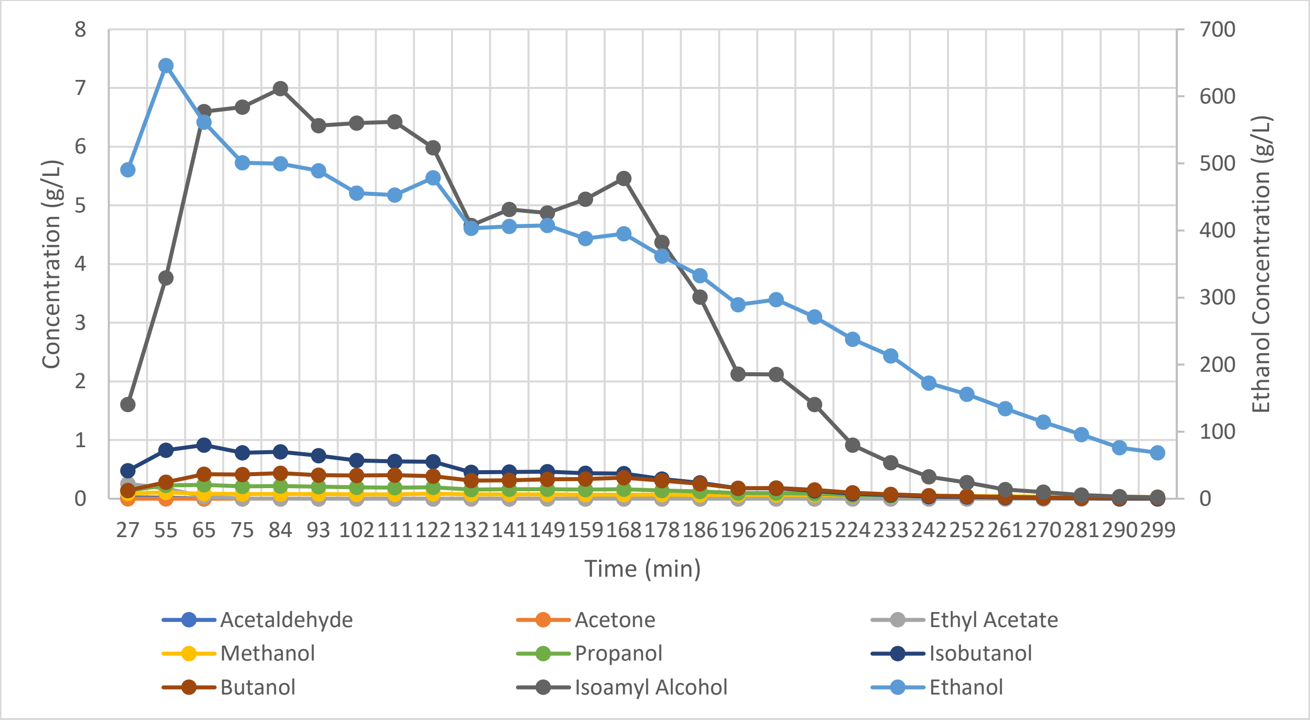

Figure A.14 Cyclic Distillation 2 (Vapor 6 min, Liquid 3 min) , Tray 2 Graphical Results

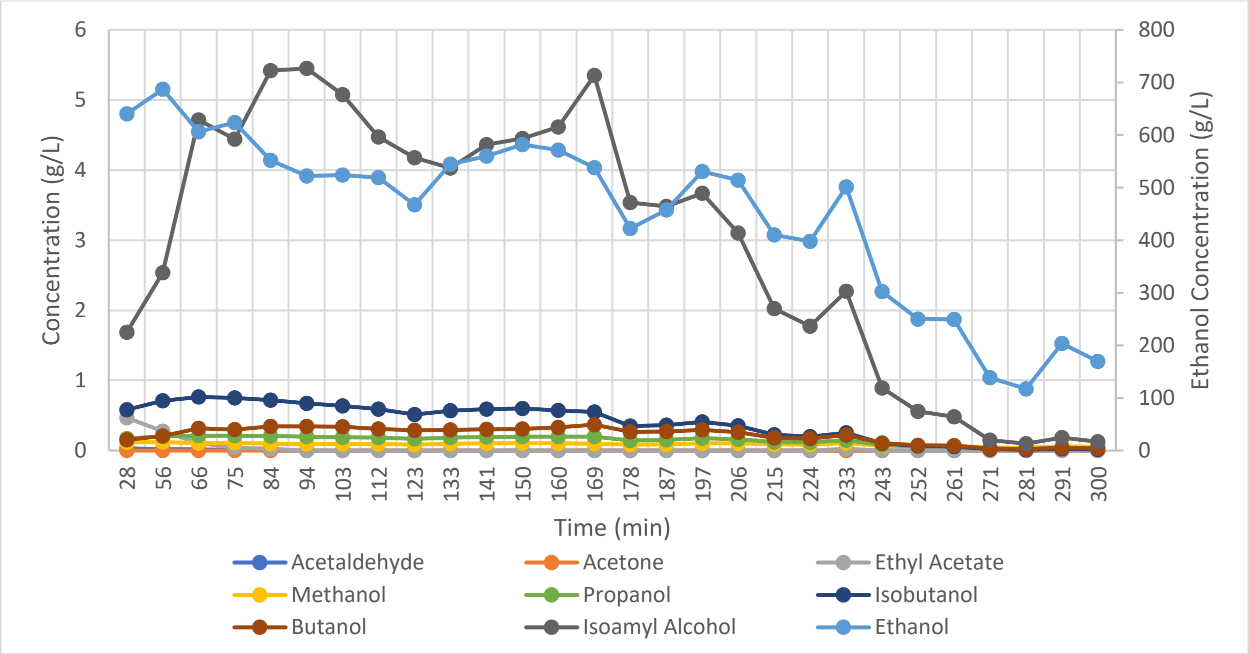

Figure A.15 Cyclic Distillation 2 (Vapor 6 min, Liquid 3 min) , Tray 3 Graphical Results

Distillation 6

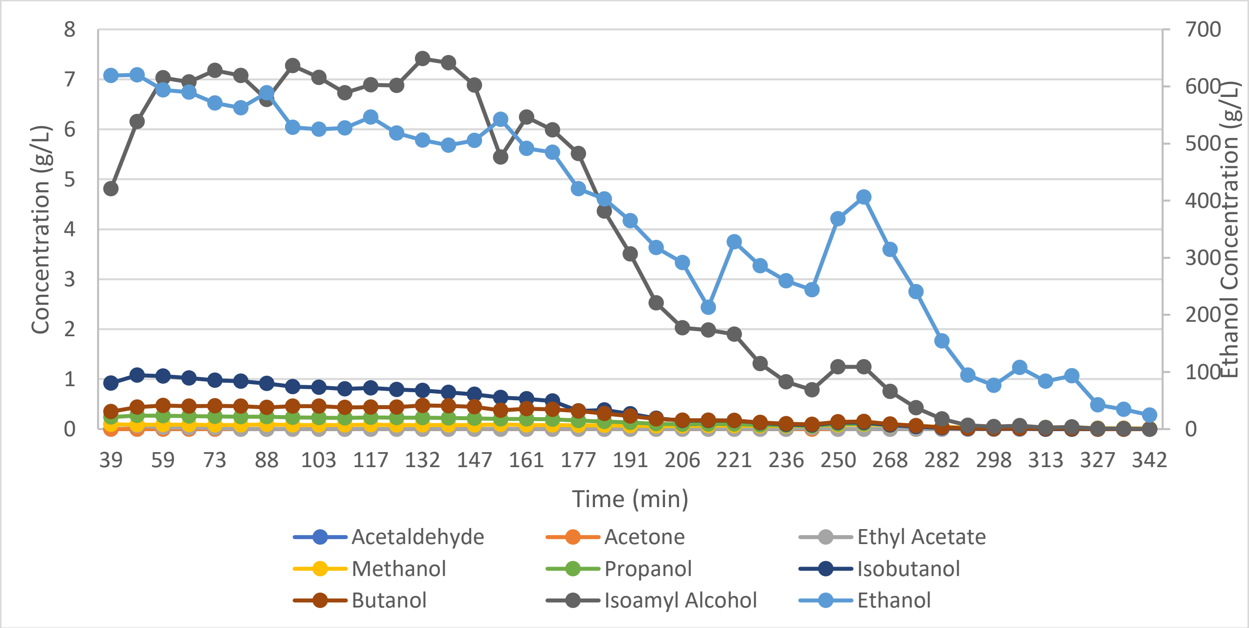

Figure A.16 Cyclic Distillation 3 (Vapor 4 min, Liquid 3 min) , Tray 1 Graphical Results

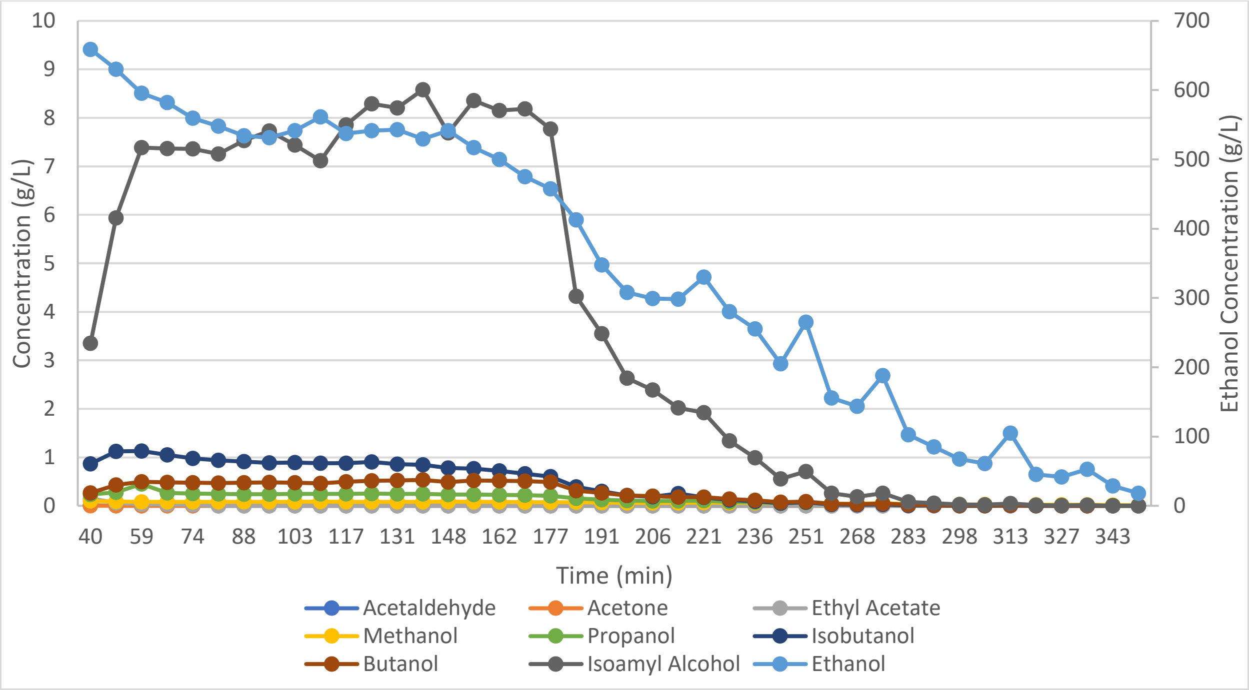

Figure A.17 Cyclic Distillation 3 (Vapor 4 min, Liquid 3 min) , Tray 2 Graphical Results

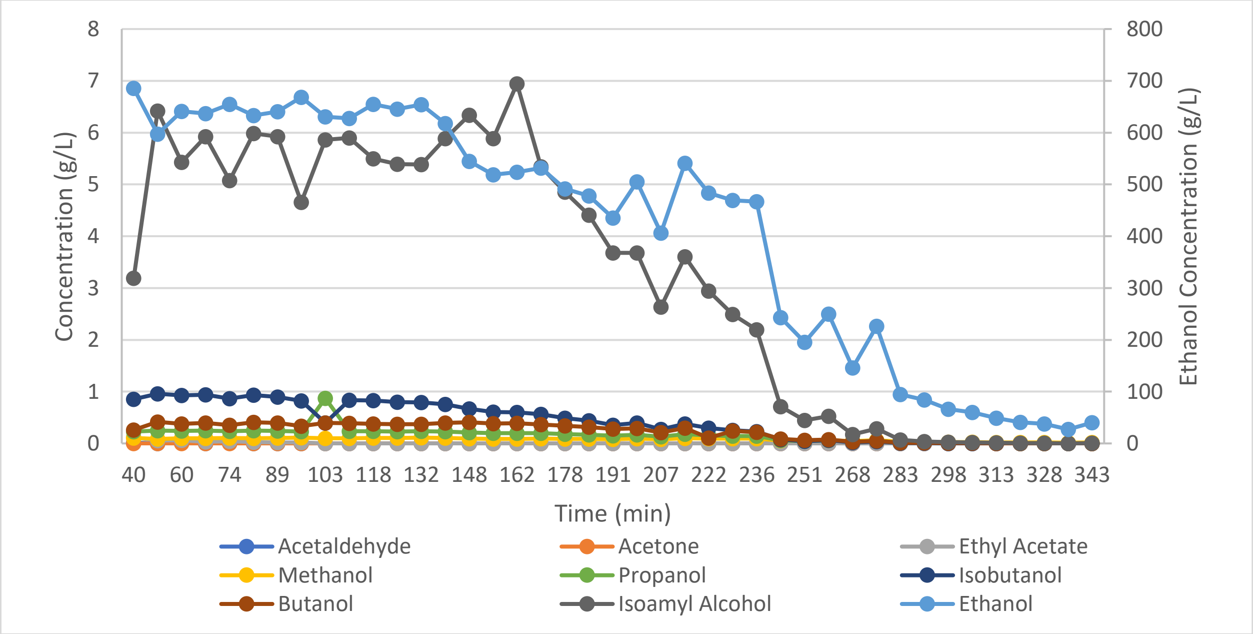

Figure A.18 Cyclic Distillation 3 (Vapor 4 min, Liquid 3 min) , Tray 3 Graphical Results

Distillation 7

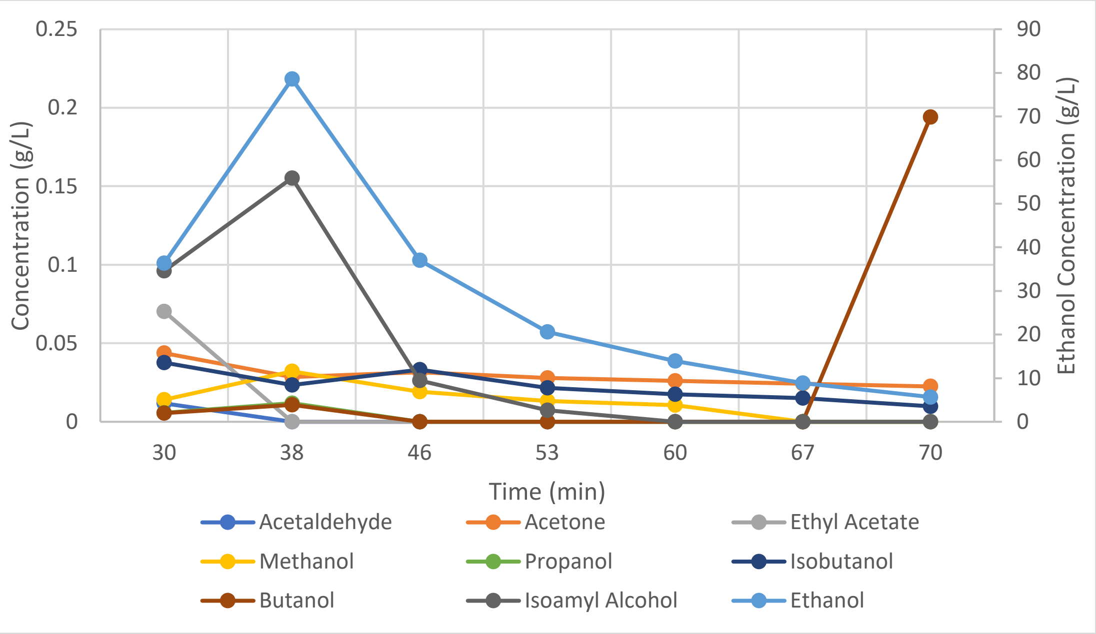

Figure A.19 Normal Operation – Low Wines , Tray 1 Graphical Results

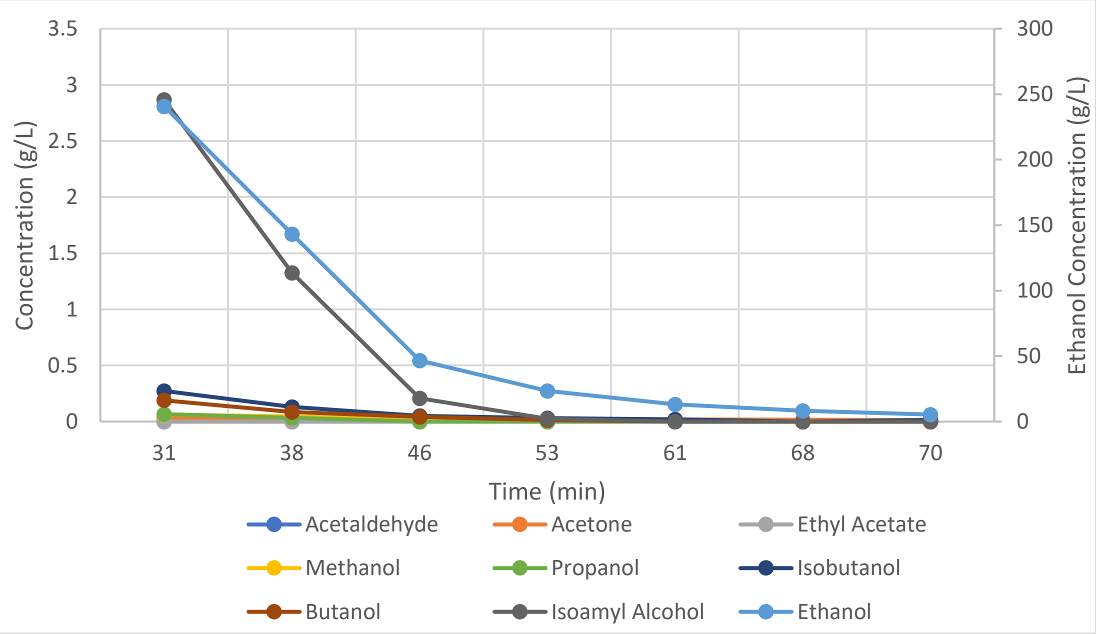

Figure A.20 Normal Operation – Low Wines , Tray 2 Graphical Results

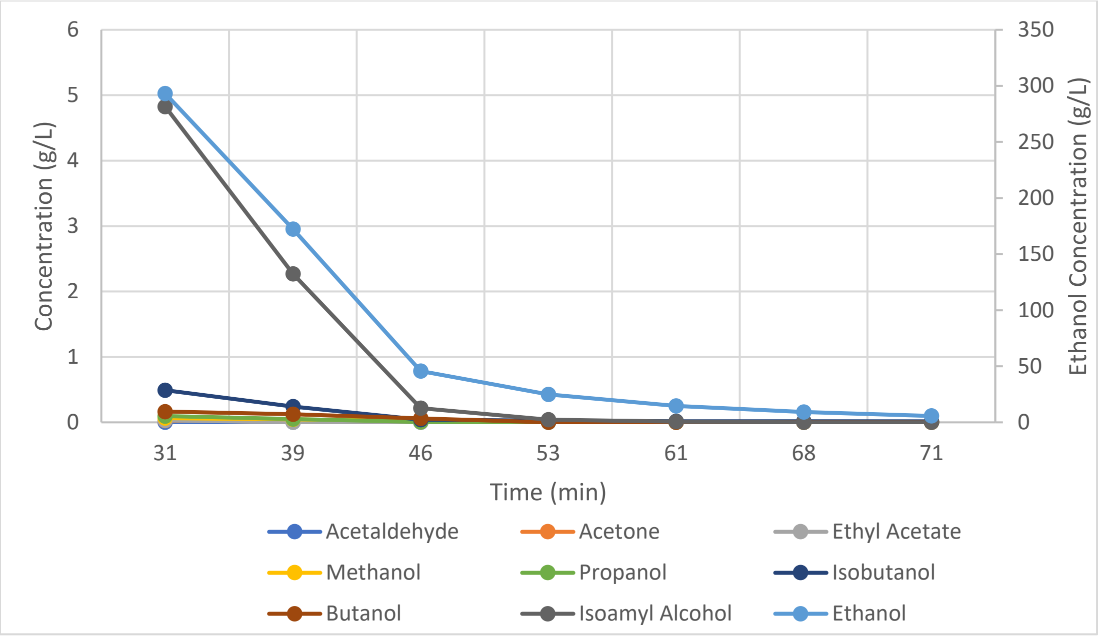

Figure A.21 Normal Operation – Low Wines , Tray 3 Graphical Results

Distillation 8

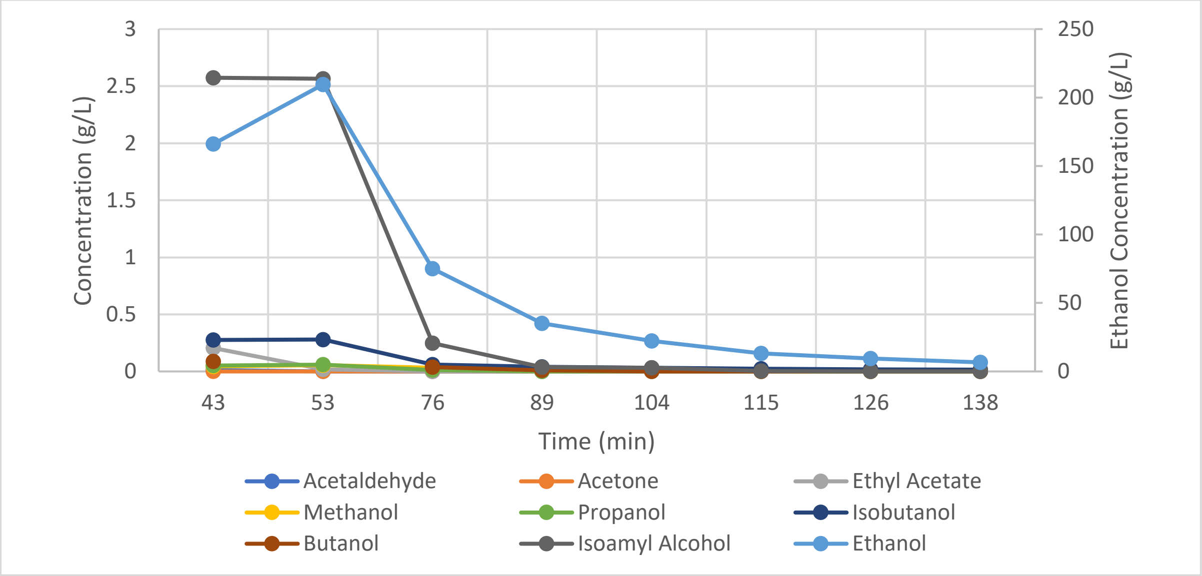

Figure A.22 Cyclic Operation – Low Wines, Cyclic Distillation (Vapor 9 min, Liquid 3 min) Tray 1 Graphical Results

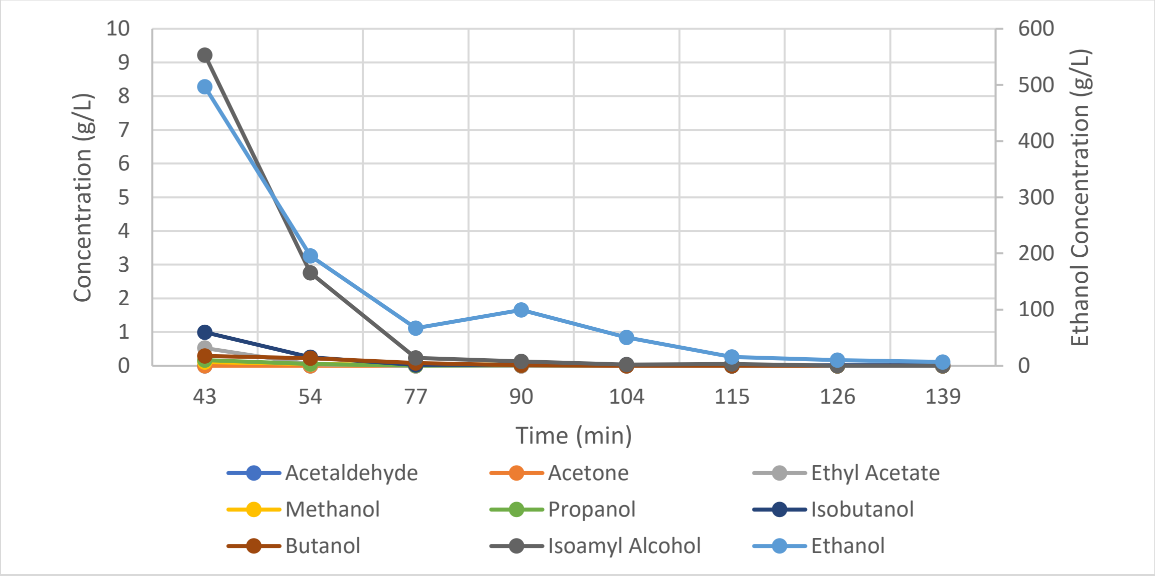

Figure A.23 Cyclic Operation – Low Wines, Cyclic Distillation (Vapor 9 min, Liquid 3 min) Tray 2 Graphical Results

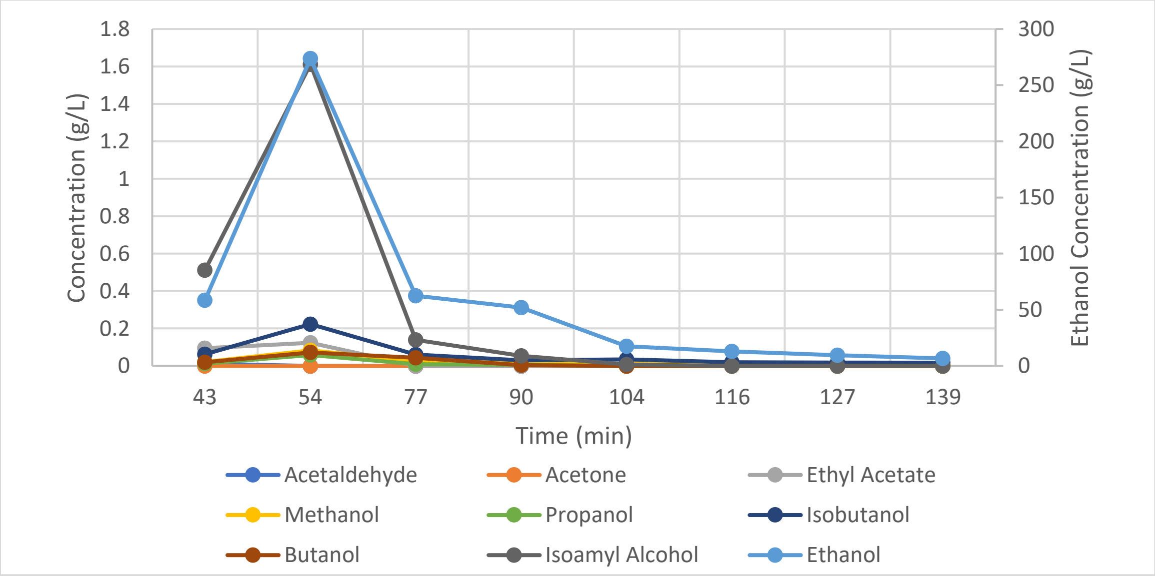

Figure A.24 Cyclic Operation – Low Wines, Cyclic Distillation (Vapor 9 min, Liquid 3 min) Tray 3 Graphical Results

Distillation 9

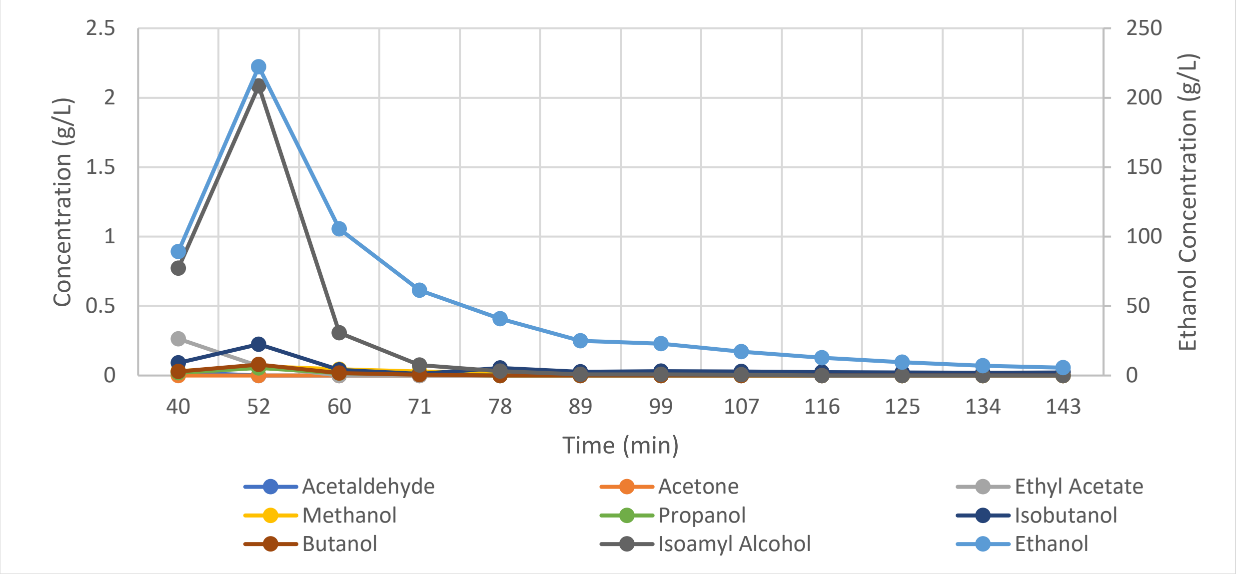

Figure A.25 Cyclic Operation – Low Wines, Cyclic Distillation (Vapor 6 min, Liquid 3 min) Tray 1 Graphical Results

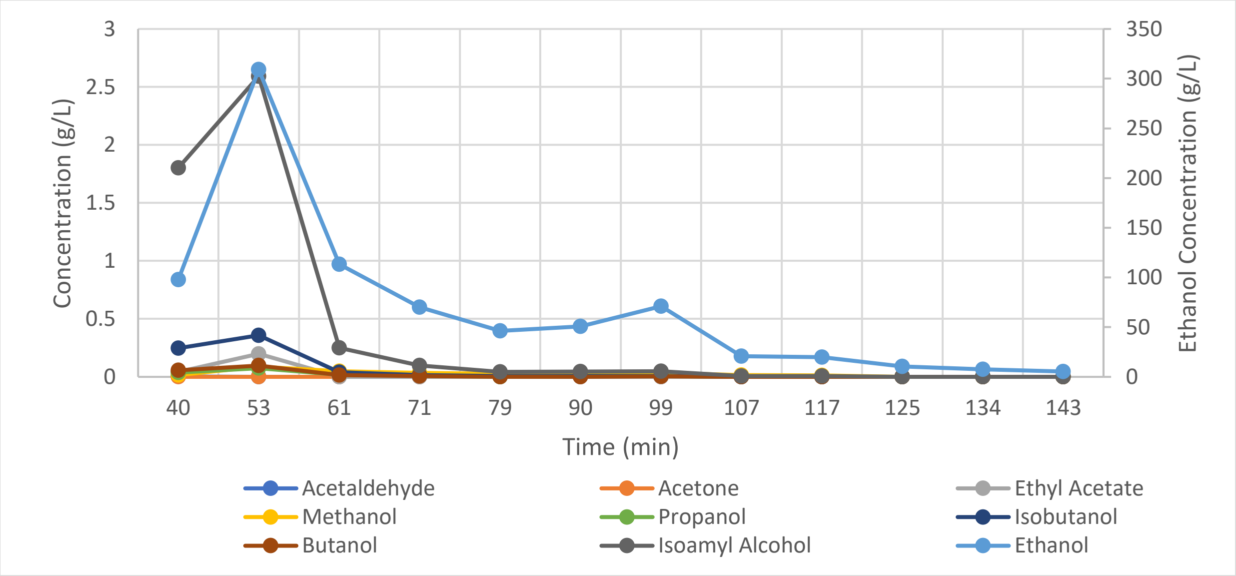

Figure A.26 Cyclic Operation – Low Wines, Cyclic Distillation (Vapor 6 min, Liquid 3 min) Tray 2 Graphical Results

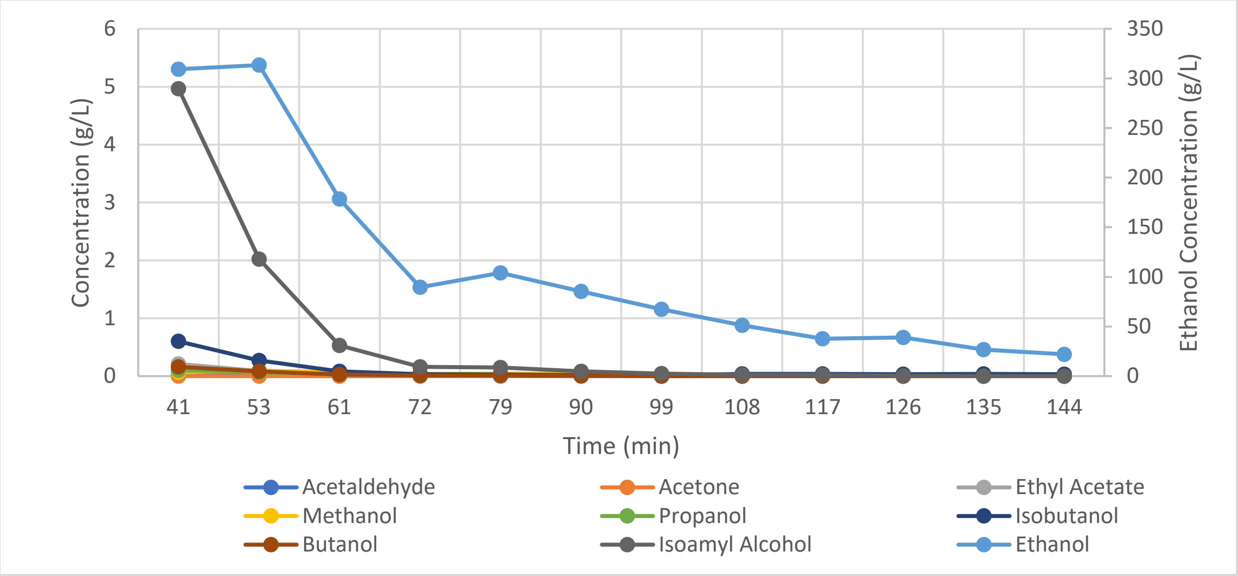

Figure A.27 Cyclic Operation – Low Wines, Cyclic Distillation (Vapor 6 min, Liquid 3 min) Tray 3 Graphical Results

Distillation 10

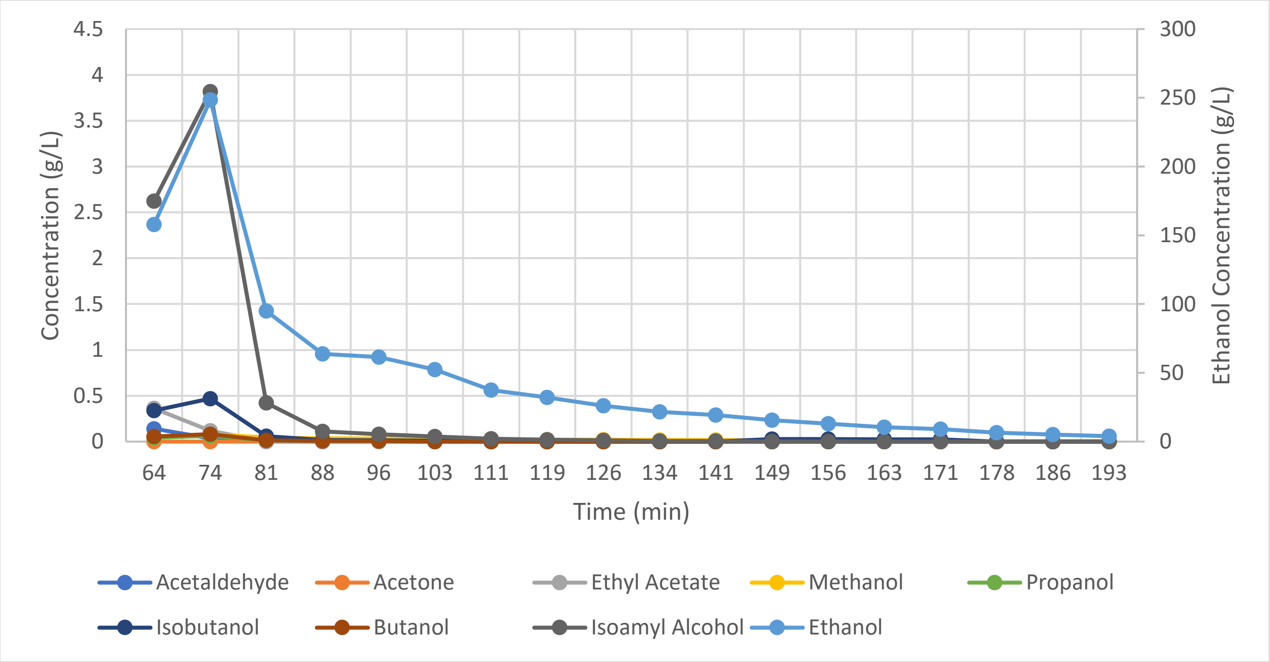

Figure A.28 Cyclic Operation – Low Wines, Cyclic Distillation (Vapor 4 min, Liquid 3 min) Tray 1 Graphical Results

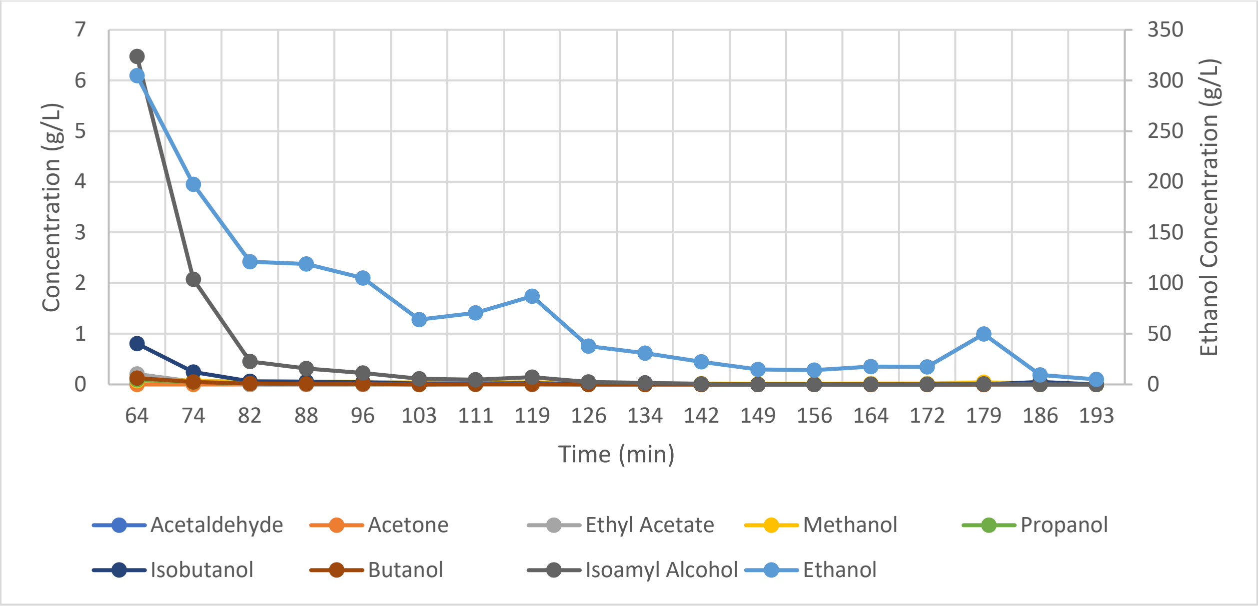

Figure A.29 Cyclic Operation – Low Wines, Cyclic Distillation (Vapor 4 min, Liquid 3 min) Tray 2 Graphical Results

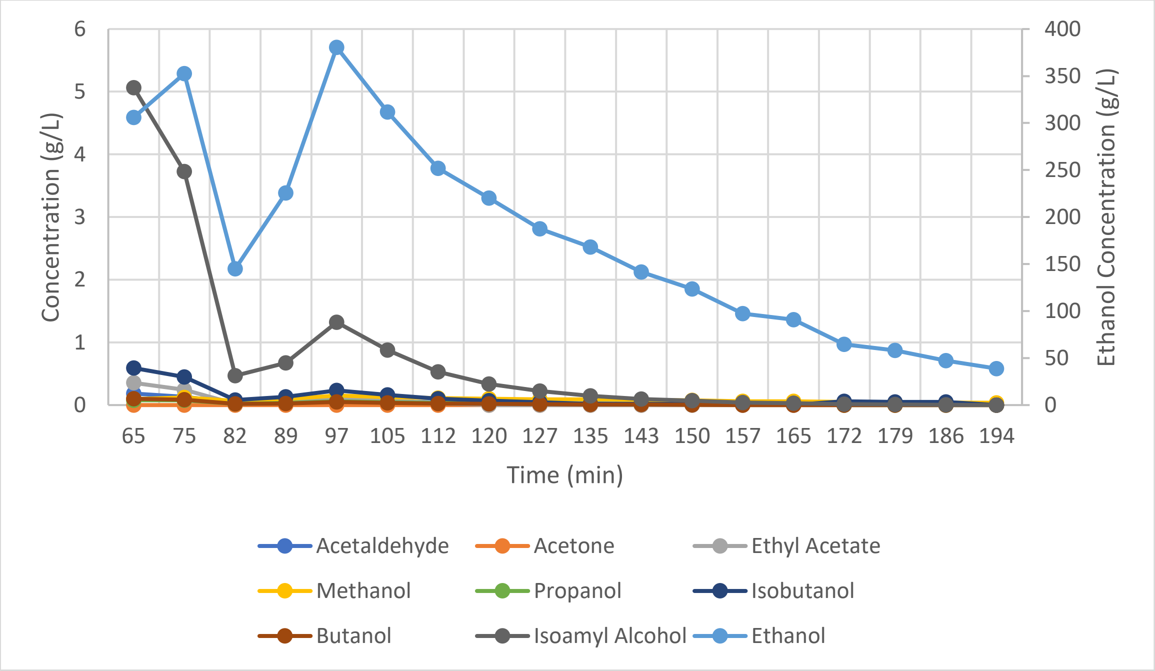

Figure A.30 Cyclic Operation – Low Wines, Cyclic Distillation (Vapor 4 min, Liquid 3 min) Tray 3 Graphical Results

Distillation 11

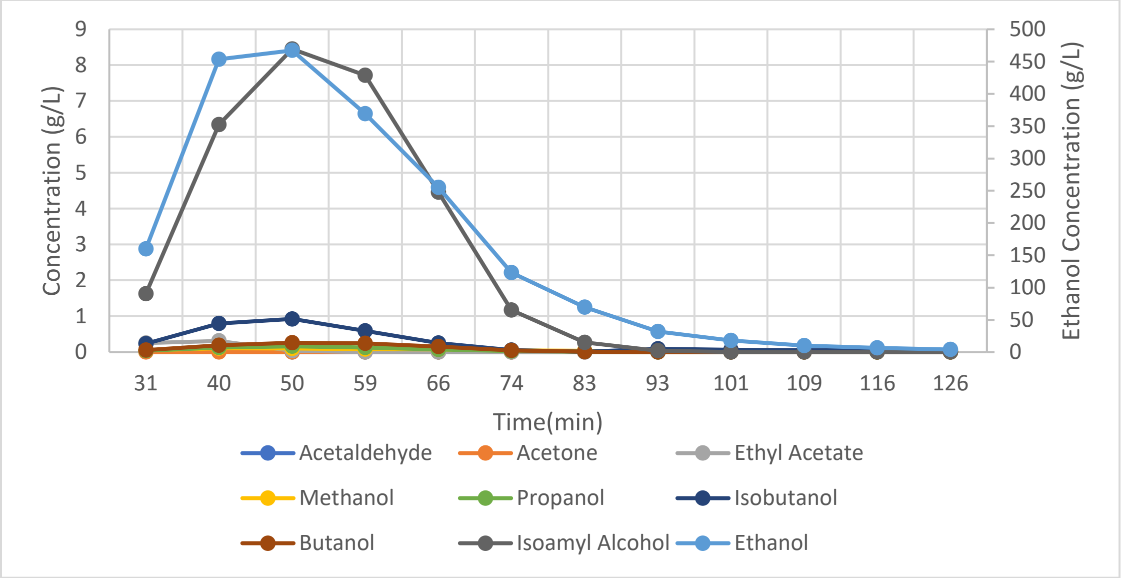

Figure A.31 Normal Operation – Brandy Finishing Run w/ reflux - Tray 1 Graphical Results

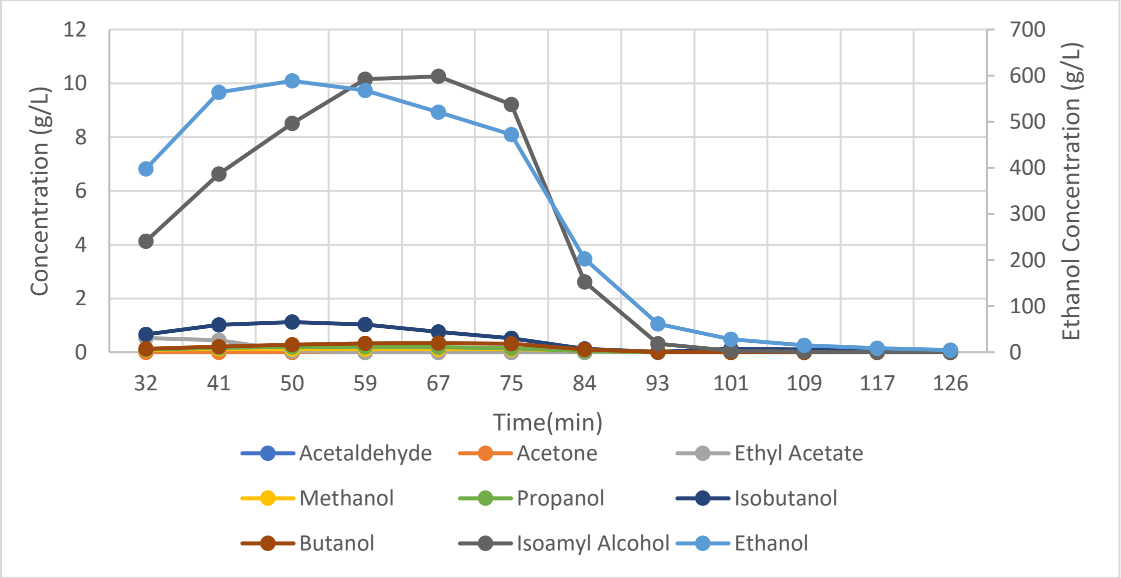

Figure A.32 Normal Operation – Brandy Finishing Run w/ reflux - Tray 2 Graphical Results

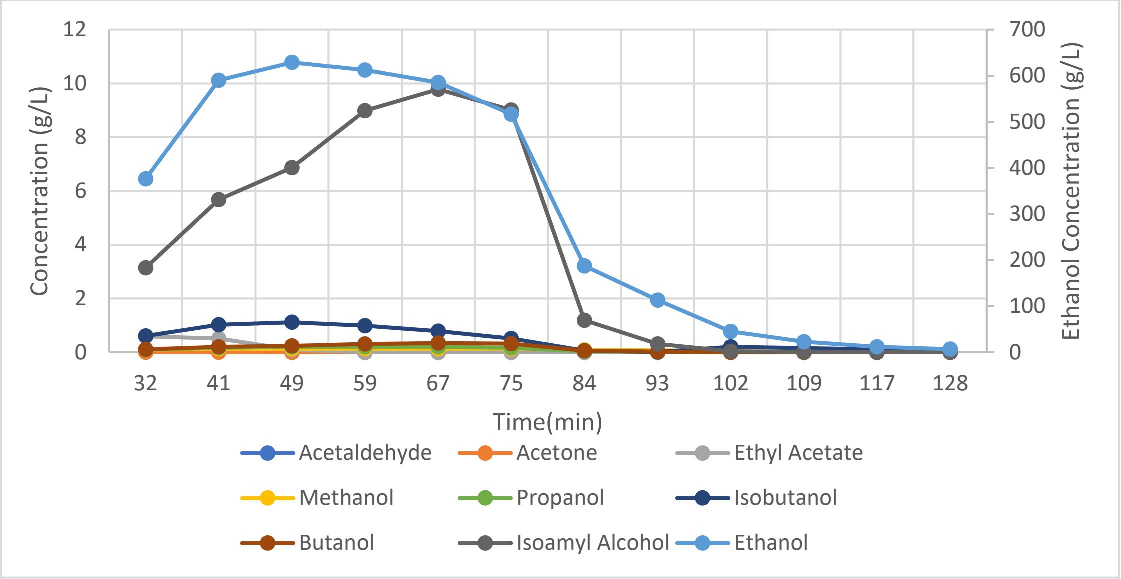

Figure A.33 Normal Operation – Brandy Finishing Run w/ reflux - Tray 3 Graphical Results

Distillation 12

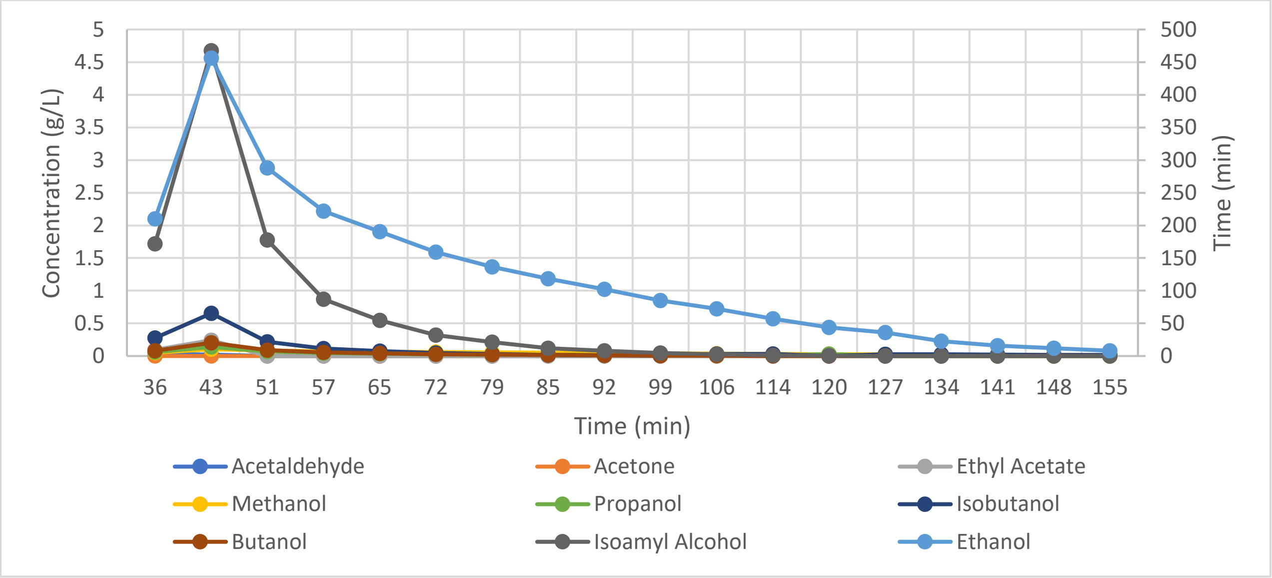

Figure A.34 Normal Operation – Brandy Finishing Run w/o reflux - Tray 1 Graphical Results

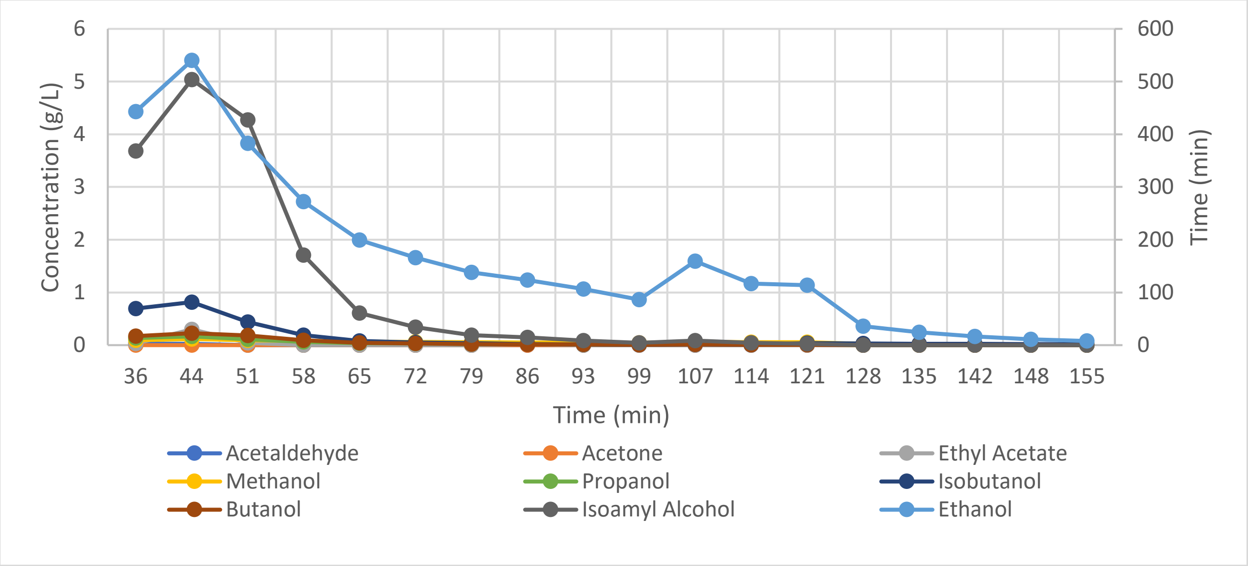

Figure A.35 Normal Operation – Brandy Finishing Run w/o reflux - Tray 2 Graphical Results

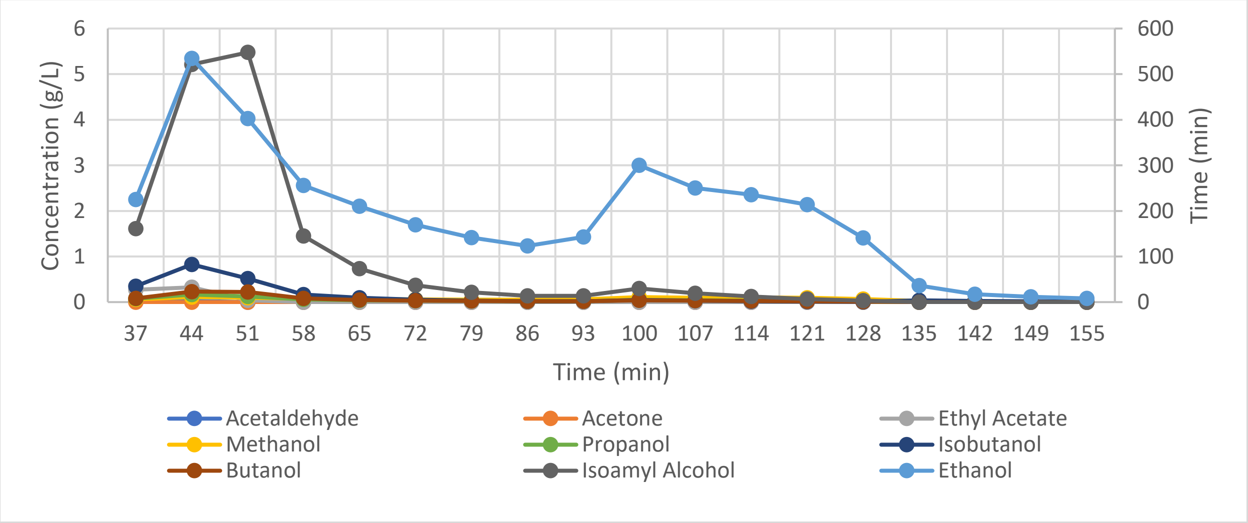

Figure A.36 Normal Operation – Brandy Finishing Run w/o reflux - Tray 3 Graphical Results

Distillation 13

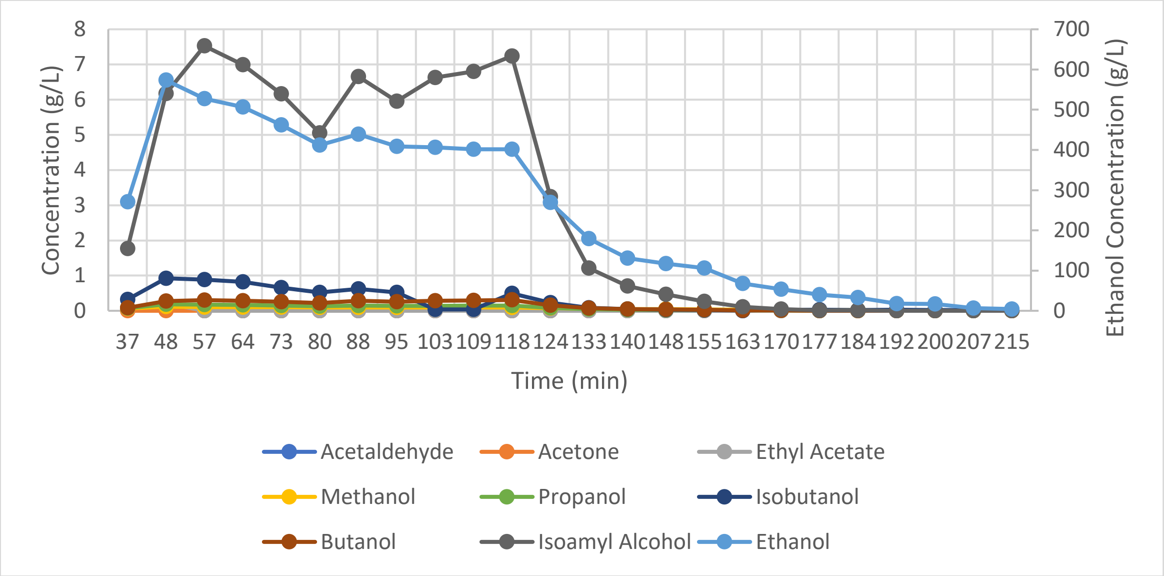

Figure A.37 Cyclic Operation – Brandy Finishing Tray by Tray w/ Reflux - Tray 1 Graphical Results

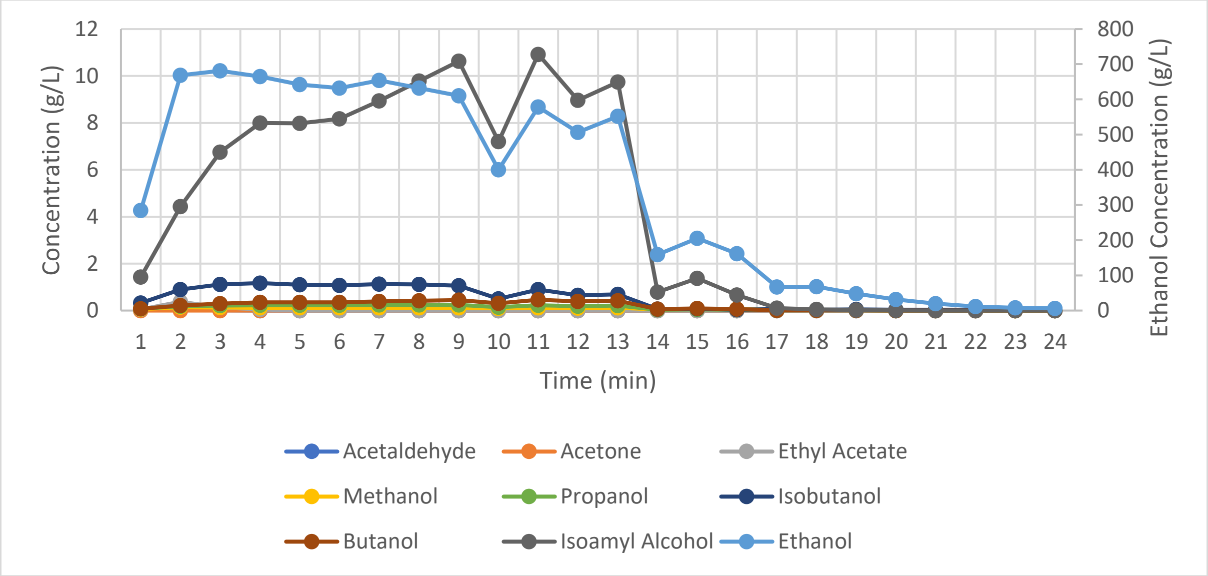

Figure A.38 Cyclic Operation – Brandy Finishing Tray by Tray w/ Reflux - Tray 2 Graphical Results

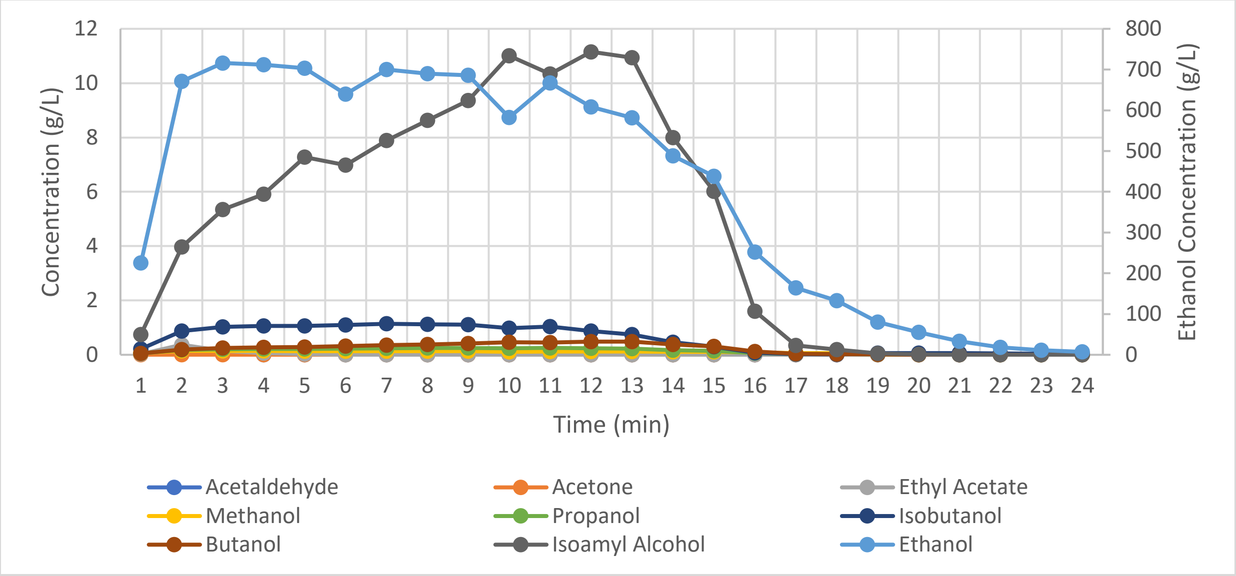

Figure A.39 Cyclic Operation – Brandy Finishing Tray by Tray w/ Reflux - Tray 3 Graphical Results

Distillation 14

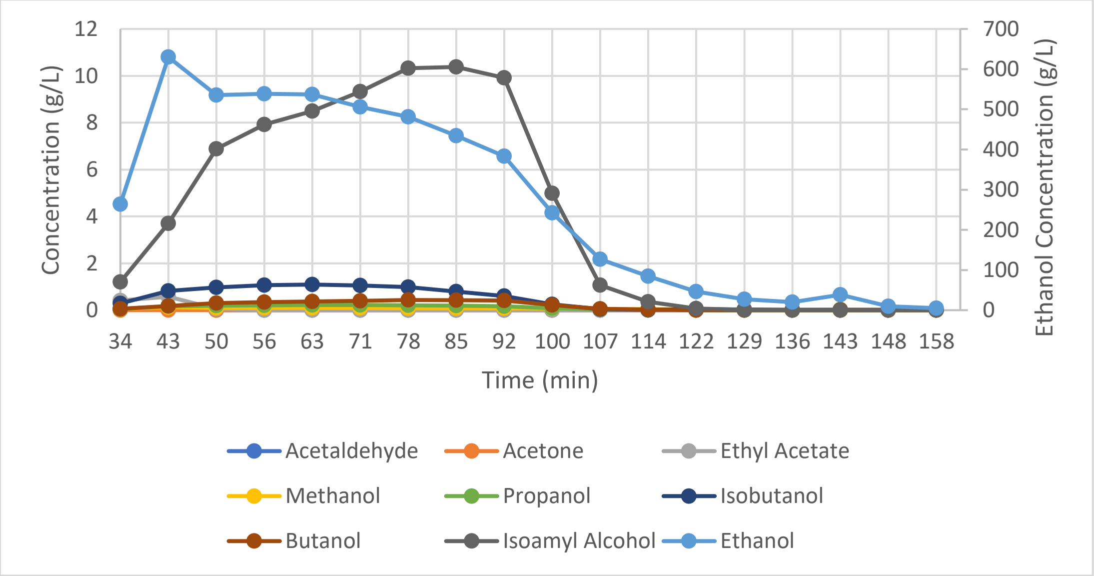

Figure A.40 Cyclic Operation – Brandy Finishing Tray by Tray w/ Reflux - Tray 1 Graphical Results

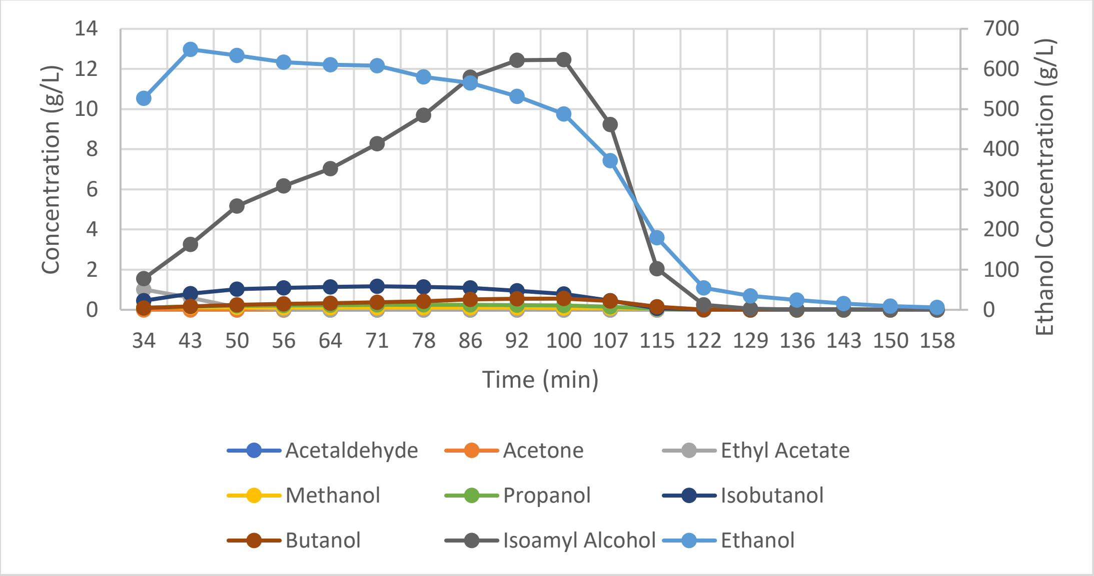

Figure A.41 Cyclic Operation – Brandy Finishing Tray by Tray w/ Reflux - Tray 2 Graphical Results

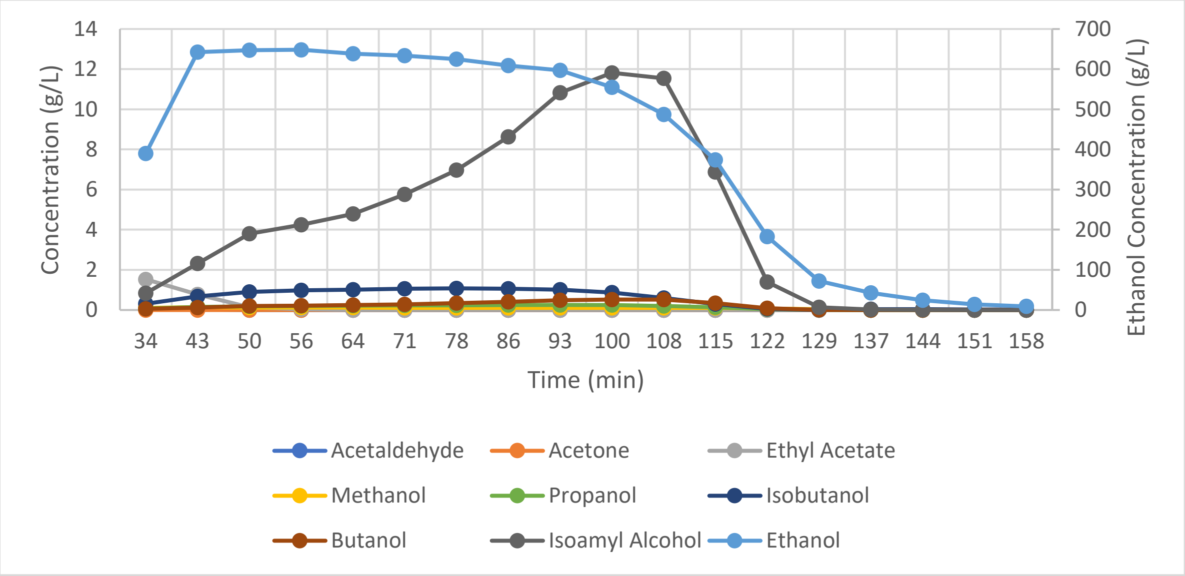

Figure A.42 Cyclic Operation – Brandy Finishing Tray by Tray w/ Reflux - Tray 3 Graphical Results

Distillation 15

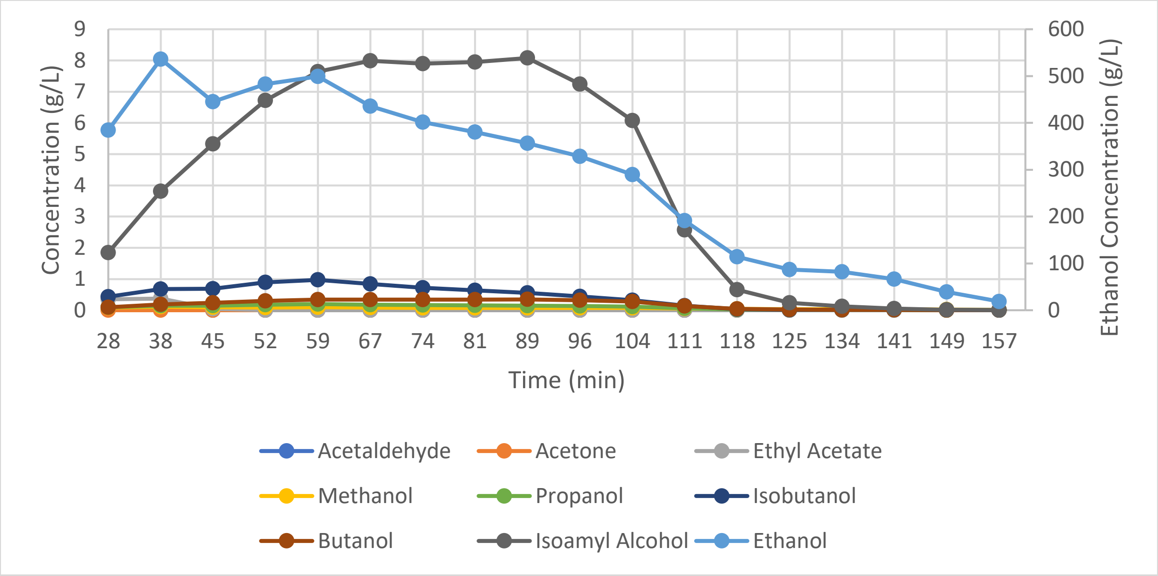

Figure A.43 Cyclic Operation – Brandy Finishing Tray by Tray w/ Reflux - Tray 1 Graphical Results

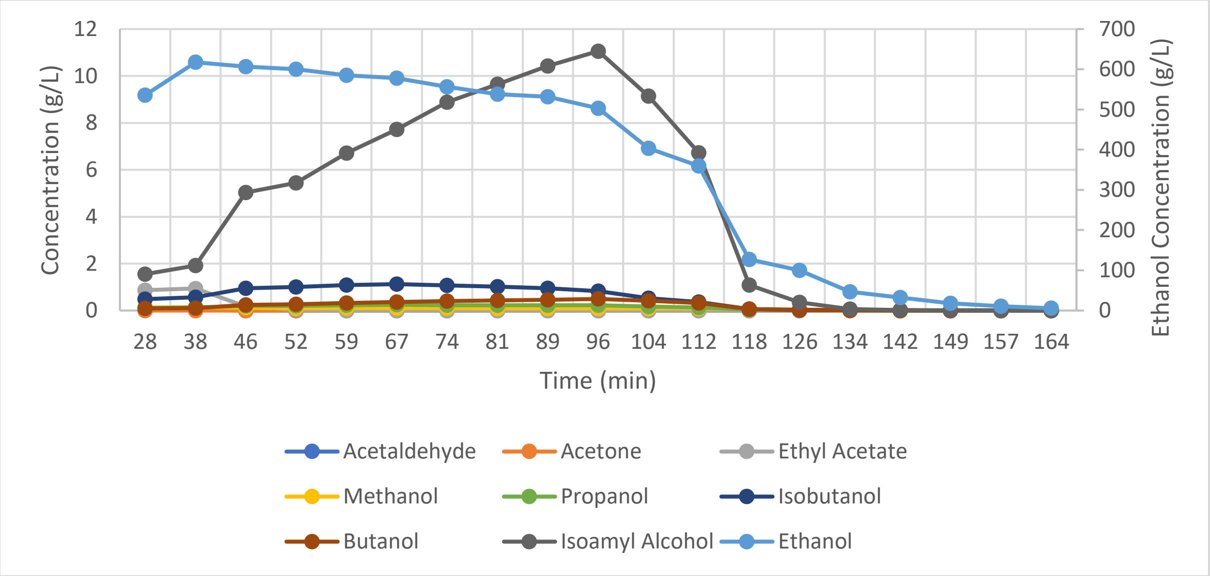

Figure A.44 Cyclic Operation – Brandy Finishing Tray by Tray w/ Reflux - Tray 2 Graphical Results

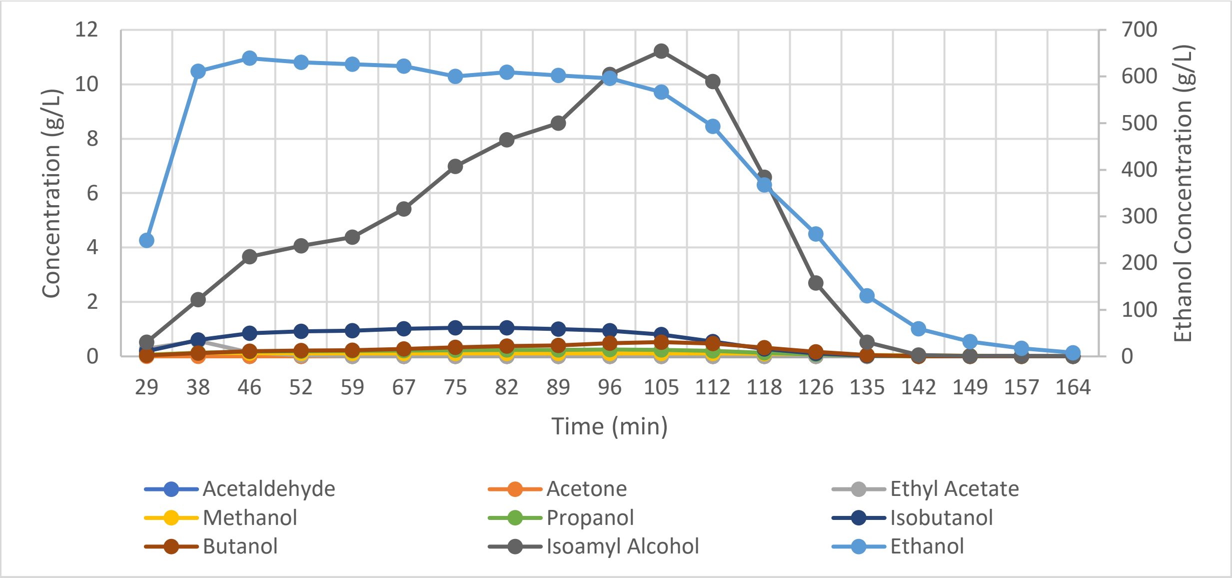

Figure A.45 Cyclic Operation – Brandy Finishing Tray by Tray w/ Reflux - Tray 3 Graphical Results

Distillate Results

Distillation 1

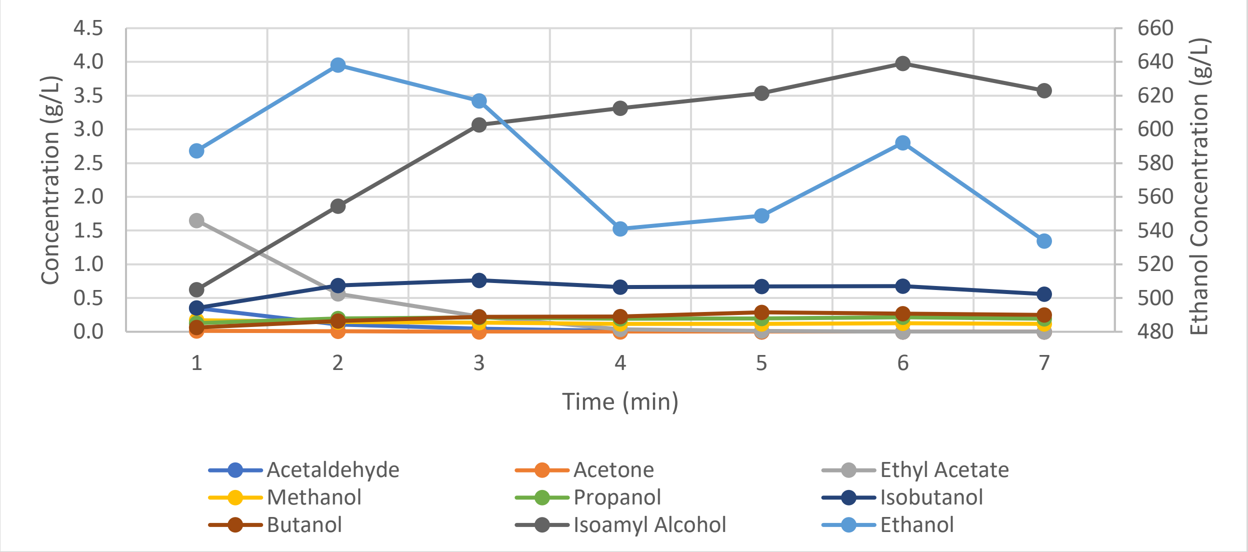

Figure A.46 Normal Operation 1 – Distillate Graphical Results

Distillation 2

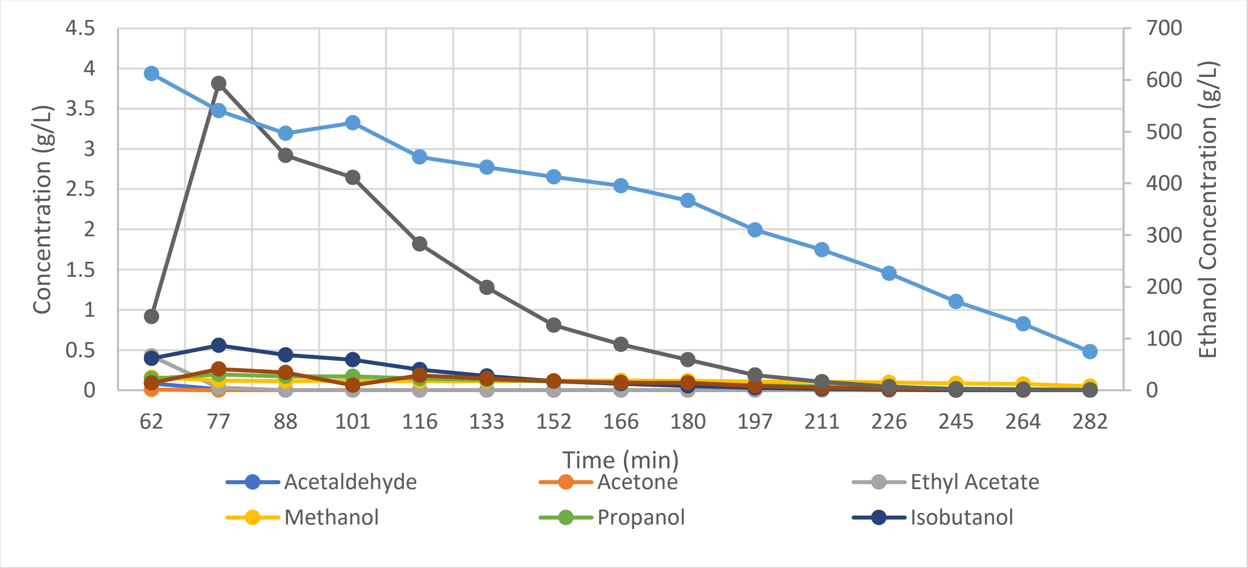

Figure A.47 Normal Operation 2 – Distillate Graphical Results

Distillation 3

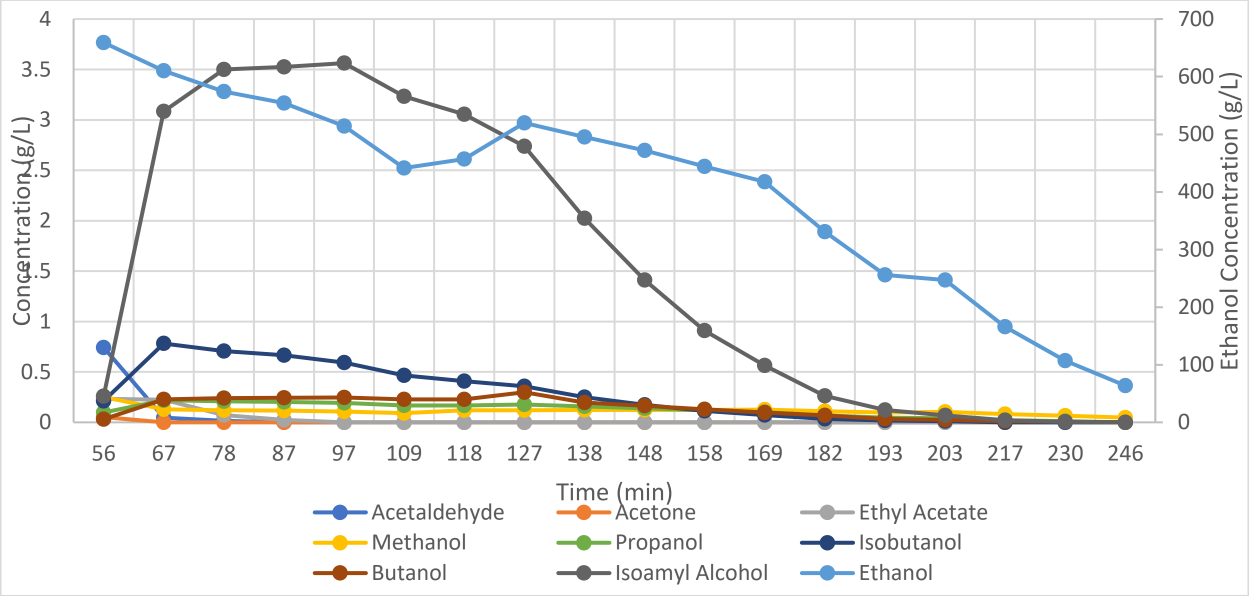

Figure A.48 Normal Operation 3 – Distillate Graphical Results

Distillation 4

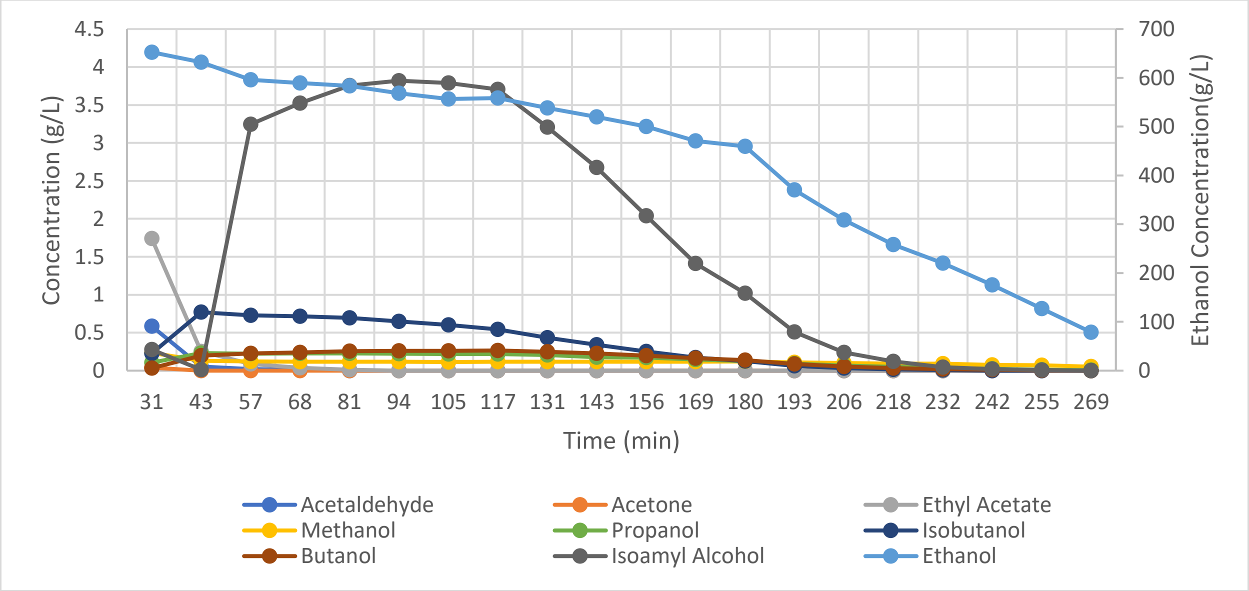

Figure A.49 Cyclic Distillation 1 (Vapor 9 min, Liquid 3 min) – Distillate Graphical Results

Distillation 5

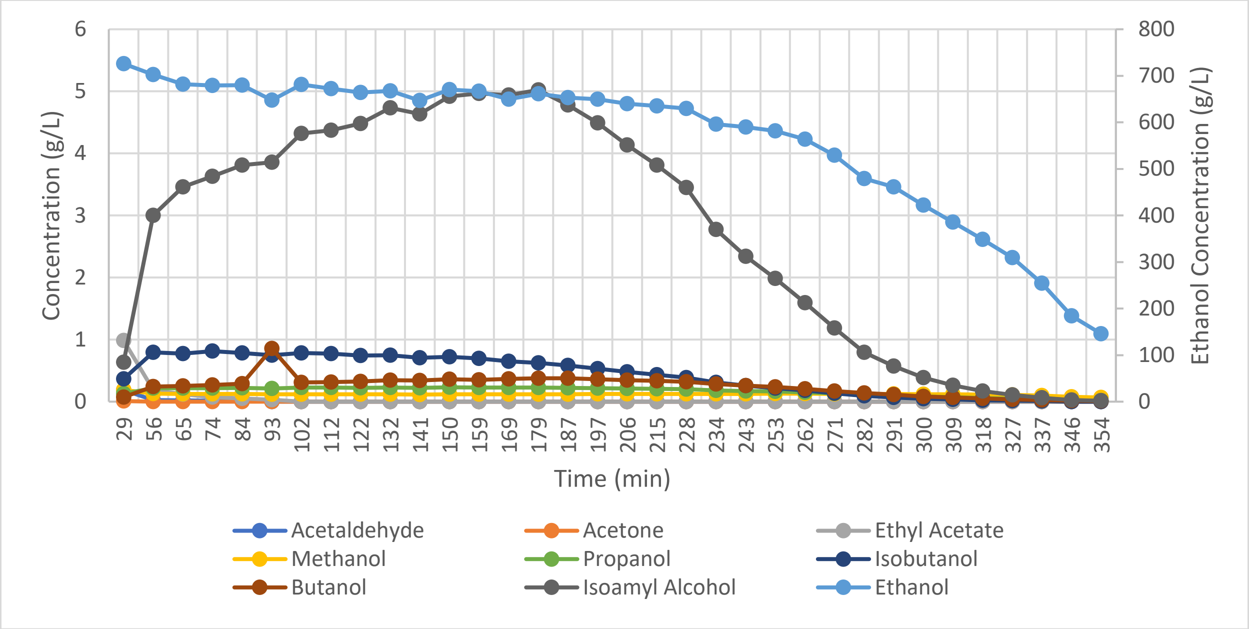

Figure A.50 Cyclic Distillation 1 (Vapor 6 min, Liquid 3 min) – Distillate Graphical Results

Distillation 6

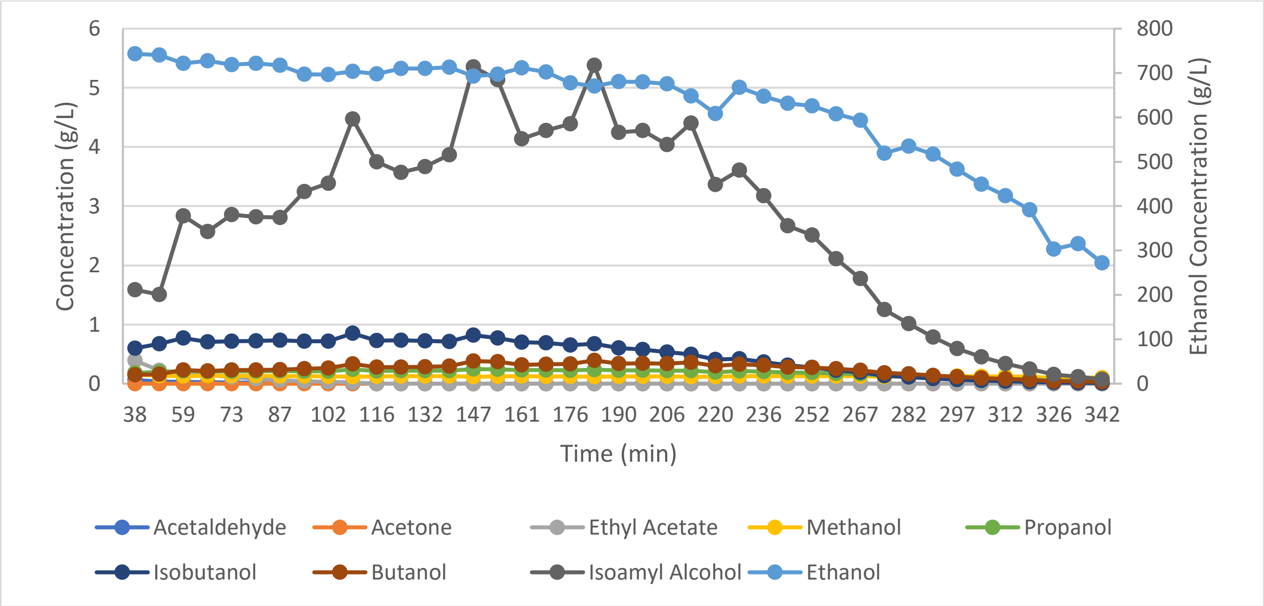

Figure A.51 Cyclic Distillation 1 (Vapor 4 min, Liquid 3 min) – Distillate Graphical Results

Distillation 7

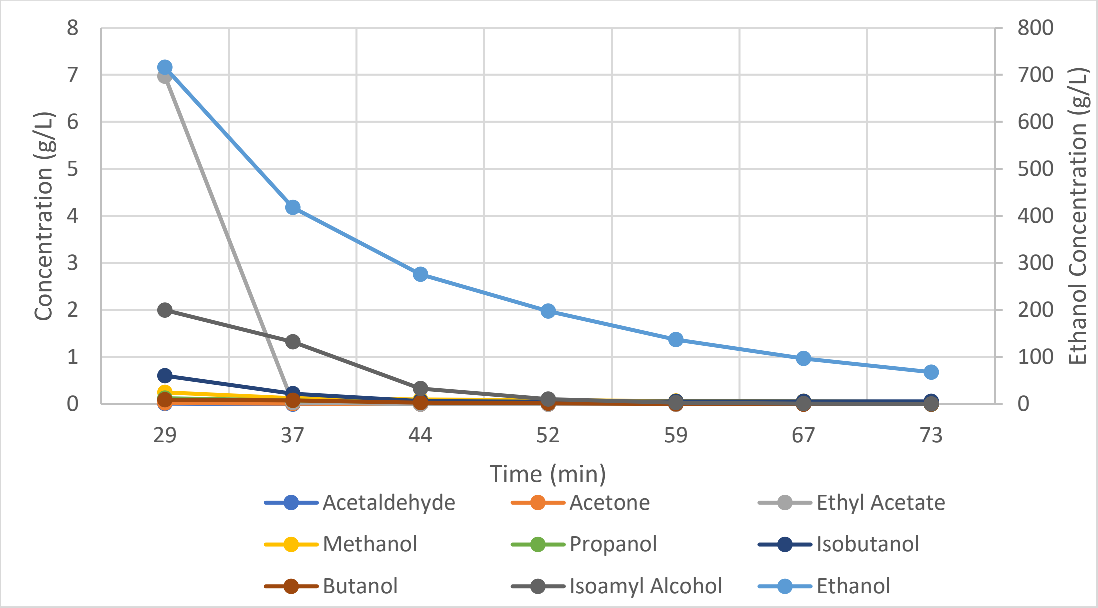

Figure A.52 Normal Operation – Low Wines – Distillate Graphical Results

Distillation 8

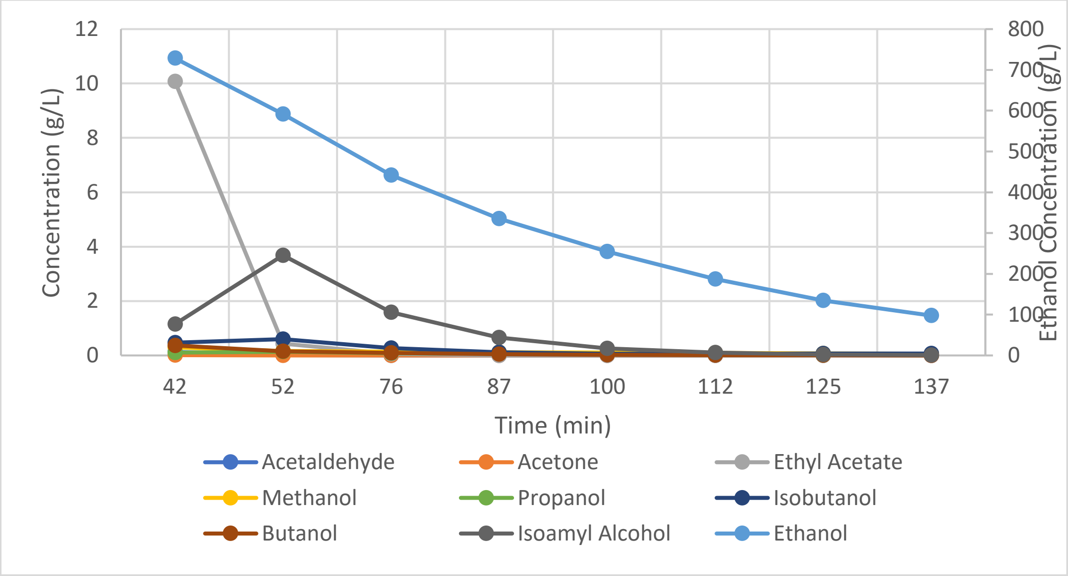

Figure A.53 Cyclic Operation – Low Wines, Cyclic Distillation (Vapor 9 min, Liquid 3 min) Distillate Graphical Results

Distillation 9

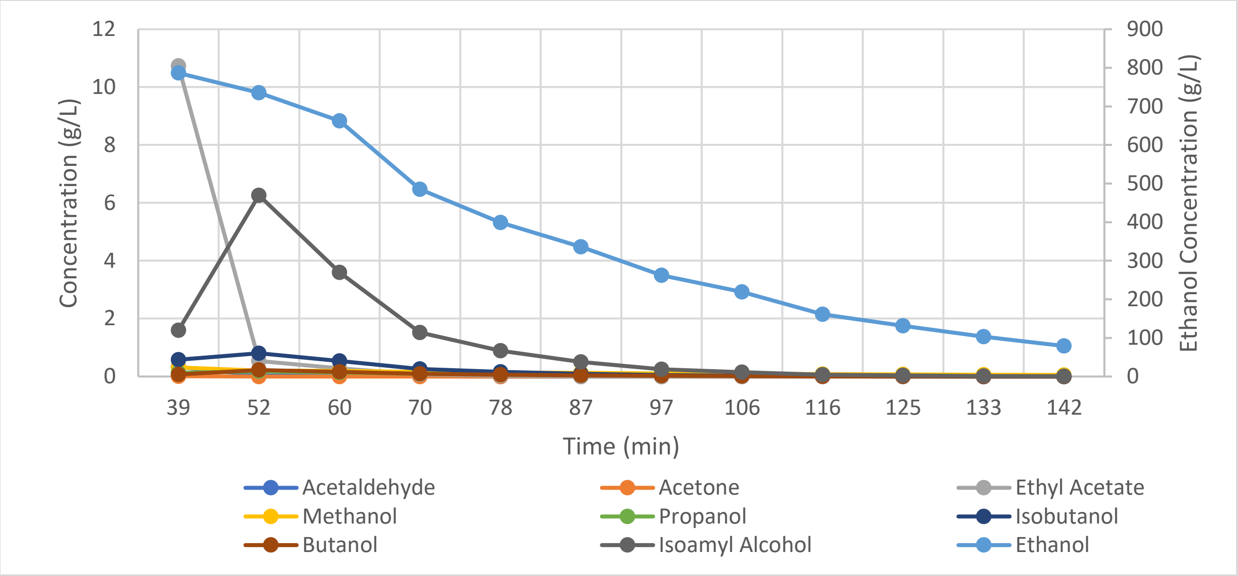

Figure A.54 Cyclic Operation – Low Wines, Cyclic Distillation (Vapor 6 min, Liquid 3 min) Distillate Graphical Results

Distillation 10

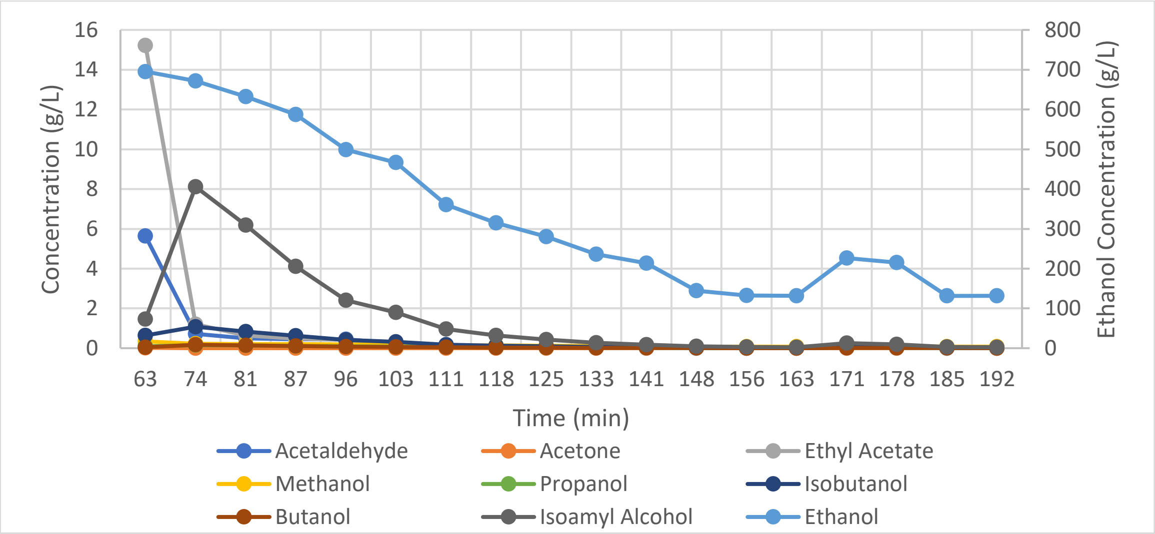

Figure A.55 Cyclic Operation – Low Wines, Cyclic Distillation (Vapor 4 min, Liquid 3 min) Distillate Graphical Results

Distillation 11

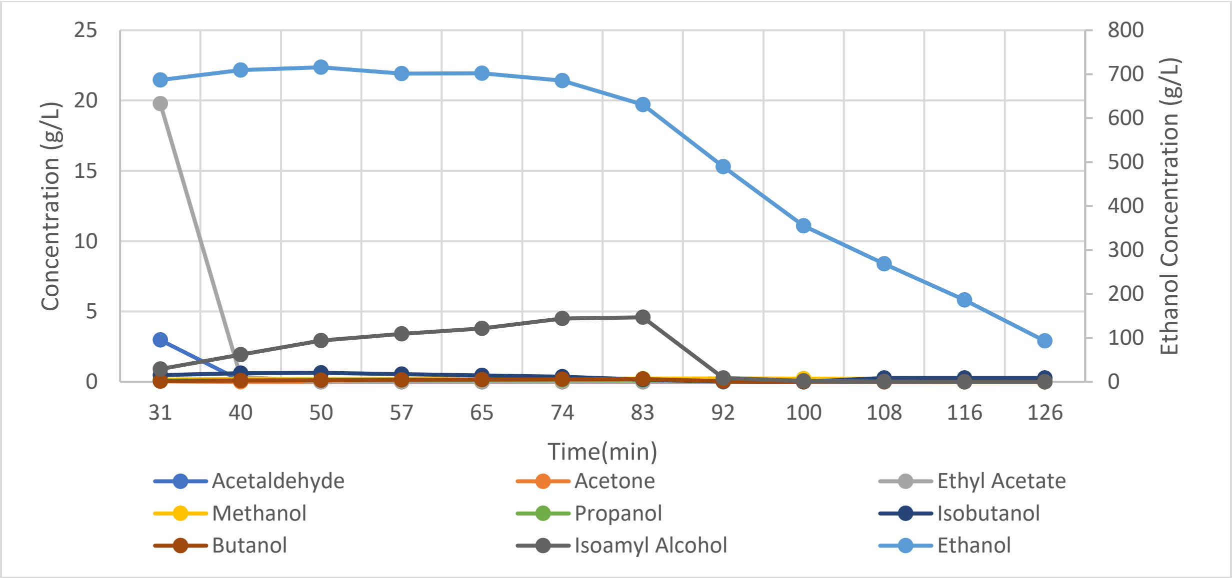

Figure A.56 Normal Operation – Brandy Finishing Run w/o reflux - Distillate Graphical Results

Distillation 12

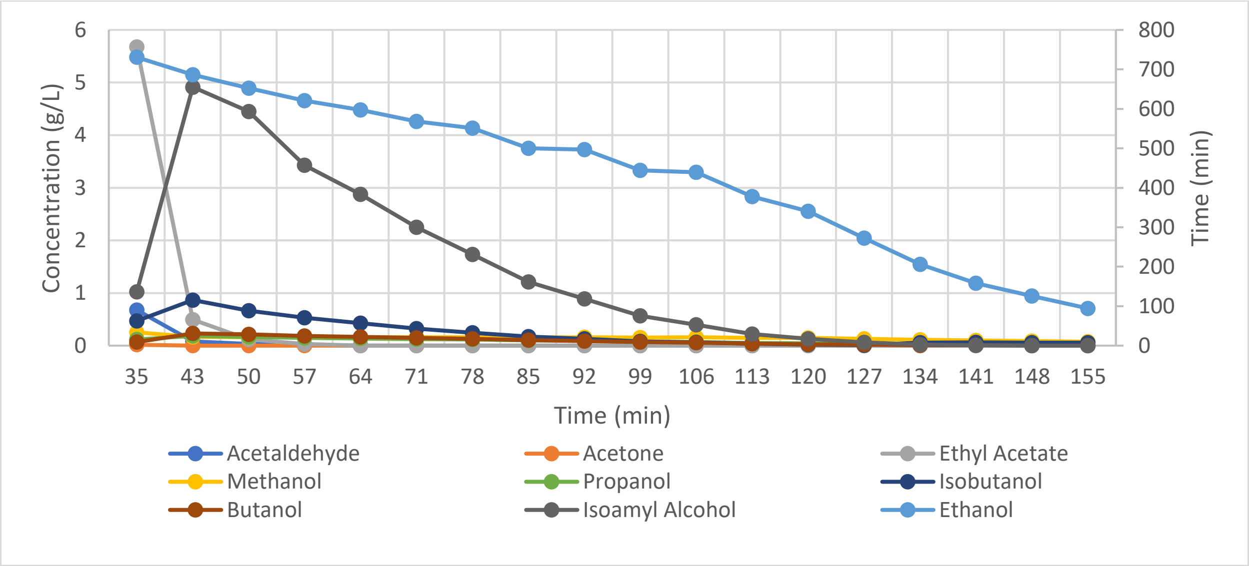

Figure A.57 Normal Operation – Brandy Finishing Run w/ reflux - Distillate Graphical Results

Distillation 13

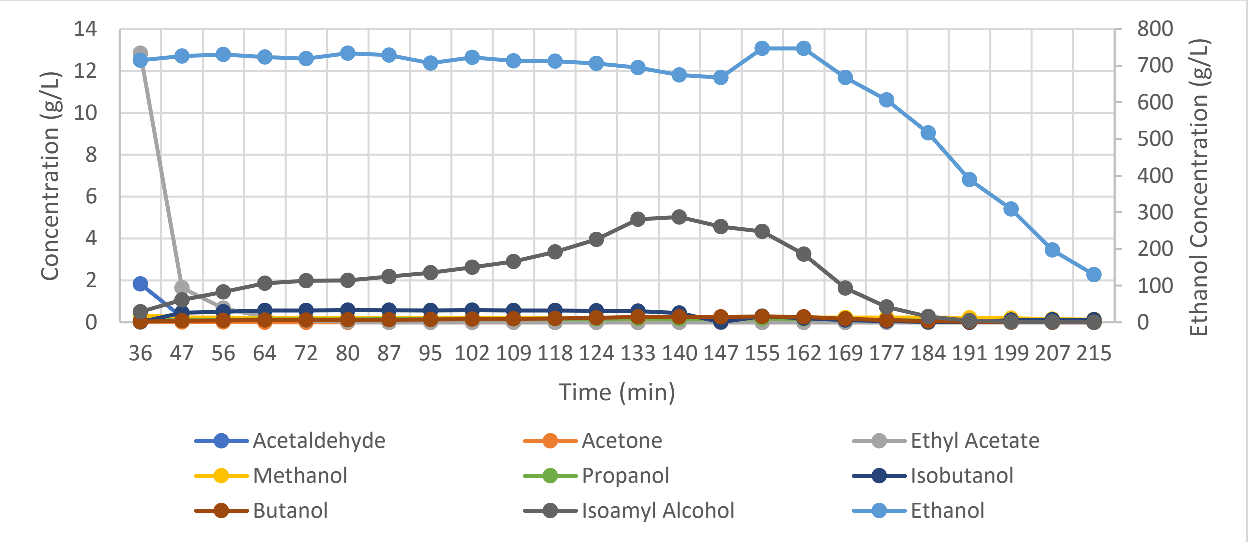

Figure A.58 Cyclic Operation – Tray by Tray Finishing Run w/ reflux – Distillate Graphical Results

Distillation 14

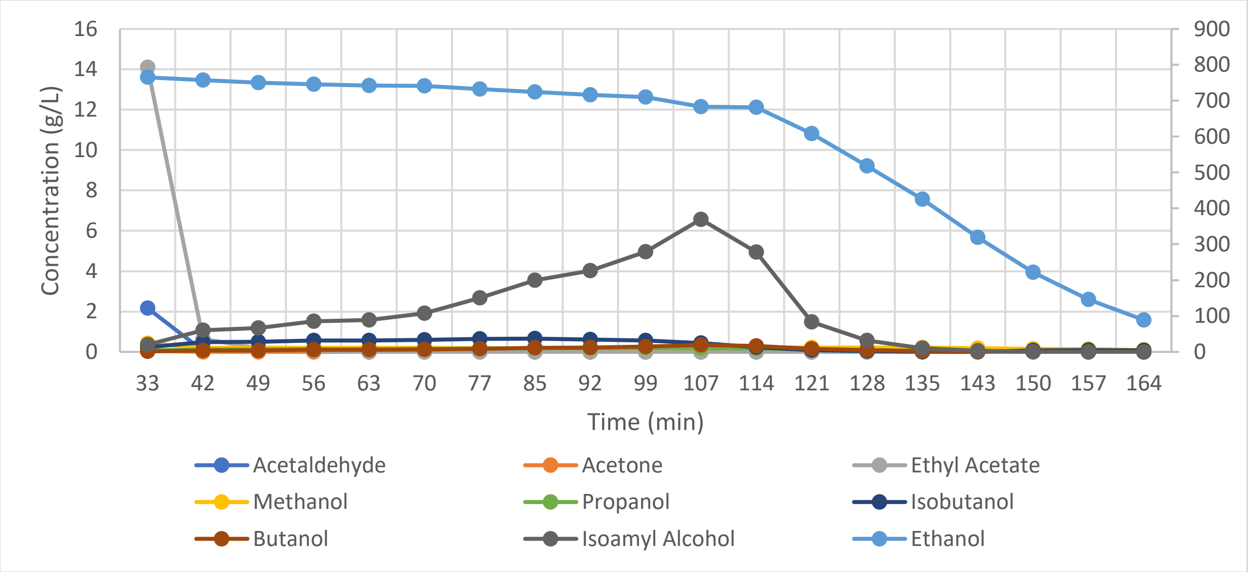

Figure A.59 Cyclic Operation – Tray by Tray Finishing Run w/ reflux – Distillate Graphical Results

Distillation 15

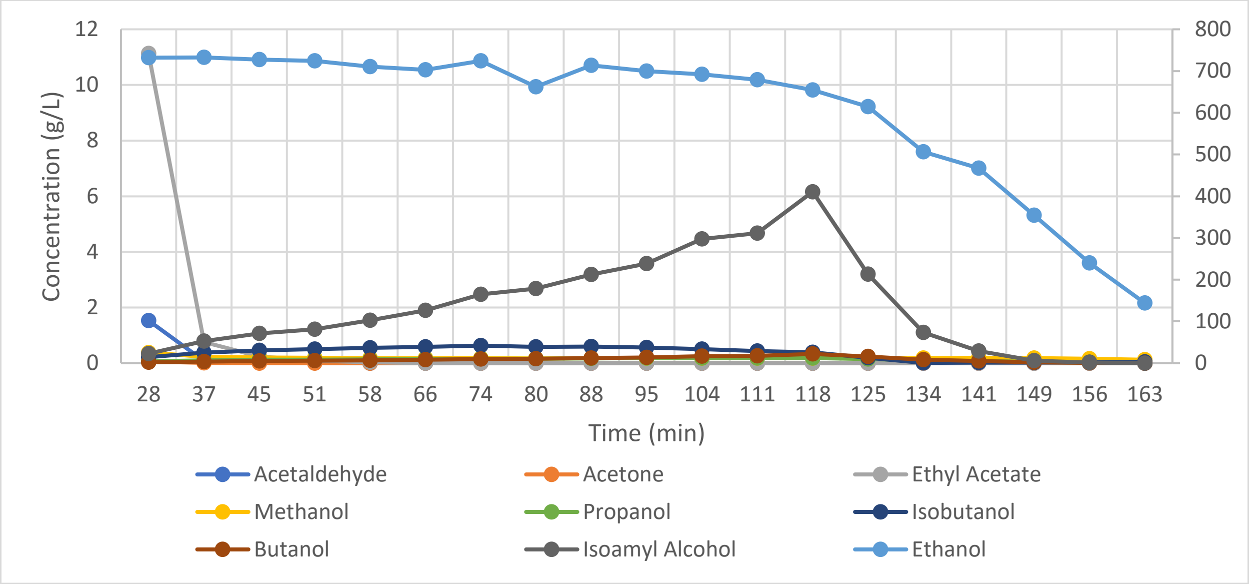

Figure A.60 Cyclic Operation – Tray by Tray Finishing Run w/ reflux – Distillate Graphical Results

Bottom Column and Cycled Volume Results

Distillation 1

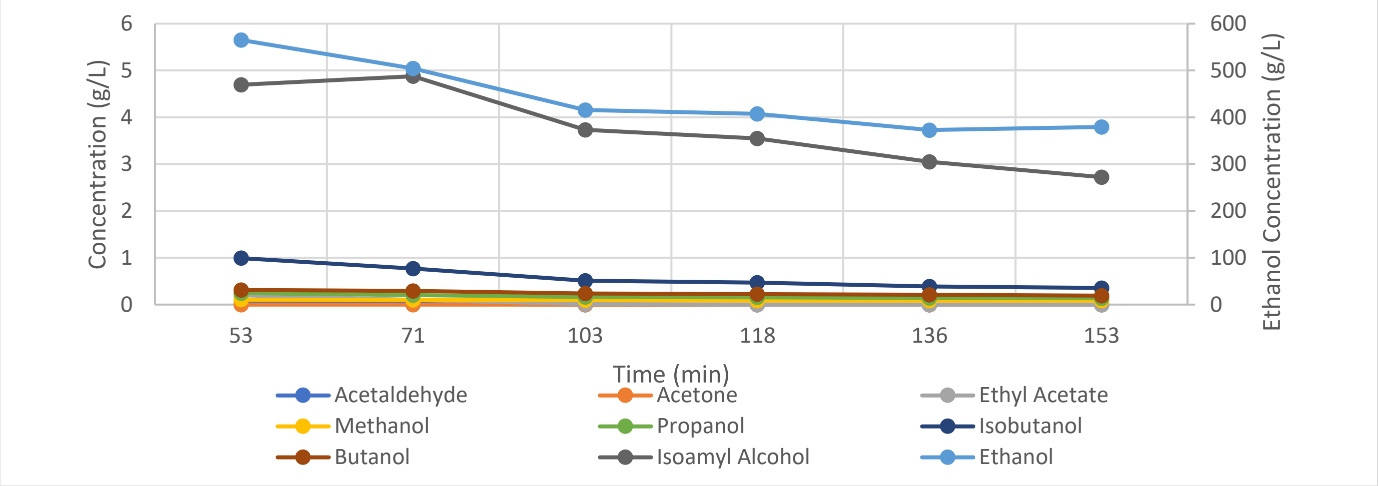

Figure A.61 Normal Operation 1 – Bottom Column Graphical Results

Distillation 2

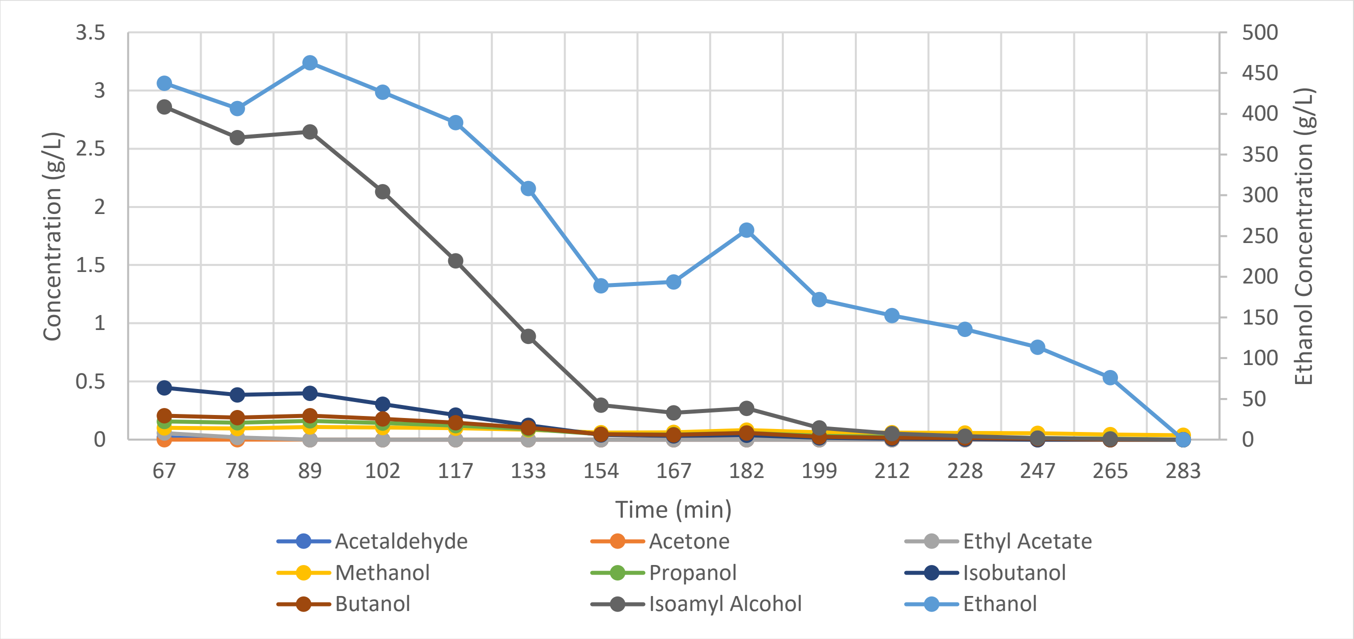

Figure A.62 Normal Operation 2 – Bottom Column Graphical Results

Distillation 3

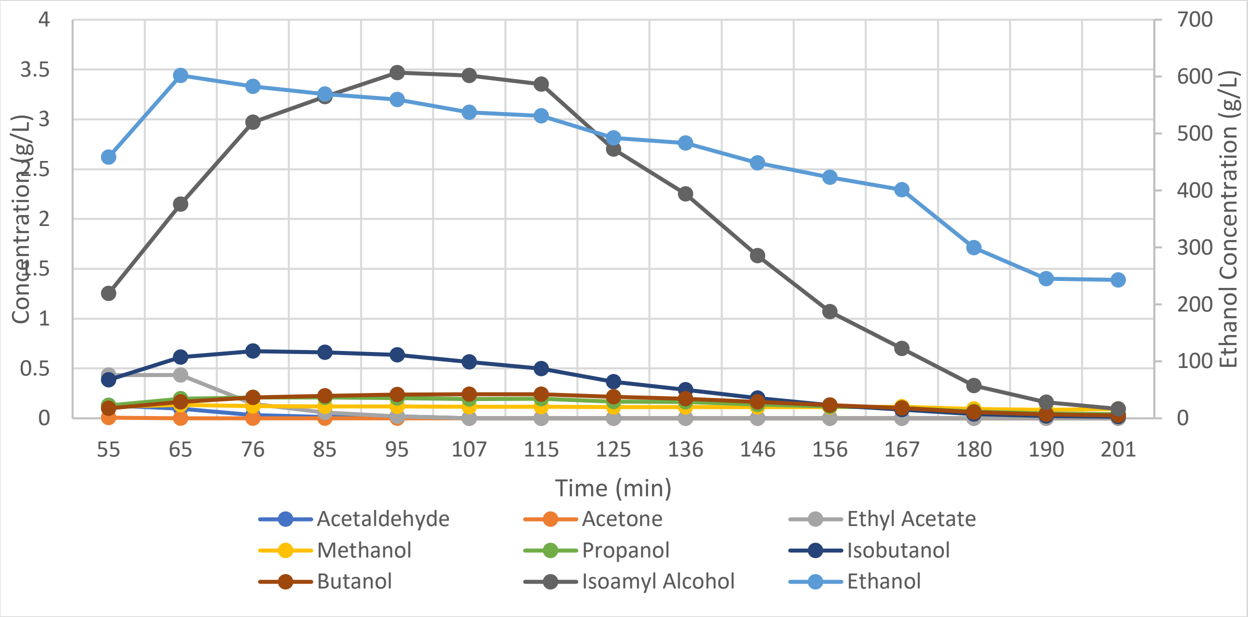

Figure A.63 Normal Operation 3 – Bottom Column Graphical Results

Distillation 4

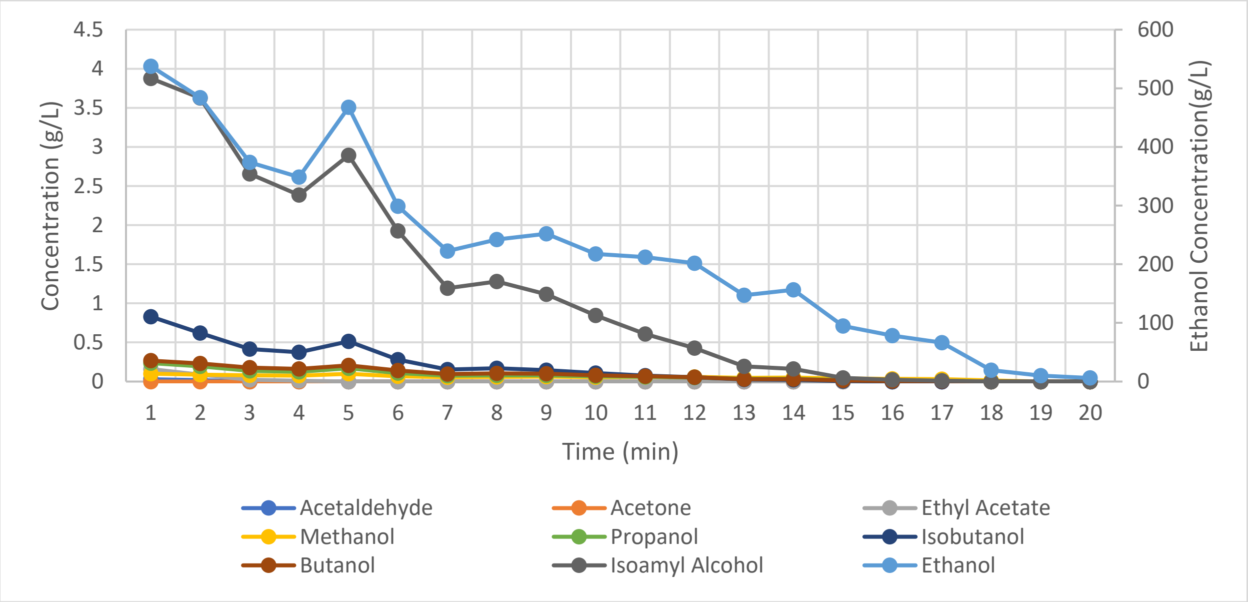

Figure A.64 Cyclic Distillation 1 (Vapor 9 min, Liquid 3 min) – Cycled Volume Graphical Results

Distillation 5

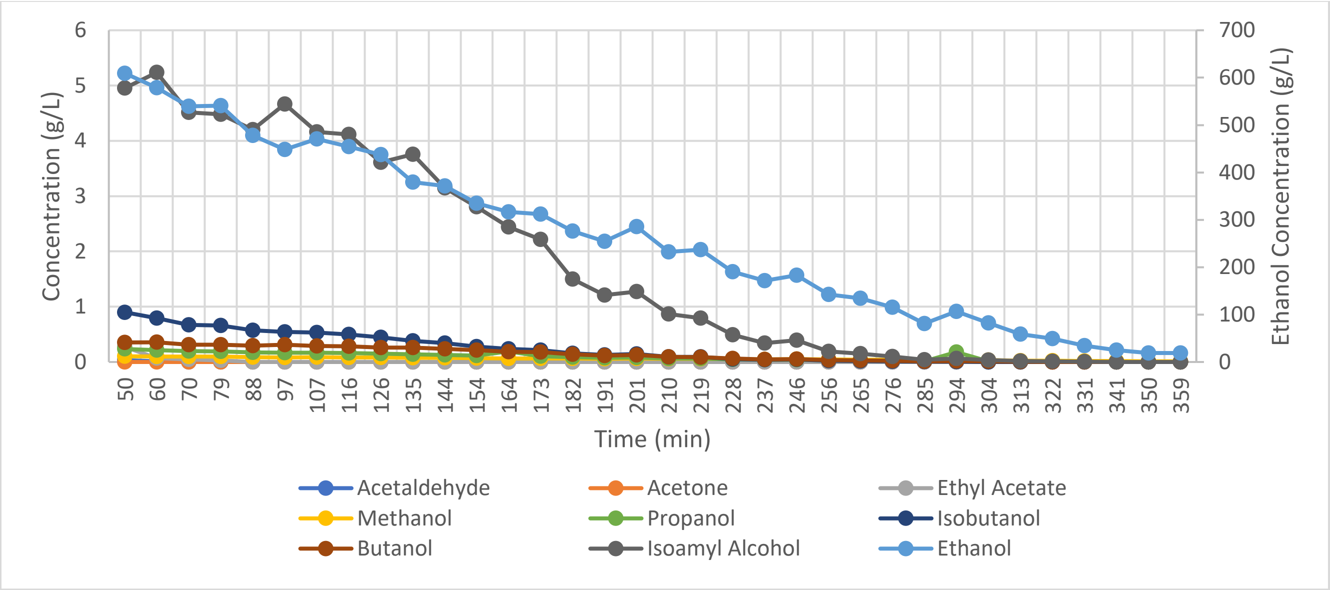

Figure A.65 Cyclic Distillation 1 (Vapor 6 min, Liquid 3 min) – Cycled Volume Graphical Results

Distillation 6

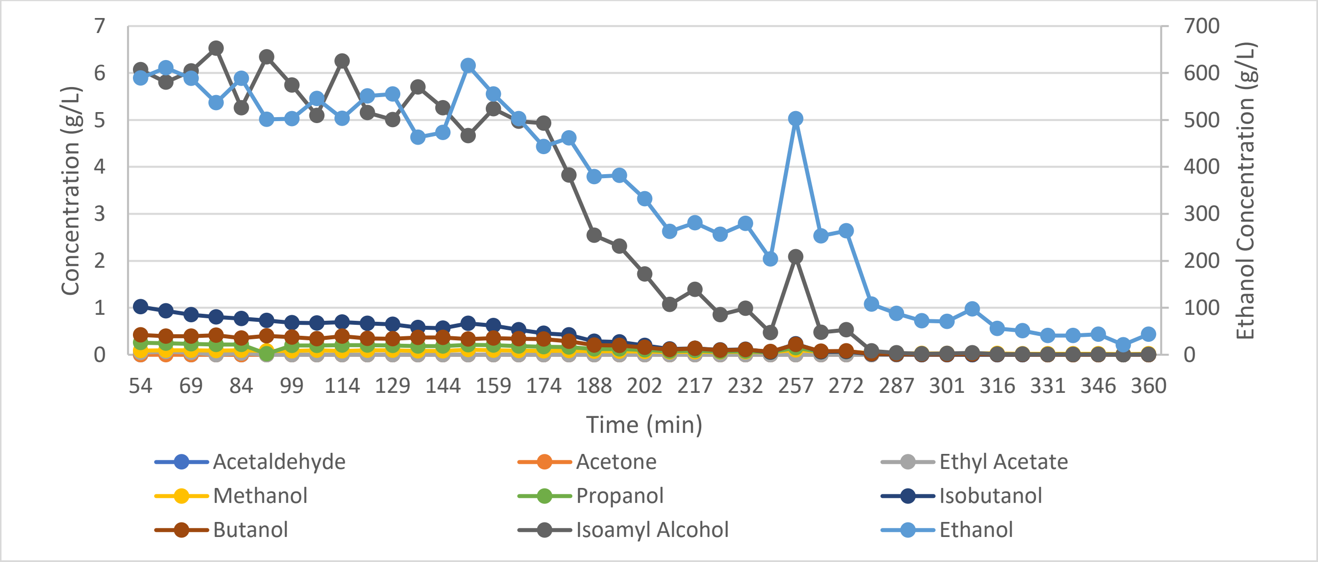

Figure A.66 Cyclic Distillation 1 (Vapor 4 min, Liquid 3 min) – Cycled Volume Graphical Results

Distillation 7

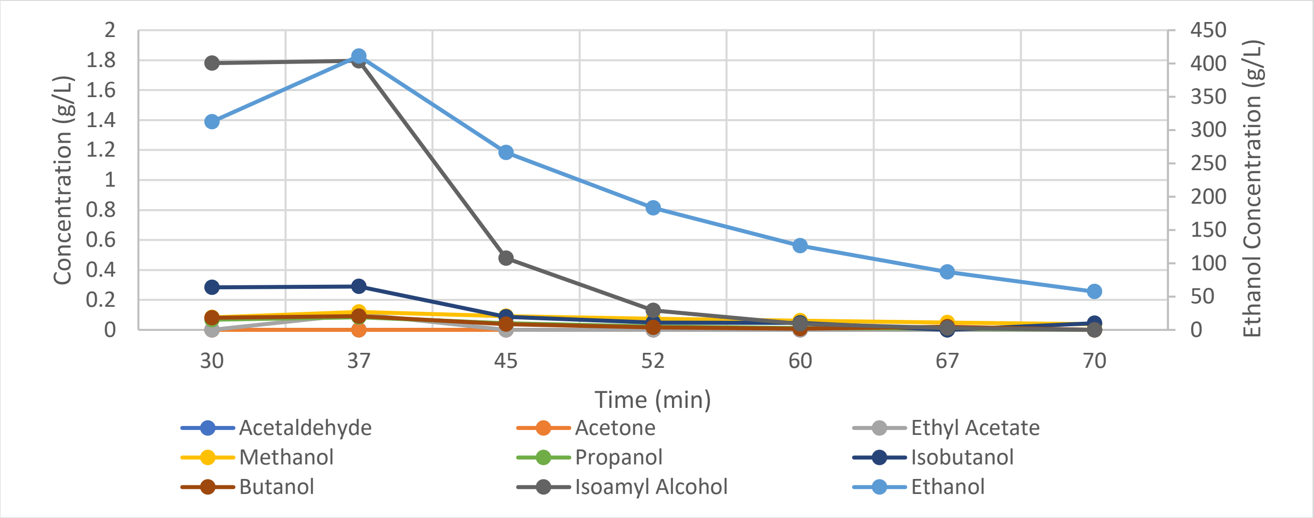

Figure A.67 Normal Operation – Low Wines – Bottom Column Graphical Results

Distillation 8

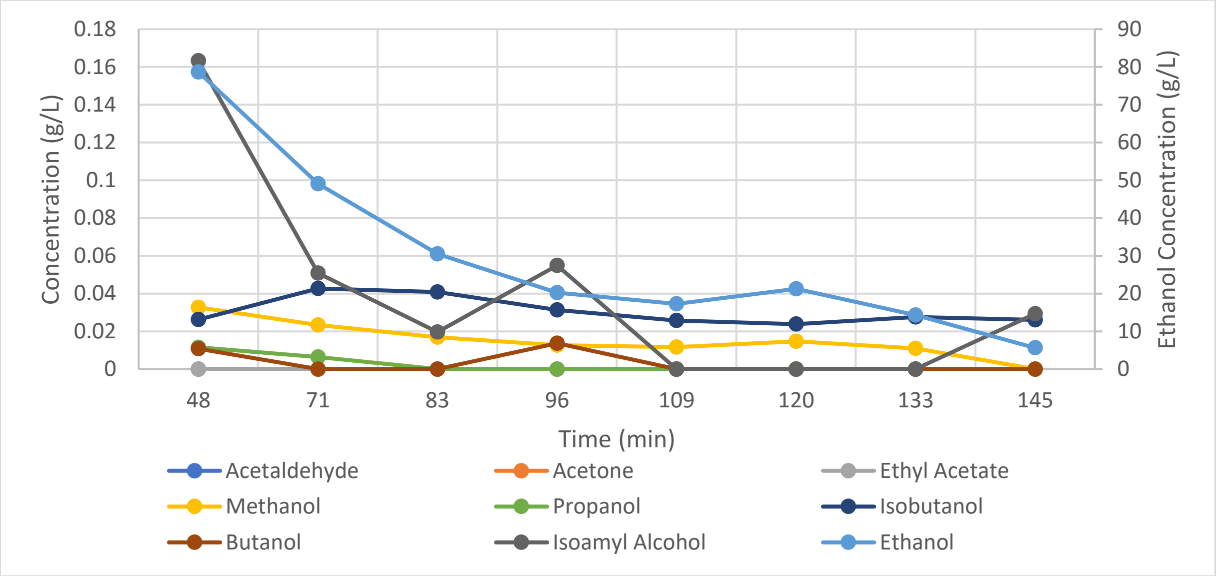

Figure A.68 Cyclic Operation – Low Wines, Cyclic Distillation (Vapor 9 min, Liquid 3 min) Cycled Volume Graphical Results

Distillation 9

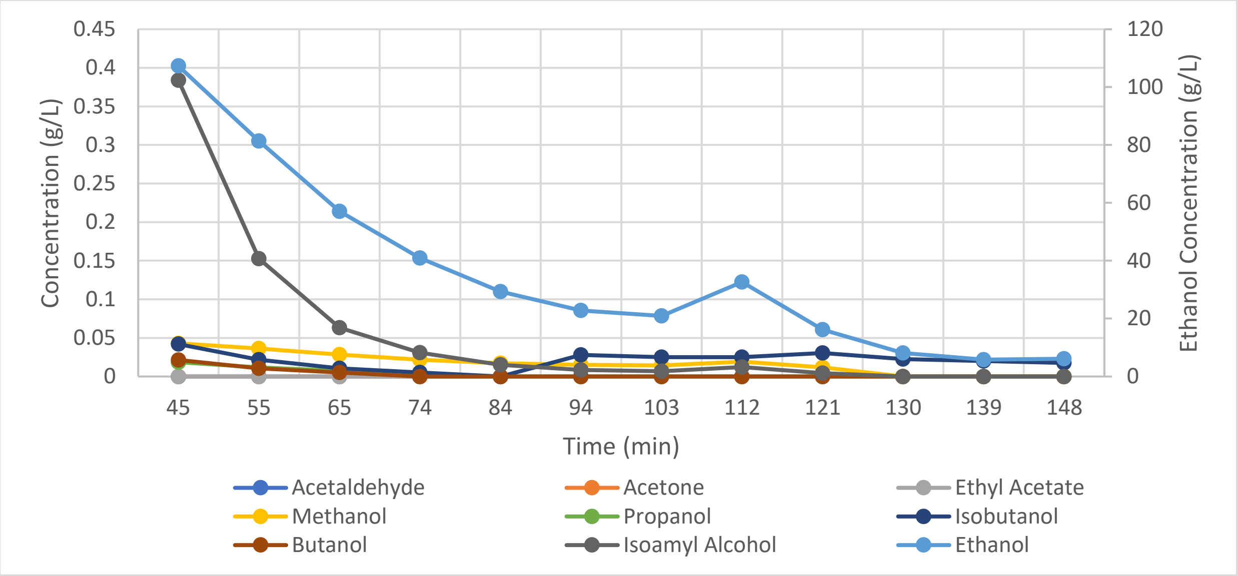

Figure A.69 Cyclic Operation – Low Wines, Cyclic Distillation (Vapor 6 min, Liquid 3 min) Cycled Volume Graphical Results

Distillation 10

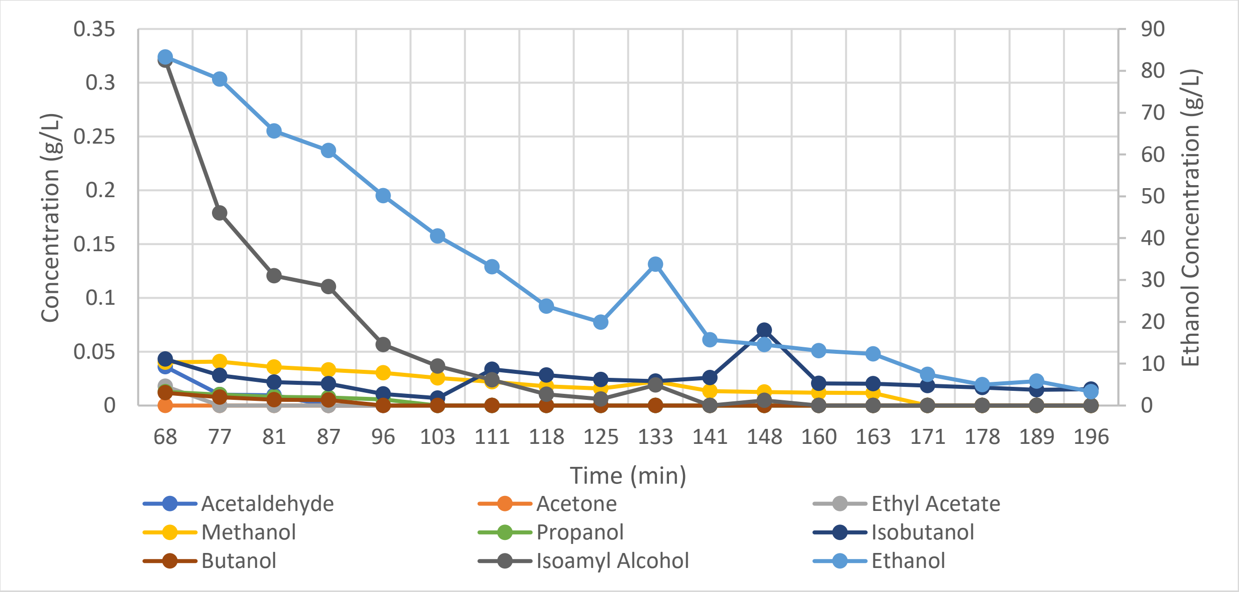

Figure A.70 Cyclic Operation – Low Wines, Cyclic Distillation (Vapor 4 min, Liquid 3 min) Cycled Volume Graphical Results

Distillation 11

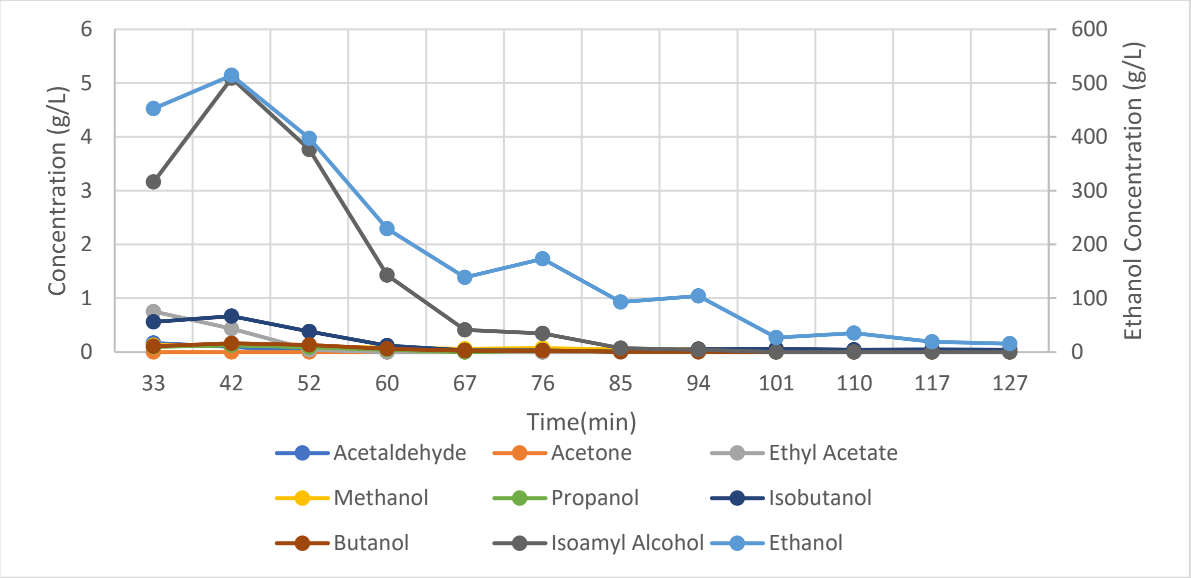

Figure A.71 Normal Operation – Brandy Finishing Run w/o reflux - Bottom Column Graphical Results

Distillation 12

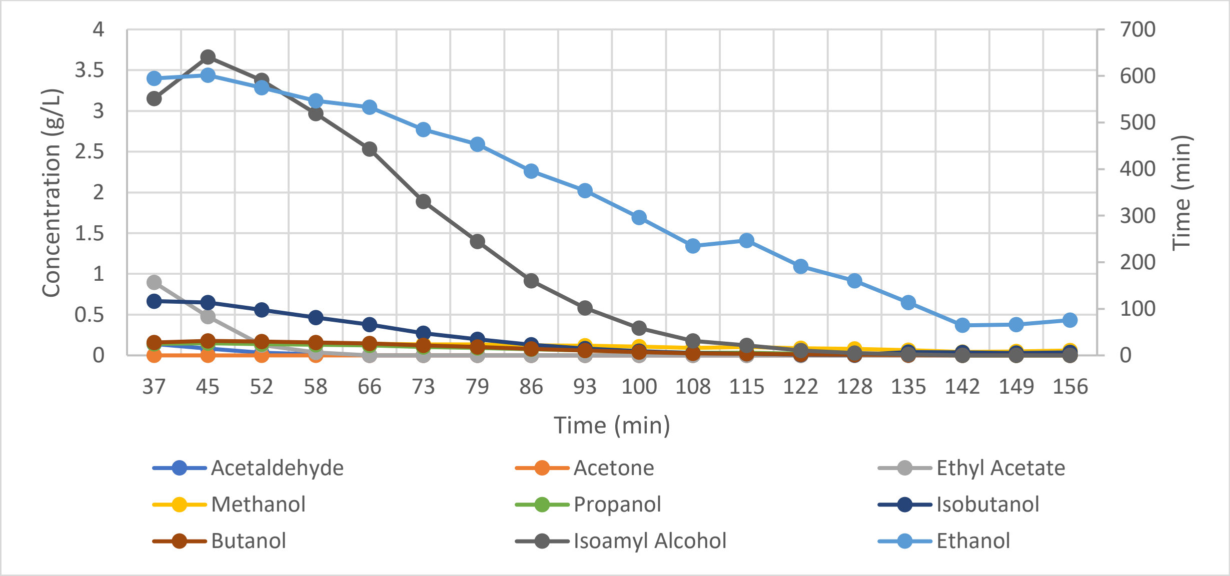

Figure A.72 Normal Operation – Brandy Finishing Run w/ reflux - Bottom Column Graphical Results

Distillation 13

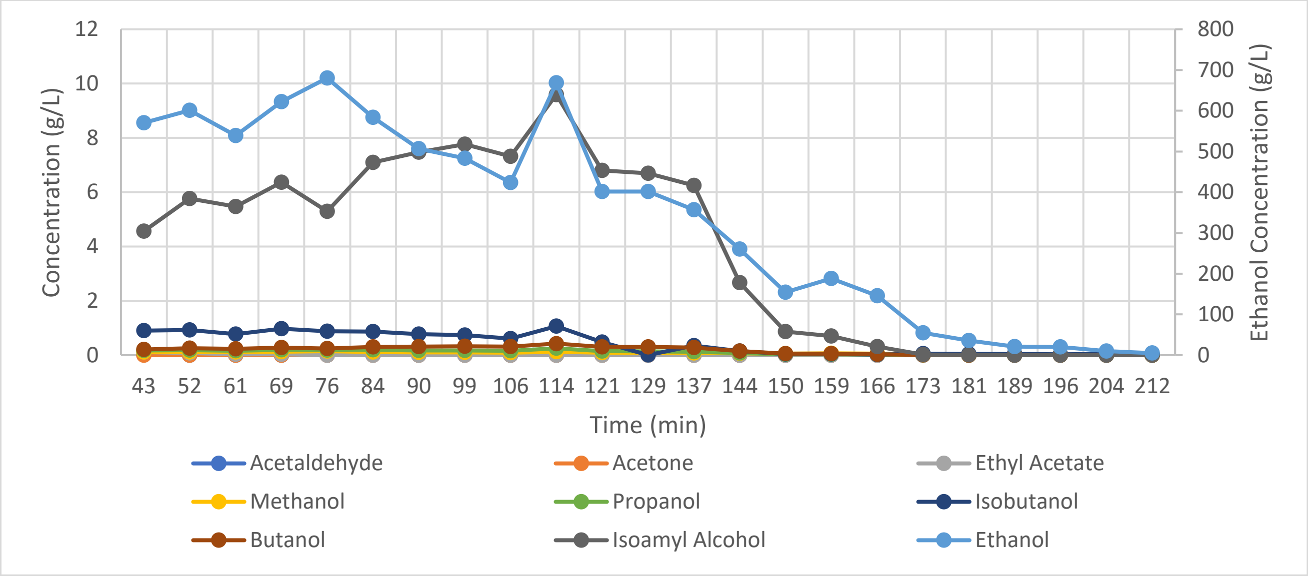

Figure A.73 Cyclic Operation – Tray by Tray Finishing Run w/ reflux – Cycled Volume Graphical Results

Distillation 14

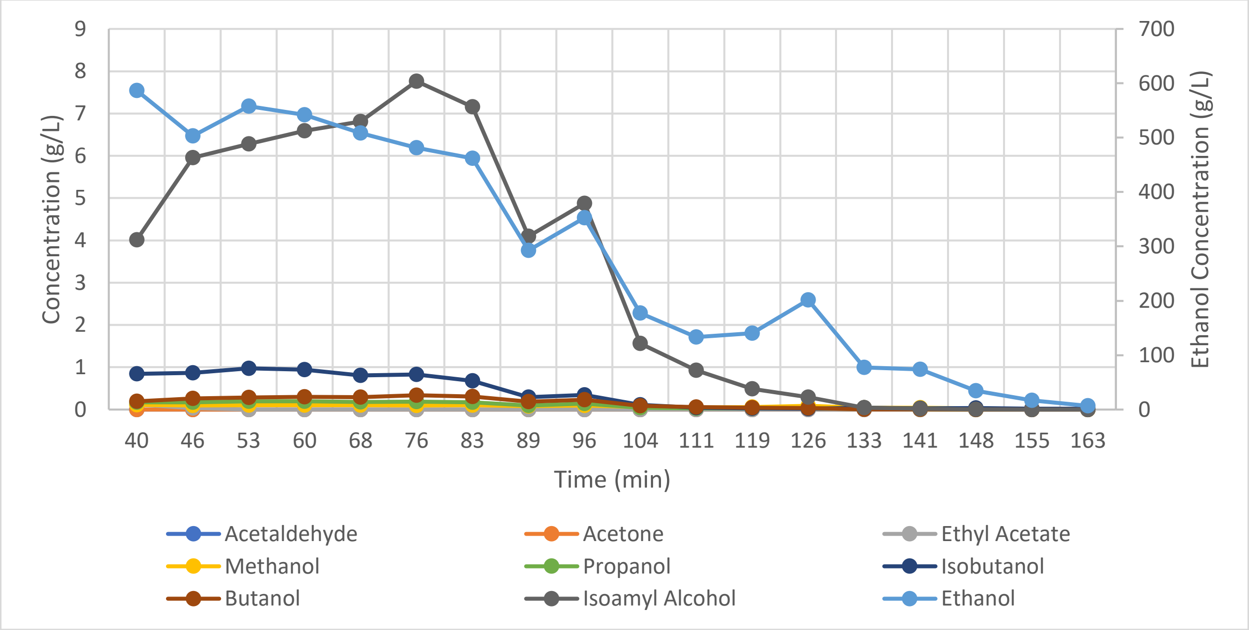

Figure A.74 Cyclic Operation – Tray by Tray Finishing Run w/ reflux – Cycled Volume Graphical Results

Distillation 15

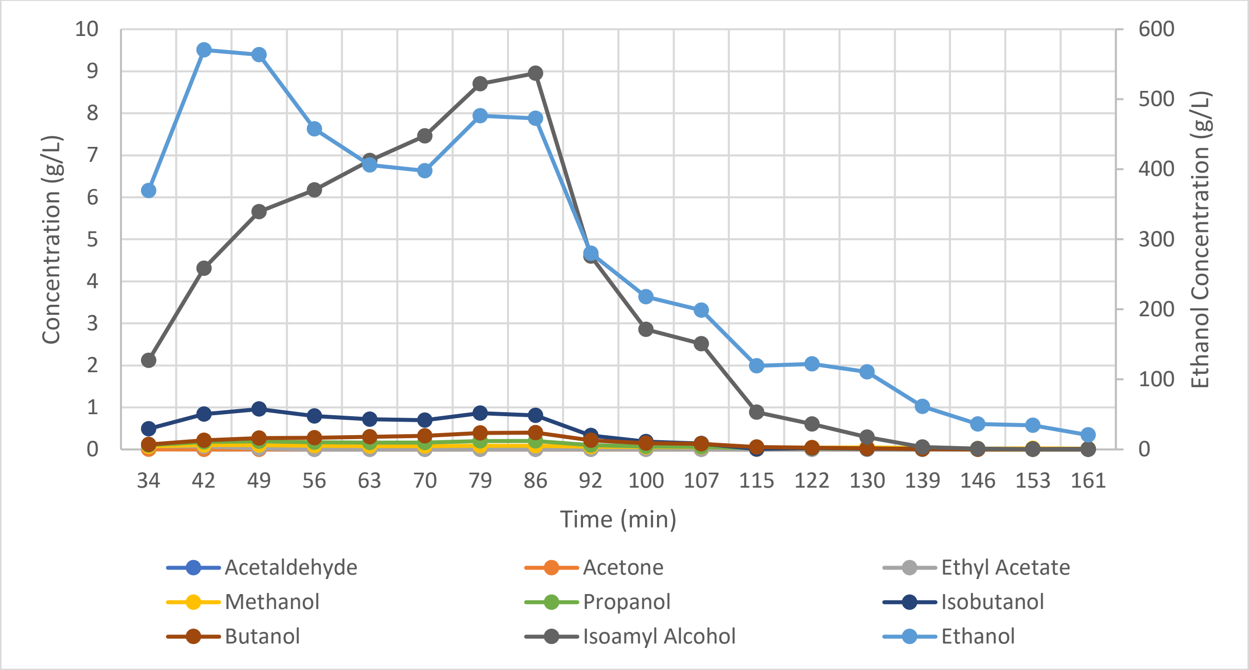

Figure A.75 Cyclic Operation – Tray by Tray Finishing Run w/ reflux – Cycled Volume Graphical Results

Component Results

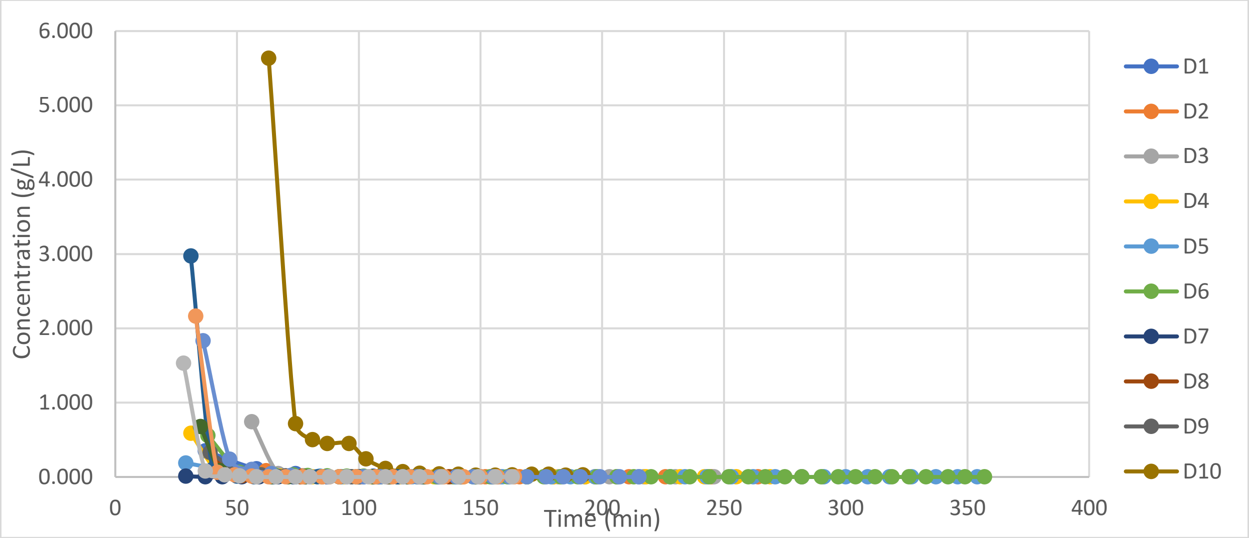

Figure A.76 Acetaldehyde Concentration vs Time for All Distillations

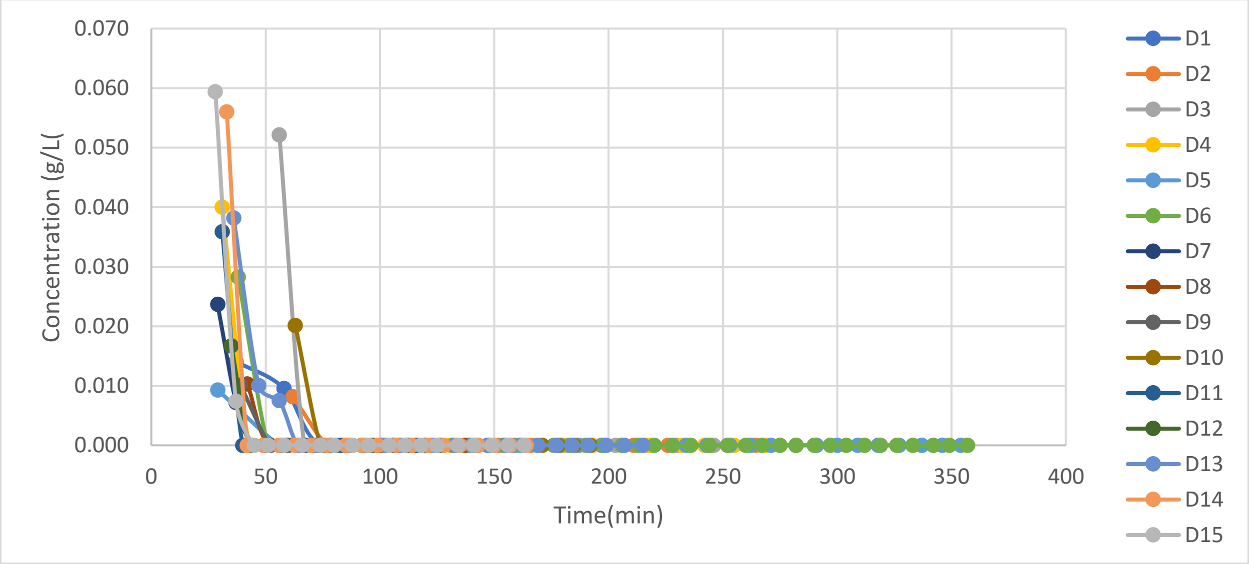

Figure A.77 Acetone Concentration vs Time for All Distillations

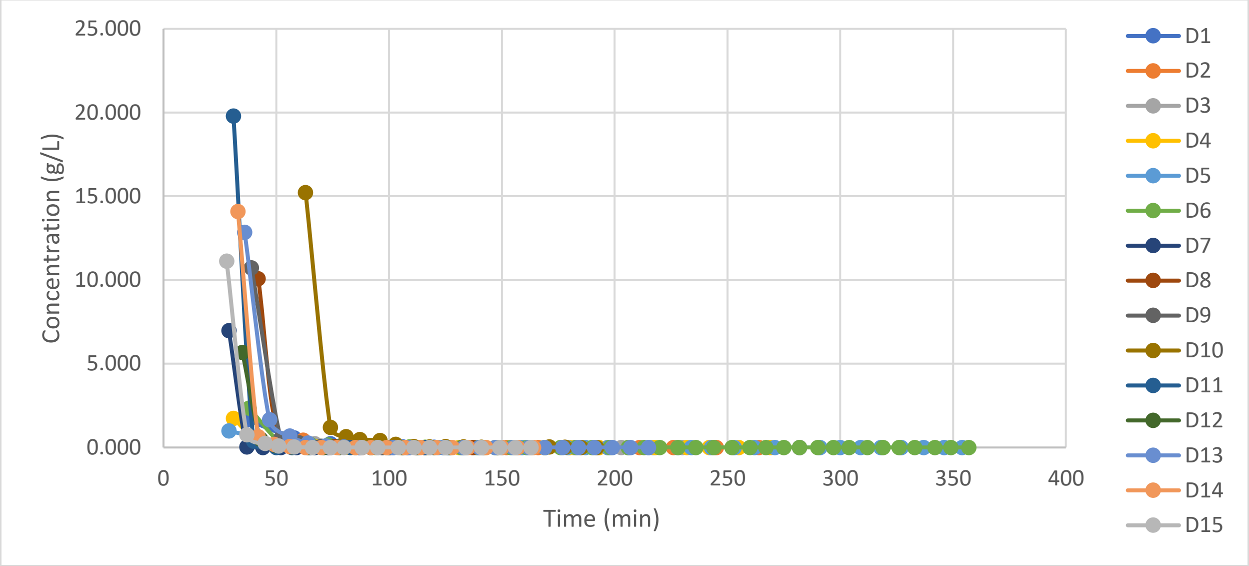

Figure A.78 Ethyl Acetate Concentration vs Time for All Distillations

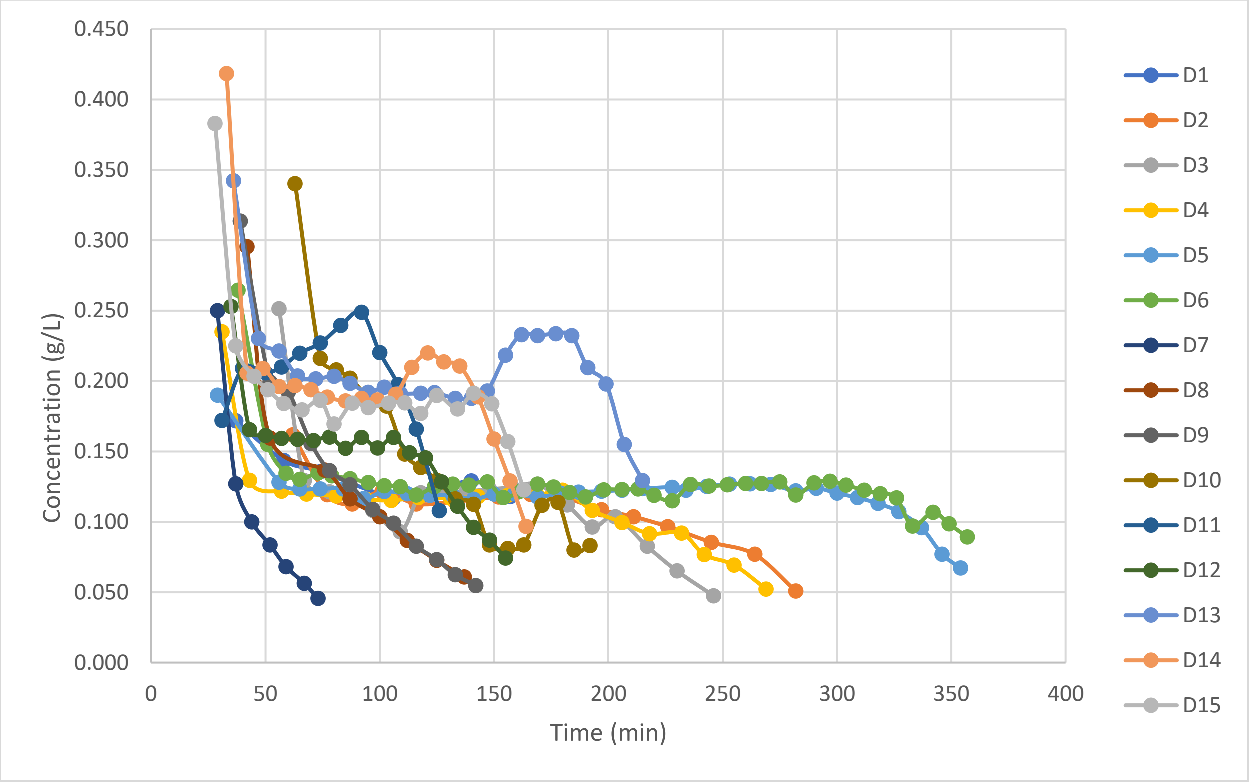

Figure A.79 Methanol Concentration vs Time for All Distillations

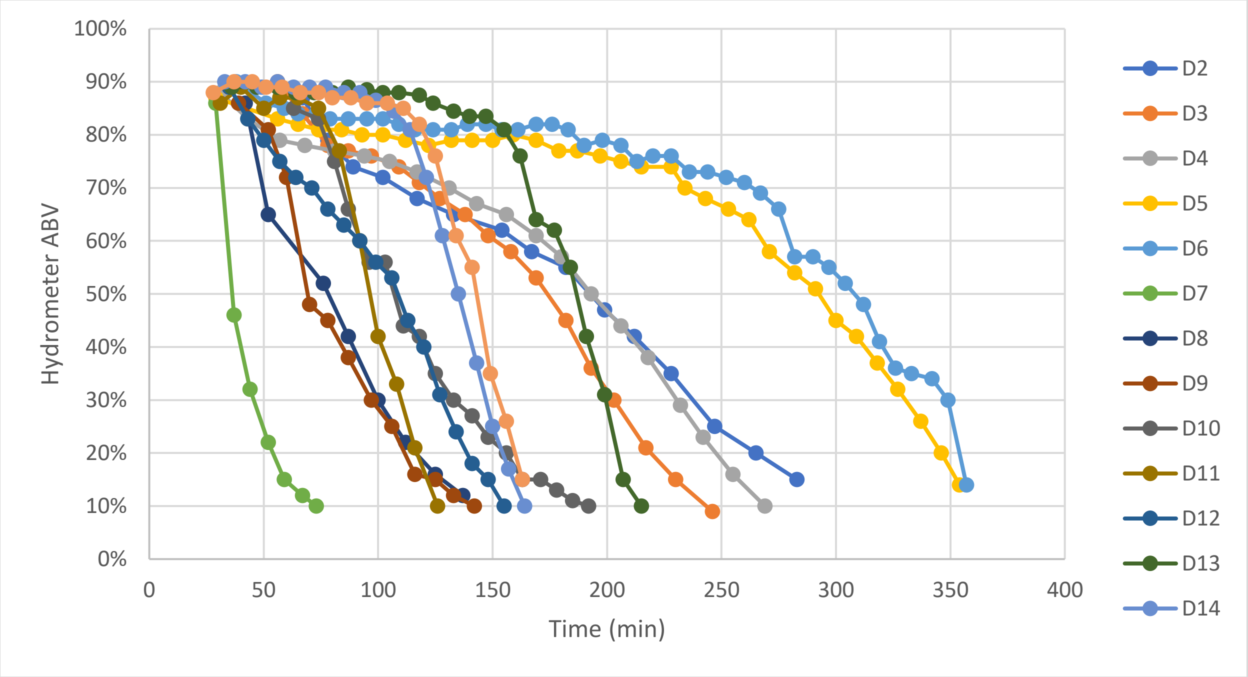

Figure A.80 Ethanol Concentration vs Time for All Distillations

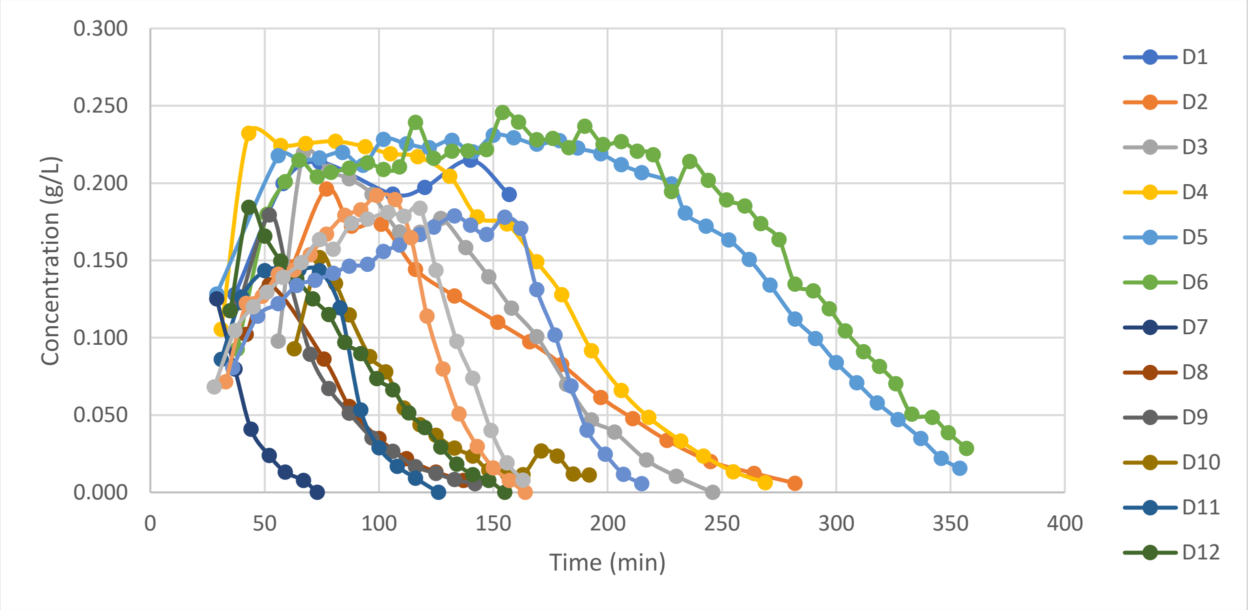

Figure A.81 Propanol Concentration vs Time for All Distillations

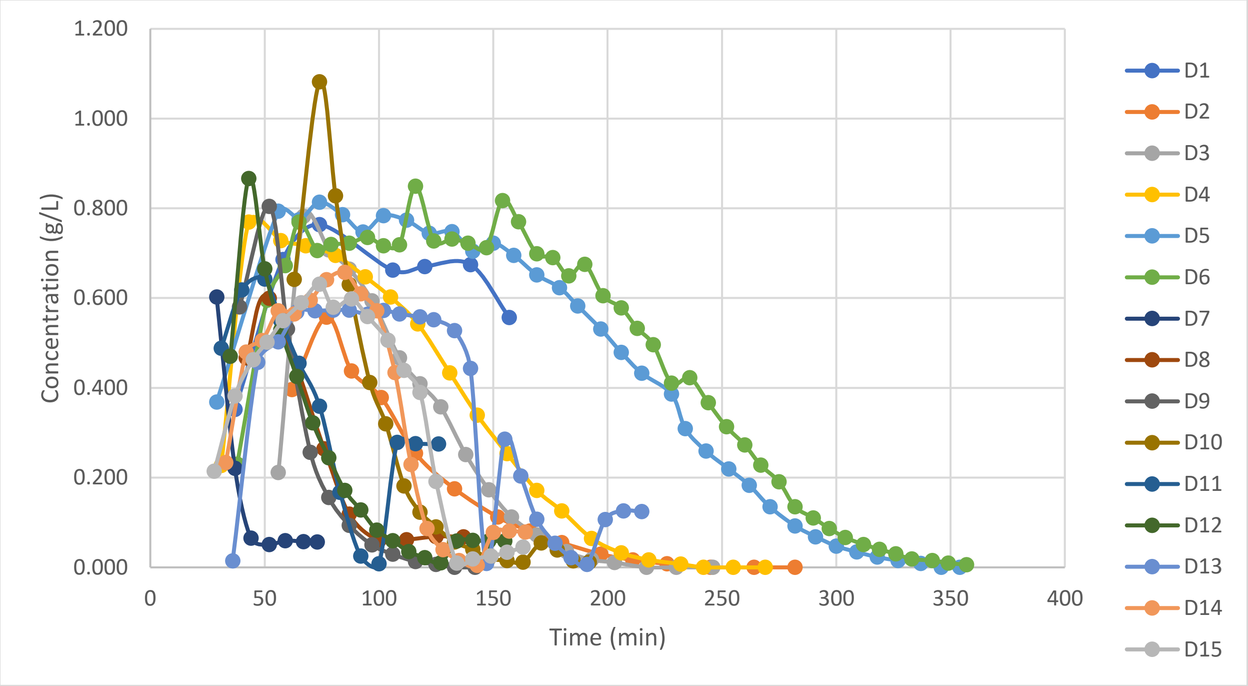

Figure A.82 Isobutanol Concentration vs Time for All Distillations

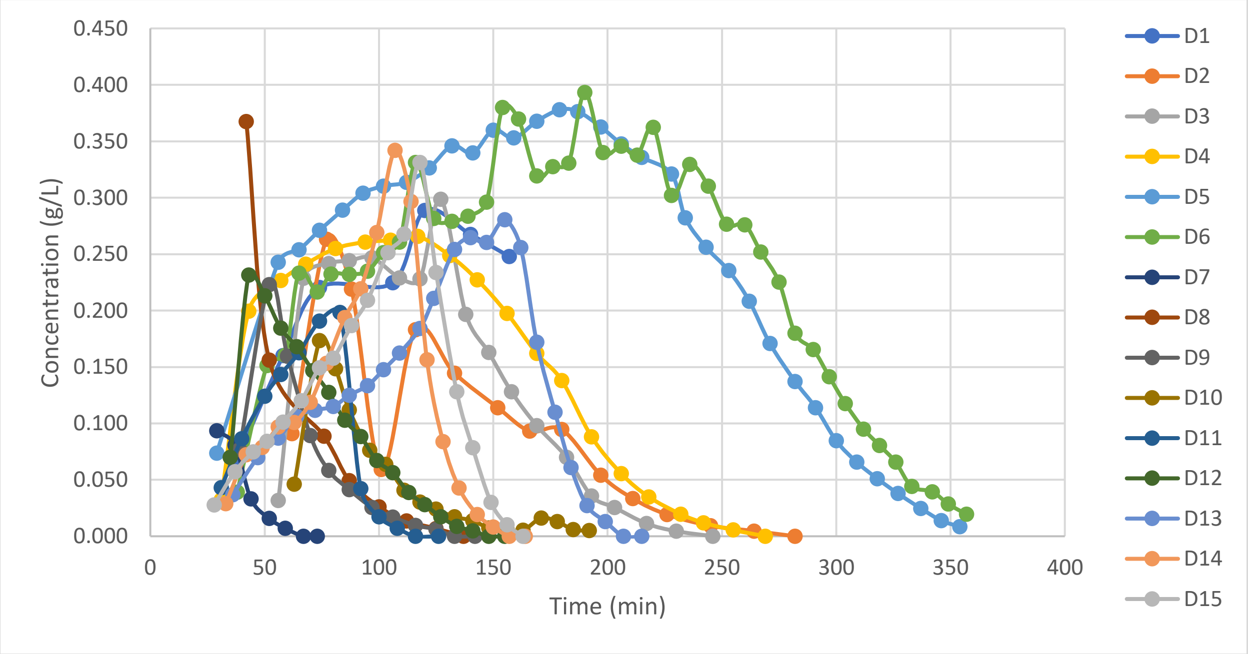

Figure A.83 Butanol Concentration vs Time for All Distillations

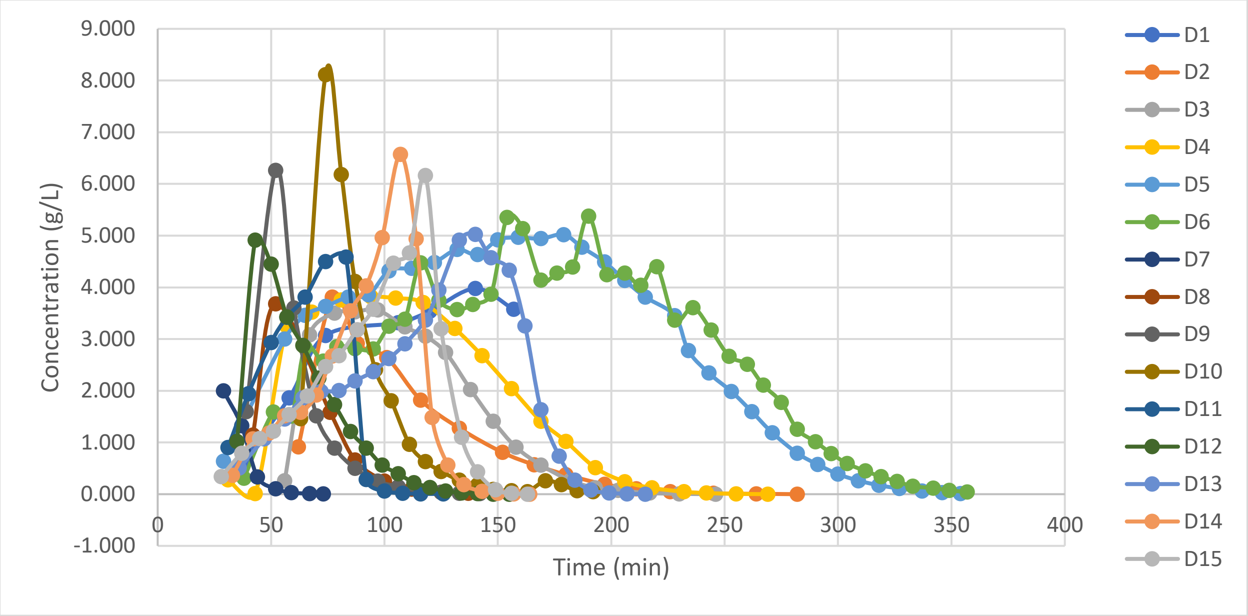

Figure A.84 Isoamyl Alcohol Concentration vs Time for All Distillations

APPENDIX B: MATLAB Codes

Conventional Simulation MATLAB Codes

```
%This code models a 5 stage distillaion column separeating ethanol and water. It
utilizes the van laar thermodynamic model for equilbrium caluculaitons.


function xdot=Ethanol_Water_Conventional(t,x,flag)
if isempty(flag),

% Pressure is 760 mmHg
P=760;

% liquid phase mole fractions in the plates, condenser and still
x1=x(1);
x2=x(2);
x3=x(3);
x4=x(4);
x5=x(5);
x0=x(7);
xB=x(8);

% temperatures in the various plates and in the still
T1=x(10);
T2=x(11);
T3=x(12);
T4=x(13);
T5=x(14);
TB=x(15);

% coefficients for vapor pressure calculation of ethanol (1) and water (2)
A1=8.11220;
B1=1592.864;
C1=226.184;
A2=8.07131;
B2=1730.63;
C2=233.426;


% NRTL coefficients of water and ethanol binary mixture
R=8.314; % Gas Constant - J/mol*K
A12 = -633; %NRTL Parameter
A21= 5823.1; %NRTL Parameter

T12_1=A12/(R*(T1+273.15));
T12_2=A12/(R*(T2+273.15));
T12_3=A12/(R*(T3+273.15));
T12_4=A12/(R*(T4+273.15));
T12_5=A12/(R*(T5+273.15));
T12_B=A12/(R*(TB+273.15));

T21_1=A21/(R*(T1+273.15));
T21_2=A21/(R*(T2+273.15));
T21_3=A21/(R*(T3+273.15));
```

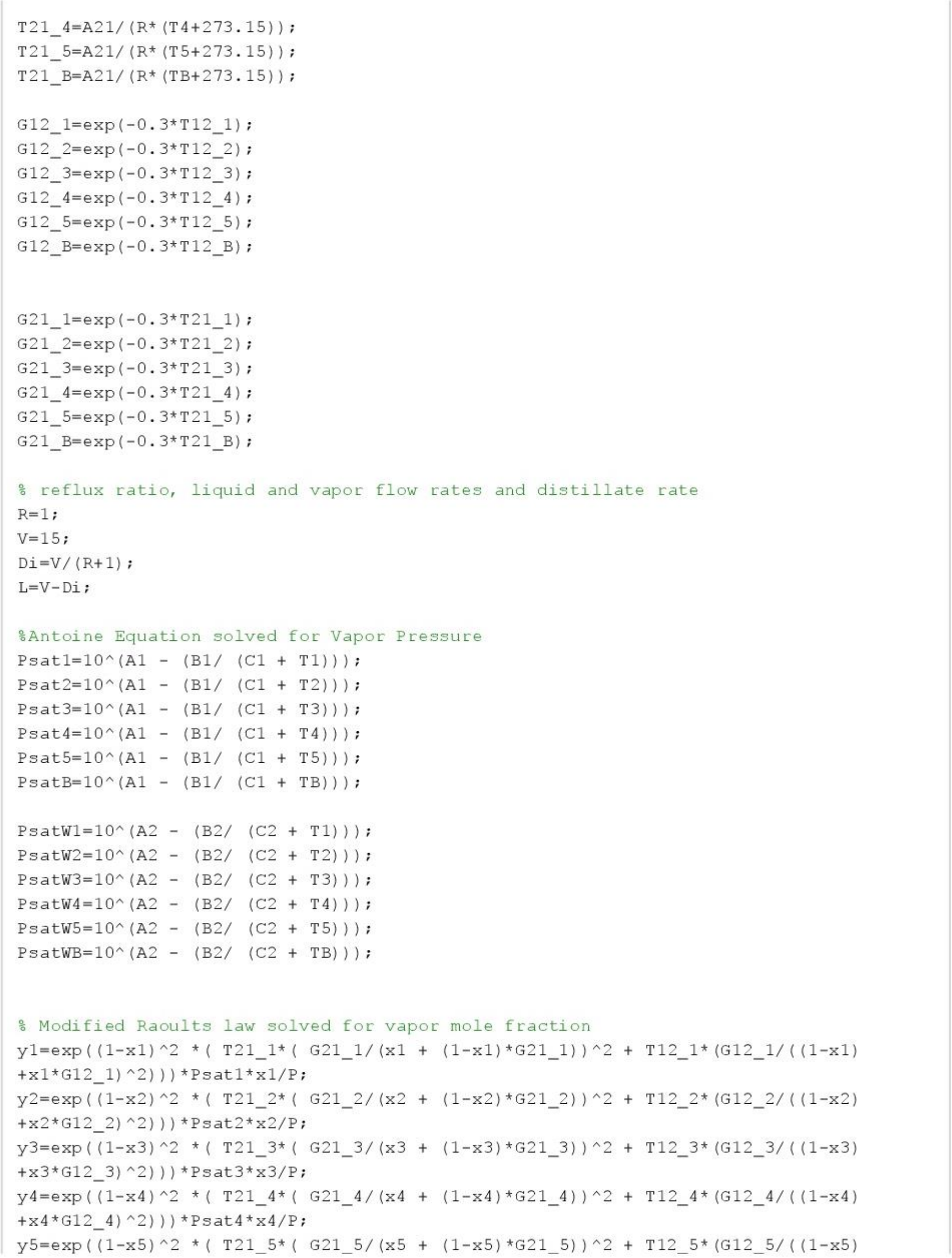

```
T21_4=A21/(R*(T4+273.15));
T21_5=A21/(R*(T5+273.15));
T21_B=A21/(R*(TB+273.15));

G12_1=exp(-0.3*T12_1);
G12_2=exp(-0.3*T12_2);
G12_3=exp(-0.3*T12_3);
G12_4=exp(-0.3*T12_4);
G12_5=exp(-0.3*T12_5);
G12_B=exp(-0.3*T12_B);


G21_1=exp(-0.3*T21_1);
G21_2=exp(-0.3*T21_2);
G21_3=exp(-0.3*T21_3);
G21_4=exp(-0.3*T21_4);
G21_5=exp(-0.3*T21_5);
G21_B=exp(-0.3*T21_B);

% reflux ratio, liquid and vapor flow rates and distillate rate
R=1;
V=15;
Di=V/(R+1);
L=V-Di;

%Antoine Equation solved for Vapor Pressure
Psat1=10^(A1 - (B1/ (C1 + T1)));
Psat2=10^(A1 - (B1/ (C1 + T2)));
Psat3=10^(A1 - (B1/ (C1 + T3)));
Psat4=10^(A1 - (B1/ (C1 + T4)));
Psat5=10^(A1 - (B1/ (C1 + T5)));
PsatB=10^(A1 - (B1/ (C1 + TB)));

PsatW1=10^(A2 - (B2/ (C2 + T1)));
PsatW2=10^(A2 - (B2/ (C2 + T2)));
PsatW3=10^(A2 - (B2/ (C2 + T3)));
PsatW4=10^(A2 - (B2/ (C2 + T4)));
PsatW5=10^(A2 - (B2/ (C2 + T5)));
PsatWB=10^(A2 - (B2/ (C2 + TB)));


% Modified Raoults law solved for vapor mole fraction
y1=exp((1-x1)^2 *( T21_1*( G21_1/(x1 + (1-x1)*G21_1))^2 + T12_1*(G12_1/((1-x1)
+x1*G12_1)^2)))*Psat1*x1/P;
y2=exp((1-x2)^2 *( T21_2*( G21_2/(x2 + (1-x2)*G21_2))^2 + T12_2*(G12_2/((1-x2)
+x2*G12_2)^2)))*Psat2*x2/P;
y3=exp((1-x3)^2 *( T21_3*( G21_3/(x3 + (1-x3)*G21_3))^2 + T12_3*(G12_3/((1-x3)
+x3*G12_3)^2)))*Psat3*x3/P;
y4=exp((1-x4)^2 *( T21_4*( G21_4/(x4 + (1-x4)*G21_4))^2 + T12_4*(G12_4/((1-x4)
+x4*G12_4)^2)))*Psat4*x4/P;
y5=exp((1-x5)^2 *( T21_5*( G21_5/(x5 + (1-x5)*G21_5))^2 + T12_5*(G12_5/((1-x5)
```

```
+x5*G12_5)^2)))*Psat5*x5/P;
yB=exp((1-xB)^2 *( T21_B*( G21_B/(xB + (1-xB)*G21_B))^2 + T12_B*(G12_B/((1-xB)
+xB*G12_B)^2)))*PsatB*xB/P;

% Molar holdup for the four stages and the still
MH0=112;
MH=56;

% governing equations are 13 Differential and Algebraic Equations
xdot(1)=1/MH*(L*(x0-x1)+V*(y2-y1));
xdot(2)=1/MH*(L*(x1-x2)+V*(y3-y2));
xdot(3)=1/MH*(L*(x2-x3)+V*(y4-y3));
xdot(4)=1/MH*(L*(x3-x4)+V*(y5-y4));
xdot(5)=1/MH*(L*(x4-x5)+V*(yB-y5));
xdot(6)=L-V;
xdot(7)=(V/MH0*y1-(L+Di)/MH0*x0);
xdot(8)=(L*(x5-xB)-V*(yB-xB));
xdot(9)=Di;
xdot(10)=P-exp((1-x1)^2 * (T21_1*( G21_1/(x1 + (1-x1)*G21_1))^2 + T12_1*(G12_1/((1-
x1)+x1*G12_1)^2)))*Psat1*x1- exp( (x1^2)* T12_1* (G12_1/((1-x1)+x1*G12_1))^2 +
T12_1*(G21_1/(x1+(1-x1)*G21_1)^2))*PsatW1*(1-x1);
xdot(11)=P-exp((1-x2)^2 * (T21_2*( G21_2/(x2 + (1-x2)*G21_2))^2 + T12_2*(G12_2/((1-
x2)+x2*G12_2)^2)))*Psat2*x2- exp( (x2^2)* T12_2* (G12_2/((1-x2)+x2*G12_2))^2 +
T12_2*(G21_2/(x2+(1-x2)*G21_2)^2))*PsatW2*(1-x2);
xdot(12)=P-exp((1-x3)^2 * (T21_3*( G21_3/(x3 + (1-x3)*G21_3))^2 + T12_3*(G12_3/((1-
x3)+x3*G12_3)^2)))*Psat3*x3- exp( (x3^2)* T12_3* (G12_3/((1-x3)+x3*G12_3))^2 +
T12_3*(G21_3/(x3+(1-x3)*G21_3)^2))*PsatW3*(1-x3);
xdot(13)=P-exp((1-x4)^2 * (T21_4*( G21_4/(x4 + (1-x4)*G21_4))^2 + T12_4*(G12_4/((1-
x4)+x4*G12_4)^2)))*Psat4*x4- exp( (x4^2)* T12_4* (G12_4/((1-x4)+x4*G12_4))^2 +
T12_4*(G21_4/(x4+(1-x4)*G21_4)^2))*PsatW4*(1-x4);
xdot(14)=P-exp((1-x5)^2 * (T21_5*( G21_5/(x5 + (1-x5)*G21_5))^2 + T12_5*(G12_5/((1-
x5)+x5*G12_5)^2)))*Psat5*x5- exp( (x5^2)* T12_5* (G12_5/((1-x5)+x5*G12_5))^2 +
T12_5*(G21_5/(x5+(1-x5)*G21_5)^2))*PsatW5*(1-x5);
xdot(15)=P-exp((1-xB)^2 * (T21_B*( G21_B/(xB + (1-xB)*G21_B))^2 + T12_B*(G12_B/((1-
xB)+xB*G12_B)^2)))*PsatB*xB- exp( (xB^2)* T12_B* (G12_B/((1-xB)+xB*G12_B))^2 +
T12_B*(G21_B/(xB+(1-xB)*G21_B)^2))*PsatWB*(1-xB);

xdot = xdot';  % xdot must be a column vector

else

% Return M the mass matrix
   M = zeros(15,15);
      M(1,1) = 1;
      M(2,2) = 1;
      M(3,3) = 1;
      M(4,4) = 1;
      M(5,5) = 1;
      M(6,6) = 1;
      M(7,7) = 1;
      M(8,8) = x(6);
```

```
      M(9,9)=  1;
   xdot = M;
end
```

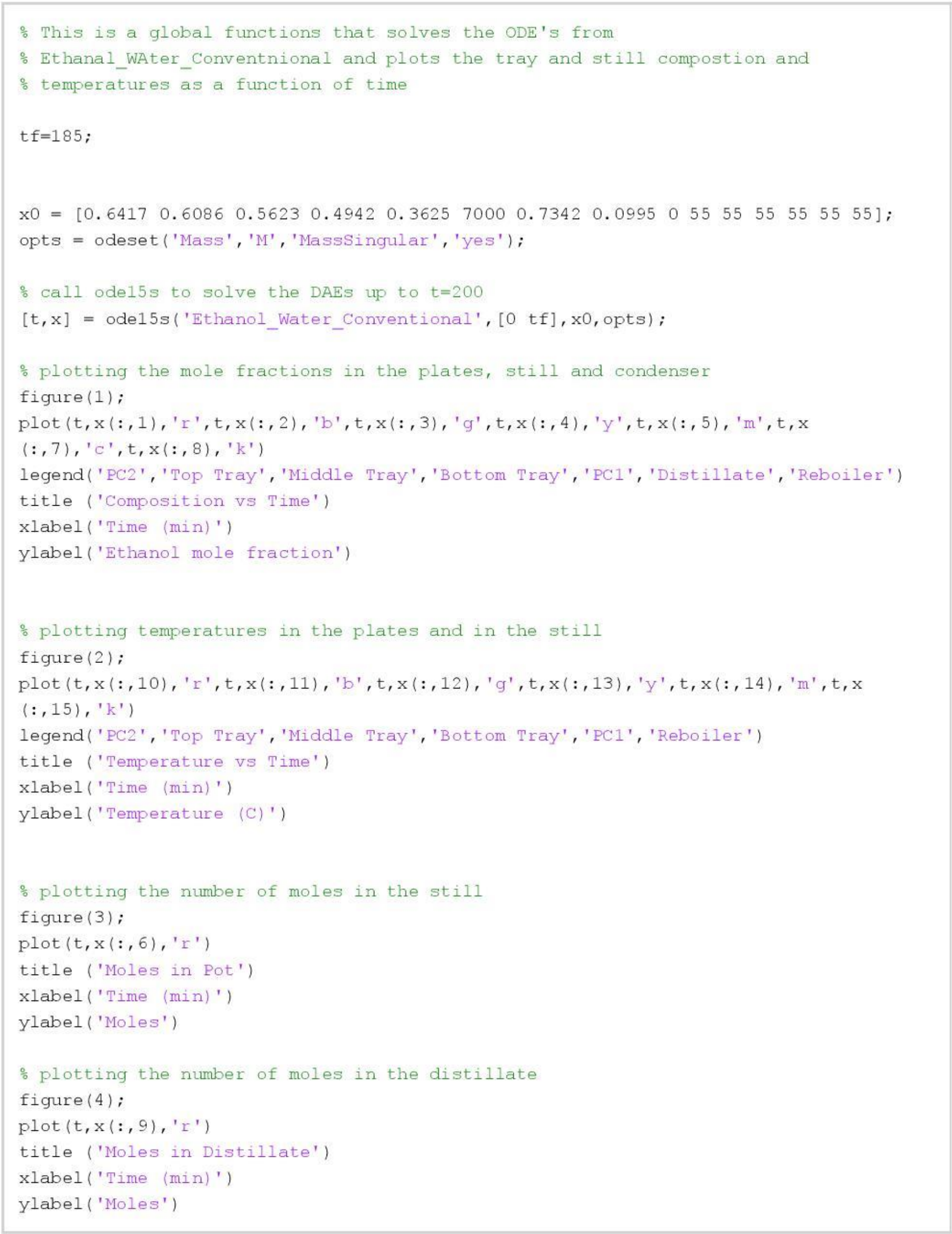

```
% This is a global functions that solves the ODE's from
% Ethanal_WAter_Conventnional and plots the tray and still compostion and
% temperatures as a function of time

tf=185;


x0 = [0.6417 0.6086 0.5623 0.4942 0.3625 7000 0.7342 0.0995 0 55 55 55 55 55 55];
opts = odeset('Mass','M','MassSingular','yes');

% call ode15s to solve the DAEs up to t=200
[t,x] = ode15s('Ethanol_Water_Conventional',[0 tf],x0,opts);

% plotting the mole fractions in the plates, still and condenser
figure(1);
plot(t,x(:,1),'r',t,x(:,2),'b',t,x(:,3),'g',t,x(:,4),'y',t,x(:,5),'m',t,x
(:,7),'c',t,x(:,8),'k')
legend('PC2','Top Tray','Middle Tray','Bottom Tray','PC1','Distillate','Reboiler')
title ('Composition vs Time')
xlabel('Time (min)')
ylabel('Ethanol mole fraction')


% plotting temperatures in the plates and in the still
figure(2);
plot(t,x(:,10),'r',t,x(:,11),'b',t,x(:,12),'g',t,x(:,13),'y',t,x(:,14),'m',t,x
(:,15),'k')
legend('PC2','Top Tray','Middle Tray','Bottom Tray','PC1','Reboiler')
title ('Temperature vs Time')
xlabel('Time (min)')
ylabel('Temperature (C)')


% plotting the number of moles in the still
figure(3);
plot(t,x(:,6),'r')
title ('Moles in Pot')
xlabel('Time (min)')
ylabel('Moles')

% plotting the number of moles in the distillate
figure(4);
plot(t,x(:,9),'r')
title ('Moles in Distillate')
xlabel('Time (min)')
ylabel('Moles')
```

Cyclic Simulation MATLAB Codes

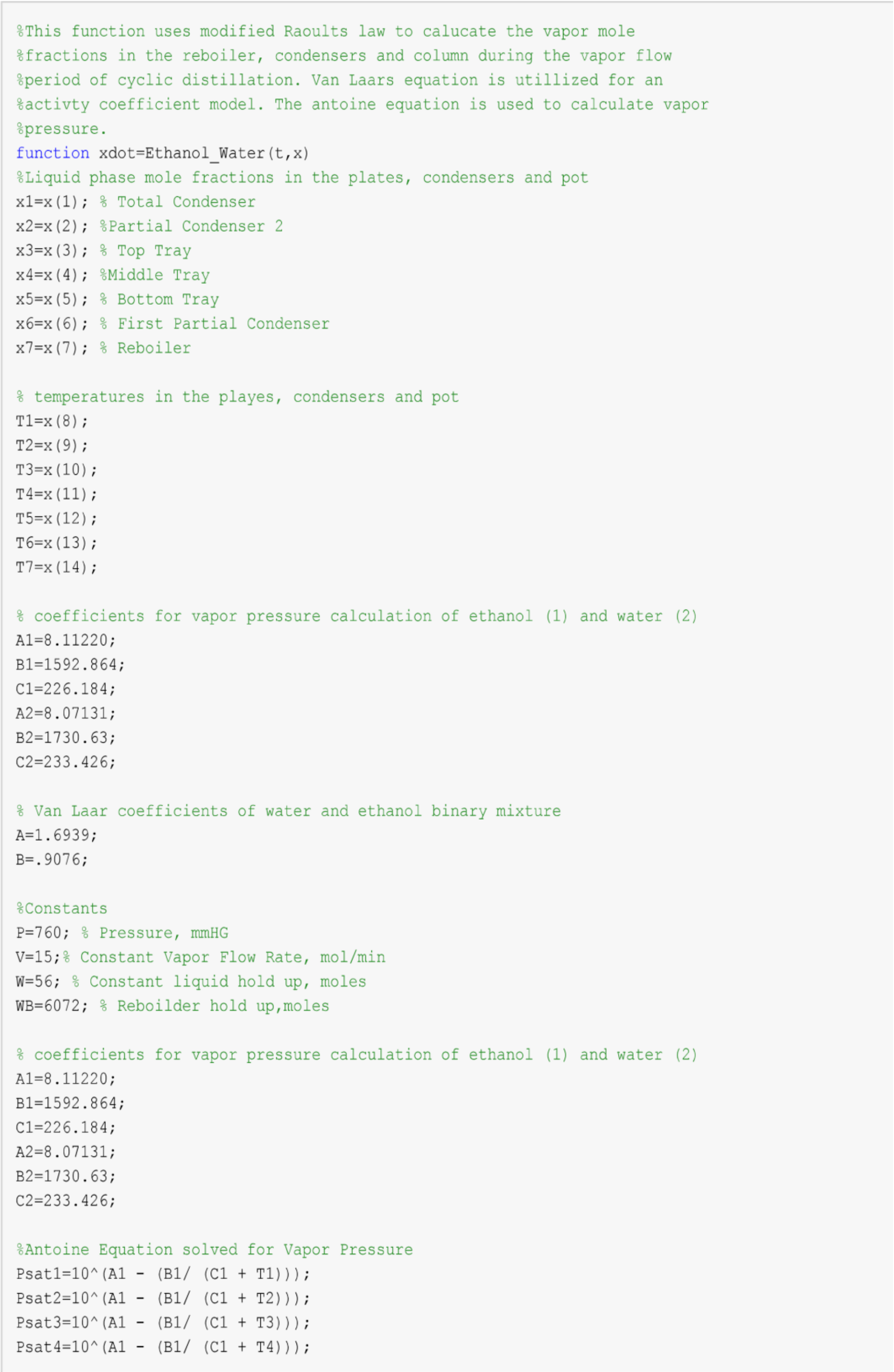

```
%This function uses modified Raoults law to calucate the vapor mole
%fractions in the reboiler, condensers and column during the vapor flow
%period of cyclic distillation. Van Laars equation is utillized for an
%activty coefficient model. The antoine equation is used to calculate vapor
%pressure.
function xdot=Ethanol_Water(t,x)
%Liquid phase mole fractions in the plates, condensers and pot
x1=x(1); % Total Condenser
x2=x(2); %Partial Condenser 2
x3=x(3); % Top Tray
x4=x(4); %Middle Tray
x5=x(5); % Bottom Tray
x6=x(6); % First Partial Condenser
x7=x(7); % Reboiler

% temperatures in the playes, condensers and pot
T1=x(8);
T2=x(9);
T3=x(10);
T4=x(11);
T5=x(12);
T6=x(13);
T7=x(14);

% coefficients for vapor pressure calculation of ethanol (1) and water (2)
A1=8.11220;
B1=1592.864;
C1=226.184;
A2=8.07131;
B2=1730.63;
C2=233.426;

% Van Laar coefficients of water and ethanol binary mixture
A=1.6939;
B=.9076;

%Constants
P=760; % Pressure, mmHG
V=15;% Constant Vapor Flow Rate, mol/min
W=56; % Constant liquid hold up, moles
WB=6072; % Reboilder hold up,moles

% coefficients for vapor pressure calculation of ethanol (1) and water (2)
A1=8.11220;
B1=1592.864;
C1=226.184;
A2=8.07131;
B2=1730.63;
C2=233.426;

%Antoine Equation solved for Vapor Pressure
Psat1=10^(A1 - (B1/ (C1 + T1)));
Psat2=10^(A1 - (B1/ (C1 + T2)));
Psat3=10^(A1 - (B1/ (C1 + T3)));
Psat4=10^(A1 - (B1/ (C1 + T4)));
```

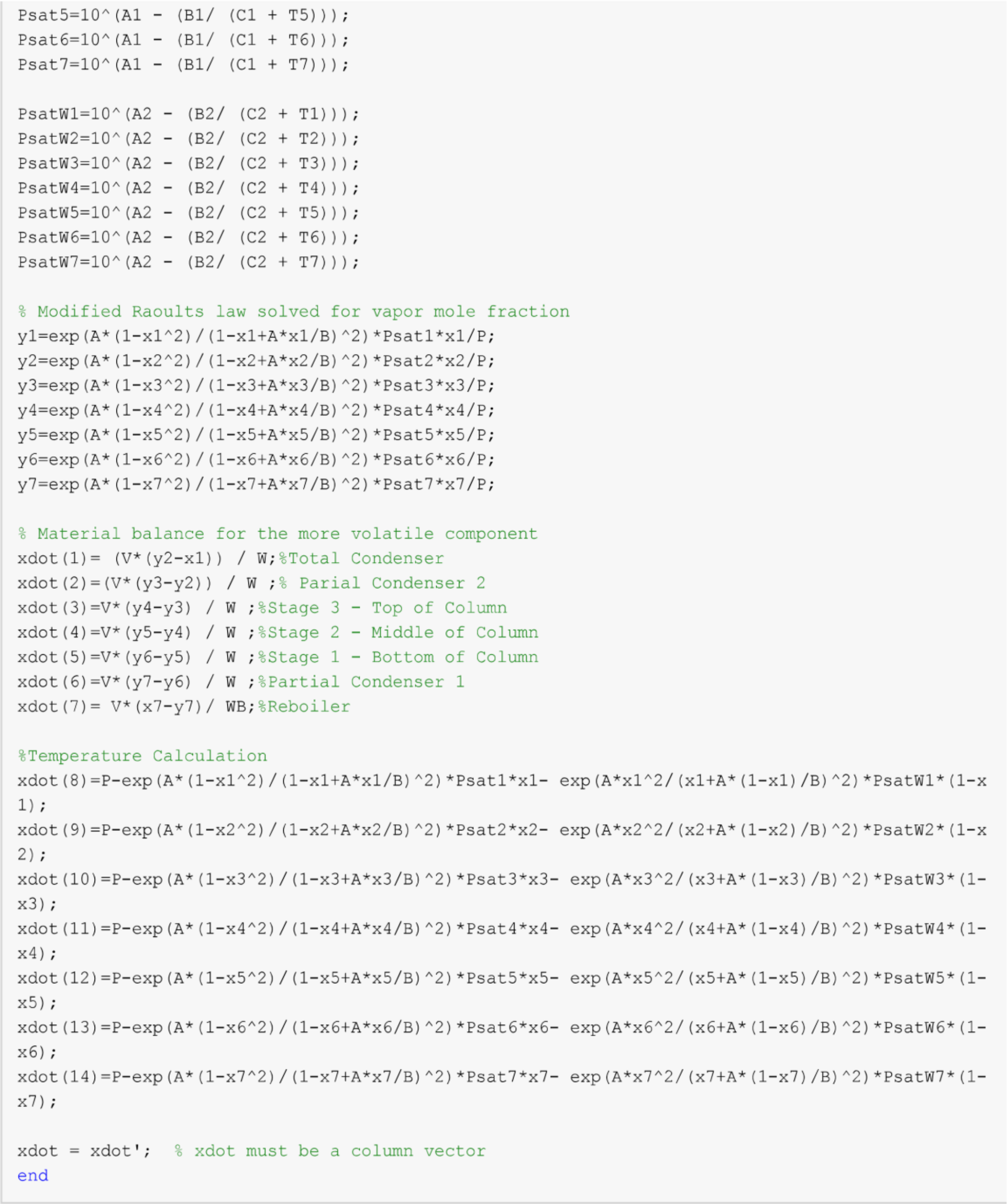

```
Psat5=10^(A1 - (B1/ (C1 + T5)));
Psat6=10^(A1 - (B1/ (C1 + T6)));
Psat7=10^(A1 - (B1/ (C1 + T7)));

PsatW1=10^(A2 - (B2/ (C2 + T1)));
PsatW2=10^(A2 - (B2/ (C2 + T2)));
PsatW3=10^(A2 - (B2/ (C2 + T3)));
PsatW4=10^(A2 - (B2/ (C2 + T4)));
PsatW5=10^(A2 - (B2/ (C2 + T5)));
PsatW6=10^(A2 - (B2/ (C2 + T6)));
PsatW7=10^(A2 - (B2/ (C2 + T7)));

% Modified Raoults law solved for vapor mole fraction
y1=exp(A*(1-x1^2)/(1-x1+A*x1/B)^2)*Psat1*x1/P;
y2=exp(A*(1-x2^2)/(1-x2+A*x2/B)^2)*Psat2*x2/P;
y3=exp(A*(1-x3^2)/(1-x3+A*x3/B)^2)*Psat3*x3/P;
y4=exp(A*(1-x4^2)/(1-x4+A*x4/B)^2)*Psat4*x4/P;
y5=exp(A*(1-x5^2)/(1-x5+A*x5/B)^2)*Psat5*x5/P;
y6=exp(A*(1-x6^2)/(1-x6+A*x6/B)^2)*Psat6*x6/P;
y7=exp(A*(1-x7^2)/(1-x7+A*x7/B)^2)*Psat7*x7/P;

% Material balance for the more volatile component
xdot(1)= (V*(y2-x1)) / W;%Total Condenser
xdot(2)=(V*(y3-y2)) / W ;% Parial Condenser 2
xdot(3)=V*(y4-y3) / W ;%Stage 3 - Top of Column
xdot(4)=V*(y5-y4) / W ;%Stage 2 - Middle of Column
xdot(5)=V*(y6-y5) / W ;%Stage 1 - Bottom of Column
xdot(6)=V*(y7-y6) / W ;%Partial Condenser 1
xdot(7)= V*(x7-y7)/ WB;%Reboiler

%Temperature Calculation
xdot(8)=P-exp(A*(1-x1^2)/(1-x1+A*x1/B)^2)*Psat1*x1- exp(A*x1^2/(x1+A*(1-x1)/B)^2)*PsatW1*(1-x
1);
xdot(9)=P-exp(A*(1-x2^2)/(1-x2+A*x2/B)^2)*Psat2*x2- exp(A*x2^2/(x2+A*(1-x2)/B)^2)*PsatW2*(1-x
2);
xdot(10)=P-exp(A*(1-x3^2)/(1-x3+A*x3/B)^2)*Psat3*x3- exp(A*x3^2/(x3+A*(1-x3)/B)^2)*PsatW3*(1-
x3);
xdot(11)=P-exp(A*(1-x4^2)/(1-x4+A*x4/B)^2)*Psat4*x4- exp(A*x4^2/(x4+A*(1-x4)/B)^2)*PsatW4*(1-
x4);
xdot(12)=P-exp(A*(1-x5^2)/(1-x5+A*x5/B)^2)*Psat5*x5- exp(A*x5^2/(x5+A*(1-x5)/B)^2)*PsatW5*(1-
x5);
xdot(13)=P-exp(A*(1-x6^2)/(1-x6+A*x6/B)^2)*Psat6*x6- exp(A*x6^2/(x6+A*(1-x6)/B)^2)*PsatW6*(1-
x6);
xdot(14)=P-exp(A*(1-x7^2)/(1-x7+A*x7/B)^2)*Psat7*x7- exp(A*x7^2/(x7+A*(1-x7)/B)^2)*PsatW7*(1-
x7);

xdot = xdot';  % xdot must be a column vector
end
```

```
%This is a global function which uses ode15s to integrate the set of cycic
%distillation functions for the vapor flow period using the Ethanol_Water
%function. It then plots the results as a functin of time. Laslty, the
%outputs are the inputs for the liquid flow period.
```

```
tvap=6;

x0 = [.7342 .6417 .6086 .5623 .4942 .3625 .0995 55 55 55 55 55 55 55 ];%Initial values used f
or Cycle 1
%x0=[X1_new X2_new X3_new X4_new X5_new X6_new X7_new x(end,8) x(end,9) x(end,10) x(end,11) x
(end,12) x(end,13) x(end,14) ]

% call ode15s to solve the DAEs up to t=tvap
[t,x] = ode15s('Ethanol_Water',[0 tvap],x0);

% plotting the mole fractions in the plates, condensers and pot
figure(1);
plot(t,x(:,1),'r',t,x(:,2),'g',t,x(:,3),'b',t,x(:,4),'c',t,x(:,5),'m',t,x(:,6),'y',t,x(:,7),'
k');
legend('x1','x2','x3','x4','x5','x6','x7')
title ('Tray Composition vs Time')
xlabel('Time (min)')
ylabel('Ethanol mole fraction')

% plotting temperatures in the plates, condensers and pot
figure(2);
plot(t,x(:,8),'r',t,x(:,9),'g',t,x(:,10),'b',t,x(:,11),'c',t,x(:,12),'m',t,x(:,13),'y',t,x(:,
14),'k');

legend('T1','T2','T3','T4','T5','T6','T7')
title ('Tray temperature vs Time')
xlabel('Time (min)')
ylabel('Temp (deg C)')

xfinal=x(end,:)
```

```
xfinal =

  Columns 1 through 7

    0.7898    0.6308    0.5902    0.5136    0.3232    0.1253    0.0935

  Columns 8 through 14

   74.1203   73.7323   73.7326   73.8455   75.2116   81.7470   84.2646
```

```
% This function takes as input the liquid concentrations from the end of
% the vapor flow period and calculates the liquid concentrations after the
% liquid flow period is over aka the intital values for the next vapor flow
% period

%Inputs
theta = .8;
W = 56;
WB =5982; % Volume in the reboiler at the beginning of the LFP
WBI =6038; %moles in the reboiler at the end of the LFP

%Liquid  Compositions from previous cycle
%Condenser
X1_old=x(end,1);
%Stages/Partial Condensers
X2_old= x(end,2);
X3_old= x(end,3);
X4_old=x(end,4);
X5_old=x(end,5);
X6_old=x(end,6);
%Reboiler
X7_old=x(end,7);

%Calculating new liquid compositions
%Condenser
X1_new=X1_old;
%Partial Condenser 2
X2_new=X1_new;
%Stage 1 - Top of Column
X3_new=theta*X2_new + (1-theta)*X3_old;
%Stage 2 - Middle of Column
X4_new=theta*X3_new + (1-theta)*X4_old;
%Stage 3 - Bottom of Column
X5_new=theta*X4_new + (1-theta)*X5_old;
%Reboiler
X7_new = ((WB*X7_old)/WBI)+ ((W*X6_old)/WBI);
%Partial Condenser 1
X6_new=X7_new;



X_NEW=[X1_new X2_new X3_new X4_new X5_new X6_new X7_new]
```

```
X_NEW =

    0.7898    0.7898    0.7499    0.7027    0.6268    0.0938    0.0938
```

MATLAB Cyclic Data

Table B.1 Cyclic Distillation Simulation Data

Cycle	Period	Reboiler	Total Con.		Part. Cond. 2		Top Tray		Middle Tray		Bottom Tray		Part. Cond. 1		Reboiler	
		Hold Up	X1	T1	X2	T2	X3	T3	X4	T4	X5	T5	X6	T6	X7	T7
Initial	-	7000	0.7342	55	0.6417	55	0.6086	55	0.5623	55	0.4942	55	0.3625	55	0.0995	55
1	VFP	6798	0.7898	74.1203	0.6308	73.7323	0.5902	73.7326	0.5137	73.8453	0.3238	75.204	0.1261	81.694	0.0943	84.194
	LFP	6854	0.7898	74.1203	0.7898	73.7323	0.7499	73.7326	0.7027	73.8453	0.6269	75.204	0.0946	81.694	0.0946	84.194
2	VFP	6764	0.8252	74.3334	0.775	74.0509	0.7269	73.8816	0.5966	73.7298	0.225	77.236	0.0907	84.529	0.0893	84.6559
	LFP	6820	0.8252	74.3334	0.8252	74.0509	0.8055	73.8816	0.7637	73.7298	0.656	77.236	0.0893	84.529	0.0892	84.6559
3	VFP	6730	0.8401	74.4487	0.814	74.2591	0.7797	74.073	0.647	73.7435	0.2271	77.171	0.0854	85.0367	0.0841	85.1597
	LFP	6786	0.8401	74.4487	0.8401	74.2591	0.8281	74.073	0.7919	73.7435	0.6789	77.171	0.0842	85.0367	0.0842	85.1597
4	VFP	6696	0.8472	74.5093	0.8306	74.3744	0.8012	74.1828	0.6702	73.7688	0.225	77.2287	0.0802	85.563	0.0791	85.683
	LFP	6752	0.8472	74.5093	0.8472	74.3744	0.838	74.1828	0.8044	73.7688	0.6885	77.2287	0.0791	85.563	0.0791	85.683
5	VFP	6662	0.8507	74.5408	0.8383	74.434	0.8102	74.236	0.6766	73.7781	0.2145	77.5449	0.0751	86.1087	0.0741	86.2252
	LFP	6718	0.8507	74.5408	0.8507	74.434	0.8426	74.236	0.8094	73.7781	0.6904	77.5449	0.0741	86.1087	0.0741	86.2252
6	VFP	6628	0.8524	74.557	0.8418	74.4636	0.8137	74.4636	0.6744	73.775	0.1988	78.0698	0.0701	86.673	0.0692	86.7857
	LFP	6684	0.8524	74.557	0.8524	74.4636	0.8447	74.4636	0.8106	73.775	0.6883	78.0698	0.0692	86.673	0.0692	86.7857
7	VFP	6594	0.8533	74.565	0.8435	74.4774	0.8147	74.2648	0.667	73.7651	0.1808	78.7612	0.0653	87.2548	0.0644	87.3634
	LFP	6650	0.8533	74.565	0.8533	74.4774	0.8456	74.2648	0.8099	73.7651	0.684	78.7612	0.0644	87.2548	0.0644	87.3634
8	VFP	6560	0.8537	74.5688	0.8441	74.4826	0.8143	74.2621	0.6564	73.7529	0.1617	79.6105	0.0605	87.8528	0.0597	87.9568
	LFP	6616	0.8537	74.5688	0.8537	74.4826	0.8458	74.2621	0.8079	73.7529	0.6787	79.6105	0.0597	87.8528	0.0597	87.9568
9	VFP	6526	0.8538	74.5701	0.8441	74.4832	0.813	74.2532	0.643	73.741	0.1425	80.6161	0.0559	88.4649	0.0552	88.564
	LFP	6582	0.8538	74.5701	0.8538	74.4832	0.8457	74.2532	0.8051	73.741	0.6727	80.6161	0.0552	88.4649	0.0552	88.564
10	VFP	6492	0.8538	74.5702	0.8439	74.4812	0.8112	74.2431	0.627	73.7319	0.1236	81.783	0.0515	89.0888	0.0509	89.1828
	LFP	6548	0.8538	74.5702	0.8538	74.4812	0.8452	74.2431	0.8017	73.7319	0.6661	81.783	0.0509	89.0888	0.0509	89.1828
11	VFP	6458	0.8538	74.5699	0.8535	74.4782	0.8092	74.2307	0.6086	73.728	0.1054	83.1273	0.0473	89.7218	0.0467	89.8106
	LFP	6514	0.8538	74.5699	0.8538	74.4782	0.8499	74.2307	0.7976	73.728	0.6592	83.1273	0.0467	89.7218	0.0467	89.8106
12	VFP	6424	0.8537	74.569	0.8431	74.4741	0.8067	74.2162	0.5875	73.7332	0.0883	84.6185	0.0432	90.3607	0.0427	90.4441
	LFP	6480	0.8537	74.569	0.8537	74.4741	0.8443	74.2162	0.793	73.7332	0.652	84.6185	0.0427	90.3607	0.0427	90.4441
13	VFP	6390	0.8535	74.5676	0.8423	74.4681	0.8035	74.1975	0.5631	73.7515	0.0738	86.1187	0.0393	91.0016	0.0393	91.0795
	LFP	6446	0.8535	74.5676	0.8535	74.4681	0.8435	74.1975	0.7875	73.7515	0.6447	86.1187	0.0388	91.0016	0.0388	91.0795
14	VFP	6356	0.8534	74.566	0.8416	74.462	0.8001	74.1784	0.5358	73.7905	0.0607	87.6971	0.0356	91.6406	0.0352	91.713
	LFP	6412	0.8534	74.566	0.8534	74.462	0.8427	74.1784	0.7814	73.7905	0.6372	87.6971	0.0352	91.6406	0.0252	91.713
15	VFP	6322	0.8532	74.5646	0.8409	74.4563	0.7967	74.1594	0.5061	73.8574	0.0499	89.3456	0.0321	92.2738	0.0318	92.3407
	LFP	6378	0.8532	74.5646	0.8532	74.4563	0.8419	74.1594	0.7747	73.8574	0.6296	89.3456	0.0317	92.2738	0.0317	92.3407
16	VFP	6288	0.8531	74.563	0.8401	74.4494	0.7923	74.1367	0.473	73.9666	0.0402	90.7527	0.0288	92.9051	0.0285	92.9666
	LFP	6344	0.8531	74.563	0.8531	74.4494	0.8409	74.1367	0.7673	73.9666	0.6219	90.7527	0.0285	92.9051	0.0285	92.9666
17	VFP	6254	0.8529	74.5611	0.8392	74.4421	0.7876	74.113	0.4385	74.127	0.0329	92.0495	0.0258	93.5124	0.0255	93.5685
	LFP	6310	0.8529	74.5611	0.8529	74.4421	0.8398	74.113	0.7595	74.127	0.6142	92.0495	0.0255	93.5124	0.0255	93.5685
18	VFP	6220	0.8526	74.5588	0.8381	74.4332	0.782	74.0858	0.4028	74.3536	0.0276	93.0784	0.023	94.0998	0.0227	94.1509
	LFP	6276	0.8526	74.5588	0.8526	74.4332	0.8385	74.0858	0.7514	74.3536	0.6066	93.0784	0.0227	94.0998	0.0227	94.1509
19	VFP	6186	0.8524	74.5568	0.8371	74.4253	0.7763	74.0601	0.3665	74.664	0.0232	94.0043	0.0204	94.6639	0.0201	94.7101
	LFP	6242	0.8524	74.5568	0.8524	74.4253	0.8372	74.0601	0.743	74.664	0.5991	94.0043	0.0202	94.6639	0.0202	94.7101
20	VFP	6152	0.8522	74.5568	0.836	74.4253	0.7698	74.0601	0.3309	74.664	0.0197	94.0043	0.018	94.6639	0.0178	94.7101
	LFP	6208	0.8522	74.5568	0.8522	74.4253	0.8357	74.0601	0.7347	74.664	0.5917	94.0043	0.0178	94.6639	0.0178	94.7101
21	VFP	6118	0.8519	74.5523	0.8349	74.4078	0.7627	74.0037	0.2964	75.5731	0.0169	95.4286	0.0158	95.707	0.0156	95.7442
	LFP	6174	0.8519	74.5523	0.8519	74.4078	0.8341	74.0037	0.7265	75.5731	0.5846	95.4286	0.0156	95.707	0.0156	95.7442
22	VFP	6084	0.8517	74.55	0.8337	74.3988	0.7552	73.9756	0.2635	76.1954	0.0145	95.9995	0.0138	96.1806	0.0137	96.2137
	LFP	6140	0.8517	74.55	0.8517	74.3988	0.8324	73.9756	0.7186	76.1954	0.5778	95.9995	0.0137	96.1806	0.0137	96.2137
23	VFP	6050	0.8514	74.5476	0.8325	74.3897	0.7471	73.9474	0.2327	76.9317	0.0125	96.4989	0.0121	96.6196	0.012	96.6489
	LFP	6106	0.8514	74.5476	0.8514	74.3897	0.8305	73.9474	0.711	76.9317	0.5713	96.4989	0.012	96.6196	0.012	96.6489
24	VFP	6016	0.8511	74.5452	0.8313	74.3806	0.7386	73.92	0.2044	77.7805	0.0108	96.9454	0.0108	97.0232	0.0105	97.0491
	LFP	6072	0.8511	74.5452	0.8511	74.3806	0.8286	73.92	0.7038	77.7805	0.5652	96.9454	0.0104	97.0232	0.0104	97.0491
25	VFP	5982	0.8509	74.5429	0.8301	74.3716	0.7297	73.8938	0.1787	78.7341	0.0093	97.3312	0.0091	97.3912	0.009	97.4139
	LFP	6038	0.8509	74.5429	0.8509	74.3716	0.8267	73.8938	0.6971	78.7341	0.5595	97.3312	0.009	97.3912	0.009	97.4139

APPENDIX C: Miscellaneous Figures/Tables

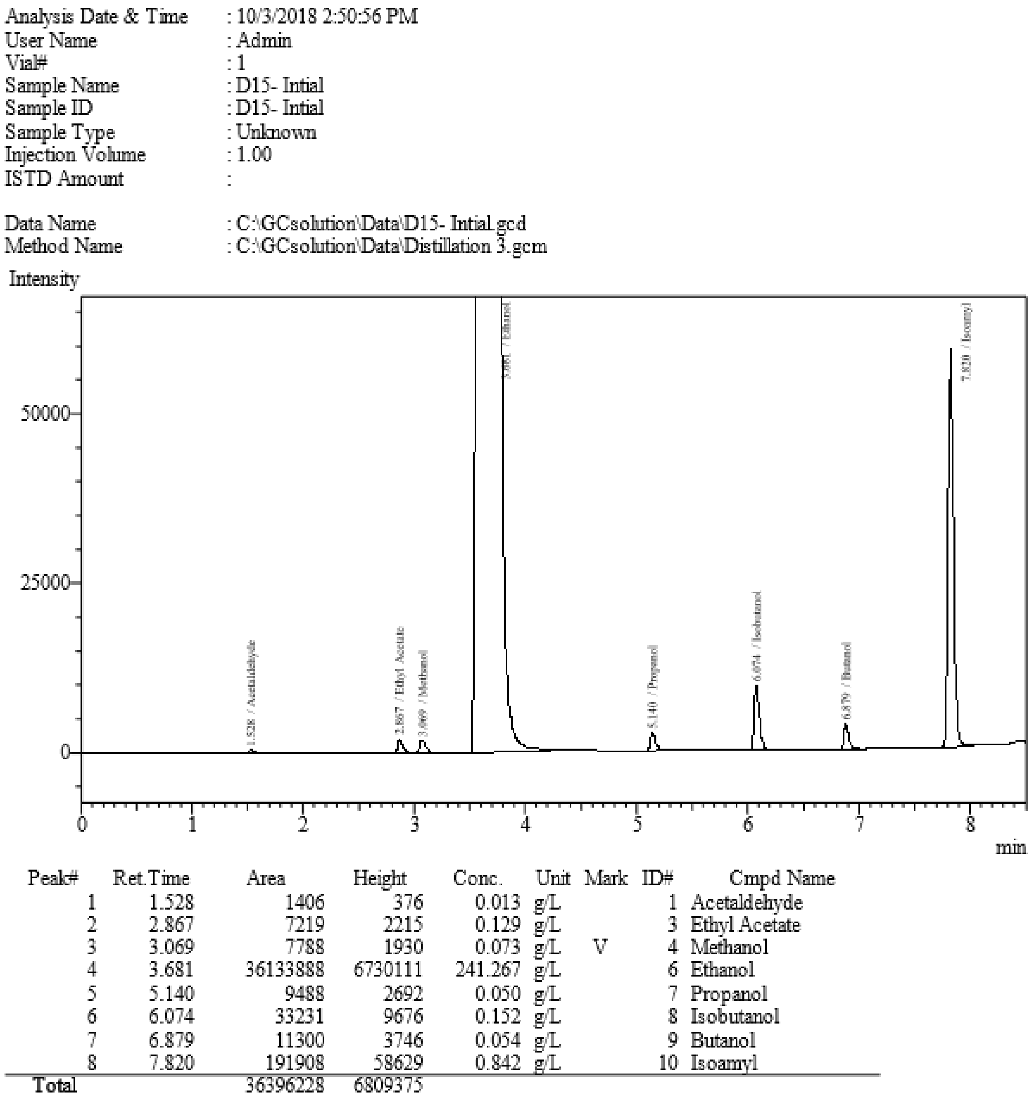

Analysis Date & Time : 10/3/2018 2:50:56 PM
User Name : Admin
Vial# : 1
Sample Name : D15- Intial
Sample ID : D15- Intial
Sample Type : Unknown
Injection Volume : 1.00
ISTD Amount :

Data Name : C:\GCsolution\Data\D15- Intial.gcd
Method Name : C:\GCsolution\Data\Distillation 3.gcm

Peak#	Ret.Time	Area	Height	Conc.	Unit	Mark	ID#	Cmpd Name
1	1.528	1406	376	0.013	g/L		1	Acetaldehyde
2	2.867	7219	2215	0.129	g/L		3	Ethyl Acetate
3	3.069	7788	1930	0.073	g/L	V	4	Methanol
4	3.681	36133888	6730111	241.267	g/L		6	Ethanol
5	5.140	9488	2692	0.050	g/L		7	Propanol
6	6.074	33231	9676	0.152	g/L		8	Isobutanol
7	6.879	11300	3746	0.054	g/L		9	Butanol
8	7.820	191908	58629	0.842	g/L		10	Isoamyl
Total		36396228	6809375					

Figure C1. Example Chromatograph Results

BIBLIOGRAPHY

BIBLIOGRAPHY

1) Cannon MR. Controlled Cycling Improves Various Processes. *Ind Eng Chem*. 1961;53:629-629.

2) Gaska RA, Cannon MR. Controlled Cycling Distillation in Sieve and Screen Plate Towers. *Ind Eng Chem*. 1961;52:630-631.

3) McWhirter JR, Cannon MR. Controlled Cycling Distillation in a Packed-Plate Column. *Ind Eng Chem*. 1961;52:632-634.

4) Schrodt VN. Controlled Cycle Operations. *Ind. Engng Chem. Fundls.* 1965;4:108-110.

5) Sommferfeld JT, Schrodt VN, Parisot PE, Chien HH. Studies of Controlled Cyclic Distillation: I. Computer Simulations and the Analogy with Conventional Operation. *Separat. Sci.* 1966;1:245-279.

6) Chien HH, Sommferfeld JT, Schrodt VN, Parisot PE. Studies of Controlled Cyclic Distillation: II. Analytical Transient Solution and Asymptotic Plate Efficiencies. *Separat. Sci.* 1966;1:281-317.

7) Schrodt VN, Sommerfeld JT, Martin OP, Parisot PE, Chien HH. Plant-scale study of controlled cyclic distillation. *Chem Eng Sci*. 1966;22:759-767.

8) Horn FJM. Periodic Countercurrent Processes. *I&EC Process Design and Develop.* 1966;6:30-35.

9) Robinson RG, Engel AJ. An Analysis of Controlled Cycling Mass Transfer Operations. *Ind Eng Chem*. 1967;59:22-29.

10) May RA, Horn FJM. Stage Efficiency of a Periodically Operated Distillation Column. *I&EC Process Design and Develop.* 1968;7:61-64

11) May RA, Horn FJM. Effect of Mixing on Periodic Countercurrent Processes. *I&EC Process Design and Develop.* 1968;7:349-354.

12) Furzer IA. Periodic Cycling of Plate Columns. *Chem Eng Sci.* 1973;28:296-299.

13) Gel’Perin NI, Polotskii LM, Potapov TG. Operation of a Bubble-Cap Fractionating Column in a Cyclic Regime. *Chem Petro Eng*. 1976;11:707-709.

14) Rivas OR. An Analytical Solution of Cyclic Mass Transfer Operations. *Ind Eng Chem, Process Des Dev.* 1977;16:400-402.

15) Duffy GJ, Furzer IA. Periodic Cycling of Plate Columns. *Chem Eng Sci*. 1978;33:897-904

16) Furzer IA. The Discrete Residence Time Distribution of a Distillation Column Operated with Microprocessor Controlled Periodic Cycling. *Canadian Journal of Chem Eng.* 1978;56:747-750.

17) Goss DW, Furzer IA. Mass Transfer in Periodically Cycled Plate Columns Containing Multiple Sieve Plates. *AIChe Journa*l. 1980;26:663-669.

18) Baron G, Wajc S, Lavie R. Stepwise Periodic Distillation – I: Total Reflux Operation. *Chem Eng Sci.* 1980.;35:859-865

19) Baron G, Wajc S, Lavie R. Stepwise Periodic Distillation – II: Separation of a Binary Mixture. *Chem Eng Sci.* 1981;36:1819-1827.

20) Matsubara M, Watanabe N, Kurimoto H. Binary Periodic Distillation Scheme with Enhanced Energy Conservation. *Chem Eng Sci*. 1985;40:715-721.

21) Matsubara M, Watanabe N, Kurimoto H, Shimizu K. Binary Periodic Distillation Scheme with Enhanced Energy Conservation - II. *Chem Eng Sci*. 1985;40:755-758.

22) Thompson MF, Furzer IA. Hydrodynamic Modelling for Liquid Holdups in Periodically Cycled Plate Columns. *AIChe Journal.* 1984;30:496-500.

23) Szonyi L, Furzer IA. Periodic Cycling of Distillation Columns Using a New Tray Design. *AIChe Journal.* 1985;31:1707-1713.

24) Bausa J, Tsatsaronis G. Reducing the Energy Demand of Continuous Distillation Processes by Optimal Controlled Forced Periodic Operation. *Comp Chem Eng.* 2001;25:359-370.

25) Flodman HR, Timm DC. Batch Distillation Employing Cyclic Rectification and Stripping Operations. *ISA Trans*. 2012;51:454-460.

26) Lita I, Bilde CS, Kiss AA. Modeling, Design and Control of Cyclic Distillation Systems. *Procedia Eng*. 2012;42:1202-1213.

27) Maleta B, MaletaO. Mass Exchange Contact Device. US Patent 8,158,073, 2012.

28) Maleta BV, Shevchenko A, Bedryk O, Kiss AA. Pilot-Scale Studies of Process Intensification by Cyclic Distillation.

29) Kiss AA. Distillation technology – still young and full of breakthrough opportunities. *J Chem Technol Biotechnol.* 2014; 89:479-498.

30) Gerven TV, Stankiewicz A. Structure, Energy, Synergy, Time – The Fundamentals of Process Intensification. *Ind.Eng. Chem. Res.* 2009;48:2465-2474.

31) White DC. Optimize Energy use in Distillation. *Chem Eng. Prog*. 2012;35-41.

32) Bildea CS, Patrut C, Jorgensen SB, Abildskov J, Kiss AA. Cyclic distillation technology – a mini-review. *J Chem Technol Biotechnol.*2016;91:1215-1223.

33) Kiss AA. Cyclic Distillation. *Advanced Distillation Technologies: Design, Control and Applications*. Chichester, West Sussex: Wiley, a John Wiley & Sons. 2013:311-351.

34) Waterbury M. 1,000 Craft Distilleries - and Counting! – Now operating in the USA. *Thewhiskeywash.com*. 2016.

35) Distilled Spirits Council of the United States. Economic Contributions of Distilled Spirits Industry. *Discus.org/economics.* 2016.

36) Boes RE, Berglund KA. Real Time Spirit Distillation Analysis using Gas Chromatography with a Flow Vial Sampler.

37) Toftegard B, Jorgensen SB. An Integration Method for Dynamic Simulation of Cycled Processes. *Computers chem. Eng.* 1989;13:927-930.

38) Sorensen E, Prenzler M. A Cyclic Operating Policy For Batch Distillation – Theory and Practice. *Computers chem. Eng.* 1997;21:S1215-S1220.

39) Sorensen E. A Cyclic Operating Policy for Batch Distillation – Theory and Practice. *Computers chem. Eng.* 1999.;23:533-542.

40) Distilled Spirits Council. "Distilled Spirits Council Reports Record Spirits Sales" DistiledSpirits.org. February 1, 2018. https://www.distilledspirits.org/news/distilled-spirits-council-reports-record-spirits-sales/

41) Hadrich B, Kechaou N. Identification of Best Model for Equilibrium Data of Ethanol-Water Mixture. *Journal of Chemistry and Chemical Engineering.* 2010;4:46-48.

42) Seader J ,Henley E, RoperD. Separation Process Principals: Chemical and Biochemical Operations.2011;3:481-483.

43) Claus M, Berglund K. Fruit Brandy Production By Batch Column Distillation With Reflux. *Journal of Food Processing Engineering.*2004;28:53-67.

44) National Institute of Standards and Technology. NIST Chemistry WebBook. 2018. https://webbook.nist.gov/chemistry/